



Corso di dottorato di ricerca in:

“Food and Human Health”

Ciclo XXXII

Titolo della tesi

**“Development of an electrochemical
biosensor for food safety:
detection of food pathogens”**

Dottoranda

Priya Vizzini

Supervisore

Prof.ssa Marisa Manzano

2019

Acknowledgments

I would like to express my gratitude to my supervisor, Prof. Marisa Manzano, for her guidance and help throughout each stage of the research project and for inspiring my interest in the development of innovative technologies.

A special thank goes to Dr. Jasmina Vidic, for all her suggestions on my work and career during my period at INRA. I'll take your advice to heart.

I wish to thank also Prof. Rosanna Toniolo for the help, support and teaching.

Thanks to my parents, they supported me throughout all these hard years.

I wish to thank my lab mates for their continued support, there are too many wonderful memories of these years together. A special thanks to the wonderful and strong woman of the lab Federica, Paola, Sabrina, Francesca and Debbie. Furthermore, I would like to say thanks to former student, now friend and colleague, Matteo, for his support, encouragement and for the sleepless nights and weekend we were working together.

A special thank to RCG, the first to believe in the importance of my role and work,

ABSTRACT

Listeria monocytogenes and *Campylobacter* spp. are two important foodborne pathogens. They can be acquired by ingestion of contaminated food mainly ready to eat (RTE), undercooked chicken, and milk and dairy products respectively. The symptoms are gastrointestinal disorders that can switch in a serious disease like listeriosis and campylobacteriosis in weak individuals.

The currently recommended ISO standard methods are sensitive and ensure compliance with microbiological criteria, but require long times and a lot of work.

In order to avoid recalls or economic losses, food industries need rapid protocols that can provide results in short times.

In this thesis, with the perspective to develop rapid and efficient molecular detection methods, species-specific primers and probes were designed for *L. monocytogenes* and *C. jejuni*, *C. coli*, *C. lari*, and *C. upsaliensis*.

For the detection of *L. monocytogenes* in cold-smoked salmon samples and ham factory samples designed MAR1- MARB primers were applied in PCR and qPCR protocols.

Two probes, ListCapt and ListE, were tested for the detection of *Listeria monocytogenes*. The ListCapt probe was applied on a DNA-biosensor based on the organic electrochemical transistor (OECT), after preliminary optimization tests with dot blot assay. Instead, the ListE probe was applied on a DNA- electrochemical biosensor based on voltammetry.

Samples of cold-smoked salmon (CSS) and Ham factories samples (from food and environment) were analyzed by electrochemical biosensors. In parallel to molecular methods, AFNOR validated *Listeria* Precis[™] method (ISO standard equivalent method) was applied to the food samples, to compare traditional plate count methods to molecular techniques, in both traditional and molecular approaches. *L. monocytogenes* was detected in only one of the tested CSS samples. Instead, six samples from ham factories were positive to the presence of *L. monocytogenes*. Both PCR and qPCR protocols allowed the detection of *L. monocytogenes*, confirming the capability of primers to detect the pathogen from a complex matrix. However, an enrichment step of 24 h was necessary.

After dot blot protocol optimization to assess specificity and sensitivity of oligonucleotide probes were employed to evaluate the development of a DNA-electrochemical biosensor based on OECT and voltammetry. The studies have been made with promising results, anticipating the prospective potential of the system for label-free DNA sensing.

For the detection of *Campylobacter* spp. designed primers CampyP were applied in PCR and qPCR protocols in 20 chicken meat samples. The probe CampyP3 was tested for the detection of *Campylobacter* spp. and was applied to a DNA-electrochemical biosensor based on voltammetry.

Chicken meat samples were analyzed by the electrochemical biosensor. In parallel to molecular method, ISO 10272-1:2006 was applied to food samples, to compare traditional plate count methods to molecular techniques. With both traditional and molecular approaches, *Campylobacter* was detected in five tested samples.

Both PCR and qPCR protocols allowed the detection of *Campylobacter* spp., confirming the capability of primers to detect the pathogen matrix without enrichment for the application of

qPCR technique. After dot blot protocol optimization, to assess specificity and sensitivity CampyP3 was employed to evaluate the development of a DNA-electrochemical biosensor based on OECT and voltammetry. After the optimization, some food samples were analyzed and confirmed the data obtained by ISO and qPCR.

TABLE OF CONTENTS

ACKNOWLEDGMENTS.....	1
ABSTRACT.....	3
CHAPTER I.....	9
INTRODUCTION	9
1.1 FOODBORNE PATHOGENS	11
1.2 <i>LISTERIA MONOCYTOGENES</i>	11
1.2.1 LINEAGE AND SEROTYPE	12
1.2.2 MORPHOLOGY AND PHYSIOLOGY	13
1.2.3 LISTERIOSIS.....	13
1.2.4 FOOD SAFETY REGULATION.....	14
1.2.5 PREVALENCE	15
1.2.6 <i>LISTERIA MONOCYTOGENES</i> IN FOOD.....	15
1.2.7 CULTURE METHODS FOR <i>L. MONOCYTOGENES</i>	16
1.3 <i>CAMPYLOBACTER SPP.</i>.....	18
1.3.1 MORPHOLOGY AND PHYSIOLOGY	18
1.3.2 CAMPYLOBACTERIOSIS.....	18
1.3.3 FOOD SAFETY REGULATION.....	19
1.3.4 PREVALENCE	19
1.3.5 <i>CAMPYLOBATER</i> IN FOOD	19
1.3.6 GOLD STANDARD METHOD: ISO 10272	20
1.4 BIOSENSOR	22
1.4.1 ELECTROCHEMICAL BIOSENSOR	23
1.4.2 THIOL-GOLD DNA INTERACTION	23
1.4.3 OECT: ORGANIC ELECTROCHEMICAL TRANSISTOR	24

1.4.4 ELECTROCHEMICAL BIOSENSOR BASED ON VOLTAMMETRY	26
REFERENCES	30
AIM OF THE PROJECT.....	41
CHAPTER II	43
<i>LISTERIA MONOCYTOGENES</i>	43
2.1 MATERIALS AND METHODS	45
2.1.1 BACTERIAL STRAINS AND CULTURE MEDIA	45
2.1.2 COLD-SMOKED SALMON SAMPLES.....	46
2.1.3 SAMPLES FROM HAM FACTORIES	48
2.1.4 PRIMER DESIGN FOR THE DETECTION OF <i>L. monocytogenes</i>	49
2.1.5 PCR PROTOCOL	50
2.1.6 AGAROSE GEL ELECTROPHORESIS	51
2.1.7 qPCR PROTOCOL.....	51
2.1.8 DNA PROBE FOR OECT (organic electrochemical transistor)	51
2.1.9 DOT BLOT PROTOCOL (ListCapt)	52
2.1.10 ATOMIC FORCE MICROSCOPE	53
2.1.11 OECT ELECTROCHEMICAL BIOSENSOR	54
2.1.12 ELECTROCHEMICAL BIOSENSOR BASED ON VOLTAMMETRY.....	56
2.2 RESULTS AND DISCUSSION	59
2.2.1 COLD-SMOKED SALMON SAMPLES.....	59
2.2.2 HAM SAMPLES	61
2.2.3 PCR.....	64
2.2.4 qPCR.....	66
2.2.5 CaptList DNA PROBE	71
2.2.6 ListE PROBE	83
2.2.7 CONCLUSIONS AND FUTURE PERSPECTIVE.....	90
REFERENCES	91
CHAPTER III	95
<i>CAMPYLOBACTER SPP.</i>	95

3.1 MATERIAL AND METHODS	97
3.1.1 BACTERIAL STRAINS AND CULTURE MEDIA	97
3.1.2 SAMPLES	97
3.1.3 PRIMER DESIGN FOR THE DETECTION OF <i>CAMPYLOBACTER</i>	100
3.1.4 PCR PROTOCOL.....	103
3.1.5 ELECTROPHORESIS	103
3.1.6 qPCR PROTOCOL.....	103
3.1.7 SEQUENCING.....	104
3.1.8 DNA PROBE DESIGN	104
3.1.9 SPECIFICITY TEST FOR CAMPYP3 by DOT BLOT ASSAYS	105
3.1.10 ELECTROCHEMICAL BIOSENSOR BASED ON VOLTAMMETRY	109
3.2 RESULTS AND DISCUSSION.....	113
3.2.1 CHICKEN SAMPLES.....	113
3.2.2 PRIMER CAMPYP FW CAMPYPRW	116
3.2.3 PCR.....	118
3.2.4 qPCR.....	121
3.2.5 CAMPYP3 PROBE	133
3.2.6 DOT BLOT ALKALINE PHOSPHATASE (ALP) ASSAY	135
3.2.7 DOT BLO CHEMILUMINESCENT ASSAY	135
3.2.8 DOT BLOT Si-NPs CHEMILUMINESCENT ASSAY	136
3.2.9 ELECTROCHEMICAL BIOSENSOR	139
REFERENCES	155
CONCLUSIONS AND FUTURE PERSPECTIVE	156

Chapter I

INTRODUCTION

1.1 Foodborne pathogens

Zoonoses are infections or diseases that can be transmitted directly or indirectly between animals and humans.

Food-borne zoonoses are caused, for instance, by consuming contaminated foodstuffs or through contact with infected animals.

The food-borne diseases are a significant and widespread public health threat particularly for very young and elderly people as well as pregnant women, and people susceptible to a weakened immune system (Scallan et al., 2011).

About 246,158 foodborne disease human cases are confirmed with a rate of 64.8 per 100,000 population in the European Union. EFSA (2018) presents the report of confirmed human cases of 14 zoonoses, the majority are caused by *Campylobacter* spp., *Salmonella*, *Yersinia*, *Listeria monocytogenes*, *Escherichia coli*, and *Brucella*. Campylobacteriosis was the most common from 2005, with a higher number of confirmed and hospitalized cases. Instead, the higher number of deaths reported was caused by listeriosis. The real global incidence is difficult to estimate, the real number is likely to be much higher.

Moreover, outbreaks generate billions of dollars in worth of damage, public health problems, and agricultural product losses (Yeni et al., 2016). In Europe, only the cost of public health caused by this disease is 2.4 billion euros per year (EFSA, 2014).

Human pathogens are commonly found in the intestines of healthy food-producing animals. The risks of contamination are present from farm to fork and require prevention and control throughout food analysis. The public health authorities set up strict measures and regulations for food control systems such as hazard analysis critical control point system (HACCP) in order to prevent the spread of these food-borne pathogens at the level of the food processing. HACCP is a method of food safety assurance based on the application of good hygiene practices and identifies control measures necessary in food operations and in hygienic practices (Fortin, 2013). Thus, the detection of foodborne pathogenic bacteria is an important key to the prevention and control of some hazardous points in food processing. Therefore, the food industry needs a new analytical method to monitor food production.

1.2 *Listeria monocytogenes*

Listeria monocytogenes is a facultative intracellular foodborne pathogen that may cause listeriosis following the ingestion of contaminated food. Therefore, this pathogen poses a potential public health problem related to the consumption of contaminated food. The ability of the microorganism to tolerate high concentrations of salt and to survive and multiply at refrigeration temperatures facilitate food contamination (Lorber, 2000).

Both pathogenic and non-pathogenic *Listeria* species are widely dispersed in nature: they can be frequently isolated from soil, flora water and from a variety of cold and warm-blooded animals, including humans (Gray and Killinger, 1966; Weis and Seelinger, 1975).

On the basis of the relatedness of species, *Listeria* spp. were divided into two distinct categories

(Figure 1.1). *Listeria* sensu stricto group includes *L. monocytogenes*, *L. marthii*, *L. innocua*, *L. welshimeri*, *L. ivanovii* and *L. seeligeri*, which share common phenotypic characteristics. *L. grayi* and other newly described 10 species (*Listeria* sensu lato) represent three distinct groups and may warrant recognition as the separate genus (Orsi and Wiedmann, 2016).

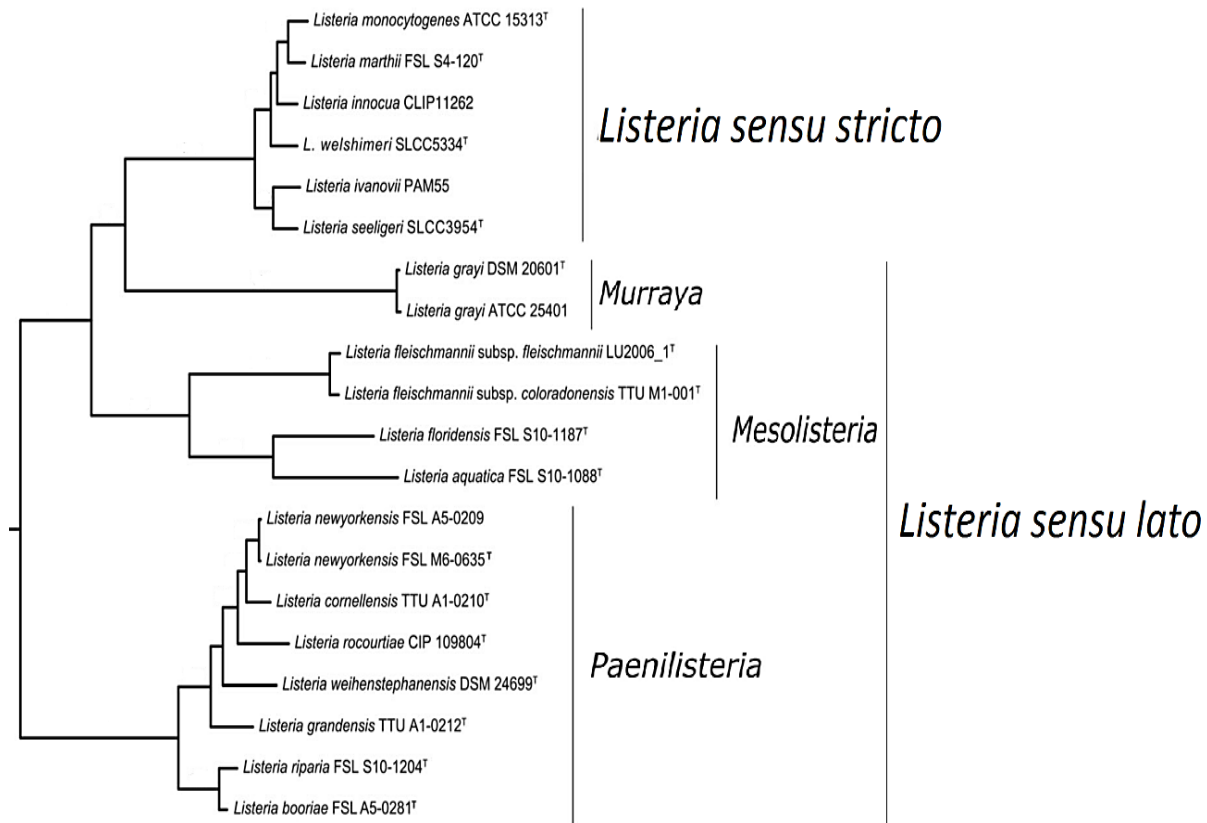


Figure 1.1 Phylogenetic tree of *Listeria* spp. *Listeria sensu stricto* group and *Listeria sensu lato* group (were classified on the basis of the relatedness to *L. monocytogenes*. (Modified from Weller et al., 2015).

1.2.1 LINEAGE AND SEROTYPE

L. monocytogenes currently consists of four evolutionary lineages (Ward et al., 2008). Most of the isolates belong to lineages I and II; lineages III and IV are rare and predominantly isolated from animal sources (Orsi et al., 2011). Among the 13 known serotypes of *L. monocytogenes*, 1/2b, 4b (lineage I), 1/2a and 1/2c (lineage II) are the most commonly involved in cases of human infections. Although serotypes 1/2a, 1/2b and 1/2c are the most frequently isolated from food and environment, more than 95% of infections in humans are caused by serotypes 1/2a, 1/2b, and 4b (Swaminathan et al., 2007; Swaminathan and Gerner-Smidt, 2007; Kathariou, 2002).

1.2.2 MORPHOLOGY AND PHYSIOLOGY

L. monocytogenes (Figure 1.2) is a short, motile, Gram-positive, non-spore forming rod, catalase-positive, oxidase-negative. It is able to grow on relatively simple culture media over a wide range of temperatures, from 1°C to 45°C with optimum growth between 30°C and 37°C (Schuchat et al., 1991). Cells dimensions vary from 0.4 to 0.5 µm in diameter and from 0.5 to 2 µm in length (Seeliger and Höhne, 1979). The organism is facultative anaerobic, with good growth in a 5% CO₂ atmosphere. *L. monocytogenes* is moderately motile at 35 °C by polar flagella. *L. monocytogenes* and *L. ivanovii* are β-hemolytic while other *Listeria* species like *L. innocua* not. This peculiar feature is used to differentiate the β-hemolytic *Listeria* species and to distinguish *L. innocua* from *L. monocytogenes* since these two species give similar results in biochemical tests. Furthermore, *L. monocytogenes* can metabolize L-rhamnose and D-glucose, but not D-xylose and D-mannitol, another distinguishing characteristic among *Listeria* species (Schuchat et al., 1991).

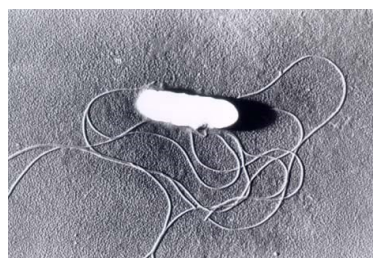


Figure 1.2 *Listeria monocytogenes*. Bureau of Social Welfare and Public Health Tokyo Metropolitan Government (<http://www.fukushihoken.metro.tokyo.jp/>)

1.2.3 LISTERIOSIS

Among the genus *Listeria*, only *L. monocytogenes* and *L. ivanovii* are considered as pathogenic strains to humans and animals, respectively (Whittaker, 2012). Human listeriosis is an atypical foodborne invasive disease: this opportunistic pathogen most frequently affects weak individuals such as pregnant women, neonates, elderly and immuno-compromised individuals (Rocourt et al., 2000). 99% of the infections caused by *L. monocytogenes* are thought to be food-borne (Swaminathan and Gerner-Smidt, 2007). In fact, the disease normally occurs following the ingestion of contaminated food (RTE products, dairy products, meat, fish, vegetables). Close contact with animals is considered a predisposing factor (CDC, 2011). *L. monocytogenes* can cause foodborne outbreaks (epidemic disease) or isolated clinical cases (sporadic disease).

For most people, contact with *L. monocytogenes* results in a transient asymptomatic carrier state (Klein et al., 1991): in fact, an immunologically competent host is sufficient to eliminate pathogens before they can settle in the organism. Conversely, if the host is not able to fight infection, he initially shows gastrointestinal symptoms, which then switch to invasive disease. Meningitis, septicemia, brain abscess, intrauterine and neonatal infections are considered

frequent complications, confirming the pathogen's hematic dissemination from a local area (the gastrointestinal tract) to the central nervous system (CNS). Atypical clinical presentation includes endocarditis, myocarditis, pneumonia, pleuritis, cholecystitis, peritonitis, arthritis, osteomyelitis, sinusitis, otitis, conjunctivitis (Ramana and Mohanty, 2013).

Human listeriosis is clinically characterized in three forms: adult, perinatal and neonatal listeriosis. In pregnant women, listeriosis is more often documented in the third trimester. Premature labor or septic abortion can occur. The infection could be vertically transmitted to the fetus (perinatal listeriosis) in this case a serious form of the disease results in a syndrome known as “granulomatosis infantiseptica”, with a near-100% mortality rate or be acquired by the newborn *post-partum* through a contaminated birth canal (neonatal listeriosis). Neonatal listeriosis results in sepsis or meningitis and occurs several days to weeks after birth; besides *post-partum* acquisition, nosocomial infections can also occur (Klein et al., 1991).

Clinical presentation of listeriosis is influenced by the physiological, pathological and immunological status of the host; his susceptibility mainly depends on cell-mediated immunity (Schuchat et al., 1991). In past, human listeriosis was confined to a selected group of population at risk, including pregnant women, neonates, elderly and immuno-compromised individuals (Papadoulas et al., 2013; Delvallée et al., 2012; Descy et al., 2012; Teodor et al., 2012; Clauss and Lorber, 2008). Other predisposing factors are chemotherapy, immunosuppressive therapy, chronic liver and kidney diseases, metabolic disorders as diabetes mellitus, autoimmune diseases (Papadoulas et al., 2013; McLauchlin and Low, 1994; Farber and Peterkin, 1991). Recently, infections in immunological competent children, invasive infections in the adult population, the occurrence of nosocomial infections and community-acquired meningitis have been reported (Dinic and Stankovic, 2013; Wang et al., 2013; Martins et al., 2010; Brouwer et al., 2006). The profile of human listeriosis has shown a significant change through time: *L. monocytogenes* became a pathogen capable of causing invasive infections not only confined to immunocompromised and debilitated patients but also in immunocompetent individuals (Pron et al., 2001). Then, *L. monocytogenes* colonizes intracellularly the intestinal epithelial cells, before invading lymph nodes and disseminating through blood, first to the liver and then to other organs (Marco et al., 1992).

Virulence factors associated with invasive infections of *Listeria* include hemolysin called listeriolysin O (LLO), phospholipases (PlcA and PlcB) lecithinase, ActA (actin-based intracellular motility) and internalins (InlA and InlB) that facilitate invasion (Vázquez-Boland et al., 2001; Travier et al., 2013).

1.2.4 FOOD SAFETY REGULATION

The high mortality rate of listeriosis has led governments and food safety agencies worldwide to take serious measurements to reduce the occurrence of *L. monocytogenes* in the food production chain (Orsi et al., 2011). European Commission Regulation No. 2073/2005 lays down microbiological criteria for *L. monocytogenes*.

A ready-to-eat (RTE) food product where the levels do not exceed 100 CFU/g is considered to pose a negligible risk for a healthy human population. Therefore, the EU microbiological criterion for *L. monocytogenes* is set as ≤ 100 CFU/g for RTE food products on the market and

the compliance must be ensured for the entire shelf-life.

Special provisions are set for RTE products intended for infants, for special medical purposes and in RTE products able to support the growth of *L. monocytogenes*: the pathogen must not be present in 25 g of sample (EC, 2005).

Regarding the US, since 1980s FDA (Food and Drug Administration) and USDA (US Department of Agriculture) have established a “zero-tolerance” policy for RTE foods: the detectable presence (≥ 1 CFU in 25 g of sample) of *L. monocytogenes* is sufficient for the non-compliance of the product (9 CFR §301.2; 21 Code of Federal Regulations §109.3; Federal Food, Drug, and Cosmetic Act. 402.a, 701.a).

This has great economic consequences for the food industry, due to recalls of the contaminated products and the temporary shutdown of food processing plants (Orsi et al., 2011).

1.2.5 PREVALENCE

Although still being relatively rare, human listeriosis is one of the most severe foodborne diseases under EU surveillance. In vulnerable individuals, such as pregnant women, infants and particularly among the elderly, it causes high morbidity, hospitalization and mortality rates. Listeriosis has the highest proportion of hospitalized cases of all zoonoses under EU surveillance: as in previous years, in 2016 almost all (97%) reported listeriosis cases were hospitalized. Despite the increasing trend since 2008, nowadays the number of human listeriosis cases appears to be stabilizing. In 2016, 28 member states reported 2,480 confirmed cases of human listeriosis. Among them, the 227 fatal listeriosis cases represent the higher number of annual deaths reported since 2007. EU case fatality was 13.8% among the 1,633 confirmed cases with a known outcome. *Listeria* infections were most commonly reported in the age group over 64 years: the proportion of cases and case fatality in elderly people have steadily increased from 2008 (EFSA, 2017).

1.2.6 LISTERIA MONOCYTOGENES IN FOOD

In 2017, EFSA conducted a survey to estimate prevalence levels of *L. monocytogenes* in certain RTE foods at retail coming from 26 different EU member states. They evaluated presence and counts of the organism at the moment of sampling and *L. monocytogenes* occurrences was highest in fish and fishery products (6%), followed by RTE salad (4.2%), RTE meat and meat products (1.8%), soft and semisoft cheese (0.9%), fruit and vegetables (0.6%) and hard cheeses (0.1%)

Although the percentage of non-compliance is fairly low, the presence of *L. monocytogenes* in foods raises concern for public health due to severity and high case fatality of human listeriosis.

1.2.6.1 Cold-smoked salmon

According to recent EFSA reports previously mentioned, RTE fishery products (especially smoked fish) are the food products with a higher prevalence of *L. monocytogenes*. Cold-smoked salmon (CSS) is a slightly preserved RTE seafood typically distributed chilled

after slicing and vacuum packaging. CSS represents a high-risk product as the process does not include a CCP (critical control point) for *L. monocytogenes* hazard. The product is subjected to potential re-contamination after processing and the risk for abusive handling by distributor or consumers is substantial. Moreover, as an RTE product, there is no terminal heat process before consumption. CSS is a highly appreciate food commodity, but careful handling and control measures during process and storage are essential to avoid human infection (Huss et al., 1995).

1.2.6.2 Dry-cured ham

Dry-cured ham is considered a “ready-to-eat” product that does not support the growth of *L. monocytogenes*. For this reason in Europe, it is regulated with EEC Reg. 2073/05. As previously mentioned, this regulation sets up a limit of 100 *L. monocytogenes*/ g. Dry-cured ham production technology blocks the development of any pathogen derived from raw meat or the environment (Grisenti et al., 2004). Yet, *L. monocytogenes* can be found in dry-cured ham if accidentally introduced during the deboning or slicing phases. However, ham producers have implemented severe measures which resulted in a significant reduction (below 0.2%) of the presence of *L. monocytogenes* during all phases of the production process. Therefore, it is very important to emphasize that no cases of listeriosis have been reported in people who have eaten dry-cured ham.

1.2.7 CULTURE METHODS FOR *L. MONOCYTOGENES*

1.2.7.1 Gold standard method: ISO 11290-1:2004

In 1996 the ISO method 11290 was published (then amended in 2004): “Microbiology of food and animal feeding stuffs - Horizontal method for the detection and enumeration of *Listeria monocytogenes*”. The method is divided into two parts, the first for the detection (ISO, 2004a) and the second for the enumeration (ISO, 2004b) of *L. monocytogenes* in food and feed. The standard protocol consists of a primary and a secondary enrichment of 24 hours each in broth selective media, which are half-Fraser broth and Fraser broth respectively. The culture is then plated on differential selective media, ALOA as first choice medium and either Oxford or PALCAM agar as a second choice medium. After 24-48 hours, plates are examined for the presence of characteristics colonies which are presumed to be *Listeria* spp. Confirmation of the presence of *L. monocytogenes* is achieved by means of appropriate morphological, physiological and biochemical tests carried out on five presumptive colonies. The scheme is reported in Figure 1.3.

1.2.7.2 *Listeria* Precis™ Method

The *Listeria* Precis™ Method, an easy method for the detection of *Listeria monocytogenes* in food samples, represents an alternative to the classic ISO 11290-1:1996 (amended 2004). It has been validated and approved by AFNOR in 2013 (NF Validation, 2013). This method utilizes a single enrichment step and the use of a single selective medium. For the enrichment step, the selective broth ONE™ Broth-*Listeria* is used. This medium provides the nutrients for the

revitalization and optimal growth of *Listeria* spp. while inhibiting the potential competitors. After the incubation at 30°C for 24 hours, 10 µL of the broth is spread on Brilliance™ *Listeria* agar base, a selective medium that allows the differentiation of *Listeria* spp. by the evaluation of specific enzymes activity. The β-glucosidase common to all *Listeria* spp. reacts with the chromogen X-glucosidase present in the medium and leads to the formation of green-blue colonies. *Listeria monocytogenes* and *Listeria ivanovii* have a specific enzyme, the lecithinase, that catalyzes the hydrolysis of lecithin present in the culture medium inducing the production of an opaque halo around the colonies. Finally, the presumptive colonies grown onto agar plates are tested for confirmation with the classic ISO confirmation test (Haemolysis test, carbohydrate test, CAMP test) or with the O.B.I.S mono test (Oxoid, Milan, Italy) validated method, a colorimetric assessment that evaluates the D-alanyl-aminopeptidase activity. This enzyme reacts with the D-alanyl-7-amido-4-methylcoumarin substrate with the formation of dimethylamino-cinnamaldehyde a violet color compound. All *Listeria* spp. but not *L. monocytogenes* have this enzyme, thus colonies tested and not producing a color change are considered *Listeria monocytogenes*. The scheme is reported in Figure 1.3.

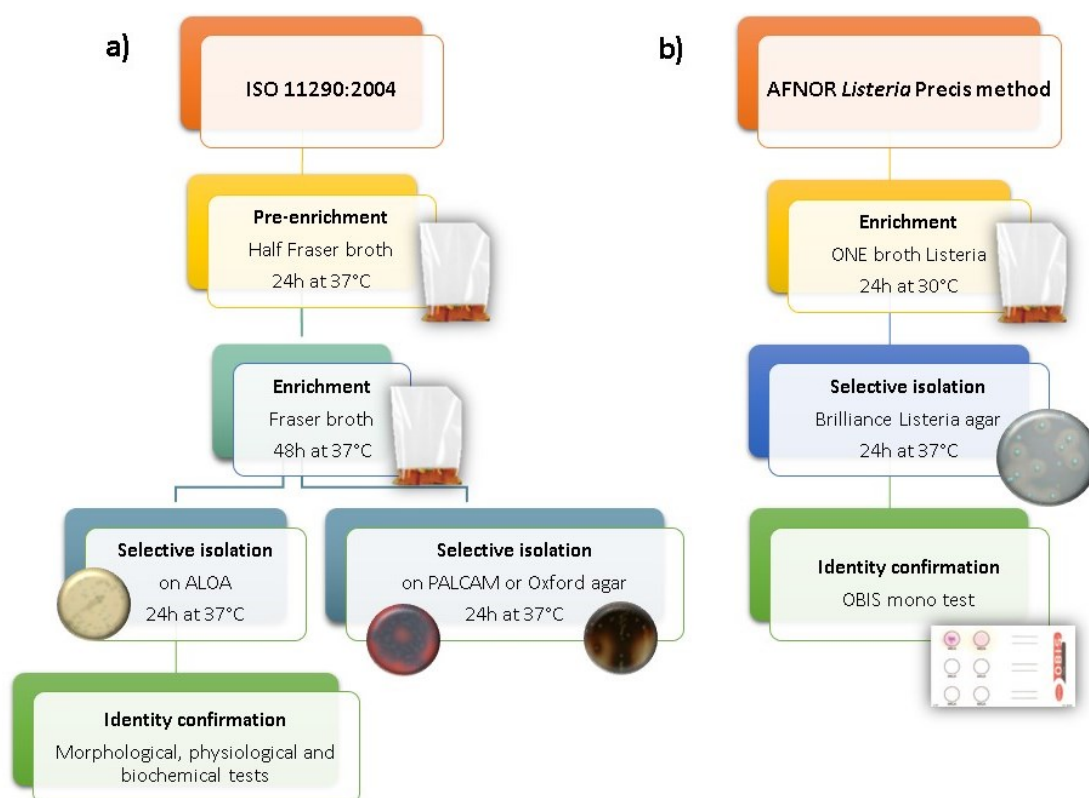


Figure 1.3 a) Standard ISO method 112290:1-2004; b) Listeria Precis™ method for the detection and isolation of *L. monocytogenes*.

1.3 *Campylobacter* spp.

1.3.1 MORPHOLOGY AND PHYSIOLOGY

Campylobacter is a Gram-negative bacterium belonging to the Campylobacteraceae family, is well known worldwide to be a pathogen causing gastroenteritis in humans. This spiral and small microorganism (0.2-0.8 μm x 0.5-5 μm) is oxidase positive and has a movement defined as “corkscrew”, with a single flagellum present at one or both ends of the cell (Silva et al., 2011). There are, however, two exceptions: *Campylobacter gracilis*, which is not motile, and *Campylobacter showae*, which has multiple flagella (Bolton, 2015). Different species of *Campylobacter* are able to grow at temperatures between 37°C and 42°C, with an optimum temperature of 41.5°C (Silva et al., 2011), under microaerophilic conditions, characterized by a very low level of oxygen. Being so sensitive to temperature, it can then be easily eliminated through heat treatments.

1.3.2 CAMPYLOBACTERIOSIS

Campylobacter is a pathogen capable of proliferating both in animals, especially poultry, and in humans, although with similar but not identical invasion mechanisms. In poultry, in fact, the first site of colonization is the caecum, where it can reach 10^6 – 10^8 CFU/g (Meade et al., 2009). In humans, however, the infection mainly occurs in the small intestine (Bolton, 2015). The virulence factors with which this micro-organism colonizes the host are flagella-mediated motility, bacterial adherence to the intestinal mucosa, invasive ability and toxins production (Van Vliet and Ketley, 2001; Asakura et al., 2007; Dasti et al., 2010). The flagella are essential for the colonization of the small intestine, after which the pathogen moves towards the target organ: the colon (Van Vliet and Ketley, 2001; Poly and Guerry, 2008). It is also thought that these have a second function related to the secretion of non-flagellated proteins during the invasion of the host (Poly and Guerry, 2008). Another fundamental requirement is the adherence to gastrointestinal epithelial cells, mediated by several adhesins on the bacterial surface (Jin et al., 2001). Invasion, the cause of inflammation of cells, on the other hand, is probably the result of the production of cytotoxins, followed by a reduction in the absorption capability of the intestine (Van Deun et al., 2007). In particular, the toxin CDT (Cytotoxin Distending Toxin) causes the stopping of eukaryotic cells in the G2/M phase of the cell cycle, preventing them from entering mitosis and consequently leading to the death of the cell itself (Yamasaki et al., 2006; Ge et al., 2008; Zilbauer et al., 2008). It is also thought that the capability of *Campylobacter* spp. to reach the intestinal tract is due to resistance to gastric acids and bile salts (Van Deun et al., 2007). *Campylobacter jejuni* and *Campylobacter coli* found in the gastrointestinal tract of several animal species (Epps et al., 2013), account for about 90% of all bacterial *Campylobacter* diagnosed in humans in the EU (Bolton, 2015; EFSA, 2014). In addition to these species, *C. upsaliensis*, *C. lari* and *C. fetus* are also responsible for this pathogenicity. This disease, with an incubation period of 1 to 5 days, is self-limiting

gastroenteritis that lasts 5 to 7 days and is characterized by aqueous diarrhea, sometimes blood, fever, abdominal cramps and vomiting (Skarp et al., 2016). In some sporadic cases, *Campylobacter* can also be the precursor to serious illnesses, such as Guillain-Barré syndrome and Miller-Fisher syndrome, a form of chronic and potentially fatal paralysis (EFSA, 2011). *Campylobacter* spp. colonizes the last gastrointestinal tract, consisting of ileus, caecum, and colon, without any symptoms. The manifestation of the disease depends on the host's immune status and the virulence characteristics of the *Campylobacter* strain encountered (Bolton, 2015).

1.3.3 FOOD SAFETY REGULATION

European Commission Regulation No. 2073/2005 which establishes microbiological criteria for specific food categories was amended with the commission regulation (EU) 2017/1495 that added carcasses of broilers as a new food category and introduced a hygiene criterion process for *Campylobacter*. This modification was based on the scientific opinion published on EFSA 2010, 2011 and 2012 on a public health hazard and risk from the consumption of broiler meat which identifies *Campylobacter* as of high public health relevance. Thus, the criteria for *Campylobacter* spp. are set as ≤ 1000 CFU/g in the carcass of broiler after chilling.

Instead, EU Regulation No. 2073/2005 for the food products on the market lays down microbial criteria for the pathogen that must be absent in 25 g of sample.

1.3.4 PREVALENCE

Since 2005, *Campylobacter* spp. has continued to be the most commonly reported gastrointestinal disease bacterium in humans in the European Union, with a number of cases of human campylobacteriosis of 246,158 (EFSA, 2017). Despite the high number of human campylobacteriosis cases, their severity in reported case fatality was low (0.04%), even though this was the third most common cause of mortality among the pathogens considered. Between 2013 and 2017 there was a clear seasonality in the number of confirmed campylobacteriosis cases reported with a peak in the summer months.

The report EFSA 2017 showed that for 54.1% of confirmed cases of campylobacteriosis in the EU, species were also provided: 84.4 % *C. jejuni*, 9.2 % *C. coli*, 0.1 % *C. lari*, 0.1 % *C. upsaliensis* and 0.1% *C. fetus*.

1.3.5 CAMPYLOBACTER IN FOOD

Campylobacteriosis occurs after eating contaminated food. The minor source is milk and milk products including cheese with an occurrence lower than 2%. Instead, the occurrence of *Campylobacter* in fresh meat is still high, 37.4% for broiler and 31.5% for turkey meat. The *Campylobacter* major species identified from fresh meat and meat products from broiler are for the 73% *C. jejuni* and for 26.3% for *C. coli*. Only one strain was reported as *C. lari*. From fresh meat and meat product from turkeys 60% were *C. jejuni* and 40% were *C. coli*. For milk products, *C. jejuni* was mostly reported (95%) followed by *C. coli*. (EFSA, 2017).

1.3.5.1 The major source of *Campylobacter*: chicken meat

Studies have shown that chickens (*Gallus gallus*) are the main source of campylobacteriosis for humans: the consumption of poultry meat is considered the most common route for human infection (Oh et al., 2015; Prachantasena et al., 2016; Young et al., 2007). *Campylobacter* spp. colonizes the caecum mucosa in these animals, which becomes the first site of infection by 24 h (Coward et al., 2008). However, this colonization does not cause diseases, nor changes in the intestinal mucosa (Meade et al., 2009), which is why the micro-organism is difficult to detect at the production level.

The chicken production and consumption chain consist of primary production, transport to the slaughterhouse, slaughter and subsequent processing of meat products, retail sale and consumption thereof. Each of these steps, although the first three, in particular, has a role to play in the transmission of *Campylobacter* spp. (Skarp et al., 2016) at the level of primary production, the risk factors are different, such as season, age of poultry, use of extended breeding, non-drinking water supply and use of antimicrobials (EFSA, 2011).

In fact, chickens at the farm are *Campylobacter*-negative for the first three weeks of life, and only after this period, there is an increase in the prevalence of contaminated animals. However, in poultry over 8 to 9 weeks of age, the presence of positive samples is subsequently observed (EFSA, 2011). The problem, in this case, is that animals of different ages are often present on farms, increasing the likelihood of cross-contamination. The use of non-chlorinated water, for example from wells, a possible *Campylobacter* reservoir, may also increase the possibility of infections of poultry (EFSA, 2011). In the end, the use of antimicrobials tends to induce antibiotic resistance in bacteria susceptible to antibiotics, which will proliferate in the matrix (EFSA, 2011). In the transport phase to the slaughterhouse, the main risk lies in the plastic crates used, which often cause cross-contamination (Allen et al., 2008a; 2008b 2008c Slader et al., 2002) and in the actual act of catching and positioning animals within them (Slader et al., 2002). During slaughter, as some authors suggest, the critical phases are plowing and evisceration (Gruntar et al., 2015; Johnsen et al., 2006; Sasaki et al., 2013). In a study reported by García-Sánchez et al., (2017), 90 *Campylobacter* spp. were isolated after cleaning and disinfection. (37.8%), 61 of which are in machinery for flushing and evisceration.

1.3.6 GOLD STANDARD METHOD: ISO 10272

The ISO standard method 10272- 1: 2006 for the detection of *Campylobacter* spp. recently replaced by the first edition, ISO 10272-1:2017 (Anonymous, 2017a; Anonymous, 2017b) was not optimal for the detection in several food matrices with different background flora. Therefore the following main changes were proposed: the detection method was extended to include the option of a second enrichment broth (Preston broth); the detection method was extended to include the option of direct plating on mCCDA; the note on the use of closed containers with reduced headspace as an alternative to incubation in a microaerobic atmosphere was deleted; the confirmation tests on study of microaerobic growth at 25 °C and aerobic growth at 41.5 °C were replaced by the study of aerobic growth at 25 °C. As described in the study of Biesta - Petters et al. (2018), with the retelling ISO 10272-1:2017 standard method, three detection procedures exist that enable to treat different matrices depending on the estimated level of

Campylobacter spp. and background flora. From the result of this study, the new method is able to detect *Campylobacter* spp. from different matrices as frozen spinach, minced meat, chicken skin, raw milk, broiler caecum material. The choice of an appropriate enrichment broth and a selective plating medium is an important step. Bolton broth (BB) is able to resuscitation of the *Campylobacter* spp. in comparison to Preston Broth, but several studies showed antibiotics that it is not selective (Moran et al., 2011). This enrichment broth contains several antibiotics such as Cefoperazone, Cycloheximide, Vancomycin, and Trimethoprim. Cefoperazone is an antibiotic belonging to the group of third-generation cephalosporins, and the β -lactam ring in this antibiotic is easily hydrolyzed by extended-spectrum beta-lactamase (ESBL) producing bacteria, making them insensitive to the selective compound. Bacterial groups known to produce ESBLs are Gram-negative and include Enterobacteriaceae such as *Escherichia coli*, *Klebsiella pneumoniae*, *Pseudomonas aeruginosa*, *Proteus mirabilis*, *Salmonella enterica*, *Enterobacter aerogenes*, *Enterobacter cloacae*, etc. Microorganisms can found in the flora of chicken meat. Therefore, the isolation of *Campylobacter* spp. is a problem involving underestimation. The growing of the ESBL bacteria, in particular, *E. coli* (Jasson et al., 2009 and Depoorter et al., 2012) causes a decrement of *Campylobacter* spp. from 8 Log₁₀ CFU / mL to 4–6 Log₁₀ CFU/ mL as shown in the study of Hazeleger (2017).

Recently, many studies were conducted to find a new way to improve the enrichment broth's selectivity. For example, testing a new broth like CampyFood broth (Biomérieux), but it hasn't the same capability in comparison to Bolton and Preston Broths (Habib et al., 2011).

Choon et al. (2013, 2017 and 2018) modified the BB using several antibiotics: bacteriological charcoal and polymyxin B; Rifampicin and Tazobactam. The results obtained clearly demonstrated the advantage to inhibit the non-*Campylobacter* spp. with a decrement from 72.5% to 20%, from 100% to 6.9% and from 80% to 0% respectively. The improvement in *Campylobacter* spp. isolation is reported as an increment from 0 to 75.9% and from 15% to 38.8% respectively. Instead, Hazeleger et al. (2017) tested the addition of clavulanic acid in BB showed inhibition of the ESBL *E. coli*, the same obtained with Preston broth. The 11272:1-2017 ISO standard method, furthermore, recommends the utilization of mCCDA in combination with other selective media at choice. Also, in this case, the antibiotics component is cefoperazone, therefore the selectivity problem persists and the researcher tested to restore the selectivity of mCCDA adding antibiotics. Researchers tested the tazobactam (Smith et al., 2015), Potassium-clavulanate-supplemented (Choon et al., 2014) shown an improvement of the selectivity. However, another possibility is the utilization of another selective medium not recommended by ISO 10272, the selective chromogenic medium RAPID *Campylobacter* agar (Bio-Rad) tested by Seliwiorstow et al. (2015) or Brilliance *CampyCount* (BCC) and *Campy FoodAgar* (CFA) tested by Habib et al. (2011). In both cases, they showed a higher recovery of *Campylobacter* in comparison to mCCDA.

1.4 BIOSENSOR

A biosensor (Figure 1.4) is an analytical device that convert target analyte concentration into an electric signal, through a biological recognition system (enzymes, antibodies, oligonucleotides, organelles, cells or tissues) integrated or intimately associated with a suitable transducer (Lowe and Goldfinch, 1983), that can be electrochemical, optical, acoustic, thermic or magnetic.

The fundamental distinguishing feature of a biosensor is the biological recognition system for the target analyte since it determines both sensitivity and selectivity. There are different possible biological recognition systems:

Biocatalytic systems: enzymes, organelles, whole cells, tissue slices;

Affinity binding systems: antibodies and antigen-binding elements (immunosensors), DNA or RNA oligonucleotides probes (genosensors);

Synthetic biomimetic systems: molecularly imprinted polymers or aptamers.

The choice of the system to use relies on the nature of the target analyte to detect, its concentration and the presence of interfering substances. After the binding of the target analyte to the biological recognition system, the signal produced by the formed bond is converted to an electric signal.

A transducer is a device that can convert a wide range of physical, chemical or biological effects into an electric signal with high sensitivity (Lowe, 2007). Different technologies can be employed for the transducers: electrochemical, optical, acoustic, thermal or magnetic.

Biosensors offer several advantages, such as small size, low cost, selectivity, fast measurements, possible direct application on-field or remote control. Despite a great number of publications on the food application of biosensors, only a few systems are commercially available and the majority of existing biosensors on the market are based on enzymes (Schnerr, 2007). Research efforts are mainly focused on clinical applications, the most successful hand-held biosensor to date is the blood glucose monitor for diabetic patients.

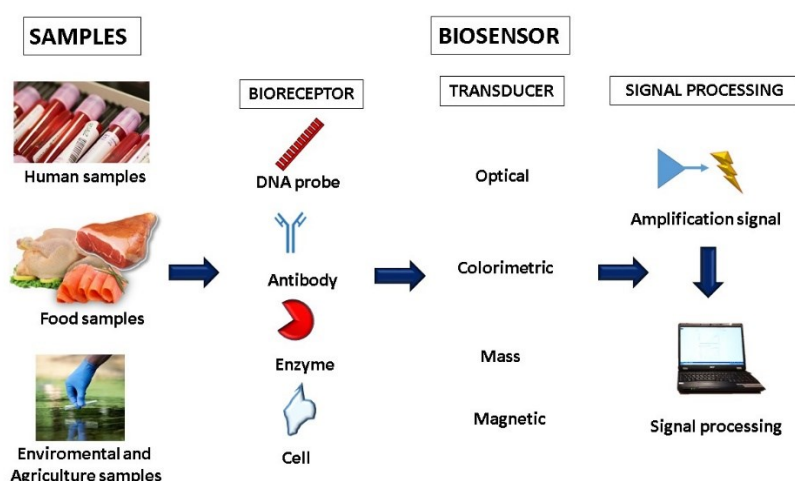


Figure 1.4 Elements of a biosensor. The biological recognition element binds the target analyte. Then the transducer converts the signal producing a detectable electric response proportional to the concentration of the analyte that is processed by a software.

1.4.1 ELECTROCHEMICAL BIOSENSOR

IUPAC defines an electrochemical biosensor as “a self-contained integrated device, which is capable of providing specific quantitative or semi-quantitative analytical information using a biological recognition element (biochemical receptor) which is retained in direct spatial contact with an electrochemical transduction element” (Thévenot et al., 2001). Biosensors based on electrochemical transducers are the most common and frequently cited in the literature (Lowe, 2007), they exhibit high sensitivity, rapidity of response, simplicity, low cost. Biomolecules are immobilized onto the chemically modified electrode (CME), constituted of electronic conducting, semiconducting or ionic materials. Electrochemical detection monitors changes of an electrical signal caused by an electrochemical reaction at an electrode surface, usually resulting from an imposed current or potential. Electrochemical methods include:

- Voltammetric detection: measurement of current resulting from the application of potential in a three-electrode (reference, auxiliary, working) electrochemical cell;
- Amperometric detection: measurement of a change of current occurring when an oxidizing or reducing potential is applied;
- Potentiometric detection: measurement of the potential difference between two electrodes without the application of current and a local equilibrium is established;
- Conductometric detection: measurement of changes in conductance due to the migration of ions when different frequencies are applied (Arya et al., 2007).

For the electrochemical detection of DNA, most biosensors use specific redox indicators (cationic metal complexes or intercalating organic compounds) that are captured following the hybridization and emit a signal (Bifulco et al., 2013; Sun et al., 2012; Steel et al., 1998). It is possible to directly detect the probe-target DNA hybrid, with potential advantages of simplicity and rapid detection using Label-free approaches which rely on the direct detection of the intrinsic electroactivity of DNA (Paleček, 1996), on oxidation of purine bases (particularly guanine) or on changes in some of the interfacial properties after hybridization (Lin et al., 2011; Wang et al., 2001; Wang et al., 1998).

1.4.2 THIOL-GOLD DNA INTERACTION

The immobilization effect of ssDNA probes on the electrode surface has a great influence on its performances, such as sensitivity, selectivity, accuracy, reproducibility and lifetime. Different methods have been described for the immobilization of ssDNA, including affinity binding, covalent attachment, adsorption and self-assembling (Sun et al., 2012). A well-known technique for a stable ssDNA probe immobilization is the chemisorption of thiol-modified oligonucleotides onto gold surfaces (Marie et al., 2002). Gold is a very useful solid substrate for biosensor electrodes: it has high conductivity, it is biocompatible and chemically inert. In order to bind the gold surface, the oligonucleotides need to be modified with functional groups that can strongly interact with gold.

The Thiol group is the most widely used for DNA-gold linkages (Li et al., 2010). Thiol groups can be introduced in a biological macromolecule, as an ssDNA probe, by appropriate modification. Thiol-gold chemistry was introduced by Nuzzo and Allara (1983) and ten years

later it was adapted to develop a procedure for binding DNA via thiolate bonds to gold surfaces (Rabke-Clemmer et al., 1994; Hegner et al., 1993). In 1997, Herne and Tarlov reported that thiol-ssDNA probes on gold surfaces are capable of hybridization with complementary DNA, showing high hybridization efficiencies. The authors also observed that DNA probes are adsorbed on the surface primarily through the sulfur atom of the thiol group, with few if any direct interactions between nitrogen-containing nucleotide side chains and gold surface. Au thiolates are known to be quite stable (Hegner et al., 1993).

Recently, Xue et al. (2014) reported the strength of the gold–sulphur (Au–S) interaction formed between thiols and gold surfaces: the strength of single bonds is strongly affected by the properties of the gold surface, the solution pH and the interacting time. Their results show that the *in situ* formation of the Au–S covalent bond requires a minimal interaction time of around 3.0 s. Focusing on the rupture mechanism of Au–S interaction, the authors also found that thiolate-bound gold atoms could be extracted from the gold surface leading to the breakage of Au–Au bonds near the Au–S binding sites.

Electrochemical biosensors for DNA detection and quantitation based on thiol-DNA probes immobilized onto gold have been described by several authors (Radish et al., 2017; Bifulco et al., 2013; Sun et al., 2012; Lin et al., 2011; Hu et al., 2008; Kang et al., 2007; Steel et al., 1998).

1.4.3 OECT: ORGANIC ELECTROCHEMICAL TRANSISTOR

Transistors work as signal amplifiers, as they take advantage of the properties of semiconductor materials, in fact, they produce a greater output signal compared to the input signal. A biosensor based on a transistor is obtained by the combination of a sensor and an amplifier. A small potential change at an interface induces a substantial variation in the channel current. These devices are highly sensitive, low cost and can be miniaturized or fabricated on various kind of substrates, easy to fabricate, flexible and biocompatible, as they operate at low voltage

(Gentile et al., 2014; Lin et al., 2011).

The signal is amplified through an electrolytic solution, which combines semiconducting properties to the characteristics of the ion transport. Semiconductors materials have a conductivity between conductor and insulator, they can be doped, positively (p-type) or negatively (n-type) based on the nature of the compound introduced as impurity, to increase the number of charge carrier (Skoog et al., 2009).

Organic electrochemical transistors (OECT) first described by Kittlesen et al. in 1984, have a gate voltage applied through an electrolyte, and the conductivity of an organic semiconductor modulated by the motion of ions between the electrolyte and the organic film (Bernards and Malliaras, 2007). An OECT (Figure 1.5) consists of a channel made of an organic p-type semiconductor with source and drain contacts and a gate electrode (gold, silver or platinum). The components are immersed into an electrolytic solution (Bernards et al., 2008). A current (ISD) is generated between drain and source by the application of voltage (VSD). The current drives holes along the polymer backbone and ionic interchange between electrolyte and polymer may take place. The application of a positive gate voltage (VG) induces a de-doping mechanism in the semiconductor, which changes the carrier concentration: cations from the electrolyte are injected into the semiconductor and each injected cation compensates one

acceptor leading to the source-drain current (I_{SD}) decrease.

An OEET was used for electrochemical label-free DNA sensing by Lin et al. (2011). They immobilized an ssDNA probe onto the gate electrode.

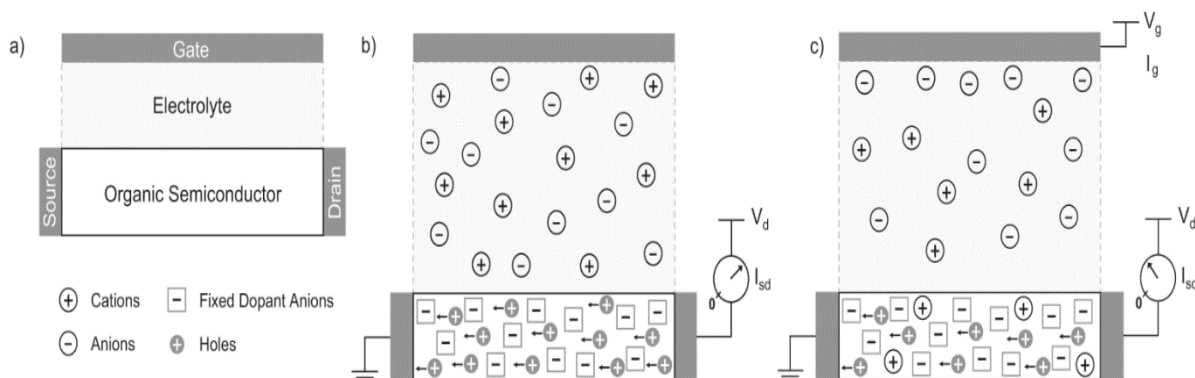


Figure 1.5 Qualitative representation of OEET behaviour (modified from Bernards and Malliaras, 2007).
a) OEET component; **b)** OEET without gate voltage applied: current is determined by the intrinsic conductance of the organic semiconductor; **c)** OEET with gate voltage applied: current is determined by the extent to which the organic semiconductor is de-doped.

One of the most used polymers for the OEET channel is PEDOT: PSS [poly(3,4-ethylenedioxythiophene) polystyrene sulfonate], a p-type doped polymer (Figure 1.6) highly sensitive to ionic species in solution, economic, stable and commercially available. PEDOT: PSS can be deposited in a thin layer on various substrates including plastic or textile inert fibers (Gentile et al., 2014).

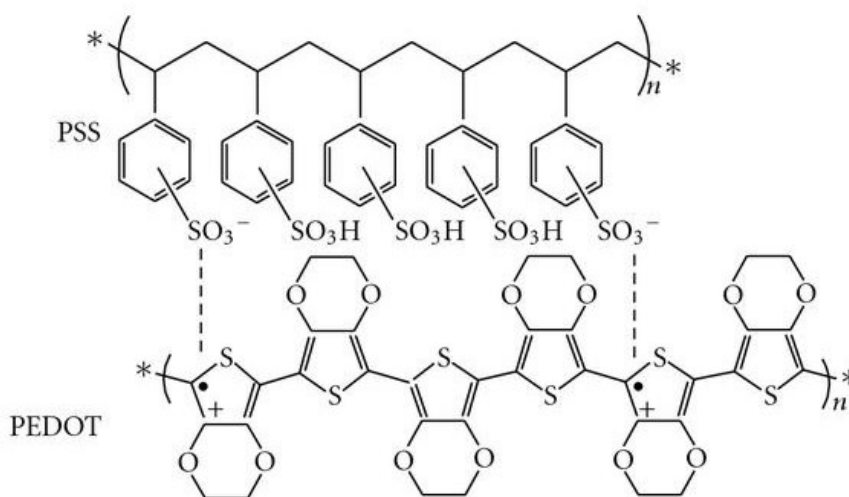


Figure 1.6 Chemical structure of PEDOT: PSS (<http://nanotechweb.org>).

1.4.4 ELECTROCHEMICAL BIOSENSOR BASED ON VOLTAMMETRY

1.4.4.1 Screen-printed electrodes

Often, electrochemical biosensors use screen printed electrodes (SPEs) (Figure 1.7) as electrochemical platform. SPEs are printed electrochemical circuits, which are commonly used for the analysis of small volume liquid samples. They consist of solid or flexible support made by a non-conductive material such as plastic or ceramic on which are printed three different electrodes: a working electrode (WE), a counter electrode (CE) and a reference electrode (RE). WE and CE can be made with gold, carbon, platinum or other metal pastes while the RE is an Ag or Ag/AgCl electrode (Mistry et al., 2014; Contreras-Naranjo et al., 2019).

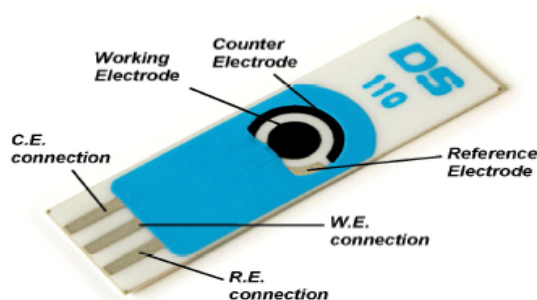


Figure 1.7 Example of Screen-Printed Electrodes.

1.4.4.2 Cyclic Voltammetry and Differential Pulse Voltammetry

Voltammetry is an electroanalytical technique widely used to study redox couples. The voltage waveform applied to the working electrode in the cyclic voltammetry (CV) is shown in Figure 1.8.

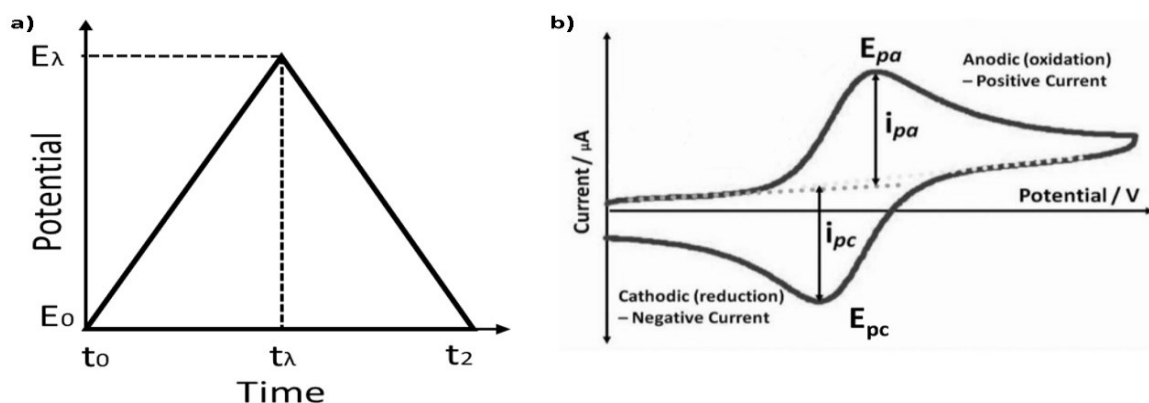


Figure 1.8 a) Cyclic voltammetry waveform. b) Typical cyclic voltammogram where i_{pa} and i_{pc} show the peak anodic and cathodic current respectively for a reversible reaction. (<https://www.slideshare.net/AfrinNirfa1/cyclic-voltammetry>).

As before t_λ , the electrode potential changes linearly with time, while at t_λ the potential scan direction reverses. Figure 1.8 shows that switching potential E_λ is both the final potential for the forward scan and the initial potential for the reverse sweep. Consequently, the potential applied to the working electrode in the forward scan is described by the following equation (eq.1):

$$(eq.1) \quad E_t = E_{in} \pm vt$$

E_t : potential at t time (V)

E_0 : starting potential (V)

v : scan rate (V/s)

t : time (s)

When this triangular waveform is adopted to investigate electrochemical processes involving a redox couple in which both partners are stable during the time required to record a voltammogram (Gau et al., 2005), the electrode reaction occurring in the backward scan involves the species electrogenerated in the forward sweep still present in the solution layer surrounding the electrode surface. When CV is performed on reversible redox couples such as ferrocyanide/ferricyanide the potential difference between the forward and the backward peaks is given by the following equation (eq.2):

$$(eq.2) \quad \Delta E_p = E_{pa}(for) - E_{pc}(back) = \pm 0.057/n$$

ΔE_p : potential different between forward and reverse

$E_{pa}(for)$: forward peak potential

$E_{pc}(back)$: backward peak potential

n : the overall number of electrons involves in change transfer

That points out that anodic-cathodic responses are symmetrical in shape with respect to $E_{1/2}$, which is essentially coincident with the standard potential (E°).

Peak currents displayed by a reversible couple are given in equation (eq. 3):

$$(eq.3) \quad i_p = 2.688 \times 10^8 n^{\frac{3}{2}} * A * D^{1/2} * v^{1/2} * C$$

2.688×10^8 : constant

n : the overall number of electrons involves in change transfer

A : electrode area (cm^2)

D : diffusion coefficient of analyzed species (cm^2/s)

ν : scan rate (V/s)

C: bulk concentration of electroactive analyzed species (mol/L)

This equation 3 points out that i_p depends linearly on both the analyte concentration (C) and the square root of both scan rate (ν) and diffusion coefficient (D). The linear dependence of i_p on C is the basis of the application of CV to quantitative analysis. There are various pulse techniques; normal pulse voltammetry (NPV), differential pulse voltammetry (DPV) and square wave voltammetry (SWV). This offers the common advantage of allowing higher faradic currents to be recorded with respect to CV while interfering capacitive currents are concomitantly minimized. In DPV potential pulses are applied with a constant frequency to electrodes and the current is recorded just before both the pulse end and the pulse starting. The shape of current-potential curves recorded by DPV is peak-shaped as can be seen in Figure 1.9.

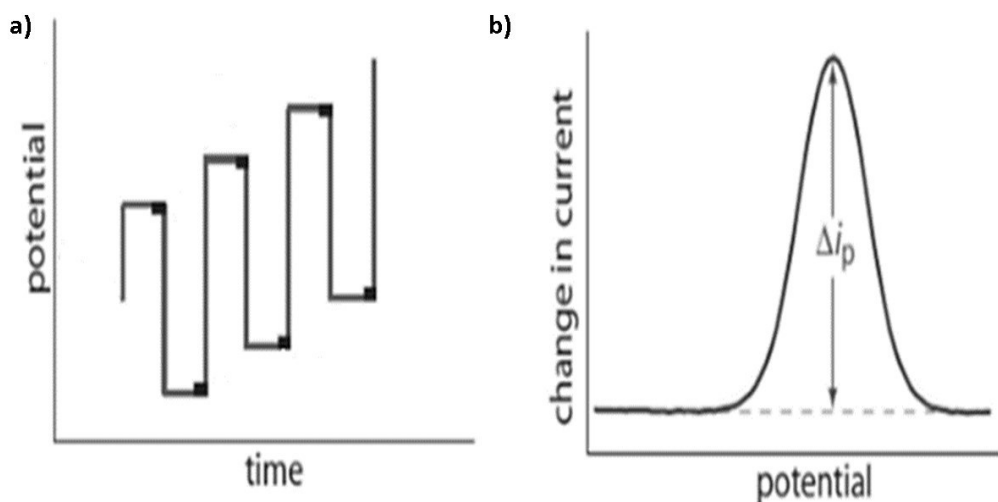


Figure 1.9 a) Differential pulse voltammetry waveform. b) Typical differential pulse voltammogram.

The most important advantage offered by DPV over CV is the increased sensitivity which leads to lower detection limits. Ferrocyanide/ferricyanide is a reversible and mono electronic system commonly adopted as a redox reference couple, often used for label-free detection in electrochemical biosensors (Settingington et al., 2012; García et al., 2012; Yan et al., 2017). In this work, this system is used to monitor changes of the electrode-solution interface due to the interaction between the ListE DNA probe and the targets as shown in Figure 1.10.

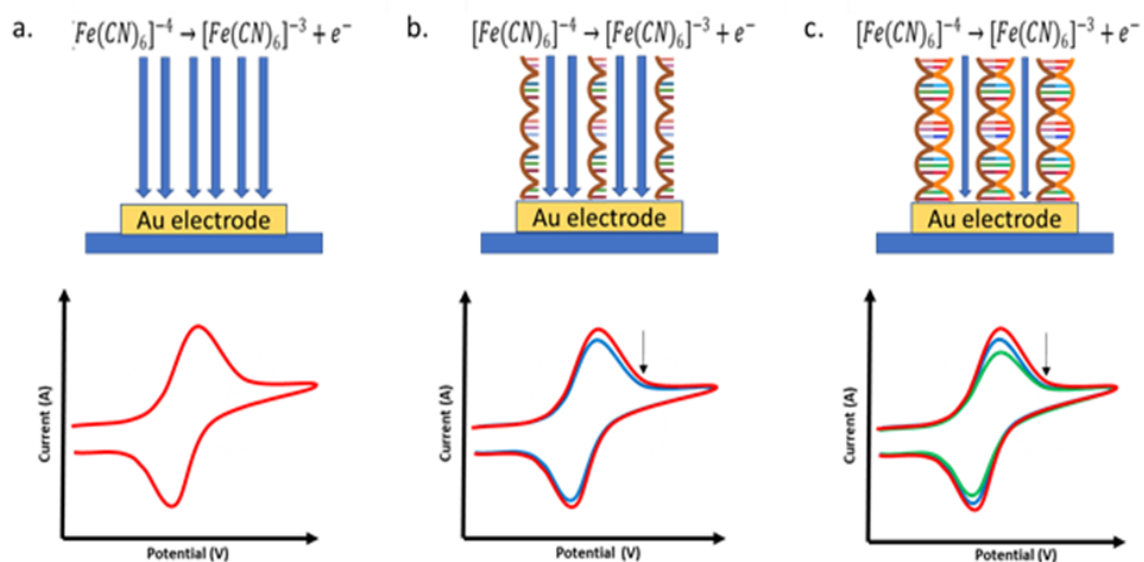


Figure 1.10 Several functionalization steps. a) Gold bare electrode b) Probe immobilization c) DNA hybridization (Braidot, 2019).

According to the process described above the ferrocyanide oxidation current recorded by CV or DPV should decrease with increasing the amount of target DNA hybridized with the capture probe on the electrode surface. In agreement with the equation (eq.3) previously reported the current decrease may be ascribed to a reduced electrode surface available to ferrocyanide for the charge transfer or to a lower diffusion coefficient due to the increase of steric hindrance caused by the hybridized target DNA. The difference between anodic peak current recorded by CV and DPV at the functionalized ListE electrode after DNA target hybridization (ipa Sample) and the anodic peak current recorded at the functionalized ListE electrode (ipa Blank) represent the analytical signal useful to evaluate the assay performance.

REFERENCES

- Allen V., Burton C., Wilkinson D., Whyte R, Harris J., Howell M., Tinker D. (2008a).Evaluation of the performance of different cleaning treatments in reducing microbial contamination of poultry transport crates. *Br Poult Sci.*, 49(3):233-40.
- Allen V.M., Weaver H., Ridley A.M., Harris J.A., Sharma M., Emery J., Sparks N., Lewis M., Edge S. (2008b). Sources and spread of thermophilic *Campylobacter* spp. during partial depopulation of broiler chicken flocks. *J Food Prot.*, 71(2):264-70.
- Allen V.M., Whyte R.T., Burton C.H., Harris J.A., Lovell R.D., Atterbury R.J., Tinker D.B. (2008c).Effect of ultrasonic treatment during cleaning on the microbiological condition of poultry transport crates. *Br Poult Sci.*, 49(4):423-8.
- Anonymous. (2017a). EN ISO 10272-1:2017 - Microbiology of the Food Chain - Horizontal Method for Detection and Enumeration of *Campylobacter* spp. - Part 1: Detection method. International Organization for Standardization, Geneva.
- Anonymous. (2017b). EN ISO 10272-2:2017 - Microbiology of the Food Chain - Horizontal Method for Detection and Enumeration of *Campylobacter* spp. - Part 2: Colony-count technique. International Organization for Standardization, Geneva.
- Arya S.K., Singh S.P., Malhotra B.D. (2007). Electrochemical techniques in biosensors. In: Marks R.S., Cullen D.C., Karube I., Lowe C.R., Weetall H.H. (eds.), *Handbook of Biosensors and Biochips* (vol. 1, pp. 341-375). Hoboken (NJ): John Wiley & Sons, Inc.
- Asakura M., Samosornsuk W., Taguchi M., Kobayashi K., Misawa N., Kusumoto M., Nishimura K., Matsuhisa A., Yamasaki S.(2007). Comparative analysis of cytolethal distending toxin (cdt) genes among *Campylobacter jejuni*, *C. coli* and *C. fetus* strains. *Microb. Pathog.*, 42(5-6):174-83.
- Bernards D.A., Macaya D.J., Nikolou M., DeFranco J.A., Takamatsu S., Malliaras G.G. (2008). Enzymatic sensing with organic electrochemical transistors. *J. Mater. Chem.*, 18(1):116-120.
- Bernards D.A., Malliaras G.G. (2007). Steady-state and transient behavior of organic electrochemical transistors. *Adv. Funct. Mater.*, 17(17):3538-3544.
- Biesta-Peters E.G., Jongernburger, I., De Boer E., Jacobs-Reitsma W.F. (2018). Validation by interlaboratory trials of EN ISO 10272 - Microbiology of the food chain - Horizontal method for detection and enumeration of *Campylobacter* spp. - Part 1: Detection method. *International journal of Food Microbiology*, 288 (2019) 39-46.
- Bifulco L., Ingianni A., Pompei R. (2013). An internalin A probe-based genosensor for *Listeria monocytogenes* detection and differentiation. *Biomed. Res. Int.*, 2013:e640163.
- Bolton J.(2015). *Campylobacter* virulence and survival factors. *Food microbial.*, 48,99-108.

- Braidot M. (2019). An explorative study to evaluate the performances of an electrochemical label-free bio-assay using Au screen printed electrodes to detect *L. monocytogenes*. Master Degree dissertation, University of Udine.
- Brouwer M.C., van de Beek D., Heckenberg S.G., Spanjaard L., de Gans J. (2006). Community-acquired *Listeria monocytogenes* meningitis in adults. *Clin. Infect. Dis.*, 43(10):1233-1238.
- CDC (2011). Multistate outbreak of listeriosis associated with Jensen Farms cantaloupe - United States, August-September 2011. *MMWR - Morb. Mortal. Wkly Rep.*, 60(39):1357-1358.
- Chon J.W., Kim H., Yim J.H., Park J.H., Kim M.S., Seo K.H (2013). Development of a selective enrichment broth supplemented with bacteriological charcoal and a high concentration of polymyxin B for the detection of *Campylobacter jejuni* and *Campylobacter coli* in chicken carcass rinses. *Int. J. Food Microbiol.*, 162(3):308-10.
- Chon J.W., Kim Y.J., Kim Y.J., Jung J.Y., Bae D., Khan S., Seo K.H., Sung K (2017). Addition of Rifampicin to Bolton Broth to Inhibit Extended-Spectrum β -Lactamase-Producing *Escherichia coli* for the Detection of *Campylobacter*. *J. Food Sci.*, 82(7):1688-1692.
- Chon J.W., Kim Y.J., Rashid F., Sung K., Khan S., Kim H., Seo K.H. (2018). Improvement of Bolton broth by supplementation with tazobactam for the isolation of *Campylobacter* from chicken rinses. *Poult Sci.*, 97(1):289-293.
- Choon J.W., Kim H.S., Kim H., Oh D.H., Seo K.H. (2014) Evaluation of potassium-clavulanate-supplemented modified charcoal-cefoperazone-deoxycholate agar for enumeration of *Campylobacter* in chicken carcass rinse. *J. Food Sci.*, 79(5): M923-6.
- Clauss H.E., Lorber B. (2008). Central nervous system infection with *Listeria monocytogenes*. *Curr. Infect. Dis. Rep.*, 10(4):300-306.
- Contreras-Naranjo J.E., Aguilar O. (2019). Suppressing Non-Specific Binding of Proteins onto Electrode Surfaces in the Development of Electrochemical Immunosensors. *Biosensors*, 9 (1):15-38.
- Coward C., van Diemen P.M., Conlan A.J., Gog J.R., Stevens M.P., Jones M.A., Maskell D.J. (2008). Competing isogenic *Campylobacter* strains exhibit variable population structures in vivo. *Appl. Environ Microbiol.* 74(12):3857-67.
- Dasti J.I., Tareen A.M., Lugert R., Zautner A.E., Gross U. (2010). *Campylobacter jejuni*: a brief overview on pathogenicity-associated factors and disease-mediating mechanisms. *Int. J. Med. Microbiol.* 300(4):205-11.
- Delvallée M., Ettahar N., Loïez C., Decoene C., Courcol R., Wallet F. (2012). An unusual case of fatal pericarditis due to *Listeria monocytogenes*. *Jpn J. Infect. Dis.*, 65(4):312-314.
- Depoorter P., Persoons D., Uyttendaele M., Butaye P., DeZutter L., Dierick K., Herman L., Imberechts H., Van Huffela X., Dewulf J. (2012) Assessment of human exposure to 3rd

- generation cephalosporin resistant *E. coli* (CREC) through consumption of broiler meat in Belgium. *I. Journal of Food Microbiology*, 159 (1) 30-38.
- Descy J., De Mol P., Hayette M.P., Huynen P., Meex C., Melin P. (2012). Acute cholecystitis with *Listeria monocytogenes*. *Acta Clin. Belg.*, 67(4):295-297.
 - Dinic M., Stankovic S. (2013). Neonatal listeriosis followed by nosocomial infection. *Indian J. Med. Microbiol.*, 31(2):187-189.
 - EC (2005). Commission Regulation (EC) No. 2073/2005 of 15 November 2005 on microbiological criteria for foodstuff. *OJ*, L 338/1.
 - EC (2017). Commission Regulation (EC) No. 2017/1495 of 23 August 2017 as regards *Campylobacter* in broiler carcasses. *OJ*, L 218/1.
 - EFSA (2010). Analysis of the baseline survey on the prevalence of *Campylobacter* in broiler batches and of *Campylobacter* and *Salmonella* on broiler carcasses, in the EU, 2008 - Part B: Analysis of factors associated with *Campylobacter* colonization of broiler batches and with *Campylobacter* contamination of broiler carcasses; and investigation of the culture method diagnostic characteristics used to analyze broiler carcass samples. *EFSA J.*, 8(8):1522.
 - EFSA (2011). Scientific Opinion on *Campylobacter* in broiler meat production: control options and performance objectives and/or targets at different stages of the food chain. *EFSA J.*, 9 9(4):2105.
 - EFSA (2012). The European Union summary report on trends and sources of zoonoses, zoonotic agents and food-borne outbreaks in 2010. *EFSA J.*, 10(3): 2597.
 - EFSA (2014). Fact sheet: EFSA explains zoonotic diseases: *Campylobacter*. <https://www.efsa.europa.eu/en/corporate/pub/factsheetcampylobacter/>
 - EFSA (2017). Scientific report of EFSA and ECDC. The European Union Summary Report on zoonoses, zoonotic agents and food-borne outbreaks in 2016. *EFSA J.*, 15(12):5077.
 - EFSA (2018). The European Union summary report on trends and sources of zoonoses, zoonotic agents and food-borne outbreaks in 2017. *EFSA J.*, 16(12):5500.
 - Epps S.V., Harvey R.B., Hume M.E., Phillips T.D., Anderson R.C., Nisbet D.J.(2013). Foodborne *Campylobacter*: infections, metabolism, pathogenesis and reservoirs. *Int. J. Environ Res Public Health*, 10(12):6292-304.
 - Farber J.M. (1991). *Listeria monocytogenes* in fish products. *J. Food Prot.*, 54(12):922-934.
 - Fortin N.D. (2013). Chapter 35 - HACCP and Other Regulatory Approaches to Prevention of Foodborne Diseases. *Food Science and Technology*, 497-510.
 - García T., Revenga-Parra M., Añorga L., Arana S., Pariente F., Lorenzo E. (2012). Disposable DNA biosensor based on thin-film gold electrodes for selective *Salmonella* detection. *Sensors and Actuators B: Chemical.*, 161 (1):1030-1037.

- García-Sánchez L., Melero B., Jaime I., Hänninen M.L., Rossi M., Rovira J. (2017). *Campylobacter jejuni* survival in a poultry processing plant environment. *Food Microbiol.*, 65:185-192.
- Gau V., Ma S.C., Wang H., Tsukuda J., Kibler J., Haake D.A.(2005). Electrochemical molecular analysis without nucleic acid amplification. *Methods.*, 37(1):73-83.
- Ge Z., Schauer D.B., Fox J.G. (2008). In vivo virulence properties of bacterial cytolethal-distending toxin. *Cell Microbiol.* 10(8):1599-607.
- Gentile F., Coppedè N., Tarabella G., Villani M., Calestani D., Candeloro P., Iannotta S., Di Fabrizio E. (2014). Microtexturing of the conductive PEDOT: PSS polymer for superhydrophobic organic electrochemical transistors. *Biomed Res. Int.*, 2014:302694.
- Gray M.L., Killinger A.H. (1966). *Listeria monocytogenes* and listeria infections. *Bacteriol. Rev.*, 30(2):309-382.
- Grisenti M., Lori D., Vicini L., Bovis N., Pedrelli B., Barbuti S. Comportamento di *Listeria monocytogenes* . *Ind. delle Conserve*, 2004, 79,3-12.
- Gruntar I., Biasizzo M., Kušar D., Pate M., Ocepek M. *Campylobacter jejuni* contamination of broiler carcasses: Population dynamics and genetic profiles at slaughterhouse level. *Food Microbiol.*, 50:97-101.
- Habib I., Uyttendaele M., De Zutter L. (2011). Evaluation of ISO 10272:2006 standard versus alternative enrichment and plating combinations for enumeration and detection of *Campylobacter* in chicken meat. *Food Microbiol.*, 28(6):1117-23.
- Hazeleger W.C., Jacobs-Reitsma W.F., den Besten H.M.W. (2016). Quantification of growth of *Campylobacter* and Extended Spectrum β -Lactamase Producing Bacteria Sheds Light on Black Box of Enrichment Procedures. *Front Microbiol.* 7: 1430.
- Hegner M., Wagner P., Semenza G. (1993). Immobilizing DNA on gold via thiol modification for atomic force microscopy imaging in buffer solutions. *FEBS Lett.*, 336(3):452-456.
- Hu K., Lan D., Li X., Zhang S. (2008). Electrochemical DNA biosensor based on nanoporous gold electrode and multifunctional encoded DNA-Au bio bar codes. *Anal. Chem.*, 80(23):9124-9130.
- Huss H.H., Ben Embarek P.K., Jeppesen V.F. (1995). Control of biological hazards in cold-smoked salmon production. *Food Control*, 6(6):335-340.
- ISO (2004a). EN ISO 11290-1:1996/Amd1:2004 Microbiology of Food and Animal Feeding Stuffs - Horizontal Method for the Detection and Enumeration of *Listeria monocytogenes* - Detection Method, Part I. Geneva: International Organization for Standardization.
- ISO (2004b). EN ISO 11290-2:1998/Amd1:2004 Microbiology of Food and Animal Feeding Stuffs - Horizontal Method for the Detection and Enumeration of *Listeria monocytogenes* - Enumeration Method, Part II. Geneva: International Organization for Standardization.

- Jasson V., Samplers I., Botteldoorn N., López-Gálvez F., Baert L., Denayer S., Rajkovic A., Habib I., De Zutter L., Debevere J., Uyttendaele M. (2009). Characterization of *Escherichia coli* from raw poultry in Belgium and impact on the detection of *Campylobacter jejuni* using Bolton broth. *International Journal of Food Microbiology*, 135 (3) 248-253.
- Jin S., Joe A., Lynett J., Hani E.K., Sherman P., Chan V.L. (2001). JlpA, a novel surface-exposed lipoprotein specific to *Campylobacter jejuni*, mediates adherence to host epithelial cells. *Mol Microbiol.*, 39(5):1225-36.
- Johnsen G., Kruse H., Hofshagen M. (2006). Genotyping of *Campylobacter jejuni* from broiler carcasses and slaughterhouse environment by amplified fragment length polymorphism. *Poult Sci.*, 85(12):2278-84.
- Kang J., Li X., Wu G., Wang Z., Lu X. (2007). A new scheme of hybridization based on the Au nano-DNA modified glassy carbon electrode. *Anal. Biochem.*, 364(2):165-170.
- Kathariou S. (2002). *Listeria monocytogenes* virulence and pathogenicity, a food safety perspective. *J. Food Prot.*, 65(11):1811-1829.
- Kittlesen G.P., White H.S., Wrighton M.S. (1984). Chemical derivatization of microelectrode arrays by oxidation of pyrrole and N-methylpyrrole: fabrication of molecule-based electronic devices. *J. Am. Chem. Soc.*, 106(24):7389-7396.
- Klein N.C., Schoch P.E., Cunha B.A. (1991). *Listeria*. *Infect. Control Hosp. Epidemiol.*, 12(5):311-314.
- Li Y., Schluesener H.J., Xu S. (2010). Gold nanoparticle-based biosensors. *Gold Bull.*, 43(1):29-41.
- Lin P., Luo X., Hsing I., Yan F. (2011). Organic electrochemical transistors integrated in flexible microfluidic systems and used for label-free DNA sensing. *Adv. Mater.*, 23(35):4035-4040.
- Lorber B. (2000). *Listeria monocytogenes*. In: Mandell G., Bennett J., Dolin R. (eds.), *Principles & Practice of Infectious Diseases*, 5th ed. (pp. 2208-2215). New York: Churchill Livingstone.
- Lowe C.R., Goldfinch M.J. (1983). Novel electrochemical sensors for clinical analysis. *Biochem. Soc. Trans.*, 11(4):448-451.
- Lowe R.L. (2007). Overview of biosensor and bioarray technologies. In: Marks R.S., Cullen D.C., Karube I., Lowe C.R., Weetall H.H. (eds.), *Handbook of Biosensors and Biochips* (vol. 1, pp. 7-18). Hoboken (NJ): John Wiley & Sons, Inc.
- Marco A.J., Prats N., Ramos J.A., Briones V., Blanco M., Dominguez L., Domingo M. (1992). A microbiological, histopathological and immunohistological study of the intragastric inoculation of *Listeria monocytogenes* in mice. *J. Comp. Pathol.*, 107(1):1-9.

- Marie R., Jensenius H., Thaysen J., Christensen C.B., Boisen A. (2002). Adsorption kinetics and mechanical properties of thiol-modified DNA-oligos on gold investigated by microcantilever sensors. *Ultramicroscopy*, 91(1-4):29-36.
- Martins I.S., Faria F.C., Miguel M.A., Dias M.P., Cardoso F.L., Magalhães A.C., Mascarenhas L.A., Nouér S.A., Barbosa A.V., Vallim D.C., Hofer E., Rabello R.F., Riley L.W., Moreira B.M. (2010). A cluster of *Listeria monocytogenes* infections in hospitalized adults. *Am. J. Infect. Control*, 38(9): e31-36.
- McLauchlin J., Low J.C. (1994). Primary cutaneous listeriosis in adults: an occupational disease of veterinarians and farmers. *Vet. Rec.*, 135(26):615-617.
- Meade K.G., Narciandi F., Cahalane S., Reiman C., Allan B., O'Farrelly C. (2009). Comparative in vivo infection models yield insights on early host immune response to *Campylobacter* in chickens. *Immunogenetics*, 61(2):101-10.
- Mistry K.K., Layek K., Mahapatra A., RoyChaudhuri C., Saha H. (2014). A review on amperometric-type immunosensors based on screen-printed electrodes. *Analyst.*, 21;139(10):2289-311.
- Moran L., Kelly C., Cormican M., McGettrick S., Madden R.H. (2011) Restoring the selectivity of Bolton broth during enrichment for *Campylobacter* spp. from raw chicken. *Lett Appl Microbiol.*, 52(6):614-8.
- NF Validation (2013). EN ISO 16140:2003 validation certificate of the *Listeria* Precis™ method for *Listeria monocytogenes* detection. Certificate No. UNI 03/04-04/05. France: AFNOR Certification.
- Nuzzo R.G., Allara D.L. (1983). Adsorption of bifunctional organic disulfides on gold surfaces. *J. Am. Chem. Soc.*, 105(13):4481-4483.
- Oh E., McMullen L., Jeon B. (2015) High Prevalence of Hyper-Aerotolerant *Campylobacter jejuni* in Retail Poultry with Potential Implication in Human Infection. *Front Microbiol.*, 12;6:1263.
- Orsi R.H., den Bakker H.C., Wiedmann M. (2011). *Listeria monocytogenes* lineages: Genomics, evolution, ecology, and phenotypic characteristics. *Int. J. Med. Microbiol.*, 301(2):79-96.
- Orsi R.H., Wiedmann M. (2016). Characteristics and distribution of *Listeria* spp., including *Listeria* species newly described since 2009. *Appl. Microbiol. Biotechnol.*, 100(12):5273-5287.
- Paleček E. (1996). From polarography of DNA to microanalysis with nucleic acid-modified electrodes. *Electro anal.*, 8(1):7-14.
- Papadoulas S.I., Kakkos S.K., Kraniotis P.A., Manousi M.E., Marangos M.N., Tsolakis I.A. (2013). Listeriosis infection of an abdominal aortic aneurysm in a diabetic patient. *J. Glob. Infect. Dis.*, 5(1):31-33.

- Poly F., Guerry P. Pathogenesis of *Campylobacter*. (2008). *Current Opinioni Gastroenterol*, 24(1):27-31.
- Prachantasena S., Charununtakorn P., Muangnoicharoen S., Hankla L., Techawal N., Chaveerach P., Tuitemwong P., Chokesajjawatee N., Williams N., Humphrey T., Luangtongkum T. (2016). Distribution and Genetic Profiles of *Campylobacter* in Commercial Broiler Production from Breeder to Slaughter in Thailand. *PLoS One*, 17;11(2).
- Pron B., Boumaila C., Jaubertetal F. (2001). Dendritic cells are early cellular targets of *Listeria monocytogenes* after intestinal delivery and are involved in bacterial spread in the host. *Cell. Microbiol.*, 3(5):331-340.
- Rabke-Clemmer C.E., Leavitt A.J., Beebe Jr T.P. (1994). Analysis of functionalized DNA adsorption on Au (111) using electron spectroscopy. *Langmuir*, 10(6):1796-1800.
- Radish J.I.A.,Yusof, N.A (2017). The strategies of DNA immobilization and hybridization detection mechanism in the construction of electrochemical DNA sensor: A review. *Sensing and Bio-Sensing Research*, 16:19-31.
- Ramana K.V., Mohanty S.K. (2013). Human Listeriosis: An Update. *Am. J. Epidemiol. Infect. Dis.*, 1(4):63-66.
- Rocourt J., Jacquet C., Reilly A. (2000). Epidemiology of human listeriosis and seafood. *Int. J. Food Microbiol.*, 62(3):197-209.
- Sasaki Y., Maruyama N., Zou B., Haruna M., Kusukawa M., Murakami M., Asai T., Tsujiyama Y., Yamada Y. (2006) *Campylobacter* cross-contamination of chicken products at an abattoir. *Zoonoses Public Health.*, 60(2):134-40
- Scallan E., Hoekstra R.M., Angulo F.J., Tauxe R.V., Widdowson M.A., Roy S.L., Jones J.L., Griffin P.M. (201). Foodborne illness acquired in the United States--major pathogens. *Emerg Infect Dis.*,17(1):7-15.
- Schnerr H.R. (2007). Food and beverage applications of biosensor technologies. In: Marks R.S., Cullen D.C., Karube I., Lowe C.R., Weetall H.H. (eds.), *Handbook of Biosensors and Biochips* (vol. 2, pp. 1191-1199). Hoboken (NJ): John Wiley & Sons, Inc.
- Schuchat A., Swaminathan B., Broome C.V. (1991). Epidemiology of human listeriosis. *Clin. Microbiol. Rev.*, 4(2):169-183.
- Seeliger H.P.R., Höhne K. (1979). Serotyping of *L. monocytogenes* and related species. In: Bergan T., Norris J.R. (eds.), *Methods in microbiology* (vol. 13, pp. 31-49). New York: Academic Press Inc.
- Seliwiorstow T., De Zutter L., Houf K., Botteldoorn N., Baré J., Van Damme I. (2015). Comparative performance of isolation methods using Preston broth, Bolton broth and their modifications for the detection of *Campylobacter* spp. from naturally contaminated fresh and frozen raw poultry meat. *International Journal of Food Microbiology*, 3 (23) 60-64

- Settingington E.B., Alocilja E.C. (2012) Electrochemical Biosensor for Rapid and Sensitive Detection of Magnetically Extracted Bacterial Pathogens. *Biosensors*, 2 (1):15-31.
- Silva J., Leite D., Fernandes M., Mena C., Gibbs P.A., Teixeira P., (2001). *Campylobacter* spp. as foodborne pathogens: a review. *Frontiers in microbiology*, 2:200.
- Skarp C.P.A., Hänninen M.L., Rautelin H.I.K. (2016). Campylobacteriosis: the role of poultry meat. *Clin Microbiol Infect*, 22(2):103-109.
- Skoog D.A., Holler F.J., Crouch S. (2009). *Chimica analitica strumentale*, 2nd ed. (cap 2, pp. 43-46). Naples (Italy): Edises.
- Slader J., Domingue G., Jørgensen F., McAlpine K., Owen R.J., Bolton F.J., Humphrey T.J. Impact of Transport Crate Reuse and of Catching and Processing on *Campylobacter* and *Salmonella* Contamination of Broiler Chickens. *Appl Environ Microbiol.*, 68(2): 713–719.
- Smith S, Meade J, McGill K, Gibbons J, Bolton D, Whyte P. Restoring the selectivity of modified charcoal cefoperazone deoxycholate agar for the isolation of *Campylobacter* species using tazobactam, a β -lactamase inhibitor. *J Food Microbiol*. 2015 Oct 1;210:131-5.
- Steel A.B., Herne T.M., Tarlov M.J. (1998). Electrochemical quantitation of DNA immobilized on gold. *Anal. Chem.*, 70(22):4670-4677.
- Sun W., Qi X., Zhang Y., Yang H., Gao H., Chen Y., Sun Z. (2012). Electrochemical DNA biosensor for the detection of *Listeria monocytogenes* with dendritic nanogold and electrochemical reduced graphene modified carbon ionic liquid electrode. *Electrochim. Acta*, 85:145-151.
- Swaminathan B., Cabanes D., Zhang W., Cossart P. (2007). *Listeria monocytogenes*. In: Doyle M., Beuchat L. (eds.), *Food Microbiology: Fundamentals and Frontiers*, 3rd ed. (pp. 457-491). Washington DC: ASM Press.
- Swaminathan B., Gerner-Smidt P. (2007). The epidemiology of human listeriosis. *Microbes Infect.*, 9(10):1236-1243.
- Teodor A., Teodor D., Miftode E., Prisăcaru D., Leca D., Petrovici C., Dorneanu O., Dorobăţ C.M. (2012). Severe invasive listeriosis--case report. *Rev. Med. Chir. Soc. Med. Nat. Iasi*, 116(3):808-11.
- Thévenot D.R., Toth K., Durst R.A., Wilson G.S. (2001). Electrochemical biosensors: recommended definitions and classifications. *Biosens. Bioelectron.*, 16(1-2):121-131.
- Travier L., Guadagnini S., Gouin E., Dufour A., Chenal-Francisque V., Cossart P., Olivo-Marin J.C., Ghigo J.M., Disson O., Lecuit M. (2013). ActA promotes *Listeria monocytogenes* aggregation, intestinal colonization and carriage. *PLOS Pathog.*, 9(1):e1003131
- Van Deun K., Haesebrouck F., Heyndrickx M., Favoreel H., Dewulf J., Ceelen L., Dumez L., Messens W., Leleu S., Van Immerseel F., Ducatelle R., Pasmans F. (2007) . Virulence properties of *Campylobacter jejuni* isolates of poultry and human origin. *J. Med. Microbiol.*, 56(Pt 10):1284-9.

- Van Vliet A.H., Ketley J.M.(2001). Pathogenesis of enteric *Campylobacter* infection. *Symp Ser Soc Appl Microbiol.*, (30):45S-56S.
- Vázquez-Boland J.A., Kuhn M., Berche P., Chakraborty T., Domínguez-Bernal G., Goebel W., González-Zorn B., Wehland J., Kreft J. (2001). *Listeria* pathogenesis and molecular virulence determinants. *Clin. Microbiol. Rev.*, 14(3):584-640.
- Wang H.L., Ghanem K.G., Wang P., Yang S., Li T.S. (2013). Listeriosis at a tertiary care hospital at Beijing, China: high prevalence of nonclustered healthcare-associated cases among adult patients. *Clin. Infect. Dis.*, 56(5):666-676.
- Wang J., Kawde A.N., Erdem A., Salazar M. (2001). Magnetic bead-based label-free electrochemical detection of DNA hybridization. *Analyst*, 126(11):2020-2024.
- Wang J., Rivas G., Fernandes J.R., Paz J.L.L., Jiang M., Waymire R. (1998). Indicator-free electrochemical DNA hybridization biosensor. *Anal. Chim. Acta*, 375(3):197-203.
- Wang R., Zhou X., Zhu X., Yang C., Liu L., Shi H. (2017). Isoelectric Bovine Serum Albumin: Robust Blocking Agent for Enhanced Performance in Optical-Fiber Based DNA. *Sensing. ACS Sensors*. 2(2)257-262.
- Ward T.J., Ducey T.F., Usgaard T., Dunn K.A., Bielawski J.P. (2008). Multilocus genotyping assays for single nucleotide polymorphism-based subtyping of *Listeria monocytogenes* isolates. *Appl. Environ. Microbiol.*, 74(24):7629-7642.
- Weis J., Seeliger H.P.R. (1975). Incidence of *Listeria monocytogenes* in nature. *Appl. Microbiol.*, 30(1):29-32.
- Weller D., Andrus A., Wiedmann M., den Bakker H.C. (2015). *Listeria booriae* sp. nov. and *Listeria newyorkensis* sp. nov., from food processing environments in the USA. *Int. J. Syst. Evol. Microbiol.*, 65(1):286-292.
- Whittaker P. (2012). Evaluating the use of fatty acid profiles to differentiate human pathogenic and nonpathogenic *Listeria* species. *J. AOAC Int.*, 95(5):1457-1459.
- Xue Y., Li X., Li H., Zhang W. (2014). Quantifying thiol-gold interactions towards the efficient strength control. *Nat. Commun.*, 5:4348.
- Yamasaki S., Asakura M., Tsukamoto T., Farique S.M., Deb R., Ramamurthy T., 2006. Cytotoxic distending toxin (CDT): Genetic diversity, structure and role in diarrheal disease. *Toxin Reviews*, 25, 61-88.
- Yan L., Zhao W., Wen Z., Li X., Niu X., Huang Y., Sun W (2017). Electrochemical DNA Sensor for hly Gene of *Listeria monocytogenes* by Three-Dimensional Graphene and Gold Nanocomposite Modified Electrode. *International Journal of electrochemical science*, 12 (4086-4095).
- Yeni F., Yavaş S., Alpas H., Soyer Y. (2016). Most Common Foodborne Pathogens and Mycotoxins on Fresh Produce: A Review of Recent Outbreaks. *Crit Rev Food Sci Nutr.*, 56(9):1532-44.

- Young K.T., Davis L.M., Dirita V.J. (2007). *Campylobacter jejuni*: molecular biology and pathogenesis. *Nat Rev Microbiol.*, 5(9):665-79.
- Zilbauer M., Dorrell N., Wren B.W., Bajaj-Elliott M. (2008). *Campylobacter jejuni*-mediated disease pathogenesis: an update. *Trans R Soc Trop Med Hyg*, 102(2):123-9.

AIM OF THE PROJECT

Listeria monocytogenes and *Campylobacter* spp. are two important foodborne pathogens and can be acquired by the ingestion of contaminated food mainly ready to eat (RTE) and undercooked chicken respectively. The symptoms are gastrointestinal disorders that can switch to a serious disease. The recommended ISO standard methods (ISO 11290:1-2017 and ISO 10272:1-2017) are time consuming and laborious. Therefore, the food industry needs rapid and sensitive analytical methods able to detect pathogens in order to comply with the legislative rules defined by food authorities, ensuring food safety and consumers' health.

The biosensors respond to this need, indeed show several advantages compared to classical and molecular methods in use.

This work is focused on the development and testing of two electrochemical biosensors that use label-free DNA probes and in the combination between bioreceptor and transducer to improve the selectivity and sensitivity. An organic electrochemical transistor (OECT) biosensor was developed to detect *L. monocytogenes*. Instead, a voltammetric biosensor (VB) was developed to detect *Campylobacter jejuni*, *C. coli*, *C. lari*, and *C. upsaliensis*.

Chapter II

LISTERIA MONOCYTOGENES

2.1 MATERIALS AND METHODS

2.1.1 BACTERIAL STRAINS AND CULTURE MEDIA

Pure strains of *L. monocytogenes*, non-pathogenic *Listeria* spp. and other microorganisms were used as positive and negative controls (Table 2.1). Due to the genomic variability among different serotypes of *L. monocytogenes*, four different strains belonging to the serotypes more frequently involved in cases of human infections (Swaminathan et al., 2007; Swaminathan and Gerner-Smith, 2007; Kathariou, 2002) were used. Negative controls were chosen among non-pathogenic *Listeria* spp., common food pathogens and natural spoilage microflora of salmon, according to literature data (Joffraud et al., 2006; Gimenez and Dalgaard, 2004).

Table 2.1. Reference bacterial strains. ^AATCC: American Type Culture Collection (Manassas, VA, USA); ^BDISTAM: Dipartimento di Scienze e Tecnologie Alimentari e Microbiologiche (Milan, Italy); ^CDSM: Deutsche Sammlung von Mikroorganismen und Zellkulturen GmbH (Braunschweig, Germany); ^DDI4A: Department of Agricultural, Food, Environmental and Animal Sciences (Udine, Italy).

Controls		Microorganism	Collection code
Positive	1	<i>Listeria monocytogenes</i> 1/2c	ATCC 7644 ^A
	2	<i>L. monocytogenes</i> 1/2a	DISTAM ^B
	3	<i>L. monocytogenes</i> 1/2b	DISTAM
	4	<i>L.monocytogenes</i> 4b	DSM 15675 ^C
Negative	1	<i>Listeria innocua</i>	DSM 20649
	2	<i>Listeria ivanovii</i>	DI4A ^D
	3	<i>Salmonella enterica</i>	DSM 9145
	4	<i>Enterobacter</i> spp.	DIA4
	5	<i>Escherichia coli</i>	DIA4
	6	<i>Bacillus cereus</i>	DSM 2301
	7	<i>Campylobacter jejuni</i>	DSM 49943
	8	<i>Lactobacillus plantarum</i>	ATCC BAA-793
	9	<i>Lactobacillus rhamnosus</i>	ATCC 53103
	10	<i>Lactobacillus paracasei</i>	DSM 5622
	11	<i>Lactobacillus brevis</i>	DSM 20054

The reference strains were preserved at -80°C in BHI broth added with glycerol in Nalgene Cryovials (Sigma-Aldrich, Milan, Italy) until revitalization in BHI broth (Brain Heart Infusion; Oxoid, Milan, Italy) for 24 h at their optimal growth temperature. Bacterial strains were then grown in appropriate medium, according to the manufacturer's instructions. Specific selective media were used for the analysis, PALCAM agar for *Listeria* spp., XLD agar for *Salmonella enterica*, Coli-ID agar for *Escherichia coli*, and *Bacillus cereus* selective agar for *Bacillus cereus*, VRBG agar for *Enterobacter* spp., all grown at 37°C for 24h. mCCD agar a blood-free selective medium was used for *Campylobacter jejuni*, at 37°C for 48 h in AnaeroJar 2.5L with CampyGen 2.5L Sachet for microaerophilic conditions.. MRS agar (de Man, Rogosa and Sharpe) for *Lactobacillus* spp. at 30 or 37°C for 48 h in AnaeroJar 2.5L with a candle for

microaerophilic conditions.

A characteristic colony of each microorganism after purification was subjected to Gram stain, morphology cell, oxidase, and catalase tests.

2.1.2 COLD-SMOKED SALMON SAMPLES

16 samples of cold-smoked salmon (CSS) from different producers purchased from local supermarkets and discounts (Table 2.2) were analyzed to evaluate natural contamination and the presence of *L. monocytogenes* with traditional Listeria PreciTM method (NF Validation, 2013) and molecular methods. For each kind of product, two packages were purchased in order to analyze the first one immediately (8 samples named from CSS 1.1 to CSS 8.1) and the other one close to expiring date (8 samples named from CSS 1.2 to CSS 8.2).

Table 2.2: CSS samples specifications.

#	Product type	Production details	Shelf-life (weeks)
1	Norwegian CSS	Bred and processed from fresh in Norway	4
2	Scottish CSS	Bred in Scotland, processed from fresh in Lithuania	4
3	Scottish CSS	Bred and processed from fresh in Scotland	4
4	Norwegian CSS	Bred in Scotland, processed from fresh in Poland	3
5	Scottish CSS	Bred and processed from fresh in Scotland, packaged in Italy	4
6	Norwegian CSS	Bred and processed from fresh in Norway, packaged in Italy	3
7	Norwegian CSS trimmings	Processed in Italy from frozen	3
8	Irish CSS	Bred in Ireland, processed in France from frozen	4

Purchased CSS samples were all dry-salted, preservative-free and vacuum-packaged, with a shelf-life of 3 or 4 weeks.

In Figure 2.1, a schematic representation of the experimental design is shown. From each sample, 10g were collected, homogenized with saline-peptone water (SPW) and subjected to plate count bacterial enumeration and DNA extraction (samples DNA named CSS_{SPW}). An aliquot of 25 g of the sample was subjected to Listeria PreciTM method for the detection of *L.*

monocytogenes. The DNA extraction was performed after 24 h of enrichment (samples DNA named CSS_{ENR}).

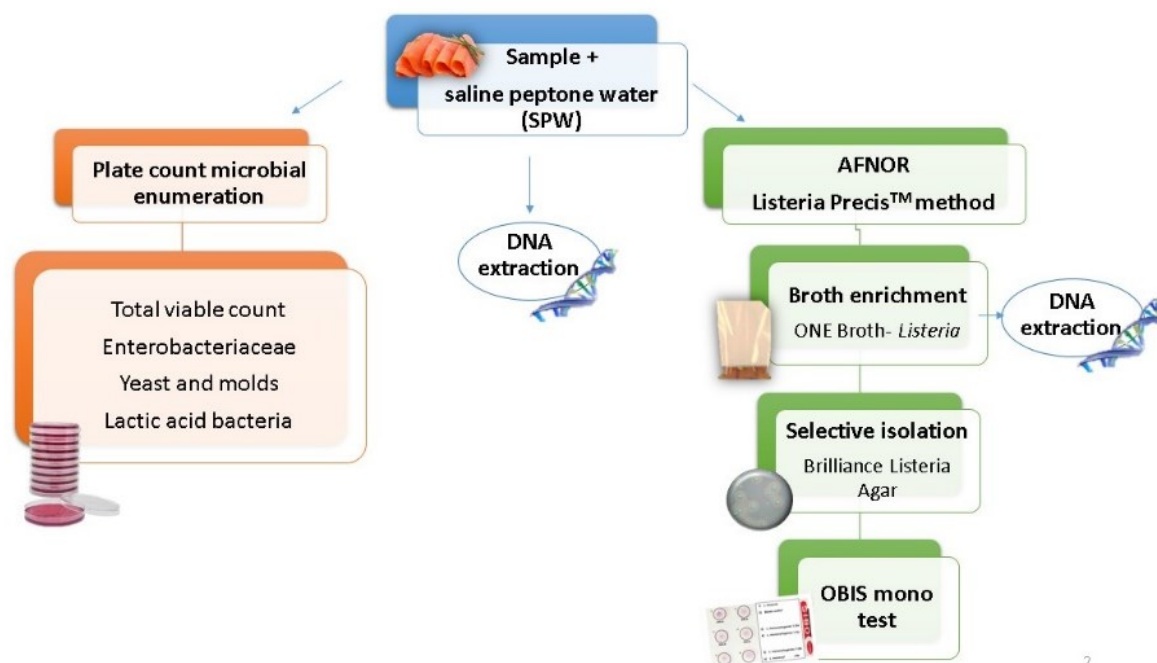


Figure 2.1 Schematic representation of the experimental design. Plate count bacterial enumeration and *Listeria PreciS™* method were performed on all the 16 CSS samples.

2.1.2.1 Plate count bacterial enumeration

10 g of salmon from each sample were transferred into a sterile filter Stomacher bag, added with 40 mL of saline-peptone water (8 g/L NaCl, 1 g/L bacteriological peptone; Oxoid), mixed for 30 sec in a Stomacher (PBI, Milan, Italy) and used for plate count bacterial enumeration:

- Total viable count on TSA (Tryptone Soya Agar, Oxoid, Milan, Italy) at 30°C for 48h;
- Lactic acid bacteria on MRS (Oxoid) at 30°C for 48 h, in AnaeroJar 2.5L (Oxoid) with a candle for microaerophilic conditions;
- Enterobacteriaceae on a double layer of VRBG agar (Oxoid) at 37°C for 24 h;
- Yeasts and molds on malt extract agar (Oxoid, Milan, Italy) added with 10 µg/mL of tetracycline; Sigma-Aldrich, Milan, Italy) at 30°C for 48 h.

2.1.2.2 *Listeria PreciS™* method

CSS is an RTE (ready-to-eat) food that allows the growth of *L. monocytogenes*. Therefore, as required by EC Reg. 2073/2005, *L. monocytogenes* must be absent in 25 g of the product. For all the CSS samples, including the inoculated samples, presence or absence of *L. monocytogenes* was determined using the AFNOR validated *Listeria PreciS™* method

(NF Validation, 2013), which has been shown to give equivalent results to ISO 11290-1:1996/Amd1:2004.

25 g of salmon from each sample was transferred into a filter sterile Stomacher bag, added with 225 mL of ONE Broth-*Listeria* (Oxoid, Milan, Italy), mixed for 30 sec in a Stomacher (PBI) and incubated for 24 h at 30°C. After enrichment, for the selective isolation of *L. monocytogenes*, Brilliance *Listeria* agar (Oxoid, Milan, Italy) was inoculated in duplicate using a 10 µL microbiological loop and then incubated for 24 h at 37°C. Presumptive *L. monocytogenes* blue/green colonies with halos were confirmed using the O.B.I.S. mono test (Oxoid, Milan, Italy).

2.1.2.3 Sample DNA extraction

As reported in the experimental design (Figure 2.1), DNA of each sample was extracted after homogenization in saline-peptone water (CSS_{SPW}) and 24 h of enrichment (CSS_{ENR}) in ONE Broth-*Listeria*. 2 mL of homogenate were collected from the Stomacher bag of each sample and centrifuged for 10 min at 13,000 rpm. The supernatant was discarded and the pellet was re-suspended in 300 µL of breaking buffer (2% Triton X-100, 1% SDS, 100 mM NaCl, 10 mM Tris-HCl, 1 mM EDTA pH 8; Sigma-Aldrich). The DNA extraction was then carried out as previously described for reference to bacterial strains. Extracted DNA was quantified with the spectrophotometer (Nanodrop 2000C; Thermoscientific, Marietta, OH, USA) and standardized at 100 ng/µL. The obtained DNA was stored at -20°C until use.

2.1.3 SAMPLES FROM HAM FACTORIES

In order to detect *L. monocytogenes*, 45 samples were recovered from different ham production factories in Friuli Venezia Giulia (Italy) during three samplings.

The first sampling included 5 raw meat samples (from 1.1 to 5.1), 5 environmental samples (from 6.1 to 10.1) and 5 dry-cured ham samples (from 11.1 to 15.1). Samples of the second sampling from 1.2 to 15.2 (raw meat from 1.2 to 5.2, environmental from 6.2 to 10.2 and cured ham from 11.2 to 15.2), the third with numbers from 1.3 to 15.3, respectively.

Sampling was performed using a sterile gauze (3.5 x 7cm), hydrated with 3 mL of saline peptone water (spw). The surface areas analyzed were 10 x 10 cm² of the leg of fresh meat and dry-cured ham. Environmental samples were taken from:

- Transport area - the starting point
- finishing point
- Cutting area
- Weight scale
- Storage area

The gauzes used for raw meat and cured ham were resuspended in 10 mL spw and subjected to plate count microbial enumeration. All samples were subjected to the *Listeria* PrecisTM method. DNA was extracted for molecular tests from, One Broth (samples from 1.1 O to 15.1 O, 1.2 O to 15.2 O and 1.3 to 15.3 respectively) while DNAs extracted from saline peptone water were

named from 1.1 F to 15.1F, 1.2 F to 15.2 F, and 1.3 to 15.3 F respectively and is shown in Figure 2.2.

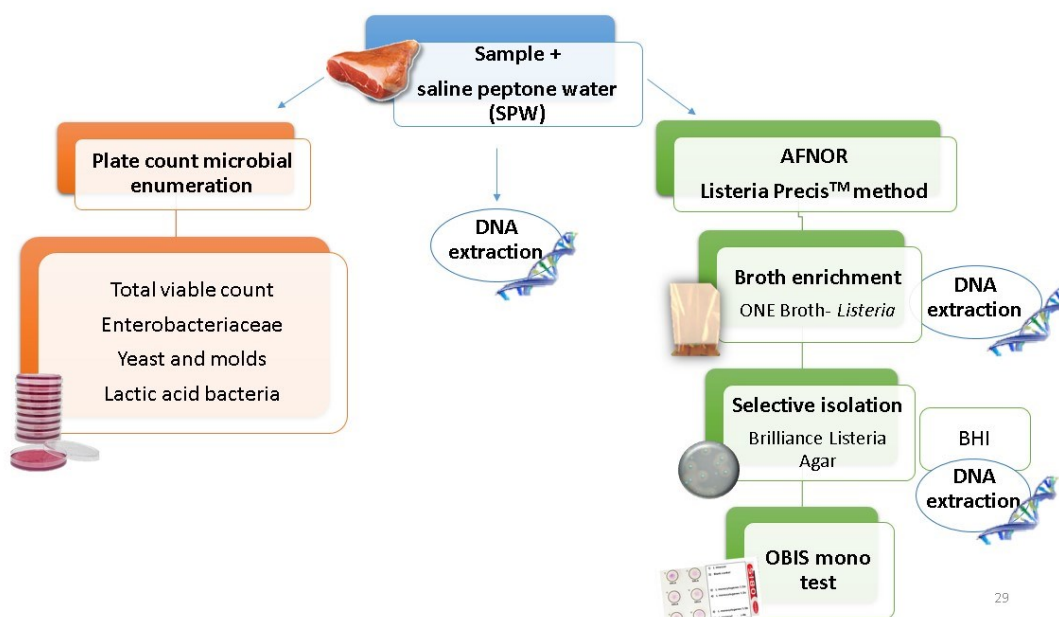


Figure 2.2 Schematic representation of the experimental design. Plate count bacterial enumeration and Listeria Precis™ method were performed on all the 45 ham factories samples.

2.1.3.1 Plate count bacteria and Listeria Precis™ method

10 mL spw were used for the total viable count, lactic acid bacteria, Enterobacteriaceae, yeast, and molds. 3 mL was added to 27 mL of ONE- Broth- Listeria, to maintain the ratio 1:10 between sample and enrichment broth. The broth was shaken on vortex for 15 sec and incubated for 24h at 30°C. After enrichment 10µL of the samples were inoculated on selective medium Brilliance Listeria agar for 24h at 37°C. The blue/green colonies with halos were confirmed using the OBIS mono test.

2.1.3.2 Sample DNA extraction

DNA was extracted from saline peptone water immediately after homogenization and after 24h enrichment in One broth-Listeria, quantified with a spectrophotometer and standardized at 100 ng/µL.

2.1.4 PRIMER DESIGN FOR THE DETECTION OF *L. monocytogenes*

As for qPCR application, the maximum length of the amplicon should be 50-150 bp in order to achieve an adequate amplification efficiency (Bustin et al., 2012), a new reverse primer was designed to be used with Mar1 forward primer (Manzano et al., 1997a) to produce an amplicon of 160 bp. *Listeria* spp. *iap* gene sequences were retrieved from GenBank and aligned using the

“Multiple sequence alignment with hierarchical clustering” (Corpet, 1988) to design the reverse MarB primer. Then primers Mar1 and MarB were tested using OligoAnalyzer 3.1 (<http://eu.idtdna.com/calc/analyzer>) and in silico with AmplifX 1.7.0 (Jullien, 2013). Selected sequences were synthesized by MWG-Biotech (Ebersberg, Germany).

Table 2.3 *L. monocytogenes* specific primers characteristics.

Primer	Mar1 (forward)	MarB (reverse)
Sequence	5'-GGG CTT TAT CCG TAA AAT A-3'	5'- NNN NNN NNN NNN NNN NN-3' ^{ab}
Length (bp)	19	17
GC content	36.8%	58%
T _m (°C)	46.9	53
Homo-dimer min. ΔG** (kcal/mol)	-4	-10
Hairpins min. ΔG** (kcal/mol)	0.48	-1
Hairpins max. T _m (°C)	20	55
Primer pairs	Mar1-MarB	
Amplicon length (bp)	160	
Annealing temperature (°C)	48	
Primer dimer min. ΔG** (kcal/mol)	-4.74	

^aAccording to the software guide, only ΔG of -9kcal/mol or more negative may be problematic (OligoAnalyzer 3.1, <http://eu.idtdna.com/calc/analyzer>).

^bPatent pending

2.1.5 PCR PROTOCOL

PCR was carried out to evaluate the specificity of primers Mar1-MarB using DNA extracted from reference strains listed in Table 2.1 at 100 ng/μL. Annealing temperature and MgCl₂ concentration were optimized to improve the stringency and specificity of the assay. To assess primers' sensitivity, a PCR was carried out using decimal dilutions (from 100 ng/μL to 1 fg/μL) of the DNA of *L. monocytogenes* 1/2b DISTAM. The reaction mixture contained the following reagents: 5 μL AmpliTaq® Buffer 10x (Applied Biosystems, Foster City, CA, USA), 1 μL MgCl₂ 25 mM (Applied Biosystems), 1 μL PCR Nucleotide Mix 10 mM each (Applied Biosystems), 1 μL of each primer at 10 μM, 0.25 μL AmpliTaq® DNA Polymerase 5 units/μL (Applied Biosystems).

The final reaction volume was 50 μL including 1 μL of template DNA. In each assay, a positive control (*L. monocytogenes* 1/2b DISTAM), a negative control (*L. innocua* DSM 20649) and no-template control (NTC) were included. Thermal cycler conditions consisted of 95°C denaturation for 5 min, 35 cycles of 95°C denaturation for 1 min, 48°C annealing for 45 sec, 72°C extension for 30 sec and a final extension at 72°C for 7 min in a Thermal Cycler (C1000 Touch™; Bio-rad, Irvine, CA, USA).

After PCR protocol optimization, DNA extracted from CSS samples (CSS_{SPW} and CSS_{ENR})

standardized at 100 ng/ μ L was subjected to PCR analysis.

The protocol was also used to confirm the identity of isolated colonies with a halo from Brilliance Agar *Listeria*.

2.1.6 AGAROSE GEL ELECTROPHORESIS

PCR products were electrophoretically resolved in a 2% agarose gel, in TBE (Tris-borate-EDTA) buffer 0.5X (Sigma-Aldrich, Milan, Italy). Added with ethidium bromide at a final concentration of 0.5 μ g/mL. A 100 bp DNA Ladder (Promega, Milan, Italy) was loaded for the recognition of the obtained fragments length. The electrophoretic run was performed at 120 V for 40 min. Each gel was observed under UV light and the image was acquired with bio-imaging system GeneGenius (SynGene, Cambridge, England).

2.1.7 qPCR PROTOCOL

qPCR was carried out using the primers Mar1-MarB, previously used for endpoint PCR. Decimal dilutions, from 100 ng/ μ L to 1 fg/ μ L of the DNA of *L. monocytogenes* 1/2b DISTAM, were used to build a standard curve by relating fluorescence with threshold cycle (Ct). The threshold limit setting was performed in an automatic mode. After qPCR protocol optimization, DNA extracted from CSS samples (CSS_{SPW}, CSS_{ENR}) standardized at 10 ng/ μ L was subjected to qPCR with Mar1-MarB primers. Absolute quantitation was performed on the basis of the standard curve built with *L. monocytogenes* 1/2b DISTAM. In each assay a positive control (*L. monocytogenes* 1/2b DISTAM), a negative control (*L. innocua* DSM 20649) and a no-template control (NTC) were included.

SsoFast™ EvaGreen® kit (Bio-rad, Irvine, CA, USA) was employed, according to the manufacturer's instructions. The reaction mixture contained the following reagents:

10 μ L SsoFast™ EvaGreen® Supermix 2x (Bio-rad), 1 μ L MgCl₂ 25 mM (Applied Biosystems), 1 μ L of each primer (Mar1-MarB at 10 μ M). The final reaction volume was of 20 μ L including 1 μ L of template DNA at various concentrations. In each assay, a blank control called NTC (no-template control) was included, in which the template DNA was replaced with an equal volume of nuclease-free water. Thermal program applied consisted of 98°C hot-start activation for 2 min, 40 cycles of 98°C denaturation for 5 sec and 60°C annealing/extension for 20 sec, followed by melting temperature analysis performed by gradually increasing the temperature from 60 to 95 °C (+0.5°C/5 sec) in the Rotor-Gene Q (Venlo, Limburg, Netherlands). Fluorescence acquisition during annealing/extension step of each cycle and final melting temperature analysis was set on the green channel (excitation at 470 nm and emission at 510 nm) of the instrument, due to the properties of the EvaGreen® dye.

2.1.8 DNA PROBE FOR OECT (organic electrochemical transistor)

ListCapt probe (Fontanot, 2014), specific for *L. monocytogenes* was used for the utilization in the construction of an OECT (organic electrochemical transistor) biosensor. The DNA probe,

34 bp length, with a 26.5% GC% content and a T_m of 54.4°C was previously tested using dot blot for specificity by labeling the 5' end with digoxigenin (DIG-ListCapt) as described in Fontanot (2014).

An ssDNA sequence, complementary to the probe, was used as a positive control for the optimization of the protocol conditions.

Listeria spp. *iap* gene sequences were retrieved from GenBank and aligned using the “Multiple sequence alignment with hierarchical clustering” (Corpet, 1988), and tested using the software Blast (Altschul et al., 1990) and OligoAnalyzer 3.1 (<http://eu.idtdna.com/calc/analyzer>). The ListCapt probe was modified by the addition of a thiol group at 5' end (Thiol-ListCapt) for the attachment to the gold electrode surface. This work was performed in collaboration with the Institute of Materials for Electronics and Magnetism – IMEM (National Research Council - CNR, Parma) (Beltrame, 2016). Probe characteristics are listed in Table 2.3.

Table 2.4 ListCapt probe and newly designed ListE probe characteristics.

Characteristics	ListCapt probe	ListE probe
Length (bp)	34	43
GC content	26.5%	30.2%
T_m (°C)	54.4	59.2
Homo-dimer min. ΔG^* (kcal/mol)	-3.61	-3.61
Hairpins min. ΔG^* (kcal/mol)	1.38	1.38
Hairpins max. T_m (°C)	-17.9	-17.9

*According to the software guide, only ΔG of -9kcal/mol or more negative may be problematic (OligoAnalyzer 3.1, <http://eu.idtdna.com/calc/analyzer>).

2.1.9 DOT BLOT PROTOCOL (ListCapt)

Dot blot technique was applied in order to verify the specificity of the probe before application to the electrochemical biosensor. The protocol was optimized by varying type of membrane (branded Sigma-Aldrich or Bio-rad), probe concentration (200, 100 and 50 ng/ μ L), hybridization temperature (44, 42, 40, 30°C and room temperature), washing temperature and the concentration of SSC buffer used for the second step of washing (1X, 0.5X or 0.1X).

The specificity of the probe was tested on the DNA extracted from reference strains listed in Table 2.1 and standardized at 100 ng/ μ L.

Briefly: DNA was denaturated at 95°C for 10 minutes, 1 μ L of DNA from samples was spotted onto a positively charged nylon membrane (Zeta-Probe GT; Bio-rad, Irvine, CA, USA) and cross-linked by exposure to UV light (254 nm) for 10 min.

The membrane was pre-hybridized in pre-warmed Dig Easy Hyb buffer (Roche Diagnostics,

Mannheim, Germany) at the optimal hybridization temperature (40°C) and then hybridized overnight at the same temperature. 7 µL of DIG-ListE probe at 200 ng/µL (previously denatured for 10 min at 95°C) were added to 7 mL of Dig Easy Hyb (Roche Diagnostics), to obtain a final probe concentration of 200 ng/mL. Washing steps: twice with 2X SSC (Promega, Milan, Italy) with 0.1% (w/v) SDS at room temperature for 5 min shaking, twice with 1X SSC (Promega) with 0.1% (w/v) SDS at room temperature for 15 min shaking, once with 1X washing buffer (Roche Diagnostics) at room temperature for 10 min shaking. The membrane was incubated with freshly prepared 1X blocking solution (obtained by tenfold dilution of 10X blocking solution with 1X maleic acid buffer; Roche Diagnostics) at room temperature for 30 min shaking and subsequently with antibody solution (AntiDIG-AP diluted in blocking solution 1:5.000; Roche Diagnostics) at room temperature for 30 min shaking. The membrane was then washed again twice with 1X washing buffer for 15 min shaking and neutralized with 1X detection buffer (Roche Diagnostic) for 5 min. For the detection of the probe-target hybrid, the membrane was incubated with detection color solution (NBT/BCIP stock solution diluted in 1X detection buffer 1:50; Roche Diagnostics) in the dark and without shaking. After 45 min, the membrane was rinsed with sterile water to stop the reaction.

2.1.10 ATOMIC FORCE MICROSCOPE

In order to study the Au surface modified by the Thiol-ListCapt probe was used the Atomic Force Microscope (AFM). Au slides on borosilicate with a thickness of 0.15 mm over titanium adhesion layer (Phasis, Rovigo, Italy) were functionalized with the List Capt probe and hybridized with *L. monocytogenes* genomic DNA.

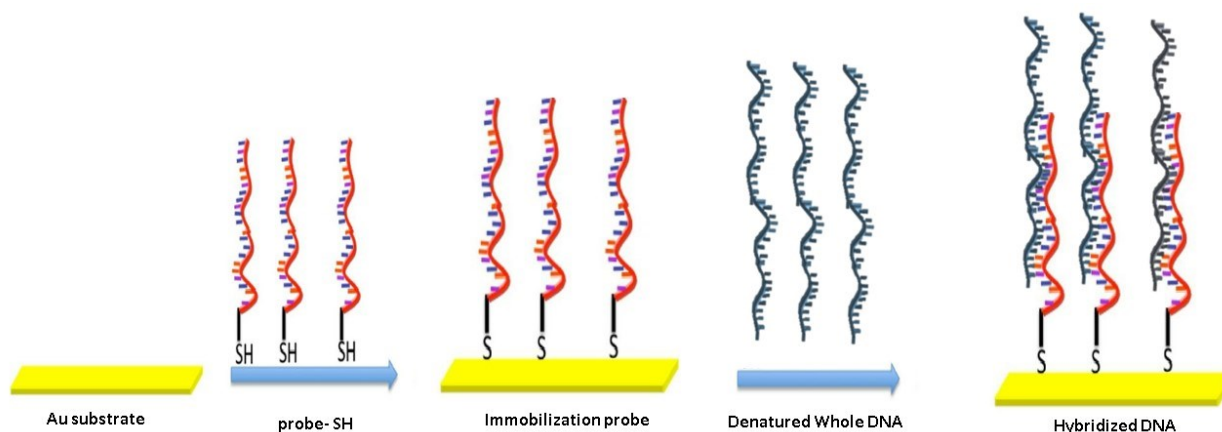


Figure 2.3 Representation of the steps used for gold functionalization and further target hybridization.

In Figure 2.3 a schematic representation of the steps performed for the analysis 1) Bare gold surface (Au substrate); 2) immobilization of the Thiol-ListCapt to the surface; 3) hybridization of the DNA of *L. monocytogenes* to the List Capt probe.

In step two, 10 µL of Thiol-List capt probe, standardized at 50 ng/µL in PBS 1X after denaturation at 95°C for 10 min, was used to functionalize the gold surface for 1 h at room temperature. The gold surface was rinsed twice with 500 µL with sterile bi-distilled water to

remove the probe in excess and PBS salts.

In step three, 10 μL of denatured *L. monocytogenes* genomic DNA, concentrated at 10 ng/ μL , were incubated for 1h at 40°C for the hybridization, and after washing twice with water and dry, the surface was analyzed. The same procedure was repeated using the sequence complementary to the ListCapt probe (positive control) and with the DNA of *L. innocua*, considered as the negative control.

The Au surface was analyzed by scanning Kelvin probe force microscopy (SKPFM) using Nanoscope III Multimode AFM equipped with an Extender TM Electronic Module. This technique is able to register topographic and Volta potential map with difference measured. The SKPFM characterization was carried out in air at room temperature. The scan height in the lift mode was 30 μm . Topography and Volta potential were sampled with a pixel density of 256 x 256 and with a scan frequency of 0.19 Hz. This scan frequency was selected in order to ensure accurate mapping to the sample surface to limit the effect of the topography on Volta potential maps for the samples with several thicknesses due to the presence or absence of hybridized DNA. The brightness of different zones of the topographic maps shown in this work corresponds to a different height of the features on the sample surface. A bright zone is higher than dark areas on the topographic maps. In a similar way, the brightness on Volta potential maps is associated with the difference in Volta potential of the features on the map. Bright areas have higher Volta potential than dark areas. (Andreatta et al., 2014).

2.1.11 OECT ELECTROCHEMICAL BIOSENSOR

In collaboration with the Institute of Materials for Electronics and Magnetism – IMEM (National Research Council - CNR, Parma), the application of a DNA probe in a DNA-biosensor based on OECT for the electrochemical detection of *L. monocytogenes* was investigated. The application of a DNA probe in a DNA-biosensor based on OECT for the electrochemical detection of *L. monocytogenes* was investigated in collaboration with the Institute of Materials for Electronics and Magnetism – IMEM (National Research Council - CNR, Parma). The OECT biosensor consisted of two main components: a gold gate electrode functionalized with Thiol-ListCapt probe, and a channel electrode made of PEDOT: PSS functionalized textile fiber realized by simply soaking a synthetic fiber of polyester into an aqueous solution of PEDOT: PSS (Clevios™ PH500, Starck GmbH, Cologne, Germany) for 5 min and by baking on a hot plate at 150°C for 2 h. The PEDOT: PSS solution was previously modified with ethylene glycol 20% (Sigma-Aldrich, Milan, Italy) and dodecylbenzene sulfonic acid (DBSA) surfactant 5% (Sigma-Aldrich, Milan, Italy) to enhance its electrical conductivity and to improve film-forming.

2.1.11.2 Gold gate functionalization

For the functionalization reaction, PBS 1X (0.01 M phosphate buffer, 0.0027 M KCl, and 0.137 M NaCl, pH 7.4) was used: a PBS tablet (Sigma-Aldrich, Milan, Italy) was solubilized in 200 mL of sterile bi-distilled water. Both The Thiol-ListCapt probe and the DNA samples were diluted in PBS 1X to proceed with the analysis.

A gold plate was obtained covering a glass slide with a thin (≈ 200 nm) gold evaporated layer. The Thiol-ListCapt probe at 100 ng/ μ L was denatured at 95°C for 10 min and immediately put on ice to avoid renaturation. For functionalization, 10 μ L of 100 ng/ μ L Thiol-ListCapt probe were spotted onto the slide. After 1 h at room temperature, the slide was rinsed twice with sterile bi-distilled water, to remove the probe in excess and PBS salts. Functionalized electrodes were kept in a dryer jar until the hybridization test to protect them from oxidation. The template DNA (genomic DNA of *L. monocytogenes*) was denatured at 95°C for 10 min and immediately put on ice to avoid renaturation. For hybridization, 10 μ L of each sample at 100 ng/ μ L were spotted onto the functionalized surface. After 1 h at 40°C, the gold electrodes gate were rinsed twice with sterile bi-distilled water, to remove the excess DNA. The hybridized electrodes were then air-dried under a sterile laminar flow cabinet and kept in a dryer jar, waiting to be measured.

2.1.11.2 Electrochemical detection

For the electrochemical measurement, the gold electrode (gate) and PEDOT: PSS wire (channel) were put nearby and both immersed in an electrolytic solution. The biosensor components were connected to an SMU – source measure unit (Agilent B2902A Precision Source/Measure Unit; Keysight Technologies, Santa Rosa, CA, USA) by silver cold welding. A constant voltage of -0.1 V was imposed on the channel (from source to drain - VSD). Then, a pulsed voltage ($+0.2$ V/2 min from 0 V to 1 V with 2 min of pause after each step) was imposed on the gate (VG). Both ISD and IG electric current variation in time were measured. Raw data were processed and OECT current response was expressed as current modulation: $\Delta I/I_0 = [(I - I_0)/I_0]$, where I is the maximum ISD current value (for $V_G > 0$ V) and I_0 is the baseline ISD value (for $V_G = 0$ V). The gold plate was placed in a little plastic tray (measurement cell) and the PEDOT: PSS wire was maintained in suspension above it. Both components were immersed in PBS 1X. Electrochemical measurements were carried out on different samples, to understand the electrochemical behavior of the biosensor:

- Non-functionalized gold electrode (bare gold).
- Functionalized but non-hybridized gold electrode (no-template control).
- Hybridized but non-functionalized gold electrode, to verify if DNA can bind gold even without the probe (no-probe control). Reference strains of *L. monocytogenes* were used.
- Decimal dilutions of ssDNA complementary sequence to check the biosensor sensitivity (from 1 ng/ μ L to 10 fg/ μ L).

DNA probe for electrochemical biosensor based on voltammetry construction after aligning *iap* gene sequences of different *L. monocytogenes* serotypes. Considering the serotype prevalence in human listeriosis epidemiology data, a new ListE probe was designed according to the genetic profile of serotypes 1/2b and 4b (lineage I). The in silico tests were conducted using the software Multalin, OlygoAnalyzer, and BLAST.

The probe of 43 bp length, 32.2 % of GC content has a T_m of 59.2°C.

Probes were labeled with digoxigenin at 5' end for the immunological detection in dot blot protocol (DIG-ListCapt and DIG-ListE). For the functionalization of the gold electrode in voltammetry biosensor application, the ListE probe was modified by the addition of a thiol group at 5' end (Thiol-ListE). The probes were synthesized by MWG-Biotech (Ebersberg, Germany). An ssDNA sequence, complementary to the probes, was used as a positive control

in probe sensitivity and optimization of hybridization conditions.

2.1.12 ELECTROCHEMICAL BIOSENSOR BASED ON VOLTAMMETRY

SPAuEs (Screen printed Au Electrodes) purchased from Metrohm-Dropsense (Asturias, Spain) were conditioned by an electrochemical pre-treatment in sulfuric acid and then functionalized. The functionalization step involved the immobilization of the thiol DNA probe on the WE gold surface. Subsequently, the WE gold surface was treated with MCH (6-mercapto-1-hexanol) solution (blocking) to avoid aspecific interaction. CV and DPV measurements were carried out to evaluate the current intensity and after used as a blank signal (ipa blank), then the SPAuEs were washed and target DNA solutions were drop-casted on the WE electrode. Finally, CV and DPV measurements were repeated after hybridization to evaluate the current intensity (ipa sample).

2.1.12.1 ListE probe

The probe (ListE) of 43 bp, with a melting temperature of 79.5°C, was previously also tested with the dot-blot technique before its utilization in the biosensor to guarantee the specificity and to evaluate the hybridization temperature (Beltrame, 2016). A sequence complementary to the capture probe was used as a positive control in both dot blot and biosensor tests.

Before being used for of the functionalizing of the gold surface, the probe must be deprotected at the 5'-end to make the thiol group reactive.

2.1.12.2 SPAuE conditioning

A solution of H₂SO₄ 0.5 M (96% sulfuric acid, Carlo Erba, Milan, Italy) were prepared and 8 ml were taken and transferred into a small electrochemical cell for the SPAuE conditioning procedure. The SPAuE was immersed into the sulfuric acid solution and the electrochemical cleaning consisting of ten voltammetric cycles from 0 to +1.3 V, was performed. After cleaning the SPAuE was washed twice on both sides with 500 µL of bi-distilled water and dried under laminar flux hood.

2.1.12.3 Functionalization

The Au WE of the SPAuE was functionalized using the DNA capture probe (ListE) specific for *Listeria monocytogenes*. The probe was diluted in a phosphate buffer solution 1X (PBS, 0.001M phosphate buffer, 0.0027M KCl e 0.137M NaCl, pH 7.4, Sigma-Aldrich, Milan, Italy) to obtain a final concentration of 10 ng/µL (7.55x10⁻⁴ mM). The probe solution was denatured at 95°C for 10 min and put on ice to avoid renaturation. The SPAuE was functionalized by drop-casting 12 µL (10 ng/µL) of the probe on the WE and incubating overnight at room temperature (RT, 25°C). After the immobilization of the ListE probe, the SPAuE was rinsed twice on both sides with 500 µL of sterile bi-distilled water. Finally, 12 µL of 6-Mercapto-1-hexanol 1 mM (MCH) solution was put on the WE surface and kept for 1 hour at RT. The solution was prepared from

a 100 mM MCH solution in absolute ethanol diluted in PBS 1X to obtain a final concentration of 1 mM. The SPAuE was incubated for 1 hour at RT and then rinsed twice with 500 μ L of sterile bi-distilled water on both sides.

2.1.12.4 Blocking solution

Finally, 12 μ L of 6-Mercapto-1-hexanol 1 mM (MCH) solution was put on the WE surface and kept for 1 hour at RT. The solution was prepared from a 100 mM MCH solution in absolute ethanol diluted in PBS 1X to obtain a final concentration of 1 mM. The SPAuE was incubated for 1 hour at RT and then rinsed twice with 500 μ L of sterile bi-distilled water on both sides. When a DNA probe is used as a recognition element a further step is needed to avoid the presence of free gold areas. Single strand DNAs present a flexible chain with a superficial charge and these characteristics can lead to non-specific adsorptions in areas of free gold (Wang et al., 2017). Consequently, a blocking strategy is required to avoid non-specific interactions. Blocking strategies consist of chemical or physical modifications. The most common chemical modifications involve polymerization, self-assembled monolayer, sol-gel, and metal nanoparticles. While, physical modifications exploit molecules that can bind directly on the surface and create a layer that prevents the non-specific interaction (Contreras-Naranjo et al., 2019). One of the most effective chemical blocking reagents is the 6-Mercapto-1-hexanol (MCH), whose thiol group permits its bound on the gold surface (Rashid et al., 2017).

2.1.12.5 Hybridization of the Compl-ListE and Genomic DNA

Hybridization tests

Five decimal dilutions of the sequence complementary to the capture probe and genomic DNA of *L. monocytogenes* and *L. innocua* were prepared in PBS 1X to obtain the following concentrations: 10 ng/ μ L, 1 ng/ μ L, 100 pg/ μ L, 10 pg/ μ L and 1 pg/ μ L.

The DNA samples were denatured at 95°C for 10 min and immediately put on ice to avoid renaturation. 12 μ L of the denatured samples were deposited on the work electrode surface and incubated for 1 hour and tested at several hybridization temperature.

Then, the SPAuE was rinsed twice on both sides with 500 μ L of sterile bi-distilled water.

The obtained five complementary probe solutions were deposited on the WE surface starting from the low concentration to the high. The concentrations of the target sequences tested are reported in Table 2.5.

Table 2.5. Probe, blocking and DNA target concentration used for the tests.

Capture probe (ListE) concentration (ng/ μ L)	MCH solution concentration (mM)	DNA target concentration
10	10	No template
10	10	1 pg/ μ L
10	10	10 pg/ μ L
10	10	100 pg/ μ L
10	10	1 ng/ μ L
10	10	10 ng/ μ L

This hybridization protocol, reagents, and target concentrations were also adopted for the tests conducted at 40°C and 59.5°C.

Hybridization of genomic DNA at room temperature

To test the DNA extracted from the bacteria, *L. monocytogenes* was used as the target and *L. innocua* was used as the negative control. The protocol used for genomic DNAs was the same used for the sequence complementary to the capture probe.

The DNA was denatured at 95°C for 10 min and immediately put on ice to avoid renaturation. 12 µl were deposited on the WE surface and incubated for 1 hour at RT. The SPAuE was rinsed twice on both sides with 500 µl sterile bi-distilled water and dried. Solutions of genomic DNA of *L. monocytogenes* at different concentrations were deposited on the WE surface starting from the lower concentration. Tests were repeated at three hybridization temperatures, RT°, 25°C and 40°C.

CV and DPV measurements

A 10 mM K₄[Fe(CN)₆]*3H₂O (Sigma Aldrich, Milan, Italy) solution in PBS 1X was prepared. Subsequently, 80 µL of this solution was drop-casted over the SPAuE. After deposition, CV and DPV measurements were carried out. The CVs were performed from -0.2V to +0.6V at 0.1 V/s while DPVs were performed from -0.2V to +0.4V at 0.01 V/s, as reported in Table 2.6.

After CVs and DPVs measurements, the SPAuE was rinsed twice on both sides with 500 µL of sterile bi-distilled water and reused for the hybridization of a higher DNA target concentration. Electrochemical measurements were performed with a computer-controlled µ-AutoLab type II potentiostat run by Nova 2.1 software (EcoChemie, Utrecht, the Netherlands). The data were collected with NOVA 2.1.2 software and the anodic peak current was measured with the same software.

Table 2.6 Staircase cycle voltammetry (CV) and differential pulse voltammetry (DPV) properties.

CV		DPV	
Start potential	-0.2 V	Start potential	-0.2 V
Upper vertex potential	0.6 V	Stop potential	0.4 V
Lower vertex potential	-0.2 V	Step	0.005 V
Stop potential	-0.19756 V	Modulation amplitude	0.15 V
Number of scans	1	Modulation time	0.05s
Scan rate	0.1 V/s	Interval time	0.5s
Step	0.00244V	Scan rate	0.01 V/s

2.2 RESULTS AND DISCUSSION

2.2.1 COLD-SMOKED SALMON SAMPLES

2.2.1.1 Plate count bacterial enumeration

Plate count method results for the enumeration of the total viable count, Enterobacteriaceae, lactic acid bacteria, yeasts, and molds are shown in Table 2.7. CSS samples analyzed immediately after purchasing showed values of total viable count ranging from 2.5×10^4 to 1.3×10^8 CFU/g, lactic acid bacteria from below 2.5×10^4 CFU/g to 9.5×10^6 CFU/g, Enterobacteriaceae were detected in two samples with values of 4.5×10^4 and 4.5×10^3 CFU/g for sample 3.1 and 5.1 respectively. Yeasts ranged from 3.7×10^1 CFU/g to 5.9×10^4 CFU/g, apart for samples 1.1 and 6.1. Molds were below the limit of detection of 25 CFU/g. CSS samples analyzed close to the expiration date showed values of total viable count between 2.4×10^5 CFU/g to 1.8×10^8 CFU/g. Lactic acid bacteria mostly ranged from below 2.5×10^4 to 5.3×10^7 CFU/g. Enterobacteriaceae were detected in three samples, with a maximum value of 2.0×10^4 CFU/g. Yeasts were found in all samples apart for sample 6.1, with values ranging from 2.6×10^2 to 9.9×10^5 CFU/g. Molds were below the limit of detection of 25 CFU/g apart for sample 2.2 with 2.6×10^4 . Samples analyzed at the end of shelf-life showed higher values as expected. CSS8 resulted the most contaminated sample, both at the beginning and at the end of the shelf-life. The data of bacterial contamination, evaluated for CSS samples purchased from local supermarkets, resulted in agreement with the data reported from literature (Gimenez and Dalgaard, 2004; Hansen and Huss, 1998; Huss et al., 1995; Paludan-Müller et al., 1998).

2.2.1.3 Listeria Precis method

The AFNOR validated *Listeria* Precis™ method (NF Validation, 2013) used to detect *L. monocytogenes* allowed to find the bacterium in one out of the 16 samples analyzed, in fact only the sample 5.2 resulted positive for *L. monocytogenes*. These data confirmed the low prevalence of this pathogen as reported in the literature (EFSA, 2015a; 2015b; 2016).

After 24 h of enrichment in ONE Broth-*Listeria* (Oxoid), samples were streaked onto the chromogenic media. On Brilliance *Listeria* agar (Oxoid), all *Listeria* spp. form blue/green colonies as they all possess β -glucosidase to metabolize the chromogen X-glucoside. *L. monocytogenes* and some pathogenic *L. ivanovii* were then differentiated from others *Listeria* spp. by their ability to produce phospholipase C (PLC), that hydrolyzes the lecithin in the medium producing an opaque white halo around the colonies (Figure 2.4).

Table 2.7. Plate count data of CSS samples expressed as Colony Forming Units (CFU)/g.

Sample	Total viable count	Lactic acid bacteria	Enterobacteriaceae	Yeasts	Molds
Samples analyzed immediately after purchasing					
1.1	1.7×10^6	8.7×10^4	$<5^*$	$<25^*$	$<25^*$
2.1	2.4×10^5	8.7×10^4	$<5^*$	3.9×10^4	$<25^*$
3.1	6.0×10^5	$<2.5 \times 10^4^*$	4.5×10^1	7.7×10^2	$<25^*$
4.1	2.5×10^4	$<2.5 \times 10^4^*$	$<5^*$	3.7×10	$<25^*$
5.1	1.2×10^6	6.2×10^4	4.5×10^3	1.8×10^3	$<25^*$
6.1	1.7×10^5	7.5×10^4	$<5^*$	$<25^*$	$<25^*$
7.1	1.3×10^8	9.5×10^6	$<5^*$	5.9×10^4	$<25^*$
8.1	7.2×10^5	1.0×10^5	$<5^*$	3.2×10^4	$<25^*$
Samples analyzed close to expiring date					
1.2	2.4×10^5	$<2.5 \times 10^4^*$	$<5^*$	$7. \times 10^3$	$<25^*$
2.2	6.9×10^7	1.5×10^7	2.0×10^4	9.9×10^5	2.6×10^4
3.2	8.2×10^5	7.5×10^4	$<5^*$	6.9×10^3	$<25^*$
4.2**	3.2×10^6	8.9×10^5	$<5^*$	5.6×10^5	$<25^*$
5.2	1.7×10^6	$<2.5 \times 10^4^*$	5.2×10^1	2.6×10^2	$<25^*$
6.2	1.3×10^6	9.1×10^5	2.3×10^2	$<25^*$	$<25^*$
7.2	1.8×10^8	5.3×10^7	$<5^*$	1.5×10^5	$<25^*$
8.2	1.2×10^6	$<2.5 \times 10^4^*$	$<5^*$	5.8×10^4	$<25^*$

*Detection limit of the method.

**Packaging of sample 4.2 was found defective: plastic film resulted to be unsealed and the product had lost vacuum atmosphere.

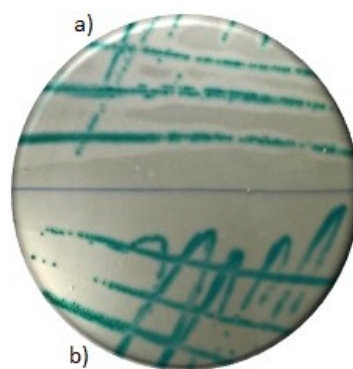


Figure 2.4. Brilliance Listeria agar plate. (a) *L. monocytogenes* 1/2bDISTAM and (b) *L. innocua* DSM20649.

The Oxoid Biochemical Identification System (O.B.I.S.) mono is a rapid colorimetric test for the determination of the enzyme D-alanyl aminopeptidase (DALAase), possessed by all *Listeria* spp. except for *L. monocytogenes*. A positive DALAase reaction rapidly develops a purple color. In the presence of *L. monocytogenes*, no color development is expected, in Figure 2.5 are showing the O.B.I.S. mono test carried out on reference strains of *L. monocytogenes* and *L. innocua* as the negative control. As can be seen, only *L. innocua* developed a clear purple color, while all *L. monocytogenes* strains developed a response comparable to the blank control.

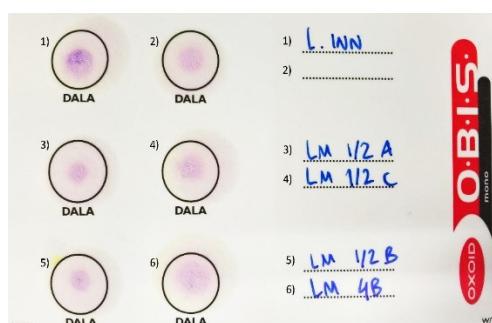


Figure 2.5 O.B.I.S. mono test results. 1) *L. innocua* DSM 20649, 2) Blank control 3) *L. monocytogenes* 1/2a DISTAM, 4) *L. monocytogenes* 1/2c ATCC 7644, 5) *L. monocytogenes* 1/2b DISTAM, 6) *L. monocytogenes* 4b DSM 15675.

O.B.I.S. mono test was applied to five blue/green colonies with halo isolated from CSS sample 5.2, which produced a negative DALAase response confirming their identity as *L. monocytogenes*. For further confirmation, DNA extracted from the isolated strain was subjected to PCR and qPCR with Mar1-MarB primers, leading to positive amplification.

2.2.2 HAM SAMPLES

2.2.2.1 Plate count bacterial enumeration

The plate count method was applied for the raw meat and dry-cured ham, and the results of the total viable count, Enterobacteriaceae, lactic acid bacteria, yeasts, and molds are shown in Table 2.7. Total bacterial contamination of fresh ham and cured ham samples ranged from 2.2×10^3 to 8.5×10^5 CFU/cm². Lactic acid bacteria ranged from 1.7×10^2 to 1.3×10^4 CFU/cm², except for some samples in which their count was below the detection limit. Enterobacteriaceae were detected mainly in fresh ham samples, with a maximum value of 5.0×10^3 CFU/g. Yeasts were found in almost all samples, with counts ranging from 5.9×10^2 to 6.7×10^4 CFU/cm². Molds were not detected.

Table 2.8 Plate count data of ham factories samples expressed as Colony Forming Units (CFU)/cm².

N.	Samples	Tot viable count	Lactic acid bacteria	Enterobacteriaceae	Yeasts	Molds	
1°Sampling	1.1	Raw meat	9.1 X 10 ³	1.9 X10 ³	9.9 X10 ²	6,6 X 10 ²	<130 *
	2.1		2.5X 10 ⁴	7.9 X 10 ³	3.3 X 10	7.4 X 10 ²	<130 *
	3.1		6.6 X 10 ⁴	8.9 X 10 ³	3.3 X 10	6.6X 10 ²	<130*
	4.1		3.2 X 10 ⁴	9. 4 X 10 ³	5.3 X 10 ²	1X 10 ³	<130*
	5.1		3.1 X 10 ⁴	1.3 X 10 ⁴	6.9 X 10 ²	5.9 X 10 ²	<130*
	11.1	Cured ham	1.1 X 10 ⁴	<130*	<33*	1.7 X 10 ³	<130*
	12.1		7.2 X 10 ⁴	<130*	<33*	1.5 X 10 ³	<130*
	13.1		1 X 10 ⁵	<130*	<33*	3.1 X 10 ³	<130*
	14.1		8.5 10 ⁵	<130*	<33*	1.4 X 10 ³	<130*
	15.1		1.6 X10 ⁴	<130*	<33*	<130*	<130*
2° Sampling	1.2	Raw meat	4.7 x 10 ⁴	7.7 x 10 ²	<33*	<130*	<130*
	2.2		2.3 x 10 ⁴	1.6 x 10 ³	<33*	<130*	<130*
	3.2		7.1 x 10 ⁴	1.8 x 10 ³	<33*	<130*	<130*
	4.2		2.5 x 10 ⁴	8.2 x 10 ³	<33*	<130*	<130*
	5.2		1.1 x 10 ⁴	<130*	4.8 x 10 ³	6.6 x 10 ²	<130*
	11.2	Cured ham	3.1 x 10 ⁴	<130*	<33*	<130*	<130*
	12.2		7.7 x 10 ⁴	<130*	<33*	<130*	<130*
	13.2		8.5 x 10 ³	1.7 x 10 ²	<33*	<130*	<130*
	14.2		2.6 x 10 ⁴	4.8 x 10 ³	<33*	<130*	<130*
	15.2		2.2 x 10 ³	<130*	<33*	<130*	<130*

3° Sampling	1.3	Raw meat	8.3 x 10 ⁴	8.3 x 10 ²	5 x 10 ³	<130*	<130*
	2.3		9.6 x 10 ³	1.2 x 10 ³	2 x 10 ³	<130*	<130*
	3.3		1.1 x 10 ⁴	9.9 x 10 ²	2.8 x 10 ³	<130*	<130*
	4.3		1.1 x 10 ⁴	8.32 x 10 ²	8.5 x 10 ²	<130*	<130*
	5.3		1.5 x 10 ⁴	2.7 x 10 ⁴	5.0 x 10 ³	<130*	<130*
	11.3	Cured ham	2.5 x 10 ⁴	<130*	<33*	6.7 x 10 ⁴	<130*
	12.3		5.0 x 10 ⁴	<130*	<33*	2.2 x 10 ⁴	<130*
	13.3		1.5 x 10 ⁴	1.1 x 10 ⁴	<33*	1.8 x 10 ⁴	<130*
	14.3		1.7 x 10 ⁴	<130*	<33*	3.2 x 10 ⁴	<130*
	15.3		3,1 x 10 ³	<130*	<33*	4,3 x 10 ³	<130*

*Detection limit of the method.

2.2.2.2 *Listeria* *Precis*TM method

The AFNOR validated *Listeria* *Precis*TM method (NF Validation, 2013) used on all the gathered 45 samples, allowed the detection of *L. monocytogenes* in six out of the 45 tested samples (Table 2.7). After 24 h of enrichment in ONE Broth-*Listeria* (Oxoid), samples were streaked onto the chromogenic media.

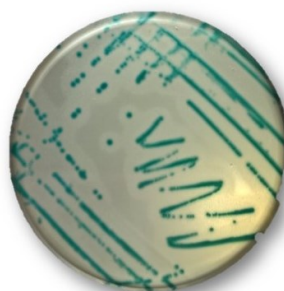


Figure 2.6 Brilliance *Listeria* agar plate. Sample 2.1 (raw meat), positive for the presence for *L. monocytogenes*.

Sample 2.1, 5.1, and 3.3 from fresh ham, sample 7.1, 10.1 and 9.2 from the environment showed an opaque white halo around the colonies (Figure 2.6), thus they were tested with O.B.I.S-mono test.

According to the O.B.I.S. mono test carried out on the suspected colonies, all the six samples that showed the opaque white halo were confirmed *L. monocytogenes*.

For further confirmation, the DNA extracted from the isolated strains were subjected to PCR

and qPCR with Mar1-MarB primers, leading to positive amplification.

Table 2.9 *Listeria* Precis™ method results in 45 ham factories samples. In red the suspected colonies subjected to the O.B.I.S. mono test. + indicates the presence of *L. monocytogenes*, – indicates the absence.

Raw meat samples					Environmental samples					Cured ham samples				
1.1	2.1	3.1	4.1	5.1	6.1	7.1	8.1	9.1	10.1	11.1	12.1	13.1	14.1	15.1
-	+	-	-	+	-	+	-	-	+	-	-	-	-	-
1.2	2.2	3.2	4.2	5.2	6.2	7.2	8.2	9.2	10.2	11.2	12.2	13.2	14.2	15.2
-	-	-	-	-	-	-	-	+	-	-	-	-	-	-
1.3	2.3	3.3	4.3	5.3	6.3	7.3	8.3	9.3	10.3	11.3	12.3	13.3	14.3	15.3
-	-	+	-	-	-	-	-	-	-	-	-	-	-	-

2.2.3 PCR

The couple of primers Mar1-MarB was tested in PCR assay to assess the specificity. A PCR was carried out on DNA from reference strains listed in Table 2.1 at 100 ng/μL. To optimize the protocol an initial annealing temperature of 46°C was tested, but negative controls of *L. ivanovii* and *B. cereus* (lines 8 and 12, Figure 2.7) were amplified suggesting to increase the annealing temperature.

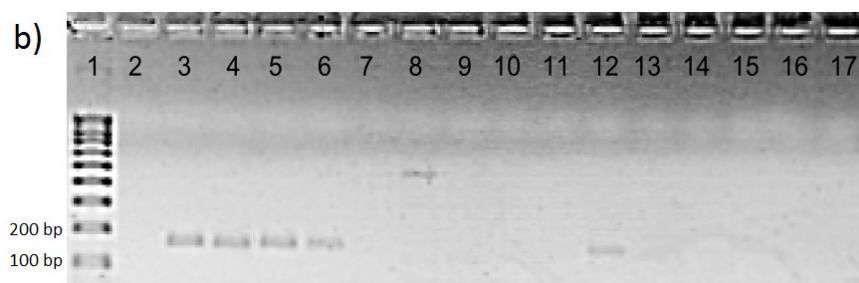


Figure 2.7 PCR specificity with Mar1-MarB couple of primers using positive and negatives controls, T_a 46°C. Line 1, 100 bp DNA ladder (Promega); line 2, NTC; line 3, *L. monocytogenes* 1/2c ATCC 7644; line 4, *L. monocytogenes* 4b DSM 15675; line 5, *L. monocytogenes* 1/2a DISTAM; line 6, *L. monocytogenes* 1/2b DISTAM; line 7, *L. innocua* DSM 20649; line 8, *L. ivanovii* DIAL; line 9, *S. enterica* DSM 9145; line 10, *Enterobacter* spp. DIAL; line 11, *E. coli* DISTAM; line 12, *B. cereus* DSM 2301; line 13, *C. jejuni* DSM 49943; line 14, *Lb. plantarum* ATCC BAA793; line 15, *Lb. paracasei* DSM 5622; line 16, *Lb. rhamnosus* ATCC 53103; line 17, *Lb. brevis* DSM 20054.

A temperature gradient from 47°C, 47.5°C and 48°C was set to define the right annealing temperature. Therefore, PCR was repeated on *Listeria* spp. and negative controls previously amplified. Figure 2.8 shows that the annealing temperature utilized avoided the amplification of *L. ivanovii* and *B. cereus*.

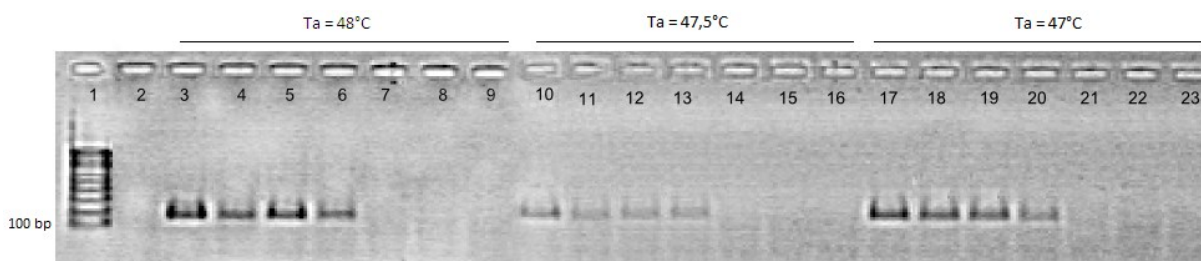


Figure 2.8 Annealing temperature optimization with Mar1-MarB using positive and negatives controls. Line 1, 100 bp DNA ladder (Promega); line 2, NTC. Lines 3-9, T_a 48°C; lines 10-16, T_a 47.5°C; lines 17-23, T_a 47°C. Lines 3, 10, 17, *L. monocytogenes* 1/2c ATCC 7644; lines 4, 11, 18, *L. monocytogenes* 4b DSM 15675; lines 5, 12, 19, *L. monocytogenes* 1/2a DISTAM; lines 6, 13, 20, *L. monocytogenes* 1/2b DISTAM; lines 7, 14, 21, *L. innocua* DSM 20649; lines 8, 15, 22, *L. ivanovii* DIAL; lines 9, 16, 23, *B. cereus* DSM 2301.

Based on these results, Mar1-MarB primers were used at an annealing temperature of 48°C for the subsequent analysis. $MgCl_2$ concentration was optimized too testing three different $MgCl_2$ concentrations: 1.5, 2 and 2.5 mM. The magnesium concentration of 2 mM was chosen to proceed with an annealing temperature of 48°C. After reagent composition optimization, the sensitivity of the primers was assessed. A PCR was carried out on decimal dilutions of *L. monocytogenes* 1/2b DISTAM, (Figure 2.9) producing the expected amplicon of 160 bp, and reaching a sensitivity of 1 pg/ μ L. In conclusion, after protocol optimization, Mar1-MarB primers showed the expected specificity for *L. monocytogenes* reference strains.



Figure 2.9 PCR sensitivity with Mar1-MarB using decimal dilutions of DNA of *L. monocytogenes* 1/2b DISTAM, T_a 48°C. Line 1, 100 bp DNA ladder (Promega); lines 2-10, *L. monocytogenes* 1/2b DISTAM: line 2, 100 ng/ μ L DNA; line 3, 10 ng/ μ L DNA; line 4, 1 ng/ μ L DNA; line 5, 100 pg/ μ L DNA; line 6, 10 pg/ μ L DNA; line 7, 1 pg/ μ L DNA; line 8, 100 fg/ μ L DNA; line 9, 10 fg/ μ L DNA; line 10, 1 fg/ μ L DNA; line 11, NTC.

2.2.3.1 Ham samples analysis

The ham factories samples were tested in PCR analys. The results obtained were confermed with O.B.I.S. mono test as shown in Figure 2.10.

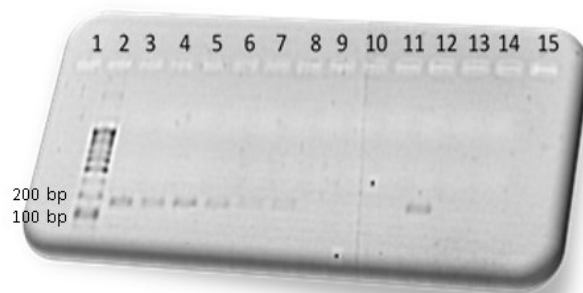


Figure 2.10 PCR results of ham factories samples. Line1-15: line2: 100pb Ladder; line3: n. 2.1 fresh ham; line4: n. 5.1 fresh ham; line5: n. 7.1 environmental sample; line6: n. 10.1 environmental sample; line7:n.9.2 environmental sample; line8:n. 3.3 fresh ham; line9: n. 1.3 fresh ham; line10: n.6.3 environmental sample; line 11: n. 12.3 cured ham; line 12: *L. monocytogenes* ATCC 7644; line 13: *L. innocua* DM 20649; line 14: blank

2.2.4 qPCR

Before testing DNA extracted from CSS samples with and without enrichment and from the isolate from sample 5.2, a standard curve was built with a serial decimal dilution of the DNA of the reference strain of *L. monocytogenes* 1/2b DISTAM.

1.2.4.1 Standard curve

Data obtained for the samples are reported in Table 2.9. Two samples were not included in the standard curve analysis due to irregular amplification curves (100 ng/ μ L and 10 pg/ μ L concentrations). Considering approximately 3 fg DNA the content of a cell of *L. monocytogenes*, the dilution at 1 fg/ μ L was expected not to produce an amplicon. From samples amplification curves (Figure 2.11), Rotor-Gene Q Series Software 2.0.2 (Build 4; Qiagen) auto-found the threshold value. The standard curve built (Figure 2.12) included DNA concentrations down to 10 fg/ μ L, corresponding to the sensitivity of the assay. The standard curve parameters are $R^2=0.997$, a slope of -2.956, which corresponds to an efficiency of 117%. Although this value is not considered as optimal, Vieira et al. (2013) obtained good results with an efficiency of 117%.

Table 2.10 Results of *L. monocytogenes* 1/2b DISTAM, samples identification and quantitation data (*Threshold cycle).

#	Col	Name	C _T *	Given Conc (ng/μl)	Calc Conc (ng/ μl)	%Var
2		<i>L. monocytogenes</i> 1/2b 10 ng/μL	19.27	10.000000	10.376867	3.8%
3		<i>L. monocytogenes</i> 1/2b 1 ng/μL	22.34	1.000000	0.952431	4.8%
4		<i>L. monocytogenes</i> 1/2b 100 pg/μL	25.52	0.100000	0.080347	19.7%
6		<i>L. monocytogenes</i> 1/2b 1 pg/μL	30.50	0.001000	0.001654	65.4%
7		<i>L. monocytogenes</i> 1/2b 100 fg/μL	34.25	0.000100	0.000090	10.4%
8		<i>L. monocytogenes</i> 1/2b 10 fg/μL	37.27	0.000010	0.000008	15.0%
9		<i>L. monocytogenes</i> 1/2b 1 fg/μL		0.000001		
10		NTC				

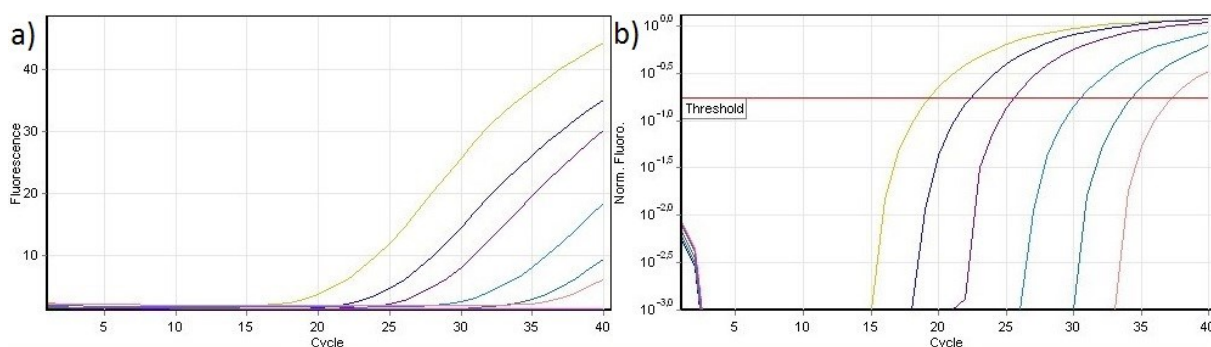


Figure 2.11 qPCR of decimal dilutions of *L. monocytogenes* 1/2b DISTAM. (a) Raw fluorescent signal vs. number of cycle. (b) Normalized fluorescent signal vs. number of cycle and individuation of the threshold value. C_T (threshold cycle) correspond to the cycle at which the template DNA reach the set threshold value. Fluorescence acquisition was performed during annealing/extension step of the amplification.

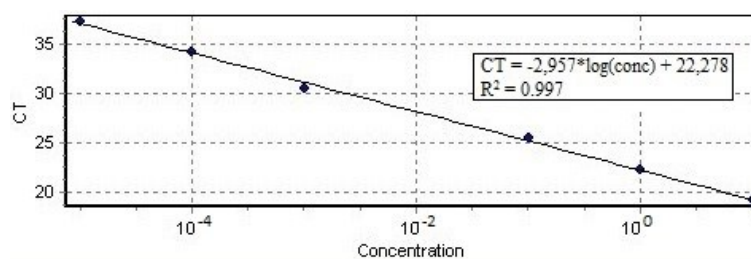


Figure 2.12 Standard curve of *L. monocytogenes* 1/2b DISTAM. The curve was obtained plotting the threshold cycle (C_T) of each DNA dilution vs. the initial DNA concentration (ng/μl). The standard curve equation obtained can be used to calculate the concentration of unknown DNA samples on the basis of their C_T values.

At the end of the cycling program, the melting curve analysis was performed in order to verify the nature of produced amplicons. Melting temperatures of produced amplicons (curve peaks) and melting curve analysis are reported in Table 2.11 and Figure 2.13, respectively. As can be seen, all samples produced comparable melting curves with the same T_m.

Table 2.11 Melting data of decimal dilutions of *L. monocytogenes* 1/2b DISTAM.

#	Col	Name	T _m (°C)
1	Red	<i>L. monocytogenes</i> 1/2b 100 ng/μL	79.75
2	Yellow	<i>L. monocytogenes</i> 1/2b 10 ng/μL	79.75
3	Blue	<i>L. monocytogenes</i> 1/2b 1 ng/μL	79.75
4	Purple	<i>L. monocytogenes</i> 1/2b 100 pg/μL	79.75
5	Pink	<i>L. monocytogenes</i> 1/2b 10 pg/μL	79.85
6	Cyan	<i>L. monocytogenes</i> 1/2b 1 pg/μL	79.75
7	Teal	<i>L. monocytogenes</i> 1/2b 100 fg/μL	79.85
8	Orange	<i>L. monocytogenes</i> 1/2b 10 fg/μL	79.75
9	Green	<i>L. monocytogenes</i> 1/2b 1 fg/μL	
10	Magenta	NTC	

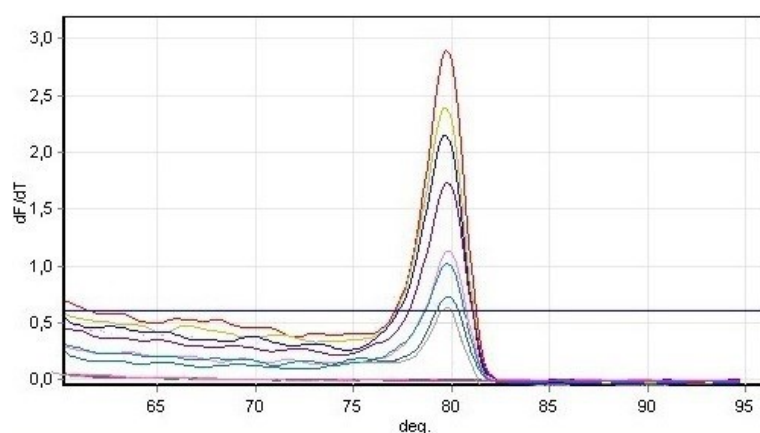


Figure 2.13 Melting curve analysis of decimal dilutions of *L. monocytogenes* 1/2b DISTAM. Decrease in fluorescent signal (expressed as dF/dT) is plotted against temperature (°C).

2.2.4.2 Specificity

To confirm the specificity of primers at qPCR amplification conditions an experiment was carried out using DNA extracted from the reference strains listed in Table 2.12 at 10 ng/μL. *L. monocytogenes*. The signal of the amplification is presented in Figure 2.14 and the analysis of the melting temperature is presented in Table 2.12 and Figure 2.15.

Table 2.12 qPCR of positive control and quantitation data (*Threshold cycle).

#	Col	Name	C _T *	Given Conc (ng/μl)	Calc Conc (ng/μl)
1	Red	<i>L. monocytogenes</i> 1/2c ATCC 7644	17.05	10	9.102275998
2	Yellow	<i>L. monocytogenes</i> 1/2a DISTAM	17.01	10	9.516041781
3	Blue	<i>L. monocytogenes</i> 1/2b DISTAM	16.94	10	10.142473766
4	Purple	<i>L. monocytogenes</i> 4b DSM 15675	16.26	10	18.264559770
16	Light Blue	NTC		10	

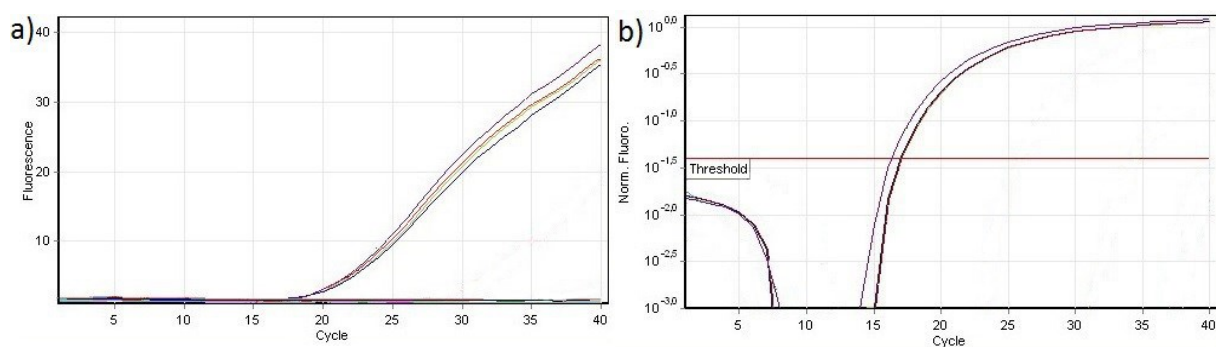


Figure 2.14 qPCR of positive control. (a) Raw fluorescent signal vs. number of cycle. (b) Normalized fluorescent signal vs. number of cycle and individuation of the threshold value. Fluorescence acquisition was performed during annealing/extension step of the amplification.

Table 2.13 Melting data of positive controls.

#	Col	Name	T_m (°C)
1	Red	<i>L. monocytogenes</i> 1/2c ATCC 7644	79.60
2	Yellow	<i>L. monocytogenes</i> 1/2a DISTAM	79.60
3	Blue	<i>L. monocytogenes</i> 1/2b DISTAM	79.75
4	Purple	<i>L. monocytogenes</i> 4b DSM 15675	79.40
16	Light Blue	NTC	

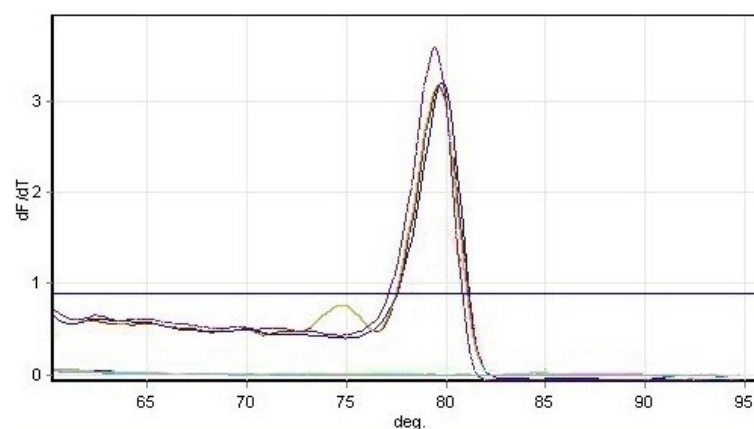








Figure 2.15 Melting curve analysis of positive controls. Decrease in fluorescent signal (expressed as dF/dT) is plotted against temperature (°C).

2.2.4.3 qPCR food sample analysis

DNA extracted from CSS samples (CSS_{SPW} and CSS_{ENR}) at 10 ng/μL was subjected to qPCR with Mar1-MarB primers. *L. monocytogenes* was not detected in samples analyzed immediately after purchasing, confirming the negative results of *Listeria* Precis[™]. Table 2.13 reports the data obtained by qPCR for CSS samples 5.1 and 5.2 in comparison with *L. monocytogenes* reference strains. Samples quantitation was performed using the standard curve (Figure 2.16). Melting curve analysis confirmed the amplicon specificity (Table 2.14 and Figure 2.17).

L. monocytogenes was successfully detected in CSS sample 5.2 (sample analyzed at the end of shelf-life) which was already considered positive using the *Listeria* Precis™ method.

Table 2.14 CSS sample 5.2 qPCR, samples identification and quantitation data (*Threshold cycle).

#	Col	Name	C _T *	Given Conc (ng/μl)	Calc Conc (ng/μl)
5		CSS 5.1 _{SPW}			
13		CSS 5.2 _{ENR}	25.61		0.052370135
17		<i>L. monocytogenes</i> CSS 5.2	19.60		9.545528969
18		<i>L. monocytogenes</i> 1/2b DISTAM	19.56	10	10
19		<i>L. innocua</i> DSM 20649			
20		NTC			

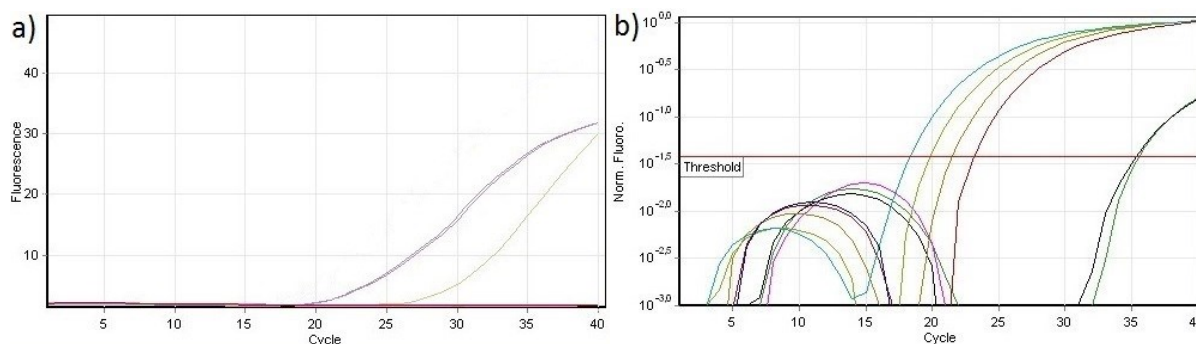








Figure 2.16 qPCR analysis of CSS sample 5.2. (a) Raw fluorescent signal vs. number of cycle. (b) Normalized fluorescent signal vs. number of cycle and individuation of the threshold value. Fluorescence acquisition was performed during annealing/extension step of the amplification.

Table 2.15 Melting data of CSS sample 5.2.

#	Col	Name	T _m (°C)
5		CSS 5.1 _{SPW}	
13		CSS 5.2 _{ENR}	79.90
17		<i>L. monocytogenes</i> CSS 5.2	79.90
18		<i>L. monocytogenes</i> 1/2b DISTAM	79.90
19		<i>L. innocua</i> DSM 20649	
20		NTC	

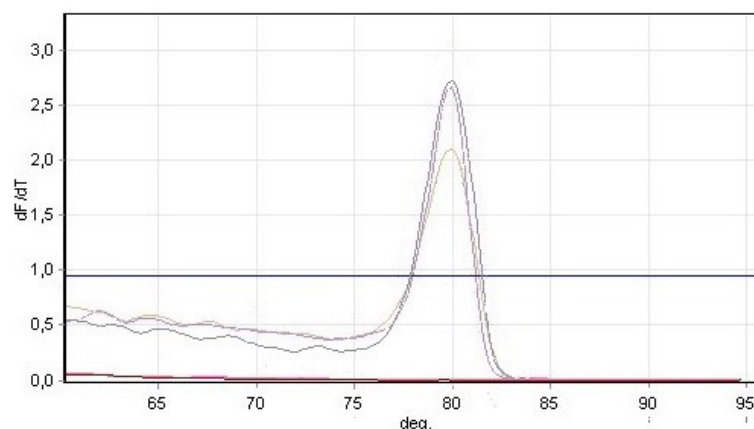


Figure 2.17 Melting curve analysis of CSS sample 5.2. Decrease in fluorescent signal (expressed as dF/dT) is plotted against temperature (°C).

Mar1-MarB primers used in qPCR were able to detect *L. monocytogenes* in a heterogeneous DNA directly extracted from a complex food matrix as cold-smoked salmon. qPCR results were also confirmed by carrying out an endpoint PCR on the same samples.

2.2.5 CaptList DNA PROBE

2.2.5.1 Dot Blot

ListCapt probe (Fontanot, 2014) showed a sensitivity of 1 ng / μ L using a probe concentration of 200 ng/ μ L (Figure 2.18).

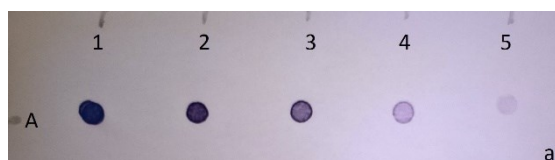
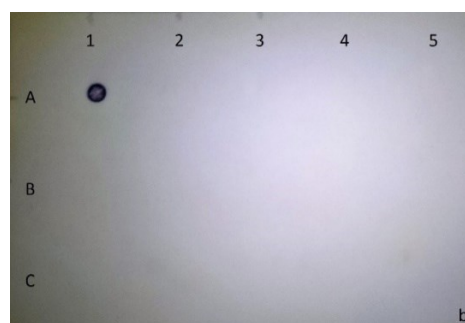


Figure 2.18 Dot blot sensitivity with DIG-ListCapt probe at 200 ng/ μ L, hybridization temperature 40°C. Row A, ssDNA complementary probe, A1: 100 ng/ μ L; A2: 50 ng/ μ L; A3: 25 ng/ μ L; A4: 10 ng/ μ L; A5: 1 ng/ μ L.

No visible spots appeared for any negative control, confirming the specificity of the assay (Figure 2.19).

Figure 2.19 Dot blot specificity with DIG-ListCapt probe at 200 ng/ μ L using negative controls (100 ng/ μ L), hybridization temperature 40°C. Row A, A1: ssDNA complementary probe 100 ng/ μ L; A2: *L. innocua* DSM 20649; A3: *L. ivanovii* DIAL; A4: *S. enterica* DSM 9145; A5: *Enterobacter* spp. DIAL. Row B, B1: *E. coli* DISTAM; B2: *B. cereus* DSM 2301; B3: *C. jejuni* DSM 49943; B4: *Lb. plantarum* ATCC BAA793; B5: *Lb. paracasei* DSM 5622. Row C, C1: *Lb. rhamnosus* ATCC 53103; C2: *Lb. brevis* DSM 20054.



2.2.5.2 Atomic Force microscopy

This analysis was performed in collaboration with the Department of Chemistry Physics and Environment at the University of Udine.

The probe was labeled with a Thiol group at 5' end to allow the immobilization on the Au surface. The functionalized gold surface was confirmed using data obtained by topography, and Volta potential map analysis conducted by Atomic Force Microscopy (AFM) on the slides, confirmed the modification of the surface after functionalization.

Figure 2.20 a) shows the topography of the bare Au surface with an area 300 x 300 nm and the corresponding roughness (RA) of 0.506 nm. Figure 2.20b shows the topography of the slide Au surface (300x 300 nm) after functionalization and the corresponding RA of 21.688 nm. Figure 2.20c) shows a detail (100x 100 nm) of the Au surface after the hybridization of the DNA template with the probe. The topographic map evidences the increase of the roughness at the addition of DNA on the Au surface of the slide.

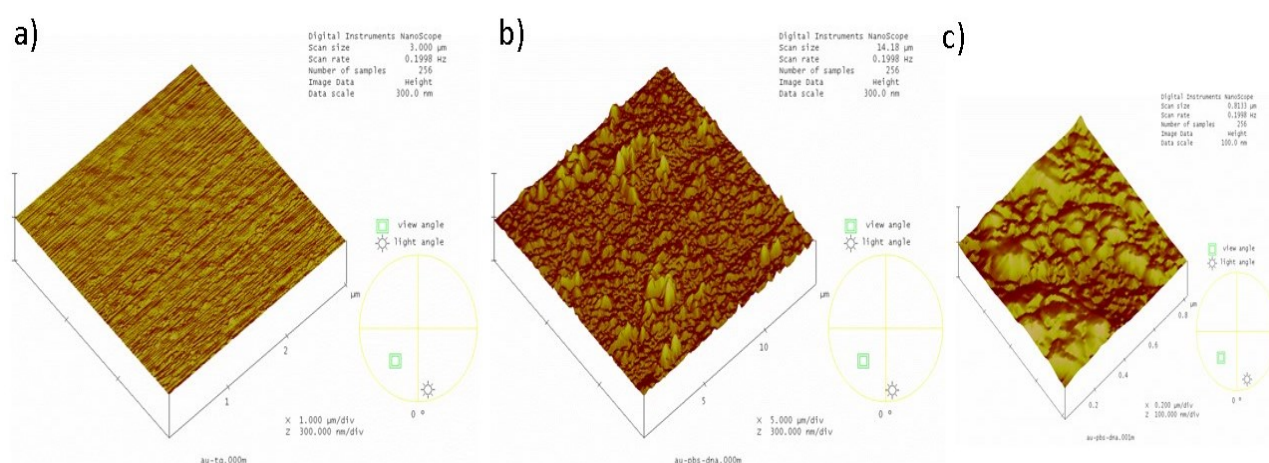


Figure 2.20 AFM roughness (RA) image. In a) bare Au surface and in b) after functionalization with ListCapt and hybridization with DNA *L. monocytogenes* and in c) a detail of the surface hybridized.

The Volta potentials were acquired for an area of 30 μ m² before the functionalization (Figure 2.21a), after functionalization (Figure 2.21b), after hybridization of the probe using DNA of *L.*

innocua (Figure 2.21c) as the negative control, and after hybridization with DNA of *L. monocytogenes* (Figure 2.21d) positive target. The Volta potential maps show that the hybridization of DNA (Figure 2.21d) produces bright contrast. Moreover, the Volta potential difference between two areas of the Au surface of the slide changes. The value of the difference between two points of the bare gold surface was 0.051 mV, after functionalization, the Volta potential difference between the red and yellow area was 16.796 mV, T the Volta potential acquired after hybridization with the negative control, *L. innocua* DNA, between the yellow and red areas was 18.052 mV. The higher difference between the yellow and red areas after hybridization was obtained with the positive target (DNA of *L. monocytogenes*) with a value of 56.867 mV. These data confirm that the activity of the addition of DNA onto the gold surface produced increasing differences between areas of the gold surface measured as Volta potential.

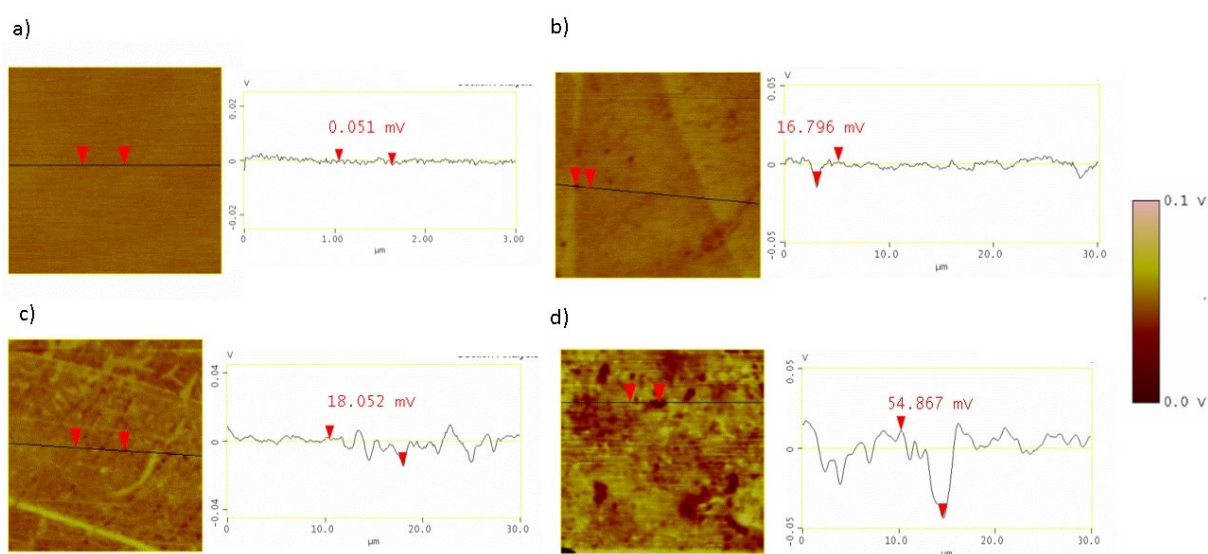


Figure 2.21 Characterization of Au electrode surface, before and after modification by AFM. a) Volta potential map of bare Au surface (left) and the topographic line scan across the line shown in the volta potential map (right); b) Volta potential map of Au surface functionalised by ListCapt (left) and the topographic line scan across the line shown in the volta potential map (right). c) Volta potential map of Au surface functionalised by ListCapt and hybridized with *L. innocua* DNA (left) and the topographic line scan across the line shown in the volta potential map (right). d) Volta potential map of Au surface functionalised by ListCapt and hybridized with *L. monocytogenes* DNA (left) and the topographic line scan across the line shown in the volta potential map (right).

The SKFPPFM measurements were complemented by surface characterization by means of SEM –EDXS. EDXS spectra acquired on the functionalized surface are represented in Figure 2.21. The chemical composition of two measured areas corresponding to spectrum 1 and spectrum 2 in Figure 2.21a. The presence of Carbon depends on the amount of DNA probe present on the gold surface after functionalization as the probe, low level of Na^+ , Cl^- , K^+ come from the residue of buffer PBS used, Si, Ti and Au come from the coverslip slide.

The data reported in Figure 2.22b demonstrates the presence of DNA on the gold surface, confirming that the functionalization step was successful.

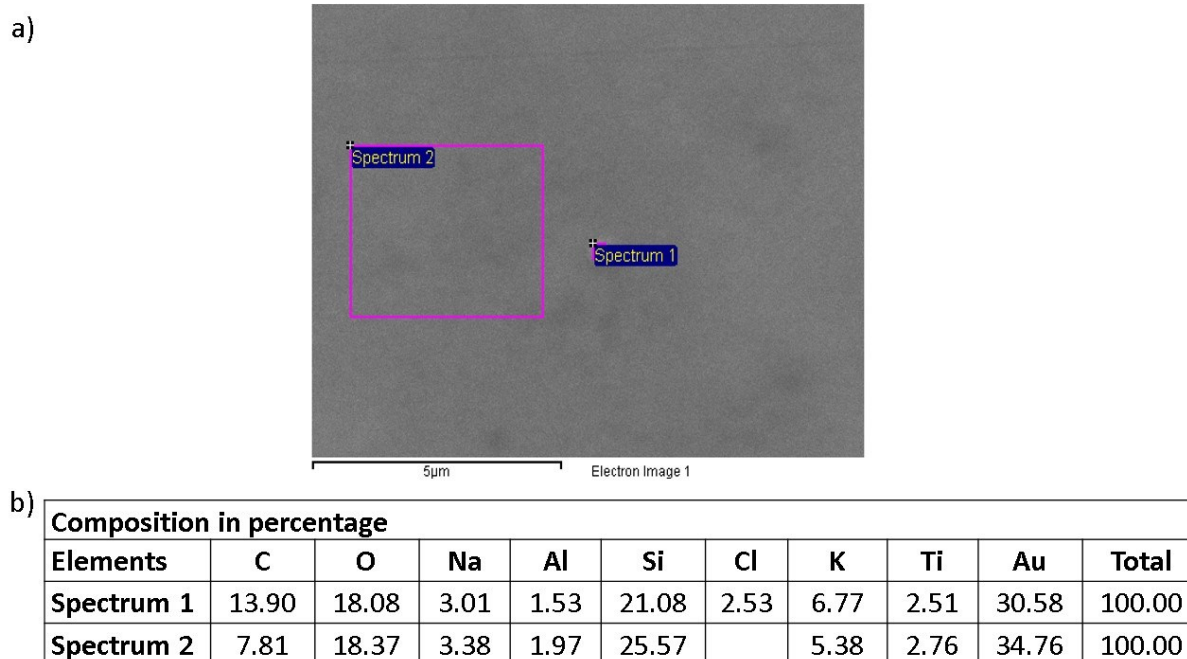


Figure 2.22 SEM-EDXS image and data. In a) the two area analyzed corresponding to spectrum 1 and 2. In b) the chemical composition of the two area expressed in percentage.

2.2.5.3 OECT biosensor

The specific ListCapt probe, modified with a thiol group at 5' end, was used to develop an electrochemical DNA-biosensor based on OECT. Previously, this kind of device was employed for the detection and quantitation of different analytes in an electrolytic solution, as salt concentration in sweat (Tarabella et al., 2012). In this work, the same system was used to detect a target DNA hybridized to the ListCapt probe, previously immobilized onto the gold gate electrode. The essential components of an OECT are an organic p-type semiconductor (PEDOT: PSS channel) with source and drain contacts, an electrolyte, and a gate electrode. Upon the application of a positive gate voltage (V_G), cations in the electrolyte are forced towards the PEDOT: PSS. The number of the available carriers in the semiconductor will be depleted and the source-drain current (I_{SD}) decreases (Bernards and Malliaras, 2007). As reported by Lin et al. (2011), the sensing mechanism of this type of DNA-biosensor may be attributed to the modulation of the surface potential of the gate electrode induced by the immobilization and the hybridization of DNA molecules on the gate surface. It was supposed that the presence of a molecule immobilized onto the gate surface may hamper the current flow between gate and electrolyte. Moreover, the inherent negative charge of DNA may entrap cations by electrostatic attraction, thus decreasing the number of cations that reach the semiconductor. Because of these two hypothesized mechanisms, in the presence of a DNA molecule (ssDNA probe) immobilized onto the gate electrode, a higher I_{SD} signal should be registered in comparison to the bare gold gate. For the same reason, a dsDNA (probe-template hybrid) should lead to an even higher signal than ssDNA. In their work, Lin et al. (2011) have successfully detected the DNA probe immobilization on gold and its hybridization with a complementary DNA sequence, registering

a horizontal shift of the measured ISD signal in function of the gate voltage applied.

In the exposition of the subsequent results, the ListCapt probe will be named ssDNA, while the probe-template hybrid will be named dsDNA, to distinguish the response of the OECT device due to a single DNA strand immobilized onto the gate electrode, or to a double DNA strand after the hybridization of the probe with the target sequence.

The measurements were carried out using glass slides of $\approx 3 \text{ cm}^2$ covered with a thin layer of gold as the gate electrode. A grid was drawn on the glass slide with a diamond tip pencil, to separate the areas for the deposition of the samples. After the functionalization of the areas of the grid with the Thiol-ListCapt probe, different samples were spotted in each sector and hybridized (2.23).

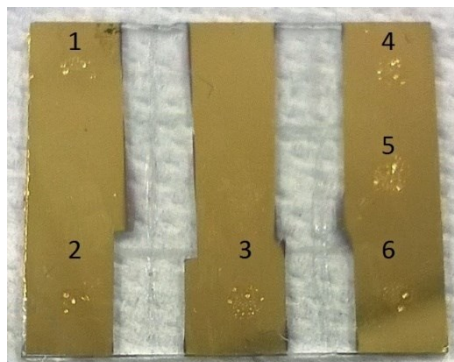


Figure 2.23 Gold slide electrode hybridized samples: 1) bare gold; 2) no-template control; 3) complementary sequence, 100 ng/ μL ; 4) *L. monocytogenes* ATCC 7644, 100 ng/ μL ; 5) *L. innocua* DSM 20649, 100 ng/ μL ; 6) *Lb. plantarum* ATCC BAA-793, 100 ng/ μL .

In order to carry out the electrochemical detection, each hybridized DNA was covered with a drop of sterile water, in which the PEDOT: PSS wire was also immersed. With the application of the pulsed voltage at the gold gate electrode (V_G , Figure 2.24), a current variation of gold gate (IG) and PEDOT: PSS channel (ISD) was detected, as shown in Figure 3.26 where variation during the analysis time of IG (Figure 2.25a) and ISD (Figure 2.25b) are plotted.

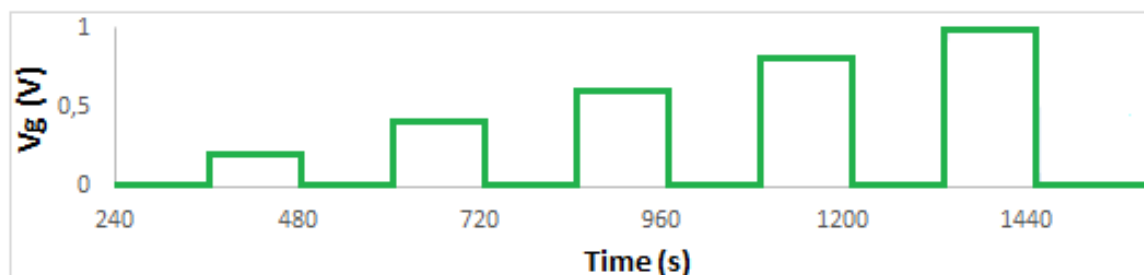


Figure 2.24 Applied gate voltage (V_G) vs time. A series of increasing gate voltages from 0.2 V to 1V has been applied (120 s/step), increasing the voltage of 0.2 V at every step with alternated steps at 0 V.

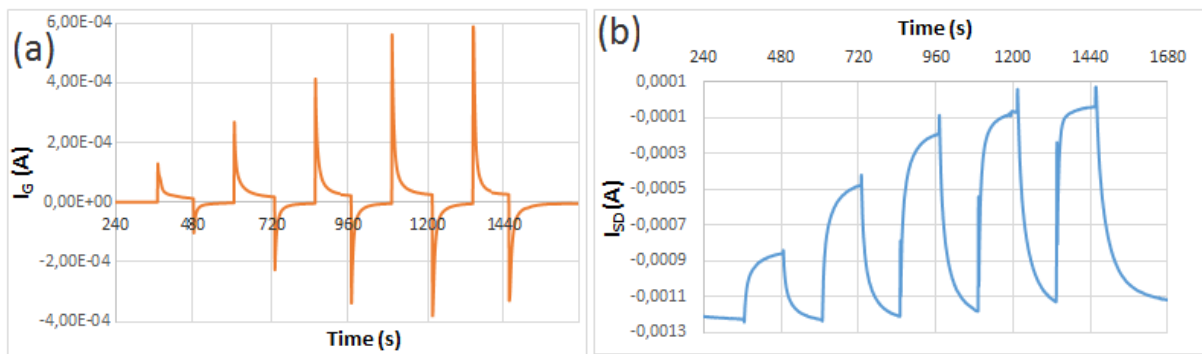


Figure 2.25 Raw current signal. (a) Gate current signal (I_G) vs. time for increasing gate voltages: the current signal represents the current flowing from gate to electrolytic solution; it is influenced by gold gate surface properties. (b) Channel source-drain current signal (I_{SD}) vs. time for increasing gate voltages: the current signal represents the variation of the current flowing through the PEDOT: PSS wire, due to the absorption of cations from the electrolytic solution that leads to the depletion of charge carriers of the semiconductor.

Processing the raw data, the modulated current response $[I - I_0/I_0]$ vs. V_G were obtained. I is the maximum I_{SD} current value (for $V_G > 0$ V) and I_0 is the baseline I_{SD} value (for $V_G = 0$ V). In Figure 2.26 differences between bare gold, gold gate electrode functionalized with the probe (ssDNA) and hybridization with complementary sequence (dsDNA) are shown. As can be noticed, for $V_G < 0.9$ V, ssDNA, and dsDNA produced an increased signal compared to bare gold, confirming the mechanisms hypothesized and the results reported by Lin et al. (2011). However, at higher V_G , the relationship among samples changed; this is maybe due to some modifications of the functionalized surface induced by the voltage applied. Therefore, for further analysis, a gate voltage range below 1 V was considered.

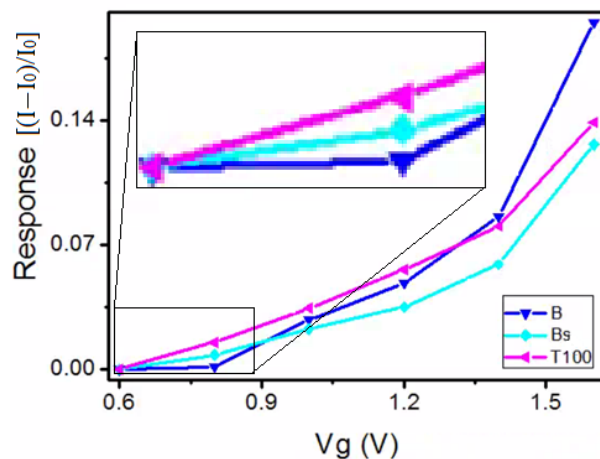


Figure 2.26 I_{SD} modulated response vs. gate voltage applied. For $V_G < 0.9$ V, the lower response is generated by the bare gold gate (B). The ListCapt probe immobilization onto the gold surface (Bs, ssDNA) generated an increased signal. A further signal increasing is generated by the hybridization of the probe with its complementary sequence at 100 ng/ μ L (T100, dsDNA). Inset plots highlights the curve shifts (Beltrame, 2016).

Signal differences between DNA samples of reference strains were also examined. A comparison between *L. monocytogenes* 1/2c ATCC 7644, *L. innocua* DSM 20649 and *Lb. plantarum* ATCC BAA-793 was carried out (Figure 2.27). It can be clearly seen that *L. monocytogenes* (positive target) generated a separate curve from curves produced by negative controls (*L. innocua* and *Lb. plantarum*), thus making it possible to obtain a clear identification of the target using the signals.

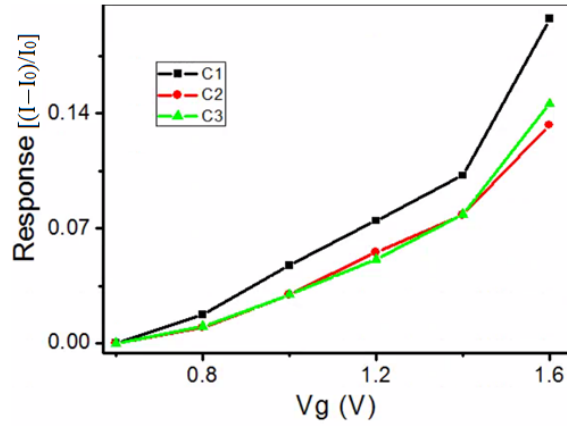


Figure 2.27 I_{SD} modulated response vs. gate voltage. C1: *L. monocytogenes* 1/2c ATCC 7644, 100 ng/ μ L; C2: *L. innocua* DSM 20649, 100 ng/ μ L; C3: *Lb. plantarum* ATCC BAA-793, 100 ng/ μ L. The hybridization of the ListCapt probe with the target sequence of the positive control (*L. monocytogenes*) generated a greater signal compared to the two negative controls (*L. innocua* and *Lb. plantarum*), that does not hybridize with the specific probe (Beltrame, 2016).

Tests using smaller ($\approx 1 \text{ cm}^2$) glass slides covered with gold for the deposition of a single sample were used. The measurement system was also modified: a multi-channel device for the simultaneous detection of 12 samples was tested. A PEDOT: PSS wire and a gold plate electrode were connected by silver cold welding at each channel of the device. Gold electrodes, placed in little plastic trays (measurement cell), were immersed together with the PEDOT: PSS wire in the electrolytic solution for measurements (Figure 2.28). In this second experiment, PBS 1X was used as an electrolytic solution to improve the measured signal.

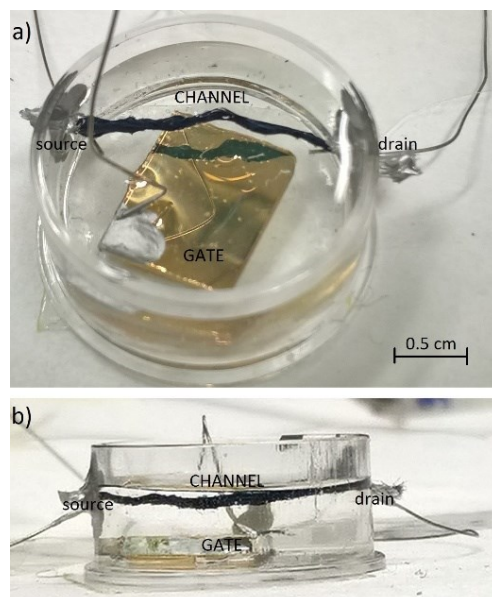


Figure 2.28 Electrochemical measurement cell. View from above (a) and view from the side (b) of the measurement system. Both gate electrode and PEDOT: PSS wire are immersed in PBS 1X and connected to the SMU by silver cold welding (Beltrame, 2016).

Usually, in OECT devices, only the I_{SD} signal is analyzed, as a concentration of ions in the electrolyte solution is measured. In the experiment performed using glass slides covered with gold for the deposition of a single sample the gate electrode was modified and acted as the biological recognition system of the biosensor. Therefore, a series of measurements were carried out to understand the behavior of the gold gate after probe functionalization (ssDNA) or template hybridization (dsDNA). The differences in I_G signal for bare gold, ssDNA, and dsDNA upon V_G application are shown in Figure 2.29. The functionalization with the List Capt probe (ssDNA) caused a drop in the registered I_G , probably due to a higher gate resistance in the presence of the immobilized DNA molecules (Figure 2.29a). The no-probe control, i.e. a DNA template hybridized onto a non-functionalized gold gate electrode, produced a response comparable to bare gold (Figure 2.29b), confirming the absence of a direct bond between the gold surface and the DNA template in the absence of the probe. The hybridization of the probe with its complementary sequence (dsDNA) produced a greater shift compared to the non-hybridized probe (ssDNA), as expected (Figure 2.29)

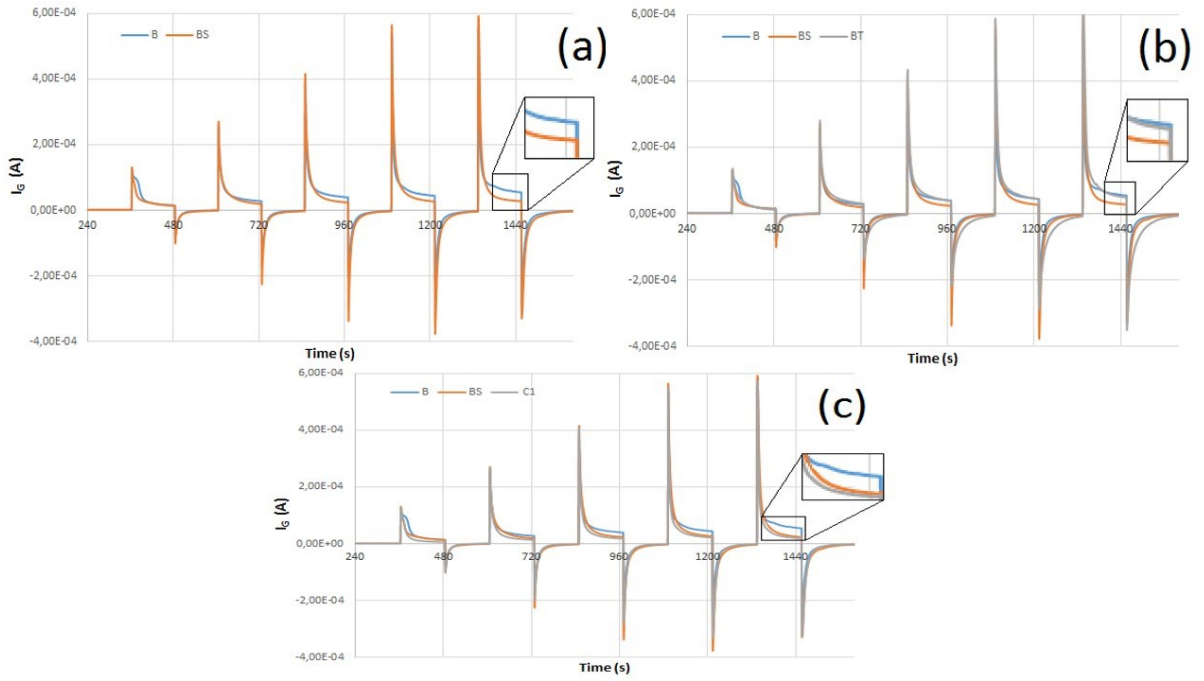


Figure 2.29 Behaviour of the gold gate (I_g) in time for increasing gate voltages, comparison between different immobilized samples. (a) Comparison between bare gold (B) and no-template control (Bs), i.e. the ListCapt probe immobilized onto the gold surface (ssDNA). (b) Comparison between bare gold (B), no-template control (Bs) and no-probe control (Br), i.e. a non-functionalized gold electrode hybridized with the DNA template. (c) Comparison between bare gold (B), no-template control (Bs) and complementary sequence at 1 ng/μL (C1), i.e. probe-template hybrid immobilized onto the gold surface dsDNA. Inset plots highlights the curve shifts (Beltrame, 2016).

After gate characterization, PEDOT: PSS channel response (I_{SD}) was analyzed comparing bare gold surface (control) and the gold surface-functionalized with the ListCapt probe (ssDNA). I_{SD} raw data were processed to obtain the modulated response $[I - I_0/I_0]$ vs. V_G shown in Figure 2.30. As reported in a previous experiment, probe immobilization onto the gold gate produced an increased signal compared to bare gold, confirming the hypothesized effect of modification of the gate surface potential due to the negative charge of DNA molecules. Decimal dilutions (from 1 ng/μL to 10 fg/μL) of the sequence complementary to the ListCapt probe were used as targets with the aim to evaluate the sensitivity of the device. Unfortunately, as shown in Figure 2.31, it was not possible to obtain clear separate signals for different concentrations of the target. This could be due to the short length of the sequence used as a target, that could have had a small modification of the surface with a consequent small variation of the signal produced.

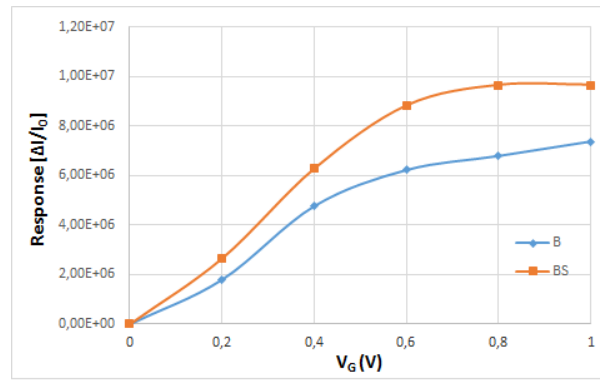


Figure 2.30 I_{SD} modulated response vs. gate voltage applied. As in the first experiment, the ListCapt probe immobilization onto the gold surface (BS, ssDNA) generated a greater signal than the bare gold gate (B) (Beltrame, 2016).

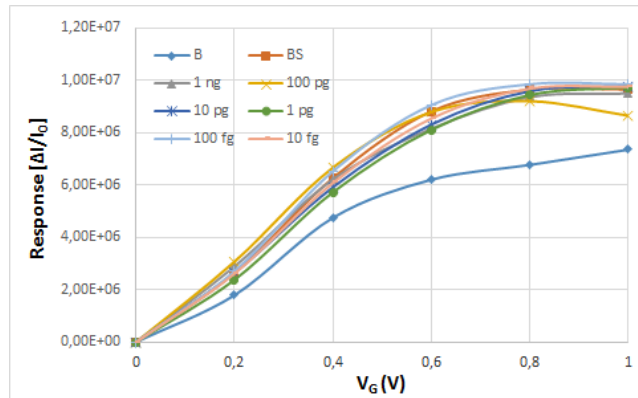


Figure 2.31 I_{SD} modulated response vs. gate voltage applied. B: bare gold control; BS: no-template control (ssDNA); decimal dilutions of complementary sequence (from 1 ng ng/ μ L to 10 fg/ μ L) (Beltrame, 2016).

One additional consideration concerns the construction of the single measurement cells that were hand-built immediately before the analysis, and lacked standardization. Differences in PEDOT: PSS wire length, the distance between semiconductor and gold gate, and gold surface characteristics may have affected the device response. Moreover, a signal could also have been generated by the silver paste used for welding, also immersed in the electrolyte solution. Standardization in the construction of the device is clearly necessary. PBS concentration should also be optimized, as the too high ions concentration of the buffer may have masked the DNA signal so that the response can be due to the salts in solution. For further analysis, a lower concentrated buffer should be considered. Another problem was represented by the limited functionalized gold surface, as only 10 μ L of DNA probe and sample were spotted in the middle of each gold plate. For the last experiment the gold gate was fully immersed in the electrolytic solution, the registered signal was produced by the entire gold surface. In fact, as previously reported (Cicoira et al., 2010; Lin et al., 2010; Bernards and Malliaras, 2007), the gate surface area and the interface between the gate and the electrolyte solution can influence OECT performances. For further analysis, a smaller gate should be tested, to avoid a high background signal. Considering the information obtained from the previous experiments a new test was conducted

optimizing the PBS concentration using PBS 1X diluted at 1:100. The functionalization of the gold surface was carried out with 50 μL of Thiol ListCapt probe at 100 ng/ μL and for the hybridization 100 μL of the solution containing the DNA target was used to cover the entire electrode.

Sensitivity test

In Figure 2.32a, is represented the I_{SD} modulate response blotted versus the voltage applied. The calibration curve was obtained with the whole DNA of *L. monocytogenes* at concentrations of 100 pg/ μL , 10 pg/ μL and 1 pg/ μL . The evaluation of the behavior of the I_{SD} was analyzed considering a voltage range between 0.8 to 1 (V) reported in detail in Figure 2.32b. Data show that there is a proportional increase of the source-drain current signal with the increase of immobilized DNA on the gate surface; compared to a functionalized surface (black curve). Considering the range tested the system seems to be able to detect a low concentration such as 1 pg/ μL .

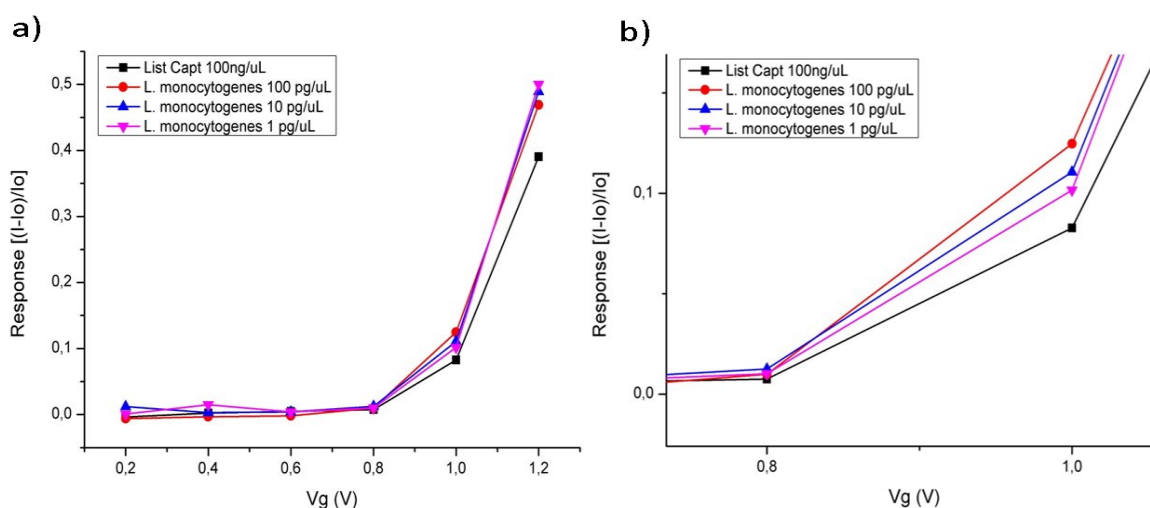


Figure 2.32 Calibration curve with *L. monocytogenes* whole DNA (a); And a detail of the curves from 0.8 to 1 Vg (V) (b).

Specificity test

Figure 2.33 shows the results of the specificity test carried out with the whole DNA of *L. innocua* (negative control) at 100 ng/ μL and *Lb. plantarum* (negative control) at 100 ng/ μL . There is no difference between the signals produced by the two negative controls that to differentiate from the signal of the Thiol ListCapt probe, as expected.

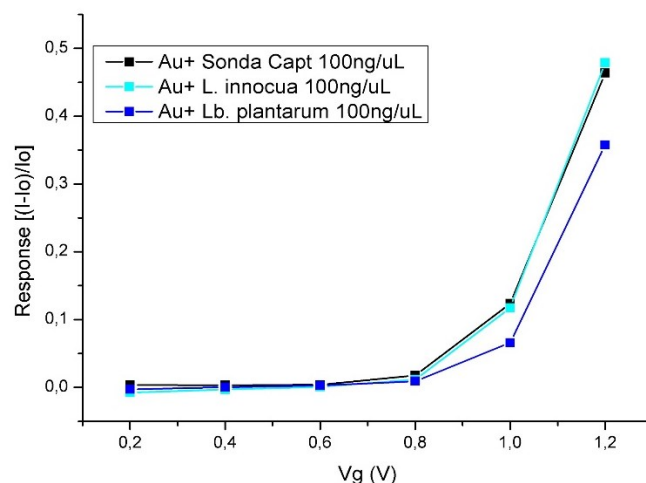


Figure 2.33 *L. innocua* and *Lb. plantarum* whole DNA analysed by OECT.

Food samples analysis

Salmon food samples were analyzed with the OECT biosensor. Figure 2.34 shows the I_{SD} modulated response of CSS samples CSS 5.2 and CSS 7.2. It can be clearly seen that the sample CSS 5.2 generated a different curve compared to CSS 7.2, with an increment of the I_{SD} . This response makes it possible to consider positive sample CSS 5.2 for the presence of *L. monocytogenes*. Sample CSS 7.2 can be considered negative for *L. monocytogenes* considering the proximity of the curve with the I_{SD} signal generated by the presence of the probe alone. The data are in agreement with the data obtained with Listeria PrecisTM method analysis.

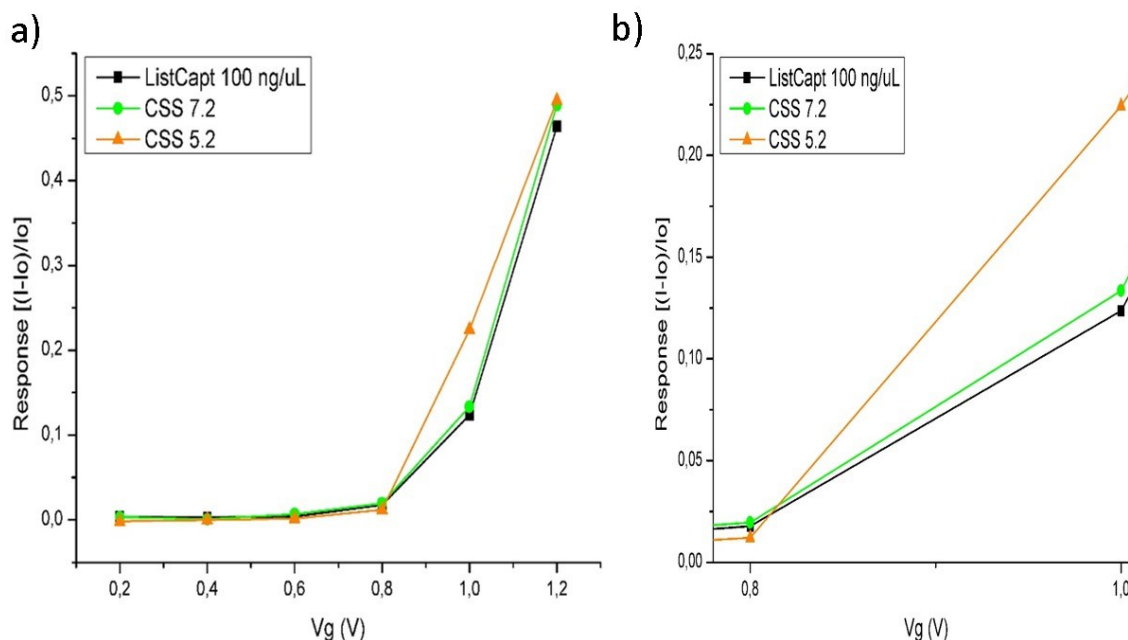


Figure 2.34 Cold-smoked salmon samples CSS 7.2 and CSS 5.2 DNA analysed by OECT biosensor. In b) a detail of the curves from 0.8 to 1 Vg (V).

Samples from ham factories were also tested with the OECT biosensor. Figure 2.35 shows that the raw ham sample 2.1 can be considered positive in comparison to the ISD signal produced by the probe. Instead, the environmental sample 8.1 can be considered negative as the produced curve is below the curve obtained for the Thiol ListCapt probe alone. These data are confirmed by *Listeria* PrecisTM method analysis (reported in Tabella 2.9).

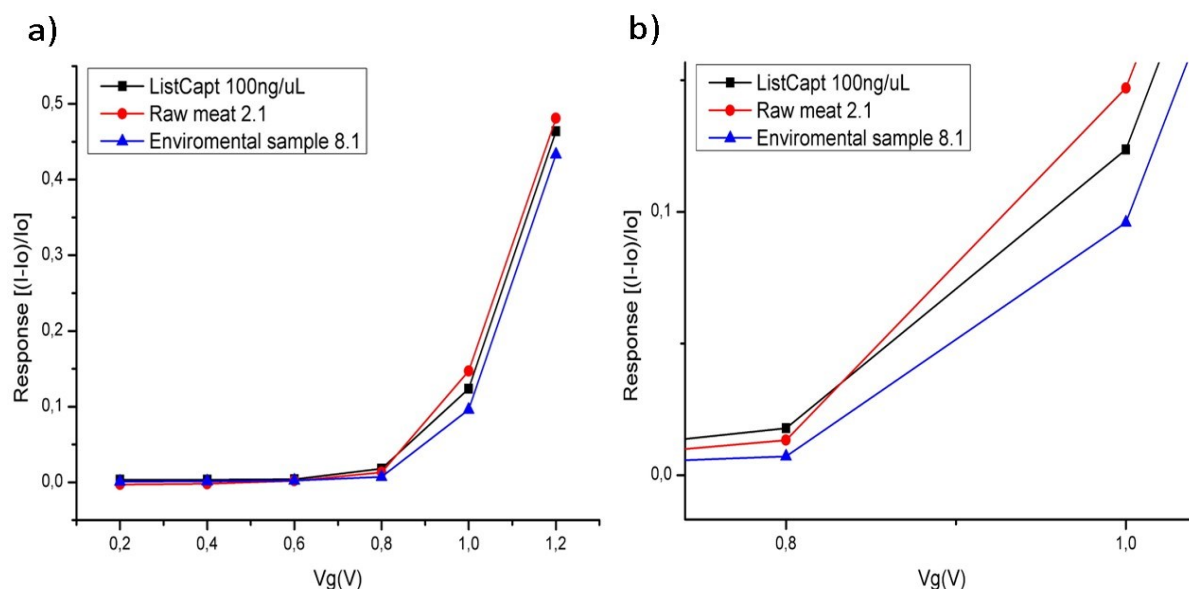


Figure 2.35 Samples from ham factory, raw ham (2.1) and environmental samples (8.1) DNA analysed by OECT biosensor (a). In b) a detail of the curves from 0.8 to 1 Vg (V).

2.2.6 ListE PROBE

2.2.6.1 Dot blot

ListE probe was tested in the dot blot assay. After protocol optimization, the best results were obtained using the following parameters: positively charged Zeta-Probe GT nylon membrane (Bio-rad), probe concentration at 200 ng/ μ L, hybridization temperature 40°C, washing steps at room temperature and SSC buffer 1X for the second step of washing. To reduce reaction volume and minimize reagent waste, dot blot assays were carried out in sterile Petri dishes.

General design rules for oligonucleotide probes recommend an ideal GC% content between 40 and 60%, as G–C pairing consists of three hydrogen bonds compared to the two bonds of A–T pairing (Ermini et al., 2011). Low GC% content may lead to a weak bond between probe and target sequence, resulting in greater hybrid instability and lower signal intensity (Xia, 2010). Despite design recommendation, in this work, the probe sequence was chosen because of the specificity and absence of secondary structures. When tested in silico, other *L. monocytogenes iap* gene regions with higher GC% content showed higher similarity to non-pathogenic *Listeria* spp. sequences or formation of secondary structures with high T_m temperatures.

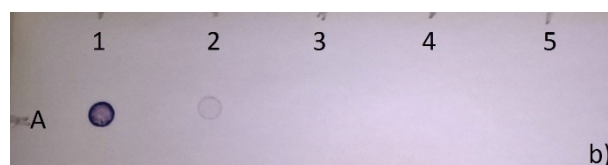


Figure 2.36 Dot blot sensitivity with DIG-ListE probe (b) at 200 ng/μL, hybridization temperature 40°C. Row A, ssDNA complementary probe, A1: 100 ng/μL; A2: 50 ng/μL; A3: 25 ng/μL; A4: 10 ng/μL; A5: 1 ng/μL.

The sensitivity of the DIG-ListE probe at the concentration of 200 ng/μL was only 50 ng/μL using the ssDNA complementary sequence as the target (Figure 2.36). Visible spots were obtained at concentrations of 100 ng/μL and 50 ng/μL (spots A1 and A2) at 45 min of incubation. No visible spots appeared for any negative control Figure 2.37 and Figure 2.38 confirming the specificity of the assay. A visible spot in A1 was obtained with the ssDNA complementary probe included as the positive control. The obtained results confirmed probe specificity allowing its utilization for the detection of *L. monocytogenes*. ListE for used for the construction of the voltammetric biosensor.

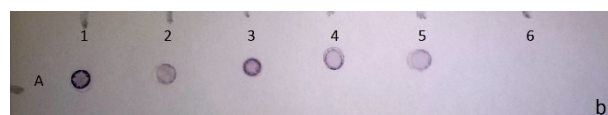


Figure 2.37 Dot blot specificity with DIG-ListE probe (b) at 200 ng/μL using positive controls (200 ng/μl), hybridization temperature 40°C. Row A, A1: ssDNA complementary probe 100 ng/μL; A2: *L. monocytogenes* 1/2c ATCC 7644; A3: *L. monocytogenes* 1/2a DIAL; A4: *L. monocytogenes* 1/2b DIAL; A5: *L. monocytogenes* 4b DSM 15675; A6: *L. innocua* DSM 20649.

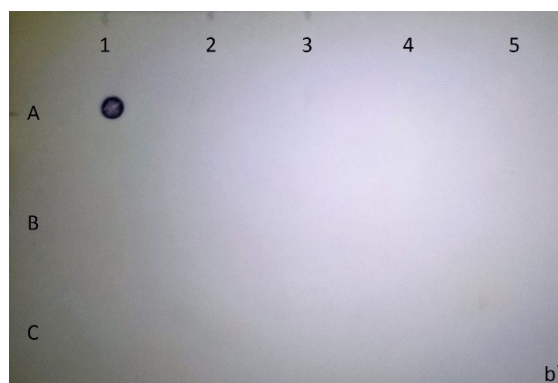


Figure 2.38 Dot blot specificity with DIG-ListE probe (b) at 200 ng/μL using negative controls (100 ng/μl), hybridization temperature 40°C. Row A, A1: ssDNA complementary probe 100 ng/μL; A2: *L. innocua* DSM 20649; A3: *L. ivanovii* DIAL; A4: *S. enterica* DSM 9145; A5: *Enterobacter* spp. DIAL. Row B, B1: *E. coli* DISTAM; B2: *B. cereus* DSM 2301; B3: *C. jejuni* DSM 49943; B4: *Lb. plantarum* ATCC BAA793; B5: *Lb. paracasei* DSM 5622. Row C, C1: *Lb. rhamnosus* ATCC 53103; C2: *Lb. brevis* DSM 20054.

2.2.6.2 Electrochemical biosensor based on voltammetry

Hybridization temperature choice

To obtain good selectivity hybridization conditions, including salt concentration and temperature, must be optimized.

Two temperatures were selected, 25°C was selected as room temperature would be the best option to simplify the protocol of analyses, while 40°C was selected because it is the best temperature for hybridization as described in the dot blot test.

DNA concentration

The DNA concentrations tested were 10 ng/μL, 1 ng/μL, 100 pg/μL, 10 pg/μL and 1 pg/μL.

Results obtained at RT

SPAuEs cleaned and functionalized as described previously were used to detect different DNA targets consisting of ListE complementary sequence, *L. monocytogenes* genomic DNA (positive) and *L. innocua* genomic DNA (negative) controls. The tests were carried out at RT using concentrations from 10 ng/μL to 1 pg/μL. The SPAuEs were covered by drop-casting of 80 μL ferrocyanide solution 10 mM and then CVs and DPVs were performed. In these measurements, the anodic current (i_{pa}) due to the oxidation of ferrocyanide showed a decrease at increasing target concentrations. CV and DPV representatives' profiles are reported in Figure 2.39.

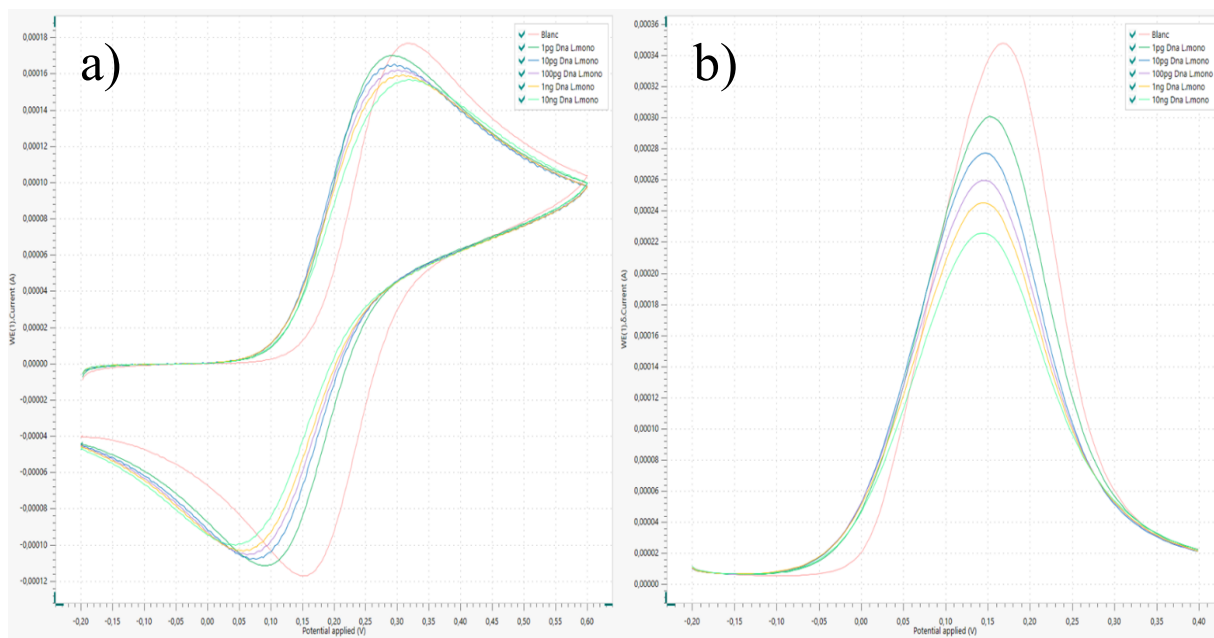


Figure 2.39 a) Example of cyclic voltammograms (CV) b) example of differential pulse voltammograms (DPV) obtained analysing genomic DNA of *L. monocytogenes* as target

Figures 2.40 and 2.41 show the calibration curves obtained by plotting the Δi_{pa} against the logarithmic concentration of the target (expressed in pg/ μ L). Δi_{pa} represents the difference between anodic peak current measured by CV and DPV of the electrode functionalized with the thiol ListE probe after hybridization with the sequence complementary to the thiol ListE probe (i_{pa} sample) and the anodic peak current recorded at the functionalized electrode (i_{pa} blank).

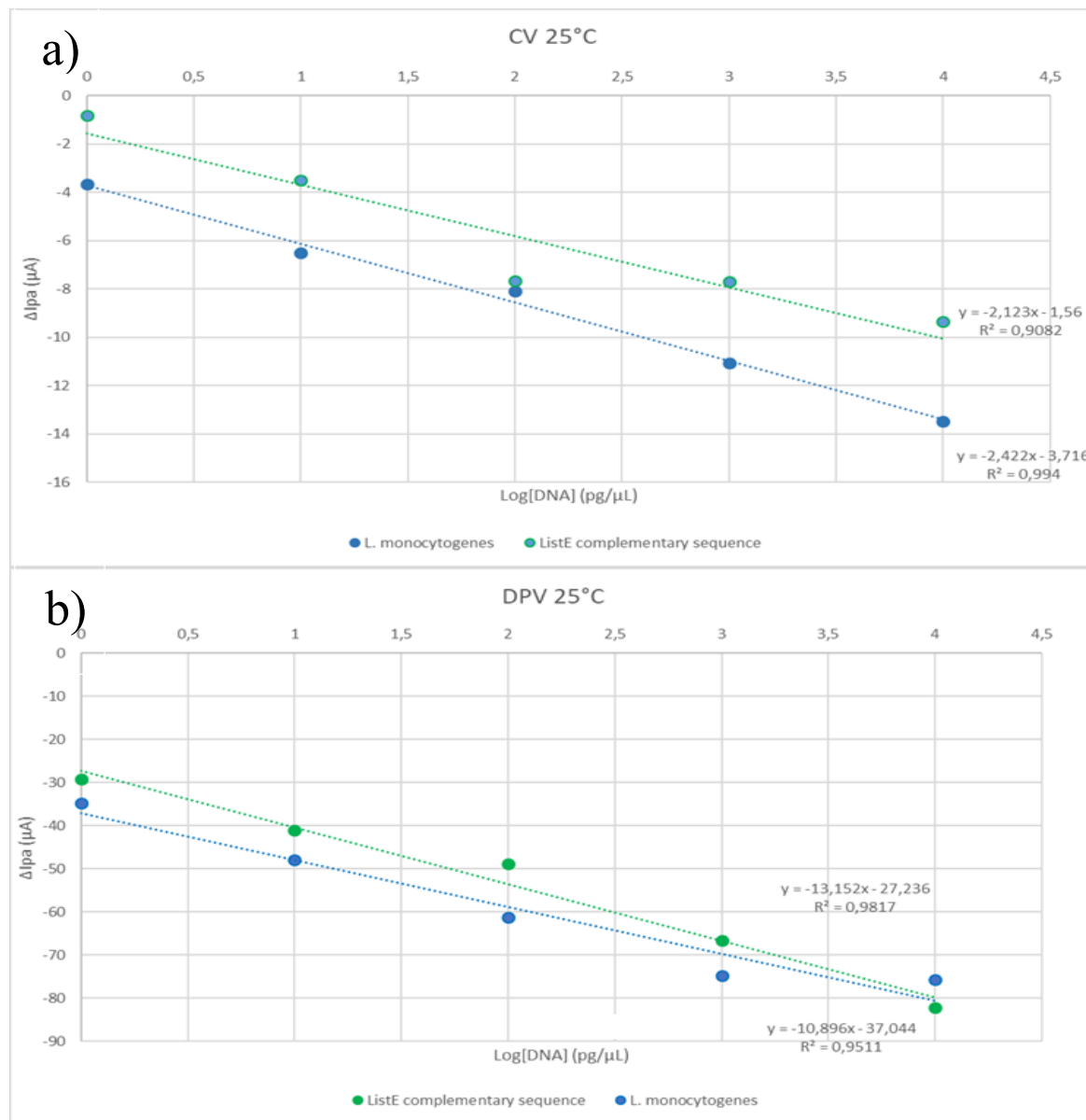


Figure 2.40 Calibration plots obtained by CV (a) and DPV (b) for ListE complementary sequence (green) and *L. monocytogenes* genomic DNA (blue) at 25°C (Braidot, 2019).

Figure 2.40 shows the calibration plots obtained with SPAuEs using CV and DPV to test as target both the ListE complementary sequence (green line) and the genomic DNA of *L. monocytogenes* (blue line). The regression line slopes have similar values indicating a similar sensitivity. Nevertheless, the genomic DNA, as expected, has shown a higher current decrement, that can be due to its greater steric hindrance that can have as a result a reduced

charge exchange between the ferrocyanide and the gold surface. This behavior was also confirmed by DPV measurements, in fact, a greater sensitivity was obtained for all genomic DNA targets compared to ListE complementary sequence. Moreover, from the data, it is clear that DPV is more sensitive when compared to CV.

However, results reported in Figure 2.41 that compare the positive control (*L. monocytogenes*) and the negative control (*L. innocua*), show that an aspecific interaction occurred with the probe. In fact, both CV and DPV measurements show the detection of a current signal produced by the hybridization of an amount of target DNA to the probe for the negative control *L. innocua*.

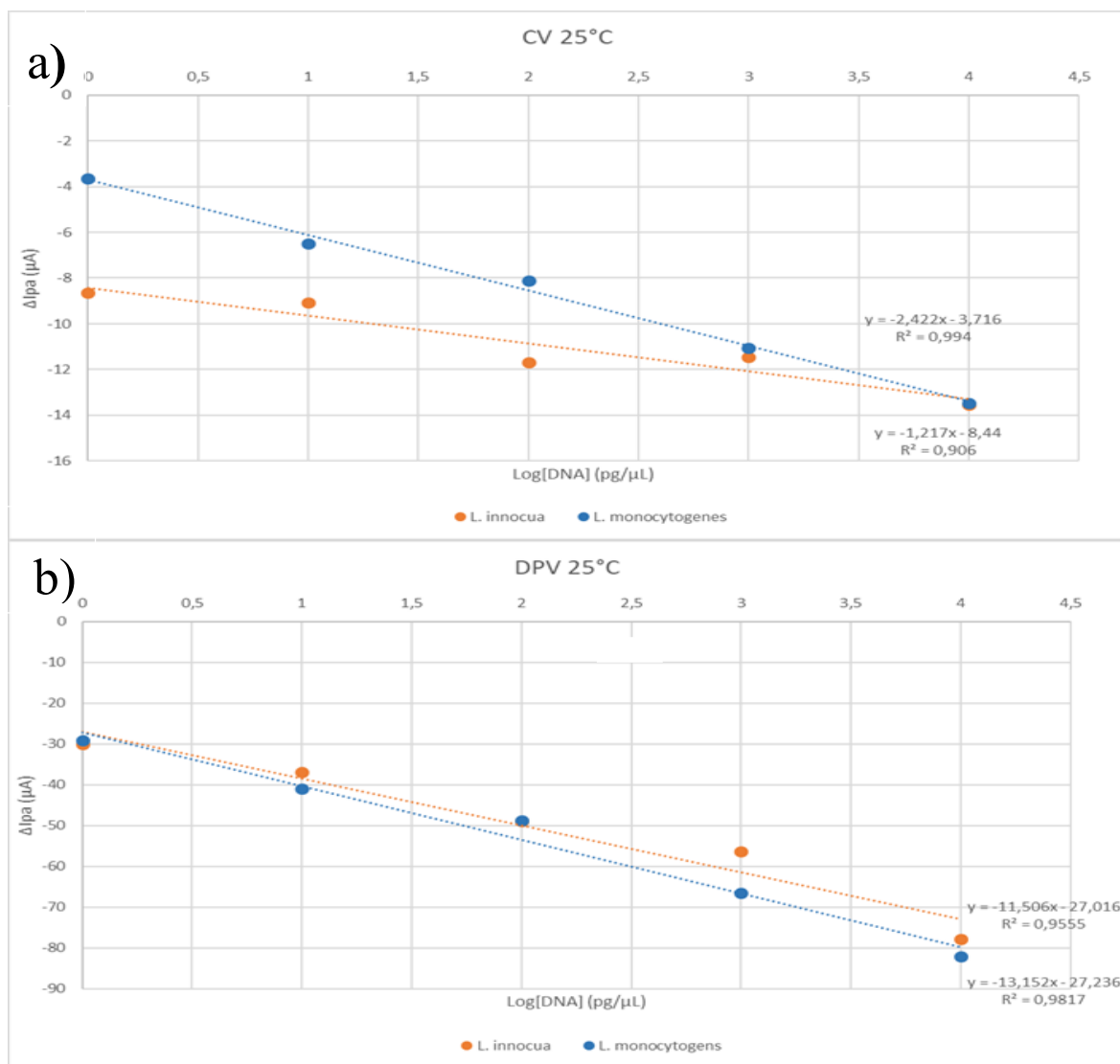


Figure 2.41 Calibration plot obtained by CV (a) and DPV (b) for *L. innocua* (orange) and *L. monocytogenes* (blue) genomic DNAs at 25°C (Braidot, 2019).

These results demonstrated that at RT the ListE capture probe has not the required selectivity. For this reason to improve the selectivity of the assay new tests were performed at an increased temperature of 40°C for the hybridization step (Braidot, 2019).

Results obtained at 40°C

The results obtained for the tests at the hybridization temperature of 40°C are reported in Figure 2.42 and 2.43.

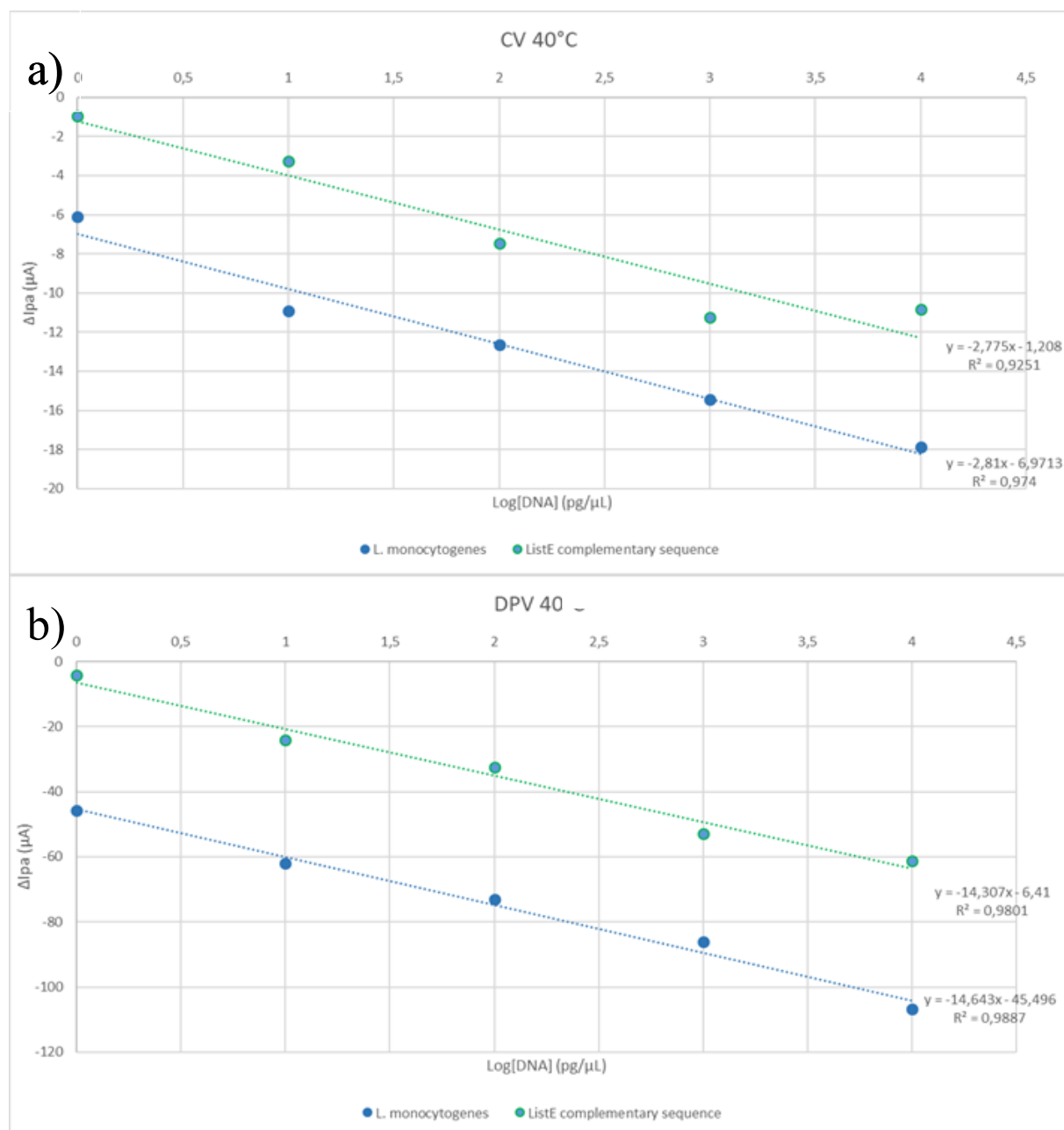


Figure 2.42 Calibration plot obtained by CV (a) and DPV (b) for ListE complementary sequence (green) and *L. monocytogenes* genomic DNA (blue) at the hybridization temperature of 40°C (Braidot, 2019).

It is clear from Figure 2.42, the similar sensitivity found for the ListE complementary sequence (green line) and the genomic DNA of *L. monocytogenes* (blue line). Although the genomic DNA, as expected, shows a higher current decrement due to its greater steric hindrance. This behavior was also confirmed by DPV measurements. Also in this experiment DPV showed a greater sensitivity for the targets compared to CV.

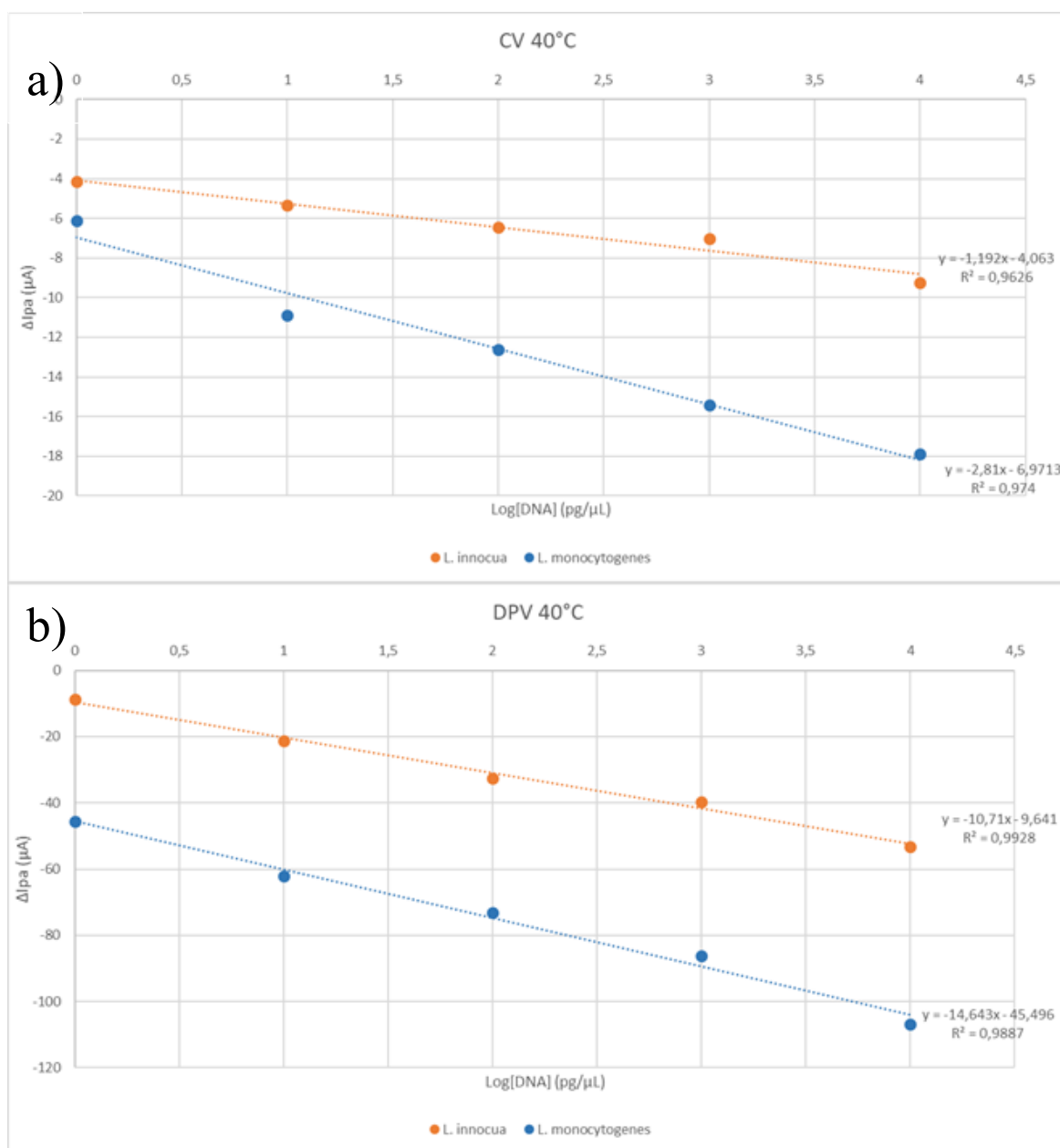


Figure 2.43 Calibration plot obtained by CV (a) and DPV (b) for *L. innocua* (orange) and *L. monocytogenes* genomic DNA (blue) at 40°C (Braidot, 2019).

Comparing the calibration plots obtained for *L. monocytogenes* genomic DNA to the calibration plot of *L. innocua* genomic DNA, it is possible to observe (Figure 2.43) that increasing the temperature of hybridization the aspecific interaction (hybridization of the negative DNA target of *L. innocua*) decreases compared to the one observed at RT. In fact, the ΔI_{pa} due to aspecific interactions of *L. innocua* DNA is clearly lower than ΔI_{pa} measured for *L. monocytogenes* DNA.

The results demonstrated that at 40°C the selectivity improves.

Table 2.15 Summary of the results.

Bacteria		25°C	40°C
CV	<i>L. monocytogenes</i>	$y = -2.422x - 3.716$	$y = -2.81x - 6.971$
	<i>L. innocua</i>	$y = -1.217x - 8.44$	$y = -1.192x - 4.06$
	Slope ratio	2.0	2.36
DPV	<i>L. monocytogenes</i>	$y = -13.152x - 27.236$	$y = -14.64x - 45.49$
	<i>L. innocua</i>	$y = -11.506x - 27.016$	$y = -10.71x - 9.64$
	Slope ratio	1.14	1.36

The results reported in Table 2.15 confirm that the right temperature for hybridization is 40°C. In fact, at 40°C the ratio between the slopes of *L. monocytogenes* and *L. innocua* results higher than the values obtained at RT. In addition, at 40°C, the relevant y-intercept for *L. innocua* is clearly smaller than the value obtained for *L. monocytogenes* (Braidot, 2019).

2.2.7 CONCLUSIONS AND FUTURE PERSPECTIVE

The results obtained lead to consider that the label-free bio-assay here investigated should be further improved in terms of selectivity and sensitivity.

For what concerns the selectivity, different negative DNA controls will be considered since our test was performed in the conditions, as we used the DNA of *L. innocua*, which is 99% similar to *L. monocytogenes*. Moreover, other parameters can be evaluated such as the buffer used for hybridization. The last solution to improve the selectivity could be the design of a new probe selecting a different gene as a target.

To improve the sensitivity further tests will be performed working on immobilization and blocking steps. Considering that a low sensitivity may be due to a low immobilization efficiency of the capture probe, different concentrations of the capture probe will be explored. In addition, the functionalization and the blocking will be done in a single step to minimize the capture probe and blocking reagent competition. Buffers used for the functionalization and hybridization steps will be evaluated.

REFERENCES

- Andreatta F., Druar M-E., W. Marin, D. Cossement, M.-G. Olivier, D. Fredizzi. (2014). Volta potential of clad AA2024 aluminium after exposure. *Contents Science*, 86,189-201.
- Beltrame E. (2016). Comparison between plate count based and molecular methods for the detection of *Listeria monocytogenes* in cold-smoked salmon. Master degree dissertation, University of Udine.
- Bernards D.A., Malliaras G.G. (2007). Steady-state and transient behavior of organic electrochemical transistors. *Adv. Funct. Mater.*, 17(17):3538-3544.
- Braidot M. (2019). An explorative study to evaluate the performances of an electrochemical label-free bio-assay using Au screen printed electrodes to detect *L. monocytogenes*. Master Degree dissertation, University of Udine.
- Bustin S.A., Zaccara S., Nolan T. (2012). An introduction to real-time polymerase chain reaction. In: Filion M. (ed.), *Quantitative Real-time PCR in Applied Microbiology* (cap. 1, pp. 3-26). Norfolk (UK): Caister Academic Press.
- Ciccoira F., Sessolo M., Yaghmazadeh O., DeFranco J.A., Yang S.Y., Malliaras G.G. (2010). Influence of device geometry on sensor characteristics of planar organic electrochemical transistors. *Adv. Mater.*, 22(9):1012-1016.
- Contreras-Naranjo JE, Aguilar O. (2019). Suppressing Non-Specific Binding of Proteins onto Electrode Surfaces in the Development of Electrochemical Immunosensors. *Biosensor*, 9 (1):15-38
- EFSA (2015a). Scientific report of EFSA and ECDC. The European Union Summary Report on trends and sources of zoonosis, zoonotic agents and food-borne outbreaks in 2013. *EFSA J.*, 13(1):3991.
- EFSA (2015b). Scientific report of EFSA and ECDC. The European Union Summary Report on trends and sources of zoonosis, zoonotic agents and food-borne outbreaks in 2014. *EFSA J.*, 13(12):4329.
- EFSA (2016). Scientific report of EFSA and ECDC. The European Union Summary Report on trends and sources of zoonosis, zoonotic agents and food-borne outbreaks in 2015. *EFSA J.*, 14(12):4634.
- Ermini M.L., Scarano S., Bini R., Banchelli M., Berti D., Mascini M., Minunni M. (2011). A rational approach in probe design for nucleic acid-based biosensing. *Biosens. Bioelectron.*, 26(12):4785-4790.
- Fontanot M. (2014). Traditional and Molecular Methods vs Biosensors for the Detection of Pathogens in Poultry Meat. Ph.D. dissertation, University of Udine.

- Gimenez B., Dalgaard P. (2004). Modeling and predicting the simultaneous growth of *Listeria monocytogenes* and spoilage micro-organisms in cold-smoked salmon. *J. Appl. Microbiol.*, 96(1):96-109.
- Hansen L.T. and Huss H.H. (1998). Comparison of the microflora isolated from spoiled cold-smoked salmon from three smokehouses. *Food Res. Int.*, 31(10):703-711.
- Huss H.H., Ben Embarek P.K., Jeppesen V.F. (1995). Control of biological hazards in cold-smoked salmon production. *Food Control*, 6(6):335-340.
- ISO (2004). EN ISO 11290-1:1996/Amd1:2004 Microbiology of Food and Animal Feeding Stuffs - Horizontal Method for the Detection and Enumeration of *Listeria monocytogenes* - Detection Method, Part I. Geneva: International Organization for Standardization.
- Joffraud J.J., Cardinal M., Cornet J., Chasles J.S., Léon S., Gigout F., Leroi F. (2006). Effect of bacterial interactions on the spoilage of cold-smoked salmon. *Int. J. Food Microbiol.*, 112(1):51-61.
- Kathariou S. (2002). *Listeria monocytogenes* virulence and pathogenicity, a food safety perspective. *J. Food Prot.*, 65(11):1811-1829.
- Lin P., Luo X., Hsing I., Yan F. (2011). Organic electrochemical transistors integrated in flexible microfluidic systems and used for label-free DNA sensing. *Adv. Mater.*, 23(35):4035-4040.
- Manzano M., Cocolin L., Cantoni C., Comi G. (1997a). Detection and identification of *Listeria monocytogenes* from milk and cheese by a single-step PCR. *Mol. Biotechnol.*, 7:85-88.
- NF Validation (2013). EN ISO 16140:2003 validation certificate of the Listeria Precis™ method for *Listeria monocytogenes* detection. Certificate No. UNI 03/04-04/05. France: AFNOR Certification.
- Paludan-Müller C., Dalgaard P., Huss H.H., Gram L. (1998). Evaluation of the role of *Carnobacterium piscicola* in spoilage of vacuum- and modified-atmosphere-packed cold-smoked salmon stored at 5 °C. *Int. J. Food. Microbiol.*, 39(3):155-166.
- Rashid J.I.A., Yusof, N.A. The strategies of DNA immobilization and hybridization detection mechanism in the construction of electrochemical DNA sensor: A review. *Sensing and Bio-Sensing Research*, 16:19-31.
- Swaminathan B. and Cabanes D., Zhang W., Cossart P. (2007). *Listeria monocytogenes*. In: Doyle M., Beuchat L. (eds.), *Food Microbiology: Fundamentals and Frontiers*, 3rd ed. (pp. 457-491). Washington DC: ASM Press.
- Swaminathan B., Gerner-Smidt P. (2007). The epidemiology of human listeriosis. *Microbes Infect.*, 9(10):1236-1243.

- Tarabella G., Villani M., Calestani D., Mosca R., Iannotta S., Zappettini A., Coppedè N. (2012). A single cotton fiber organic electrochemical transistor for liquid electrolyte saline sensing. *J. Mater. Chem.*, 22(45):23830-23834.
- Vieira P.M., Coelho A.S.G., Steindorff A.S., de Siqueira S.J.L., do Nascimento Silva R., Ulhoa C.J. (2013). Identification of differentially expressed genes from *Trichoderma harzianum* during growth on cell wall of *Fusarium solani* as a tool for biotechnological application. *BMC Genomics*, 14(1):177.
- Wang R., Zhou X., Zhu X., Yang C., Liu L., Shi H. (2017). Isoelectric Bovine Serum Albumin: Robust Blocking Agent for Enhanced Performance in Optical-Fiber Based DNA. Sensing. *ACS Sensors*. 2(2)257-262.
- Xia X. (2010). The effect of probe length and GC% on microarray signal intensity: characterizing the functional relationship. *Int. J. Syst. Synth. Biol.*, 1(2):171-183.4

SOFTWARE

- Altschul S.F., Gish W., Miller W., Myers E.W., Lipman D.J. (1990). Basic local alignment search tool. *J. Mol Biol.*, 215(3):403-410 (<http://blast.ncbi.nlm.gov/Blast.cgi>).
- Corpet F. (1988). Multiple sequence alignment with hierarchical clustering. *Nucleic Acid Res.*, 16(22):10881-10890 (<http://multalin.toulouse.inra.fr/multalin/>).
- IDT OligoAnalyzer 3.1 (<http://eu.idtdna.com/calc/analyzer>).
- Jullien N. (2013). AmplifX 1.7. CNRS, Aix-Marseille Université (<http://crn2m.univ-mrs.fr/pub/amplifx-dist>)

Chapter III

***CAMPYLOBACTER* spp.**

3.1 MATERIAL AND METHODS

3.1.1 BACTERIAL STRAINS AND CULTURE MEDIA

Bacterial strains used for the analysis in this study are listed in Table 3.1.

All the *Campylobacter* strains were cultivated in anaerobic gas jars at specific microaerophilic conditions (6% O₂, 7% CO₂, 7%H₂ and 80% N₂) generated with a Sachet Oxoid™ CampyGen™ 2.5 l (Oxoid, Milan, Italy). After revitalization in BHI the incubation was conducted at 37 °C for 48h in Brain Heart Infusion (BHI) broth (Oxoid, Milan, Italy) and on Columbia blood agar base (Oxoid, Milan, Italy), supplemented with 5% v/v of sheep defibrinated blood. These procedures were repeated twice before Gram stain, morphology cell, oxidase, and catalase tests.

Negative controls were cultivated at 30 °C or 37 °C based on the optimum growth temperature of the bacteria, in aerobic conditions, except for *Campylobacter fetus*, *C. cryaerophila*, *Helicobacter pylori*, *H. suis*, *Arcobacter butzleri*, and *Lactobacillus plantarum* which grew in microaerophilic condition. Strains were checked by Gram stain, cell morphology and selective medium for *Listeria* spp., *Salmonella*, and *Bacillus* on PALCAM Agar Base, X.L.D. Agar and Brilliance™ *Bacillus Cereus* Agar Base (Oxoid, Milan, Italy) respectively.

3.1.2 SAMPLES

For the detection of *Campylobacter* spp. microbiological and molecular analysis were conducted on 20 fresh chicken skin (CS) samples collected from local butcher shops, from 2016 to 2017 (1CS - 20CS). Microbiological enumeration and ISO 10272- 1B:2006 and DNA extraction were carried out. DNA samples from 1CSF to 20 CSF correspond to DNA samples extracted from Bolton broth before enrichment, while DNA samples from 1CSB to 20 CSB correspond to DNA extracted after 48 h enrichment step.

3.1.2.1 Sampling

In Figure 3.1 schematic representation of the experimental design is shown. From each carcass, an aliquot of 10 gr of skin was collected, homogenized with saline peptone water (SPW), subjected to plate count bacterial enumeration and DNA extraction. 10 g, were used for ISO1027-1:2006.

Table 3.1 List of bacteria used in specificity tests.^ADSM: Deutsche Sammlung von Mikroorganism und Zellkulturen GmbH (Braunschweig, Germany). ^B ICS: Isolated from Clinical samples (Hospital of Udine, Italy).^CATCC: American Type Culture Collection (Manassas, VA, USA). ^D DI4A: Department of Agricultural, Food, Environmental and Animal Sciences (Udine, Italy) ^E DISTAM: Department of Food technologies and Microbiology Science (Milan, Italy).

Control	N.	Microorganisms	Collection code
Positive	1	<i>Campylobacter jejuni subsp. jejuni</i>	DSM 4688 ^A
	2	<i>C. coli</i>	DSM 24155
	3	<i>C. lari subsp.lari</i>	DSM 11375
	4	<i>C. upsaliensis</i>	DSM5365
Negative	5	<i>C. fetus</i>	DSM 5361
	6	<i>C. cryaerophila</i>	DSM 7289
	7	<i>Helicobacter pylori</i> ¹	DSM 7492
	8	<i>H. pylori</i> ²	ICSS ^B
	9	<i>H. suis</i>	DSM 19735
	10	<i>Arcobacter butzleri</i>	DSM 8739
	11	<i>Listeria monocytogenes</i>	ATCC 7644 ^C
	12	<i>L. innocua</i>	DSM 20649
	13	<i>L. seeligeri</i>	DSM 20751
	14	<i>L. marthii</i>	DSM 23813
	15	<i>L. welshimeri</i>	DSM 15452
	16	<i>L. ivanovii</i>	DSM 52491
	17	<i>Staphylococcus aureus</i>	DI4A ^D
	18	<i>Bacillus cereus</i>	DSM 4282
	19	<i>B. cereus</i>	DI4A RC3
	20	<i>B. subtilis</i>	DSM 4181
	21	<i>Salmonella enterica</i>	DSM 9378
	22	<i>Escherichia coli</i>	DISTAM ^E
	23	<i>Lactobacillus plantarum</i>	ATCC RAA 793
	24	<i>Saccharomyces cerevisiae</i>	ATCC 36024

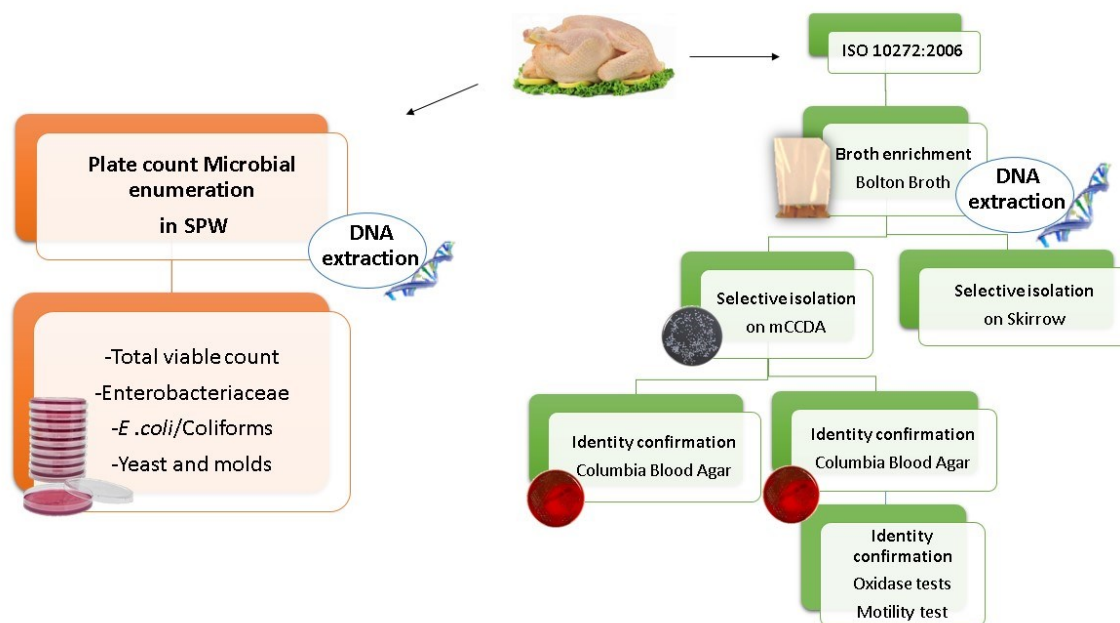


Figure 3.1 Experimental design.

3.1.2.2 Plate count Microbial enumeration

10 g chicken skin was transferred to a Stomacher filter bag added with 40 mL of saline-peptone water (8.5 g/L NaCl, 1 g/L bacteriological peptone), mixed for 30 sec in a Stomacher (PBI, Milan, Italy) and used for plate count bacterial enumeration. One mL aliquots were used for serial decimal dilutions to enumerate the following bacteria:

- Total viable count on Tryptone soya Agar (TSA) (Oxoid, Milan, Italy), incubated at 30°C for 48 h.
- Yeast and molds count on Malt extract Agar added with 10 µg/mL of tetracycline (AMT) (Oxoid, Milan, Italy), incubated at 30°C for 48 h.
- Enterobacteriaceae on Violet Red Bile Agar (VRBGA) (Oxoid, Milan, Italy), incubated at 37°C for 24h.
- *E. coli* and coliforms on Coli-ID (Biomeriux, Firenze, Italy), incubated at 37°C for 24 h.

3.1.2.3 ISO 10272-1:2006

10 g from each chicken carcass were transferred to a Stomacher filter bag added with 90 mL of Bolton broth (Oxoid, Milan, Italy) mixed for 30 sec in a Stomacher (PBI, Milan, Italy) and incubated for 4-6 h at 37°C in micro-aerophilic conditions and then incubated for 40-48 h at 41.5°C.

After enrichment, for selective isolation, a loop of the broth was streaked on two selective media

mCCDA and Skirrow (Oxoid, Milan, Italy). Then, plates incubation was conducted for 48 h at 41.5°C in micro-aerophilic conditions. Plates were examined for the presence of suspected colonies. Confirmation was carried out from 1 to 5 suspected colonies per plate by streaking on two Blood agar base plates, one was incubated at 41.5°C and one at 25°C for 48 h. *Campylobacter* spp. is not able to grow at 25°C, therefore the absence of growth at 25°C was expected. The identity confirmation includes oxidase and motility tests. The motility test was carried out using Brucella broth, formulated on the Brucella Base Medium (ThermoFisher Scientific, Monza, Italy). One colony was suspended in broth and transferred on a microscope slide. A typical corkscrew movement identifies *Campylobacter* spp.

3.1.2.4 DNA extraction

Genomic DNA from pure bacteria cultures and from food samples were extracted using the reported protocol by Cocolin et al. (2002) with some modifications.

Bacteria colonies were collected from the agar plates and suspended in a tube containing glass beads (0.5 mm diameter) and 300 µL of Breaking Buffer (Triton2%, SDS1%, NaCl 100 mM, trizma-base at pH 8 (SIGMA, Milan, Italy).

For food samples, 2 mL from Stomacher bag with SPW, and 2mL from the Enrichment broth, were centrifuged for 10 min at 13,000 rpm and resuspended in a tube containing breaking buffer and glass beads.

The DNA was treated with RNase enzyme at 37°C for 1 h. Before the concentration measurement obtained using a spectrophotometer Nanodrop™ 2000C (ThermoFisherScientific, Milan, Italy). The DNA concentration was finally standardized at 100 ng/µL using sterilized dd water. The DNA obtained was stored at -20°C before using it.

3.1.3 PRIMER DESIGN FOR THE DETECTION OF *CAMPYLOBACTER*

Primers were designed with the aim to detect, with q-PCR, the species *C. jejuni*, *C. coli*, *C. lari*, and *C. upsaliensis*, which cause gastroenteritis in humans. For the purpose the length of the amplicons should be 50-150 pb in order to achieve an adequate amplification efficiency.

Sequences of several genes were downloaded by genebank (<https://www.ncbi.nlm.nih.gov/genbank/>) and aligned with "Multiple sequence alignment with hierarchical clustering"(Corpet, 1988) (<http://multalin.toulouse.inra.fr/multalin/>) to select the primer to use in qPCR. The selected sequences were analyzed by Amplifix 1.7.0 (Julien, 2013) and then by OligoAnalyzer3.1 (<https://eu.idtdna.com/calc/analyzer>). To verify parameters: length (18-22 base pair), melting temperature (52-58°C), GC% content between 40-60%, no secondary structures (selfdimer or homodimer and hairpins).

The couple of primers was tested in silico for PCR with the software FastPCR6.1 and Amplifix 1.7.0 to verify the specificity on bacteria listed in Table 3.1 the accession number of the sequences used for this study are listed in Table 3.2. The selected primers are named CampyPFW and CampyPRW.

Table 3.2 Accession number of the sequences analyzed *in silico* to design the primer CampyP forward and reverse.

BACTERIA SEQUENCE (16S and 16S-23S ribosomal RNA gene)					
N.	Accession number	Genus, species	N.	Accession number	Genus, species
1	EF373994.1	<i>Aeromonas sobria</i>	15	AB089244.1	<i>Morganella morganii</i>
2	AM062666.1	<i>Bacillus cereus</i>	16	AF405374.1	<i>Pediococcus pentosaceus</i>
3	EF205020.1	<i>B. subtilis</i>	17	FJ518598.1	<i>Proteus vulgaris</i>
4	AF047423.1	<i>Citrobacter freundii</i>	18	JN418884.1	<i>Pseudomonas aeruginosa</i>
5	EF527445.1	<i>Escherichia coli</i>	19	AF268968.1	<i>Ps. brennerii</i>
6	FJ410387.1	<i>Enterobacter aerogenes</i>	20	AM086254.1	<i>Ps. brennerii</i>
7	AF047426.1	<i>E. aerogenes region</i>	21	EF198908.1	<i>Ps. fluorescens</i>
8	EU078570.1	<i>E.cloacae</i>	22	KF857261.1	<i>P. migulae</i>
9	AY277975.1	<i>Helicobacter ganmani</i>	23	AF046822.1	<i>Salmonella enterica</i>
10	DQ399570.1	<i>Klebsiella pneumoniae</i>	24	KX696458.1	<i>Shigella sonnei</i>
11	AB092638.1	<i>Lactobacillus plantarum</i>	25	U11784.1	<i>Staphylococcus aureus</i>
12	AF000655.1	<i>Legionella pneumophila</i>	26	AY531067.1	<i>Vibrio parahaemolyticus</i>
13	AB295116.1	<i>Leuconostoc lactis</i>	27	FJ429988.1	<i>Weissella cibaria</i>
14	AY684791.1	<i>Listeria monocytogenes</i>	28	AF293850.1	<i>Yersinia enterocolitica</i>

BACTERIAL WHOLE DNA					
N.	Accession number	Genus, species	N.	Accession number	Genus, species
1	kv861263.1	<i>Aeromonas sobria</i>	16	lvwz01000001.1	<i>Pseudomonas brenneri</i>
2	ap007209.1	<i>Bacillus cereus</i>	17	NZ_LDET01000015.1	<i>Ps. fluorescens</i>
3	nz_cp011534.1	<i>Bacillus subtilis</i>	18	fnty01000001.1	<i>Ps. migulae</i>

4	CP016762.1	<i>Citrobacter freundii</i>	19	acfl01000033.1	<i>Saccharomyces cerevisiae</i>
5	fm991728.1	<i>Helicobacter pylori</i> b38	20	NC_003197.2	<i>Salmonella enterica</i> <i>subsp. Enterica</i>
6	ba000007.2	<i>Escherichia coli</i> O157:H7	21	nz_lfwb01000312.1	<i>Morganella morganii</i>
7	NZ_LYDO0100000 4.1	<i>Enterobacter aerogenes</i>	22	nz_lyem01000481.1	<i>Shigella sonnei</i>
8	nz_cp011798.1	<i>E. cloacae</i>	23	ap008934.1	<i>Staphylococcus saprophyticus</i> <i>subsp. saprophyticus</i>
9	nz_cp010435.1	<i>Helicobacter pylori</i>	24	kn150745.1	<i>Proteus vulgaris</i> strain
10	fo203501.1	<i>Klebsiella pneumoniae</i>	25	nz_lirr01000034.1	<i>Vibrio parahaemolyticus</i>
11	nz_cp012650.1	<i>Lactobacillus plantarum</i>	26	nz_cp012873.1	<i>Weissella cibaria</i>
12	nz_cp011105.1	<i>Legionella pneumophila</i>	27	am286415.1	<i>Yersinia enterocolitica</i> <i>subsp. enterocolitica</i>
13	nz_cp011105.1	<i>Legionella pneumophila</i>	28	cp007224.1	<i>Pseudomonas aeruginosa</i>
14	ae005176.1	<i>Lactococcus lactis</i> subsp. <i>lactis</i>	29	cp015918.1	<i>Pediococcus pentosaceus</i>
15	nz_bbrp01000009.1	<i>Listeria monocytogenes</i>			

CAMPYLOBACTER SPP. (16S and 16S-23S gene)			ANIMALS (16S gene)		
N.	Accession number	Genus, species	N.	Accession number	Genus, species
1	KP064555.1	<i>Campylobacter fetus</i>	1	KP721213.1	<i>Sus scrofa domesticus</i>
2	GQ167709.1	<i>C. concisus</i>	2	DQ334849.1	<i>Meleagris gallopavo</i>
3	JX912515.1	<i>C. gracilis</i>	3	AB489247.1	<i>Gallus gallus</i>
4	L04322.1	<i>C. concisus</i> ,			
5	AB301966.1	<i>C. fetus</i> subsp. <i>fetus</i>			

6	M65011.1	<i>C. fetus subsp. venerealis</i>
7	NZ_FPBB0100000 5.1	<i>C. hyointestinalis</i>
8	nz_jhq01000009.1	<i>C. mucosalis</i>
9	nz_jmti01000045.1	<i>C. sputorum biovar sputorum</i>

3.1.4 PCR PROTOCOL

PCRs were carried out using the CampyPFW and CampyPRW primer in a reaction mixture containing the following reagents:

5 µL of AmpliTaq Buffer (1.5mM) 1µL of PCR Nucleotide Mix dNTPs (10 mM each dNTPs), 1 µL of each primer (10 µM), 0.25 µL AmpliTaq DNA polymerase (5 units/µL) and 1µL of DNA extracted standardized at 100 ng/µL. The reaction final volume was 50µL. All the reagents were purchased from Applied Biosystem (Monza, Italy).

The thermal cycler conditions used were: 95°C denaturation for 5 min; 30 cycles of 95°C for 1 min, 58°C for 30 s, 72°C for 30 s and a final extension at 72°C for 7 min. The reaction was carried out in a thermal cycler (C1000 Touch™, Bio-Rad, Irvine, CA, USA). The PCR products were electrophoresed in agarose gel.

3.1.5 ELECTROPHORESIS

Each amplicon (5 µL) was loaded after mixing with 5 µL Gel loading Buffer 1X in a 1.5% agarose gel prepared in Tris-borate-EDTA buffer 0.5X (Sigma- Aldrich, Milan, Italy).

The ethidium bromide (Sigma- Aldrich, Milan, Italy) dye for DNA detection was used in the gel at a final concentration of 0.5 µg/mL. A 100-bp ladder (Promega, Milano, Italy) was used to size products.

In each assay, a blank control was included, in which the template DNA was replaced with an equal volume of nuclease-free water. The electrophoretic run was performed at 120V for 40 min. The results were examined under UV light in a cabinet (BioImaging System GeneGenius, Syngene, England).

3.1.6 qPCR PROTOCOL

The Kit Sso Fast Tm Eva Green® was employed according to the manufacturer's instructions. The reaction mixture contained the following reagents: 10µL of SsoFastTMEvaGreen®Supermix 2X, 1 µL for each primer CampyPFW and RW (10 µM) and 1 µL of DNA template. The final reaction volume was 20 µL. In each assay, a negative control was included, in which the template DNA was replaced with an equal volume of nuclease-free water.

The program applied consisted of a hot-start activation at 98°C for 2 min, 35 cycles of denaturation at 98°C for 5 min and the annealing/extension at 60°C for 20 sec. Following a melting temperature analysis was performed by a graduated increase of the temperature from 60 to 95°C (0.5°C/5 sec) in a Rotor-gene Q (Qiagen, Milan, Italy). Fluorescence acquisition during annealing/extension step of each cycle and final melting temperature analysis was set on the green channel (excitation at 470 nm and emission at 510 nm) of the instrument, due to the properties of the EvaGreen dye.

3.1.7 SEQUENCING

Amplicons of some bacterial strains and food samples were sequenced to confirm the *Campylobacter* identification by the primer CampyPFW and CampyPRW.

Amplicons obtained using primer P1V1-P4V3 (Klijn et al., 1991) were purified before been sent to Eurofins genomics Germany GmbH (Ebersberg, Germany) for the sequencing.

Amplification conditions:

5 µL of AmpliTaq Buffer (1.5mM), 1µL of PCR Nucleotide Mix dNTPs (10 mM each dNTPs), 1 µL of each primer (10 µM), 0.25 µL AmpliTaq DNA polymerase (5 units/µL) and 1µL of DNA standardized at 100 ng/µL in a final volume of 50 µL. For each sample, the amplification was conducted in duplicate to obtain the 100 µL required from the protocol. All reagents were purchased from Applied Biosystem (Monza, Italy).

Condition used: 95°C denaturation for 5 min; 35 cycles of 95°C for 1 min, 42°C for 1 min, 72°C for 90 sec and a final extension 72°C 7 min. The reaction was carried out in a thermal cycler (C1000 Touch™, Bio-Rad, Irvine, CA, USA). The PCR products were electrophoresed in 1.5 % agarose gel. The expected PCR products were of 700 bp in length.

3.1.7.1 Identification sequences by BLAST software

The nucleotide sequences obtained were processed by BLAST (<https://blast.ncbi.nlm.nih.gov/Blast.cgi>). The sequence identification was based on the identity percentage and the E-value of the result achieved.

3.1.8 DNA PROBE DESIGN

Various sequences were downloaded from genbank (<https://www.ncbi.nlm.nih.gov/genbank/>) and aligned by "Multiple sequence alignment with hierarchical clustering"(Corpet, 1988) (<http://multalin.toulouse.inra.fr/multalin/>).

The sequences were selected for the following features by Amplifix 1.7.0 and then by OligoAnalyzer3.1 (<https://eu.idtdna.com/calc/analyzer>) length, melting temperature (60-80°C), GC% between 40-60%, absence of secondary structures (self-dimer or homo-dimer and hairpins), The selected sequence was tested in silico to verify specificity by the software FastPCR6.1 and Amplifix 1.7.0. Bacteria listed in Table 3.3.

The probe selected was named Campy P3 (CP3). A sequence complementary to the CP3 probe (CCP3), was used as a positive control in the analysis *in vitro*.

Table 3.3 Accession numbers of the sequences analyzed in silico to design the probe CampyP3.

N.	Accession number	Genus, species	N.	Accession number	Genus, species
1	nr_118514.1	<i>Campylobacter fetus</i>	16	ab089244.1	<i>Helicobacter ganmani</i>
2	jx912506.1	<i>C. concisus</i>	17	af268968.1	<i>Morganella morganii</i>
3	jx912515.1	<i>C. gracilis</i>	18	ef198908.1	<i>Pediococcus pentosaceus</i>
4	nr_117766.1	<i>C. ureolyticus</i>	19	kx186944.1	<i>Pseudomonas fluorescens</i>
5	nz_cp019944.1	<i>Escherichia coli</i>	20	kf857261.1	<i>P. fluorescens</i>
6	ef527445.1	<i>E. coli</i>	21	fj429988.1	<i>P. migulae</i>
7	eu014681.1	<i>Salmonella choleraesuis</i>	22	ay593991.1	<i>Weissella cibaria</i>
8	nr_044370.1	<i>Salmonella enterica subsp. indica</i>	23	nr_114587.1	<i>Helicobacter pylori</i>
9	nr_044372.1	<i>S. enterica subsp. salamae</i>	24	nr_043053.1	<i>H.pylori</i>
10	nr_116124.1	<i>S. bongori</i>	25	FJ573216.1	<i>H. pullorum</i>
11	nr_044373.1	<i>S. enterica subsp. diarizonae</i>	26	ay277975.1	<i>Arcobacter suis</i>
12	nr_116125.1	<i>S. enterica subsp. arizonae</i>	27	NR_043035.1	<i>A. butzleri</i>
13	jq694170.1	<i>S. enterica strain 365</i>	28	U25805.1	<i>A.cryaerophilus</i>
14	eu078570.1	<i>Enterobacter cloacae subsp. dissolvens</i>	29	DQ464344.1	<i>A.skirrowii</i>
15	ay277975.1	<i>Gallus gallus</i>			

3.1.9 SPECIFICITY TEST FOR CAMPYP3 by DOT BLOT ASSAYS

The probe CampyP3 was tested with two dot blot protocols as follows: a) the 5' end was labeled with digoxigenin to be used in dot blot with alkaline phosphatase and b) was labeled at 5'end with biotin to be applied in dot blot with chemiluminescent readout (Figure 3.2).

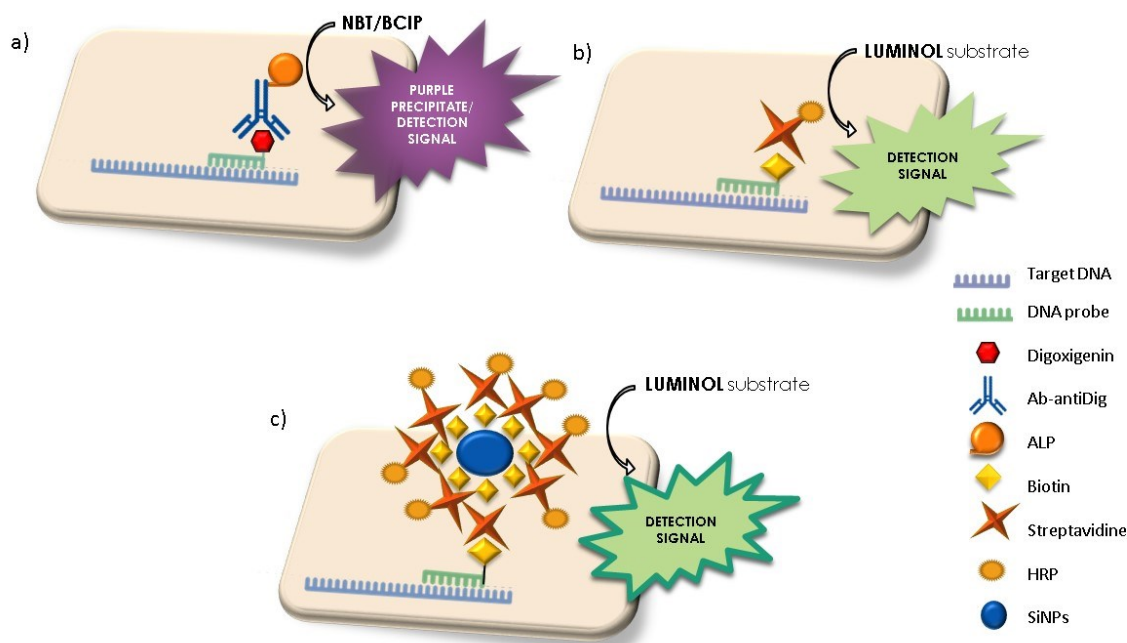


Figure 3.2 Schematic experimental procedure. Dot blot with alkaline phosphatase (AP) (a), chemiluminescent (b) and Si-NPs chemiluminescent (c) readout.

3.1.9.1 Dot blot with alkaline phosphatase (AP) assay.

The protocol was optimized for the following parameters:

- The temperature of hybridization (48, 50, 52, 54, 65 °C),
- time hybridization (30 min and overnight),
- washing temperature (hybridization temperature and room temperature)
- concentration of saline sodium citrate buffer (SSC) used in the first washing step (2X and 1X) second washing step (1X, 0.5X and 0.1X).
- addition of Formamide (2% and 5%) to DNA.

The protocol described by Fontanot et al. (2014) with some modifications was used.

The membrane was treated for the pre-hybridization step. It soaked in 7 mL of Dig Easy Hyb buffer (Roche, Italy) warmed at 65°C for 30 min, with shaking.

For the hybridization 7 µL of CampyP3 probe at 100 ng/µL, previously denatured at 98°C for 10 min, was added to 7 mL of Dig Easy Hyb buffer (Roche, Monza Italy) to obtain a final probe concentration at 100 ng/mL.

The non-hybridized probe was removed by serial washing steps. Twice 1X SSC (Sigma, Milano, Italy) with sodium 0.1 % (w/v) sodium dodecyl sulfate (SDS), for 10 min shaking at room temperature. Following twice with 0.1X SSC with sodium 0.1%SDS for 15 min shaking at room temperature.

The membrane was incubated with 10 mL of fresh prepared 1X Blocking (obtained by tenfold dilution of 10X blocking solution with 1X maleic acid buffer) (Roche, Monza, Italy) at room temperature for 30 min. Subsequently, the membrane was incubated with antibody solution (Anti-DIG-AP) diluted in blocking solution 1:5000 (Roche, Monza, Italy) at room temperature for 30

min shaking.

The membrane was washed twice with washing buffer 1X (Roche, Monza, Italy) for 15 min shaking and was neutralized with 5 mL of detection buffer 1X for 5 min.

For the detection of the probe hybridized to the target, the membrane was incubated with 100 μ L of detection color solution (NBT/BCIP stock solution) diluted in 5 mL of detection buffer 1X.

3.1.9.2 Chemiluminescent readout

The following studies were conducted in collaboration with the Institut Micalis, INRA, (Jouy en Josas, France).

The protocol was optimized by testing:

- nylon and nitrocellulose membrane
- Two hybridization buffers
A- 0.5 M Na_2HPO_4 , 0.5 M NaH_2PO_4 , 1% SDS and 10 mM EDTA at pH 7.5
B- 0.25 M Na_2HPO_4 , 7% SDS, 1 mM EDTA and 5% Dextran sulfate.
- The hybridization buffers conditions: DMSO 0% and 10%, Formamide 10, 25, 30, 35, 50%.
- Temperature of hybridization RT, 44, 55 and 65 °C.
- SSC concentrations for the washing steps: 2X -0.5X and 1X-0.1X.
- Streptavidin concentrations of 25 ng/ μ L and 50 ng/ μ L.

The whole procedure was conducted in a Petri dish 60 mm \varnothing .

The DNA was denatured at 95°C for 10 min and transferred immediately on ice for immobilization on the membrane. 1 μ L was spotted on the positively charged nylon membrane (Amersham Hybond Tm-XL, GE Healthcare, France), and fixed by exposure to UV light for 10 min.

The membrane was pre-hybridized soaking in 4 mL of hybridization buffer (0.5M Na_2HPO_4 , 0.5M NaH_2PO_4 , 10mM EDTA, 1%SDS at pH 7.5) at 65°C for 30 min, under shaking in a Petri dish.

Prior to the hybridization, the probe campyP3 was denatured at 95 °C for 5 min and placed on ice. 4 μ L denatured probe at 100 ng/ μ L was put in 4 mL of hybridization buffer. The Petri dish was closed with parafilm. The hybridization was performed at 65°C, overnight, shaking at 55 rpm. Washing steps were performed to remove the not hybridized probe, twice in 3 mL 1X SSC (Meraudex, France) with sodium 0.1 % (w/v) SDS, for 5 min shaking at 65°C, twice in 0.5X SSC with sodium 0.1%SDS for 15 min shaking at room temperature. Then 1X washing buffer (Thermofisher Tm, France), was used for 5 min at room temperature, shaking.

The membrane was incubated with 3mL of blocking buffer solution (Thermofisher Tm, France) to saturate the surface, for 15 min at RT. Subsequently, it was incubated with a new Blocking solution adding 5 μ L of 20X Stabilized streptavidin- Horseradish Peroxidase (SSHP) (EMD millipore corp., France) for 15 minutes at RT.

The membrane was washed twice with 4 mL of 1X washing buffer for 5 min shaking.

For the detection, the membrane was soaked in the substrate equilibrium buffer (Thermofisher Tm, France) for 5 min at RT shaking. Then, 500 μ L of the substrate working solution composed by Luminol/Enhancer Solution and Stable Peroxide Solution (1:1) was added and kept for 1 min at

RT without shaking. The membrane was then exposed to CCD camera (ChemiDoc™ MP Imaging System) and the data were read and processed by the program Image Lab™ Software (Biorad).

3.1.9.3 Dot Blot with Si NPs-Chemiluminescent readout

The following studies were conducted in collaboration with the Institut Micalis, INRA, (Jouy en Josas, France).

Preparation Silica NPs

The Silica NPs (Si-NPs) were prepared in Institut des Sciences Analytiques to CNRS-Université Claude Bernard Lyon 1-ENS (Lyon, France). The protocol carried out for the formation and study of Si NPs is reported by Bonnet et al. (2018).

The Si NPs of 40 nm diameter were covered with 50 biotins (Figure 3.3).

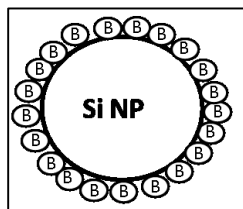


Figure 3.3 Si-NPs covered with biotins.

The stock solution was at a concentration of 1.4×10^{13} NPs/mL. Two-fold dilution were performed in PBS buffer to obtain Si-NPs solution at the final concentration of 108 NPs/mL. The Si NPs were prepared fresh for each experiment after 15 min of sonication of the stock solution.

Protocols

For this assay, the protocol was optimized testing several concentrations of Si-NPs at the concentration of 10^4 , 10^5 , 10^6 and 10^{10} .

The protocol optimized for chemiluminescent readout was applied also in the Si-NPs chemiluminescent assay until the incubation with the SSHP.

Indeed, the following steps were added to the protocol Si-NPs chemiluminescent readout.

The membrane was washed twice with 4 mL of 1X washing buffer for 5 min shaking.

Subsequently, the membrane was incubated with 80 μ L Si-NPs diluted in 7920 μ L PBS with a final concentration of 10^6 for 30 min at RT. Washing two times for 5 minutes at RT.

Then, the membrane was incubated with 3 mL 1X Blocking solution adding 5 μ L of 20X SSHPC for 15 min at RT and washing twice with 4 mL of 1X washing buffer for 5 min at RT.

The detection step proceeds as above described.

Normalized Data of the intensity measurement

The data were normalized to obtain a better qualitative comparison.

The intensity was measured and the average was calculated for each sample and for the control,

the sequence complementary to the probe (CCP3) by the software Image Lab TM Software (Biorad). The average value of the sample was divided by the average value of the control obtained.

Preparation of the samples for the Scanning electron microscopy micrographs

The samples with a surface of 1x1 cm² were prepared after the application of the protocol Si-NPs readout. The membrane was dried with a fixer, formalin, for 1h and then the membrane was left at room temperature overnight.

3.1.10 ELECTROCHEMICAL BIOSENSOR BASED ON VOLTAMMETRY

The following studies were conducted in collaboration with the Department of Chemistry of University of Udine.

3.1.10.1 Equipment and reagents

Materials and reagents used in this study are listed below:

- The screen-printed gold electrodes (SPAuEs) DropSens 220 AT (Au-Au-Ag/AgCl) (Metrohm- DropSens, Spain) were used. The electrochemical cell consists of a gold working electrode (WE), a gold auxiliary electrode (CE) and a silver reference electrode (RE). The working area was 4 mm in diameter. The screen-printed electrode with high-temperature curing inks showed the following surface (Figure 3.4).

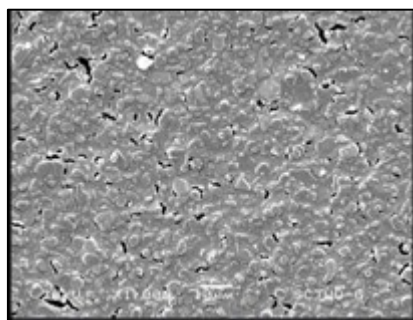


Figure 3.4 Surface of the Au screen printed electrode 220 AT (<http://www.dropsens.com>).

- H₂SO₄ at 0.5 M (96% sulfuric acid) was prepared in bidistilled sterilized water (Carlo Erba, Milan, Italy).
- PBS table, buffer 1X (0.0027 M KCl e 0.137 M NaCl, pH 7.4), solubilized in 200 mL of sterilized bidistilled water (Sigma- Aldrich, Milano, Italy).
- 6-Mercapto-1- hexanol (MCH) at 10 mM, (Sigma- Aldrich, Milan, Italy), was solubilized in Ethanol absolute anhydrous (Carlo Erba, Milan, Italy) and following the solution MCH at 1 mM was prepared in sterilized PBS buffer.
- FeCH (K₄[Fe(CN)₆·3H₂O])10 mM in sterilized PBS buffer 1X (AnalytiCals, Milan, Italy)
- The electrochemical analysis was conducted using PGSTAT101 autolab potentiostat galvanostat and NOVA 2.1 software (Methrom-Autolab B.V., Netherlands)

- Capture probe CampyP3 at 10 ng/μL was used to functionalize the Au surface.

3.1.10.2 Samples Bacterial strains preparation

To confirm the specificity of the probe used with the electrochemical biosensor protocols, *C. jejuni* (DSM 4688) was used as positive control and pure strains of *C. fetus* (DSM 5361), *E. coli* (DI4A), and *L. innocua* (DSM 20649) were used as negative controls. All the reference strains were preserved at -80°C in glycerol until revitalization on BHI broth (Thermofisher, Milan, Italy). The incubation time and temperature for *C. jejuni* and *C. fetus* were 48h at 41.5°C in microaerophilic conditions using CampyGen sachet (Thermoscientific, Milan, Italy), instead, *E. coli* and *L. innocua* were growing at 37°C 24h in aerobic conditions. The DNA of bacteria was extracted with phenol protocol previously described.

3.1.10.3 CampyP3 probe

The CampyP3 probe designed on the 16S gene was modified by the addition of a thiol group at 5' to allow to bind to the Au WE. The sequence of the probe is under patent.

Preparation and deprotection of the Capture probe CampyP3

The CampyP3 probe previously tested with the dot blot techniques, was standardized at 10 ng/μL in PBS buffer after deprotection at 5' end to make the thiol group reactive. The specific manufacturer's protocol was used:

- 200 μL of 10 mM TCEP
- Shaking 60 min at Room Temperature (RT)
- Precipitation by adding 150 μL 3 M of NaAc and addition of ethanol p.a., shaking gently and incubation for 20 min at -20°C
- Centrifuge for 5 min at 13000 rpm, discard the supernatant
- Dry pellet at room temperature.

3.1.10.4 Functionalization protocol of SPAuE

SPAuE Conditioning

All the electronic connections have been arranged, after which the screen-printed was inserted in the cable connectors and immersed in 8 mL of H₂SO₄ 0.5 M (aqueous solution), being careful to immerse all the electrodes of the screen printed. Then the following cleaning program was applied (Table.3.4). Subsequently, the electrodes were rinsed with sterile water, 500 μL of H₂O twice on both sides and dried under a laminar flow cabinet.

Table 3.4 Conditioning properties.

Start potential	0 V
Upper vertex potential	1.3 V
Lower vertex potential	-0.002 V
Stop potential	0 V
Number of scans	10
Scan rate	0.1 V/s
Step	0.00198 V

Immobilization of Campyp3 on Au electrode

The WE of the SPAuE was functionalized using 12 μL of 10 $\text{ng}/\mu\text{L}$ HS-ssDNA probe (CampyP3) in PBS overnight at 25°C, after denaturation at 95°C for 10 min. Then, the SPAuE was rinsed and dried. The resulting DNA-functionalized electrode surfaces were blocked with 12 μL of MCH 1 mM in PBS, pH 7.4 for 1 hour at 25°C. The electrode surface was then rinsed and dried under a sterile laminar flow cabinet and used for detection.

Hybridization samples

The hybridization was conducted with several nucleotide samples: sequence complementary to the Campy P3 probe, whole DNA from positive and negative controls and DNAs from food samples. Samples were diluted in PBS, then denatured at 95°C for 10 min and immediately put on ice before being used for hybridization and kept for 1 h at 25°C to hybridize. After incubation, the SPAuE was washed in order to remove the DNA not hybridized. The electrodes were then air-dried under a sterile laminar flow cabinet and used for the measurements.

3.1.10.5 Electrochemical measurement and processing data

The cyclic voltammetry (CV) and the differential pulse voltammetry (DPV) were performed in potentiostatic conditions for the functionalization and the hybridization steps. The experiment base on the detection of redox characteristics of $[\text{Fe}(\text{CN})_6]^{4-}$ that change after the surface functionalization with DNA. For the experiments CV and DPV measurements were conducted in 10 mM potassium hexacyanoferrate (II) trihydrate ($\text{K}_4[\text{Fe}(\text{CN})_6 \cdot 3\text{H}_2\text{O}]$) in PBS 1X under the following conditions (Table 3.5):

Table 3.5 Staircase cycle voltammetry (CV) and differential pulse voltammetry (DPV) properties.

CV		DPV	
Start potential	-0.2 V	Start potential	-0.2 V
Upper vertex potential	0.6 V	Stop potential	0.4 V
Lower vertex potential	-0.2 V	Step	0.005 V
Stop potential	-0.19756 V	Modulation amplitude	0.15 V
Number of scans	1	Modulation time	0.05s
Scan rate	0.1 V/s	Interval time	0.5s
Step	0.00244V	Scan rate	0.01 V/s

After each measurement, before the software, NOVA 2.1 was used to acquire data and register the height of anodic current peak (I_{pa}) by CV and DPV.

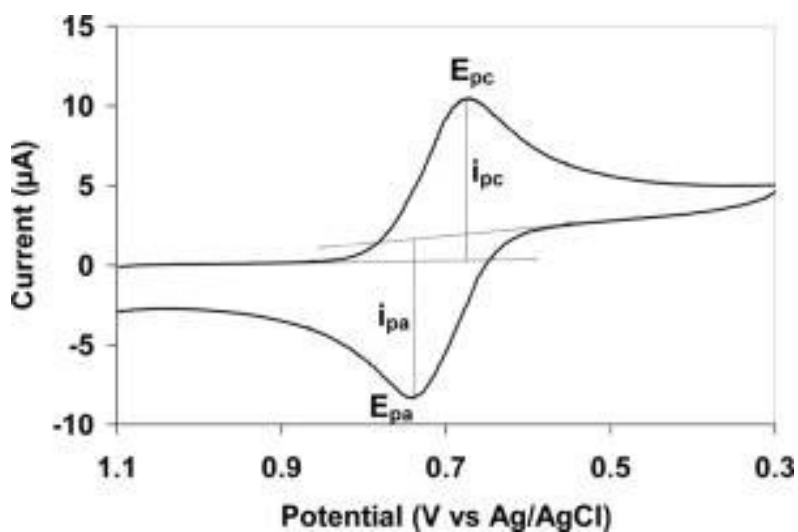


Figure 3.5 Typical cyclic voltammogram where I_{pc} and I_{pa} show the cathodic and anodic anodic current respectively for a reversible reaction. Instead, the E_{pc} and E_{pa} show the cathodic and anodic potential peak respectively.

For each sample, the delta of the anodic current peak, measured by CV and DPV, was calculated through the I_{pa} before hybridization (I_{pa} blank) and I_{pa} after hybridization (I_{pa} samples), obtained a ΔI_{pa} CV and ΔI_{pa} DPV:

$$I_{pa} \text{ blank} - I_{pa} \text{ samples} = \Delta I_{pa}$$

3.2 RESULTS AND DISCUSSION

3.2.1 CHICKEN SAMPLES

3.2.1.1 Plate count microbial enumeration

Plate count method results for the enumeration of the total viable count, Enterobacteriaceae, coliforms, *E. coli*, yeast and molds obtained for 20 chicken samples are reported in Table 3.6.

Total bacteria contamination of SC samples ranged from 1.3×10^4 to 5.1×10^9 CFU/g, except for the 17 SC sample in which count was below the detection limit. Enterobacteriaceae ranged from 2.1×10^2 to 2.4×10^4 CFU/g. Coliforms values ranged from 1.3×10^1 to 3.2×10^4 CFU/g, except for samples 12 SC and 17 SC that showed values below the limit of detection of the method applied. *E. coli* values ranged from 2×10^1 to 5.3×10^3 CFU/g, except for sample 19 SC that showed a value below the limit of detection. Yeasts ranged from 1.7×10^2 to 6.3×10^5 except sample 17 SC, molds were below the limit of detection in all samples.

Commission Regulation (EU) No 2073/2005 which establishes microbiological criteria for specific food categories was amended with the commission regulation (EU) 2017/1495 that added carcasses of broilers as a new food category and introduced a hygiene criterion process for *Campylobacter*. Nevertheless, there is still not a defined range for microorganisms detected broiler carcasses. The choice of further analysis and the evaluation is assigned to European Union Member States can choose microbial limits for analysis. Due to the defective legislation, the guideline of Piemonte Region on the analysis of risk in food microbiology approved with D.D. n. 780 on 11.18.2011, was adopted. The D.D. n 780 on 11.18.2011 declares, for the fresh and refrigerated meat, the following acceptable range: total viable mesophilic microorganisms from 10^6 to 10^7 CFU/g (FCD, 2009; Camera Commercio Torino, 2008), Enterobacteriaceae from 10^4 to 10^6 CFU/g (WQA, 2011; Circ -R nr. 8/1992) and *E. coli* from 10^3 to 10^4 CFU/g (FCD, 2009; Camera Commercio Torino, 2008).

The total viable mesophilic amount is acceptable for all chicken samples analyzed, except for 18 SC, 19 SC and 20 SC that showed a value of 2-3 logs higher. Enterobacteriaceae and *E. coli* amounts are in the range of acceptance.

Table 3.6 Plate count data expressed in Colony Forming Units (CFU)/g.

Samples	total viable count	Enterobacteriaceae	coliforms	<i>E. coli</i>	Yeasts	Molds
1 SC	9.9 x 10 ⁷	3.8 x 10 ³	2.0 x 10 ³	1.7 x 10 ³	2.3 x 10 ⁴	< 5 *
2 SC	5.1 x 10 ⁵	1.1 x 10 ³	9.8 x 10 ¹	2 x 10 ²	1.9 x 10 ³	< 5 *
3 SC	1.9 x 10 ⁵	9.4 x 10 ²	1.3 x 10 ¹	7.4 x 10 ²	7.8 x 10 ²	< 5 *
4 SC	4.8 x 10 ⁶	1.2 x 10 ⁴	3.0 x 10 ³	5.3 x 10 ³	9.4 x 10 ⁴	< 5 *
5 SC	9.5 x 10 ⁶	2.1 x 10 ⁴	7.0 x 10 ³	1.3 x 10 ³	6.3 x 10 ⁵	< 5 *
6 SC	7.3 x 10 ⁵	1.7 x 10 ³	2.3 x 10 ³	7.6 x 10 ²	6.6 x 10 ⁴	< 5 *
7 SC	9.6 x 10 ⁵	9.2 x 10 ³	6.4 x 10 ³	4.7 x 10 ²	3.3 x 10 ⁴	< 5 *
8 SC	9.8 x 10 ⁴	5.2 x 10 ³	5.2 x 10 ³	3.2 x 10 ²	1.5 x 10 ³	< 5 *
9 SC	1.8 x 10 ⁵	2.7 x 10 ³	1.4 x 10 ³	3.5 x 10 ²	2.2 x 10 ³	< 5 *
10 SC	1.3 x 10 ⁴	1.5 x 10 ³	7.7 x 10 ²	8.3 x 10 ¹	1.7 x 10 ²	< 5 *
11 SC	2.1 x 10 ⁶	2.15 x 10 ²	4.2 x 10 ¹	2 x 10 ¹	6.1 x 10 ³	< 5 *
12 SC	7.0 x 10 ⁵	2.6 x 10 ³	<5*	8 x 10 ²	2 x 10 ⁴	< 5 *
13 SC	1.2 x 10 ⁷	9.6 x 10 ³	9.5 x 10 ¹	2.7 x 10 ²	3.5 x 10 ⁴	< 5 *
14 SC	1.7 x 10 ⁷	2.4 x 10 ³	3.0 x 10 ²	0.6 x 10 ³	5.3 x 10 ⁴	< 5 *
15 SC	3.7 x 10 ⁷	6.9 x 10 ³	6.5 x 10 ¹	2.2 x 10 ³	4.5 x 10 ⁴	< 5 *
16 SC	1.1 x 10 ⁷	1.62 x 10 ⁴	5.6 x 10 ²	2.6 x 10 ²	2.4 x 10 ⁵	< 5 *
17 SC	<5 *	3.3 x 10 ²	<5*	3.1 x 10 ²	< 5 *	< 5 *
18 SC	3.3 x 10 ⁹	2.1 x 10 ⁴	3.2 x 10 ⁴	6.0 x 10 ²	4.9 x 10 ⁵	< 5 *
19 SC	3.8 x 10 ⁹	5.4 x 10 ³	1.3 x 10 ⁴	< 5 *	3.9 x 10 ⁵	< 5 *
20 SC	5.1 x 10 ⁹	2.4 x 10 ⁴	2.4 x 10 ⁴	1.5 x 10 ²	5.4 x 10 ⁵	< 5 *

*Detection limit

3.2.1.2 ISO 10272-1:2006

The same samples of chicken carcasses were analyzed applying the ISO 10272-1:2006 for the detection of *Campylobacter*. The data reported in table 3.7 show that samples 2 SC, 3 SC, 8 SC, 10 SC, 16 SC, and 17 SC must be considered positive for the presence of *Campylobacter* spp. because the results agree with the profile.

Table 3.7 The presence (+) or absence (-) of *Campylobacter* spp. assessed with the ISO1027-1:2006 protocol.

Samples	mCCDA	SKR	CAB	Confirmation medium CAB		Oxidase	Motility
				presence /absence			
				41.5 °	25 °C		
				Aerobic	microaerobic		
1 SC	+	-	+	+	-	+	-
2 SC	+	-	+	-	-	+	+
3 SC	+	-	+	-	-	+	+
4 SC	+	-	+	+	+	+	-
5 SC	+	-	+	+	+	+	-
6 SC	+	-	+	+	+	+	-
7 SC	+	-	+	+	+	+	-
8 SC	+	-	+	-	-	+	+
9 SC	+	+	+	+	+	+	-
10 SC	+	-	+	-	-	+	+
11 SC	-	-	/	/	/	/	/
12 SC	-	-	/	/	/	/	/
13 SC	-	-	/	/	/	/	/
14 SC	-	-	/	/	/	/	/
15 SC	-	-	/	/	/	/	/
16 SC	+	+	+	-	-	+	+
17 SC	+	+	+	-	-	+	+
18 SC	+	+	+	+	+	+	-
19 SC	+	+	+	+	+	+	-
20 SC	+	+	+	+	+	+	-

3.2.1.3 Quality of DNA extracted from chicken samples

The electrophoresis performed on the DNA samples extracted allowed the evaluation of good integrity of the DNA, indicating that it was useful for application in the biosensor optimization protocol. An example of the DNA extracted from the samples SCB is shown in Figure 3.6 a single defined band.

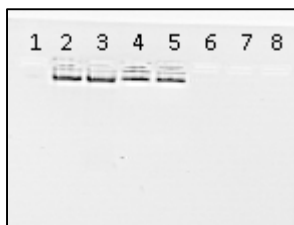


Figure 3.6 Test of Integrity DNA. Line 1, 6, 7 and 8: /, line 2: SCB1, Line3:SCB2, Line 4:SCB3, Line 5:SCB4.

3.2.2 PRIMER CAMPYP FW CAMPYPRW

3.2.2.1 Features of the primers

The primers, named CampyPFW and CampyPRW, were able to detect *C. jejuni*, *C. coli*, *C. lari*, and *C. upsaliensis*, as expected. They were designed on the 16S-23S gene. Sequences – following sequence: GQ167702.1 for *C. jejuni*, GQ167720.1 for *C. coli*, AB644222.1 for *C. lari* and DQ871249.1 for *C. upsaliensis* (Fig. 3.7) that were used for the alignment by “Multiple sequence alignment with hierarchical clustering” software.

The features taken into account for the design of the primers are represented in Table 3.8.

Table 3.8 CampyP primers features.

FEATURES	CampyP FW	CampyP RW	Score
Length	19	20	/
Melting Temperature	57°C	55	Good
Content ofGC %	57%	50	Good
Stability at 3' end	3	2	Good
Repeated sequence in tandem (Poly x)	0	0	Good
Self dimer	15	16	Good
Self end dimer	0	0	Good

The data reported show that CampyPFW and CampyPRW primers observe the optimal feature, indicated by the score: good obtained for all parameters. The sequences are under patent.

3.2.2.2 Specificity with the test *in silico*

Before the application in the experiments, specificity was tested *in silico* by the software Amplifx, Fast PCR 6.1 and Blast. The first two softwares are able to simulate the amplification as shown in Figure 3.7.

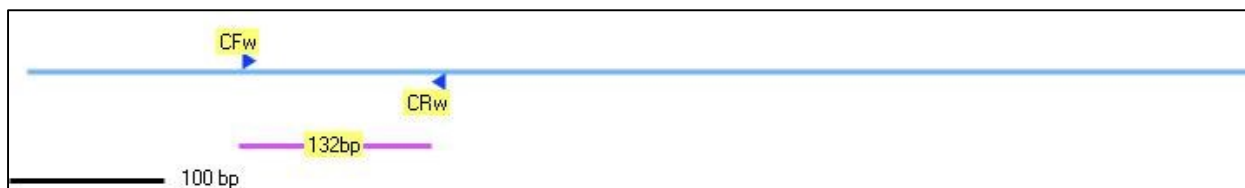


Figure 3.7 Example of amplification *in silico* using the sequence of *C. jejuni*, GQ167720.1 by Amplifx.

Positive amplification results were obtained for the following accession numbers: *Campylobacter jejuni* (GQ167702.1), *C. coli* (GQ167720.1), *C. lari* (AB644222.1), *C. upsaliensis* (DQ871249.1). The couple of primers were also tested on bacteria that can be considered natural contaminants of the food samples such as chicken and pig, including other species of *Campylobacter*. The accession numbers of species tested, that gave *in silico* negative amplification results are listed in Table 3.2. Considering the studies conducted by Zhang et al. (2000) and Morgulis et al. (2008) on BLAST software a further test was conducted on the amplified sequences obtained by PCR *in silico*. The results confirmed that the sequence produced by positive amplification of the tested species belonged to *Campylobacter* spp.: *C. jejuni* or *C. coli* or *C. lari* or *C. upsaliensis*. Following an example of the results (Table 3.9) obtained about the lineage analysis that confirm the optimal features of the primers and their specificity *in silico*. Based on these results the tests proceeded by PCR and q-PCR on samples.

Table 3.9 Results of the lineage analysis.

Organism	Blast Name	Score	N. of Hits	Description
<i>Campylobacter</i>	e-proteobacteria		100	
<i>Campylobacter jejuni</i>	e-proteobacteria		74	
<i>Campylobacter jejuni subsp. jejuni</i>	e-proteobacteria	244	6	<i>Campylobacter jejuni subsp. jejuni</i> hits
<i>Campylobacter jejuni subsp. jejuni</i> D42a	e-proteobacteria	244	1	<i>Campylobacter jejuni subsp. jejuni</i> D42a hits
<i>Campylobacter jejuni subsp. jejuni</i> M129	e-proteobacteria	244	1	<i>Campylobacter jejuni subsp. jejuni</i> M129 hits
<i>Campylobacter jejuni subsp. jejuni</i> str. RM3420	e-proteobacteria	244	1	<i>Campylobacter jejuni subsp. jejuni</i> str. RM3420 hits
<i>Campylobacter jejuni subsp. jejuni</i> PT14	e-proteobacteria	244	1	<i>Campylobacter jejuni subsp. jejuni</i> PT14 hits
<i>Campylobacter jejuni</i>	e-proteobacteria	244	74	<i>Campylobacter jejuni</i> hits
<i>Campylobacter coli</i>	e-proteobacteria	244	15	<i>Campylobacter coli</i> hits
<i>Campylobacter lari</i> CCUG 22395	e-proteobacteria	244	1	<i>Campylobacter lari</i> CCUG 22395 hits

3.2.3 PCR

3.2.3.1 Optimization of annealing temperature

The primers CampyPFW and CampyPRW tested *in vitro* by PCR assay before their application in q-PCR technique, required the optimization of the protocol, in particular, the annealing temperature and the MgCl₂ concentration in the reaction mixture. To assess the primer specificity, a PCR was carried out on the reference strains listed in Table 3.1 using a DNA concentration of 100 ng/μL. The amplification results are shown in Figure 3.8. The annealing temperature of 55 °C used in the first test allowed the production of an amplicon for the negative controls *L. innocua* (line 4), *L. seeligeri* (line 5), *L. ivanovii* (line 8), *B. cereus* (line 13), and *B. subtilis* (line 15), inducing to evaluate an increased annealing T to improve primer specificity.

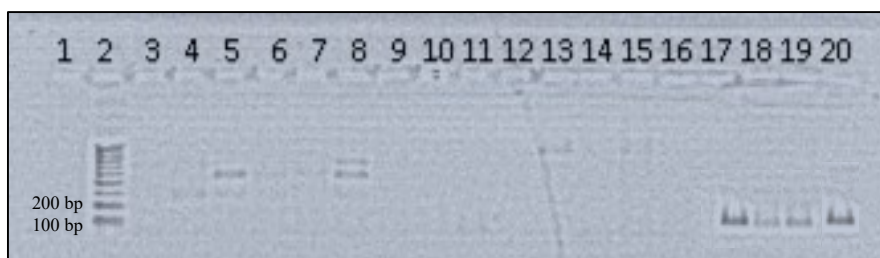


Figure 3.8 PCR specificity using positive and negative controls, Ta 55 °C. Line 1: /; line 2: 100 bp DNA ladder (Promega); line 3: *L. monocytogenes* ATCC 7644; line 4: *L. innocua* DSM 20649; line 5: *L. seeligeri* DSM 20751; line 6: *L. marthii* DSM 23813; line 7: *L. welshimeri* DSM 15452; line 8: *L. ivanovii* DSM 52491; line 9: *S. aureus* DI4A; line 10: *C. fetus* DSM 5361; line 11: *C. cryaerophila* DSM 7289; line 12: *H. pylori* DSM 7492; line 13: *B. cereus* DSM 4282; line 14: *H. suis* DSM 19375; line 15: *B. subtilis* DSM 4184; line 16: *S. enterica* DSM 9378; line 17: *C. jejuni* DSM 4688; line 18: *C. coli* DSM 24155; line 19: *C. lari* DSM 11375; line 20: *C. upsaliensis* DSM 5365.

3.2.3.2 Sensitivity test

The temperatures of 56 °C- 57 °C (Figure 3.9) and 58 °C (Figure 3.10) were tested. At 56 °C, *B. cereus* (DSM 4282) (line 6, Figure 3.10) produced an amplicon. At 57 °C, a thick band below the 50 bp value indicated by the MWM is visible for *L. ivanovii* (line 14), it can be justified as primer accumulation.

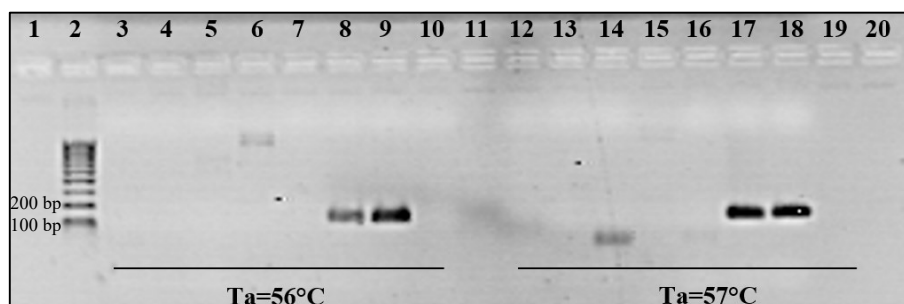


Figure 3.9 Annealing temperature optimization with CampyPFW- CampyPRW using positive and negatives controls, Ta 56 e 57°C. Line 1, 11, 20: /; Line 2: 100 bp DNA Ladder; Line 3: *L. innocua* DSM 20649; Line 4: *L. seeligeri* 20751; Line 5: *L. ivanovii* DSM 72491; Line 6: *B. cereus* DSM 4282; Line 7: *B. subtilis* DSM 4181; Line 8: *C. jejuni* DSM 4688; Line 9: *C. coli* DSM 24155; Line 10: blank; Line 12: *L. innocua* DSM 20649; Line 13: *L. seeligeri* DSM 20751; Line 14: *L. ivanovii* DSM 72491; Line 15: *B. cereus* DSM 4282; Line 16: *B. subtilis* DSM 4181; Line 17: *C. jejuni* DSM 4688; Line 18: *C. coli* DSM 24155; Line 19: blank.

The temperature of annealing of 58 °C allowed the best specificity of the primers as shown in Figure 3.10, where clear amplification DNA bands are visible for the four species of *Campylobacter* under test. Based on these results the annealing temperature of 58 °C was selected for the subsequent analysis.

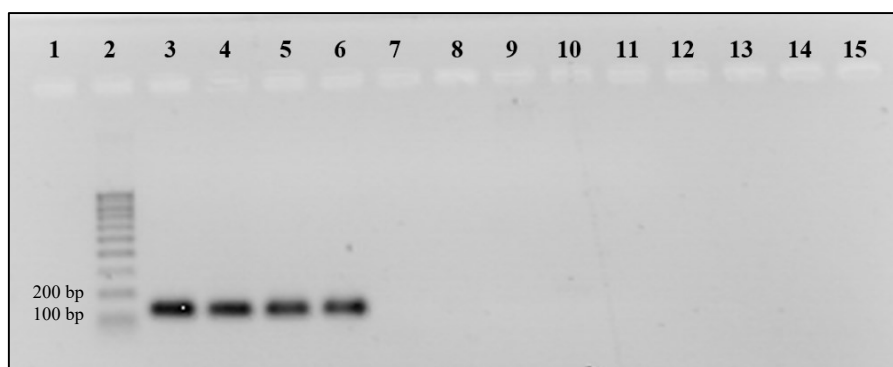


Figure 3.10 Specificity test with CampyPFW- CampyPRW at 58°C annealing temperature. Line 1: /; Line 2: 100 bp DNA Ladder; line 3: *C. jejuni* DSM 4688; line 4: *C. coli* DSM 24155; line 5: *C. lari* DSM 11375; line 6: *C. upsaliensis* DSM 5365; line 7: *C. fetus* DSM 5361; line 8: *H. suis* DSM 19735; line 9: *H. pylori* DSM 7492; line 10: *H. pylori* ICSS; line 11: *Arc. butzleri* DSM 8739; line 12: *B. cereus* DI4A RC3; line 13: *E. coli* DISTAM; line 14: *Lb. plantarum* ATCC RAA 793; line 15: *S. cerevisiae* ATCC 36024.

3.2.3.3 Optimization of $MgCl_2$

After the optimization of the annealing temperature, $MgCl_2$ concentration was optimized too. PCR was repeated on positive and negative samples, *C. jejuni*, *C. coli*, *C. fetus*, and *E. coli* at three different $MgCl_2$ concentrations: 1.5, 2 and 2.5 mM at 58°C. The best results were obtained at $MgCl_2$ 1.5 mM.

Therefore, a magnesium concentration at 1.5 mM was chosen.

3.2.3.4 PCR sensitivity

The Sensitivity of the primers was assessed using decimal dilutions of *Campylobacter jejuni* DNA (Figure 3.11). CampyPFW- CampyPRW primers reached a sensitivity of 1 pg/ μ L as reported in Figure 3.11.

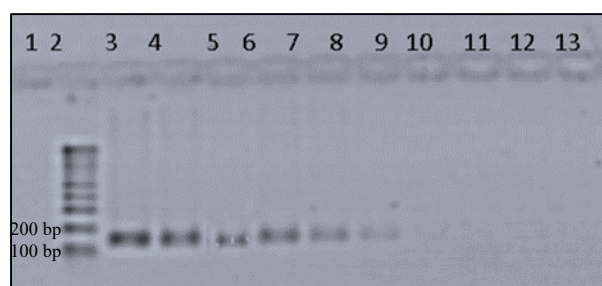


Figure 3.11 PCR sensitivity with CampyPFW-CampyPRW using decimal dilutions of DNA of *C. jejuni* DMS 468, at 58 °C. Line 1:/; line 2: Line 3: 100 bp DNA Ladder; line4: 100 ng/ μ ; line5:10 ng/ μ ; line6:1 ng/ μ ; line7:100 pg/ μ , line8: 10 pg/ μ L; line9:1 pg/ μ L, line 10: 100 fg/ μ L, line 11: 10 fg/ μ L, line12: 1 fg/ μ L, line 13: Blank.

3.2.4 qPCR

A standard curve was built with the *C. jejuni* DSM 4688 reference strain at serial decimal dilutions. Subsequently, qPCR was applied to DNA extracted from non-enriched (SCF) and enriched (SCB) samples

3.2.4. 1 Standard curve

To build a standard reference curve for absolute Quantification of samples, a qPCR assay was carried out on decimal dilutions of *C. jejuni* DSM 4688 from 10 ng/μL to 100 fg/μL samples are reported in Table 3.10.

Figure 3.12 shows the behavior of the amplification cycles performed and the threshold value obtained with the Rotor-Gene Q Series Software 2.0.2 (Build 4; Qiagen). Figure 3.13 reports the standard curve obtained with DNA concentration from 10 ng/μL to 100 fg/μL that corresponds to the sensitivity of the assay. NCT is the no template control. The standard curve shows an $R^2 = 0.99$ and a slope of -3.315, corresponding to an efficiency of 100.28 % and a threshold value of 0.0556.

Table 3.10 *C. jejuni* DSM 4688 samples and quantification data (*Threshold cycle).

#	Col	Name	C _T *	Given Conc (ng/μL)	Calc Conc (ng/μL)	% Var
1		<i>C. jejuni</i> 10 ng/μL	9.15	10.000000	10.7960	8.0%
2		<i>C. jejuni</i> 1 ng/μL	12.64	1.000000	0.9616	3.8%
3		<i>C. jejuni</i> 100 pg/μL	15.87	0.100000	0.1016	1.6%
4		<i>C. jejuni</i> 10 pg/μL	19.44	0.010000	0.0085	15.0%
5		<i>C. jejuni</i> 1 pg/μL	22.45	0.001000	0.0010	5.0%
6		<i>C. jejuni</i> 100 fg/μL	25.75	0.000100	0.0001	6.1%
7		NTC	-	-	-	-

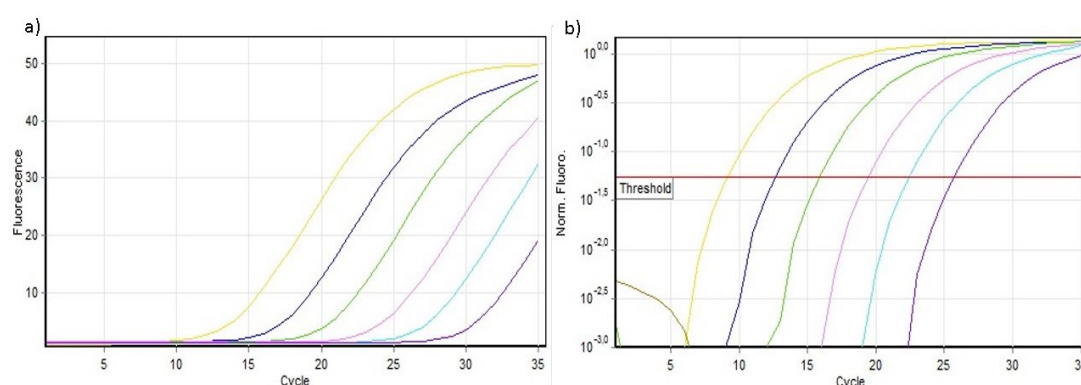


Figure 3.12 qPCR of decimal dilutions of *C. jejuni* DMS 4688. a) Raw fluorescent signal vs. number of cycles. b) Normalized fluorescent signal vs. number of cycle and individuation of the threshold value. C_t (threshold cycle) correspond to the cycle at which the template DNA reach the set threshold value. Fluorescence acquisition was performed during annealing/extension step of the amplification.

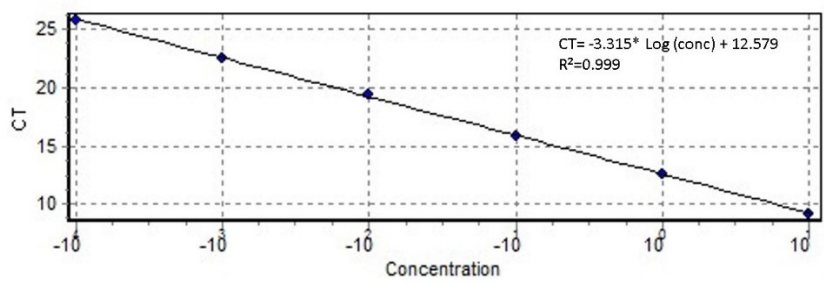


Figure 3.13 Standard curve of *C. jejuni* DSM 4688. The curve was obtained plotting the threshold cycle (C_T) of each DNA dilution vs. the initial DNA concentration (ng/ μ L). The standard curve equation obtained can be used to calculate the concentration of unknown DNA samples on the basis of their C_T values.

A melting curve analysis was performed in order to verify the nature of the produced amplicons as reported in Table 3.11 and Figure 3.14, respectively. All samples produced melting curves with the T_m in the range from 84.90 to 85.10 with the threshold df/t corresponding to 1.1993 value.

Table 3.11 Melting data of decimal dilution of *C. jejuni* DMS 4688.

#	Col	Name	T_m ($^{\circ}$ C)
1	Yellow	<i>C. jejuni</i> 10 ng/ μ L	85.10
2	Blue	<i>C. jejuni</i> 1 ng/ μ L	85.10
3	Green	<i>C. jejuni</i> 100 pg/ μ L	85.00
4	Pink	<i>C. jejuni</i> 10 pg/ μ L	85.00
5	Cyan	<i>C. jejuni</i> 1 pg/ μ L	84.90
6	Purple	<i>C. jejuni</i> 100 fg/ μ L	84.90
7	Brown	NTC	-

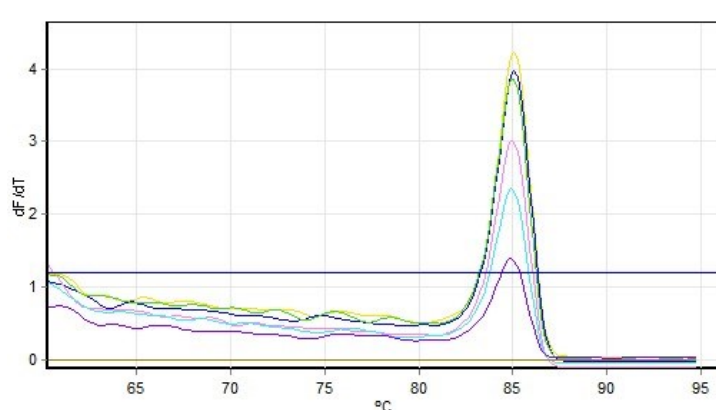


Figure 3.14 Melting curve analysis of decimal dilutions of *L. C. jejuni* DSM 4688. Decrease in fluorescent signal (expressed as dF/dT) is plotted against temperature ($^{\circ}$ C).

3.2.4.2 Specificity test

A check on specificity was carried out using DNA extracted from the reference strains listed in Table 3.12 at 50 ng/μL. Samples quantification was performed using the standard curve obtained previously and reported in Figure 3.15. *C. jejuni*, *C. coli*, *C. lari* and *C. upsaliensis*, reference strains, were amplified within 11.55 C_T . The melting curve analysis presents a range between 84.90- 85.10 °C, confirming the specificity of the protocol and primers. Although the negative controls *C. fetus*, *A. butzleri*, and *H. pylori* produced a fluorescent signal, they were considered negative because their value of C_t was over the threshold value 24.19 (Table 3.12 and Figure 3.16).

Table 3.12 qPCR of positive and negative control, C_T value and melt data.

#	Col	Name	C_T	T_m (C°)
1	■	<i>C. jejuni</i> DSM 4688	8.67	85.10
2	■	<i>C. coli</i> DSM 24155	8.14	84.90
3	■	<i>C. lari</i> DSM 11375	12.68	84.90
4	■	<i>C. upsaliensis</i> DSM 5365	9.89	85.00
5	■	<i>C. fetus</i> DSM 5361	27.14	-
6	■	<i>A. butzleri</i> DSM 8739	26.29	-
7	■	<i>H. pylori</i> DSM 7492	26.37	-
8	■	NTC	24.19	-

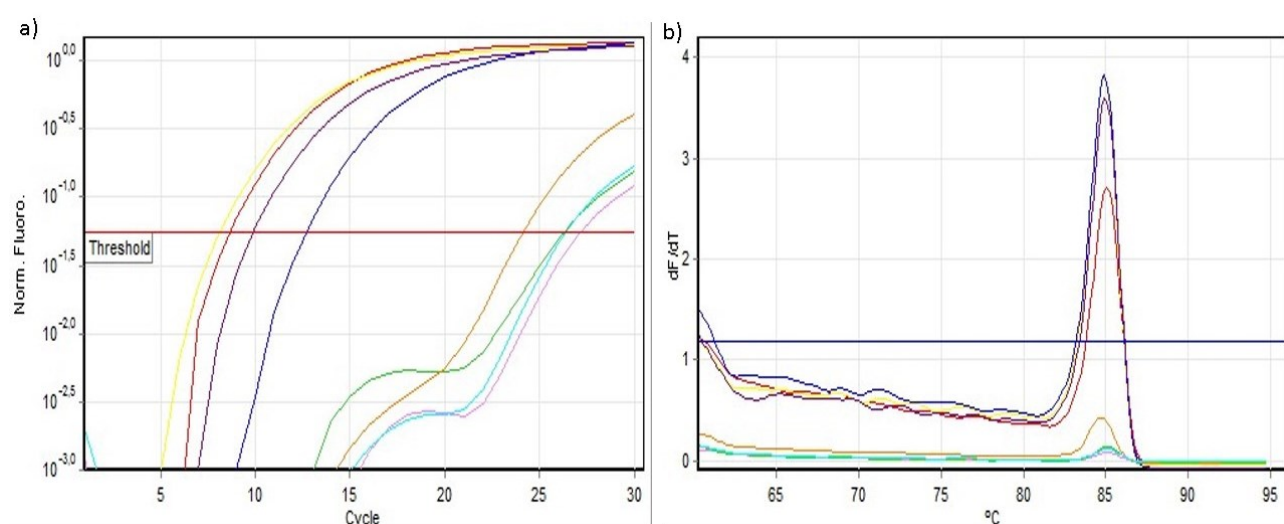


Figure 3.15 qPCR analysis of positive and negative controls. a) Normalized fluorescent signal vs. number of cycle and individuation of the threshold value. Fluorescence acquisition was performed during annealing/extension step of the amplification. b) Melting curve analysis of positive and negative controls. Decrease in fluorescent signal (expressed as dF/dT) is plotted against temperature (°C).

3.2.4.3 qPCR samples analysis

Samples extracted from saline peptone water (SCF) at 1:100 dilution

All samples SCF at the dilution 1:100 were considered negative for the presence of *Campylobacter* spp. as the signal they produced was further the C_t of the no template control (26.98) as shown in Table 3.13 and Figure 3.16.

Table 3.13 SCF samples diluted 1:100, C_t value, quantification and melting data.

#	Col	Name	C_t	Calc Conc (ng/ μ L)	T_m (C°)
1	Red	2 SCF 1:100	27.67	0.000028	-
2	Yellow	3 SCF 1:100	27.11	0.000041	84.75
3	Blue	6 SCF 1:100	27.55	0.000030	-
4	Purple	7 SCF 1:100	27.63	0.000029	-
5	Green	8 SCF 1:100	27.93	0.000023	-
6	Cyan	9 SCF 1:100	26.97	0.000046	-
7	Black	10 SCF 1:100	27.73	0.000027	-
8	Grey	NTC	26.98	0.000045	84.60

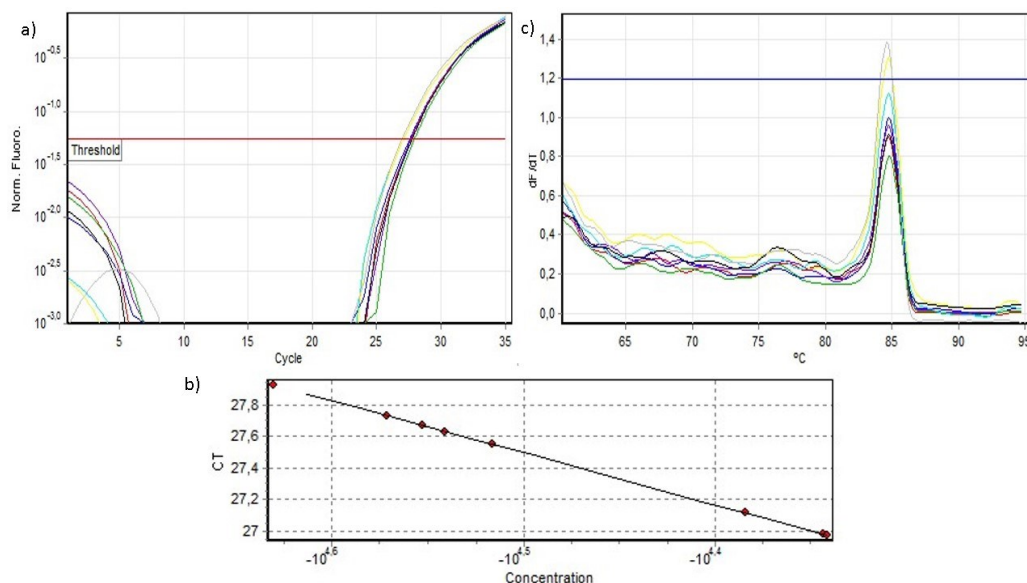


Figure 3.16 qPCR analysis of SCF samples (1-10), diluted 1:100. a) Normalized fluorescent signal vs. number of cycle and individuation of the threshold value. Fluorescence acquisition was performed during annealing/extension step of the amplification. b) Standard curve showing determination of concentration of SCF samples. c) Melting curve analysis of positive and negative controls. Decrease in fluorescent signal (expressed as dF/dT) is plotted against temperature (°C).

Samples extracted from saline peptone water (SCF) at dilution 1:10

Samples SCF at the dilution 1:10 produced a fluorescent signal over the Ct of the NTC sample (26.46 Ct), a part for sample 3SCF which Ct was 25.1, as reported in Table 3.14 and Figure 3.15, These samples were considered negative for the presence of *Campylobacter* spp.

Table 3.14 SCF samples diluted 1:10, quantification and melting data.

#	Col	Name	C _T	Calc Conc (ng/μL)	T _m (C°)
1	Red	2 SCF 1:10	27.00	0.000045	85.00
2	Yellow	3 SCF 1:10	25.14	0.000162	85.00
3	Blue	6 SCF 1:10	29.85	0.000006	-
4	Purple	7 SCF 1:10	30.55	0.000004	-
5	Green	8 SCF 1:10	30.04	0.000005	-
6	Grey	9 SCF 1:10	31.05	0.000003	-
7	Black	10 SCF 1:10	30.09	0.000005	-
8	Cyan	NTC	26.46	0.000065	85.00

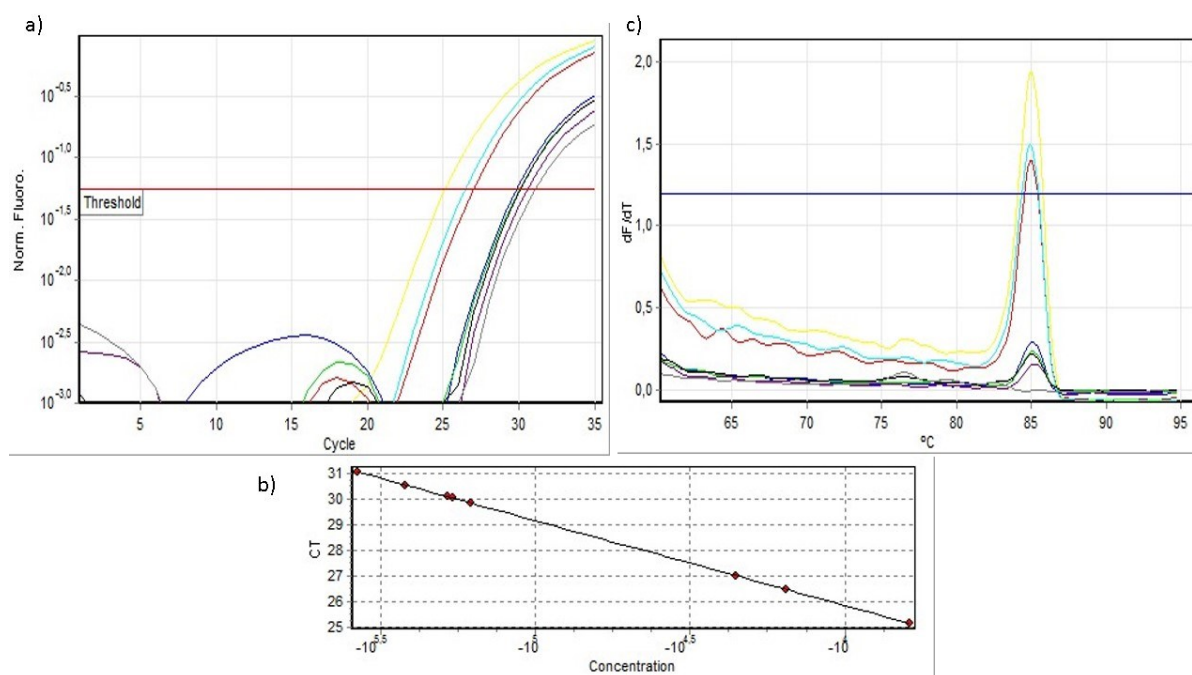


Figure 3.17 qPCR analysis of SCF samples (1-10), diluted 1:10. a) Normalized fluorescent signal vs. number of cycle and individuation of the threshold value. b) Standard curve showing determination of concentration of SCF samples. c) Melting curve analysis of positive and negative controls. Decrease in fluorescent signal (expressed as dF/dT) is plotted against temperature (°C).

Samples extracted from saline peptone water (SCF) at TQ dilution

The data of the samples not diluted are reported in Table 3.15. From the value obtained in the Table 3.15, the 2 SCF, 3SCF, 8SCF, and 10 SCF were considered positive as their fluorescent signals were obtained before the Ct value of the no template control (NTC) (27.62) as shown in Figure 3.18.

Table3.15 SCF sample, Ct value, quantification and melting data.

#	Col	Name	C _T	Calc Conc (ng/μL)	T _m (C°)
1	■	2 SCF TQ	24.75	0.000215	84.40
2	■	3 SCF TQ	23.24	0.000610	84.50
3	■	6 SCF TQ	28.11	0.000021	-
4	■	7 SCF TQ	28.16	0.000020	-
5	■	8 SCF TQ	23.90	0.000385	84.40
6	■	9 SCF TQ	27.11	0.000041	-
7	■	10 SCF TQ	26.72	0.000054	-
8	■	NTC	27.62	0.000029	-

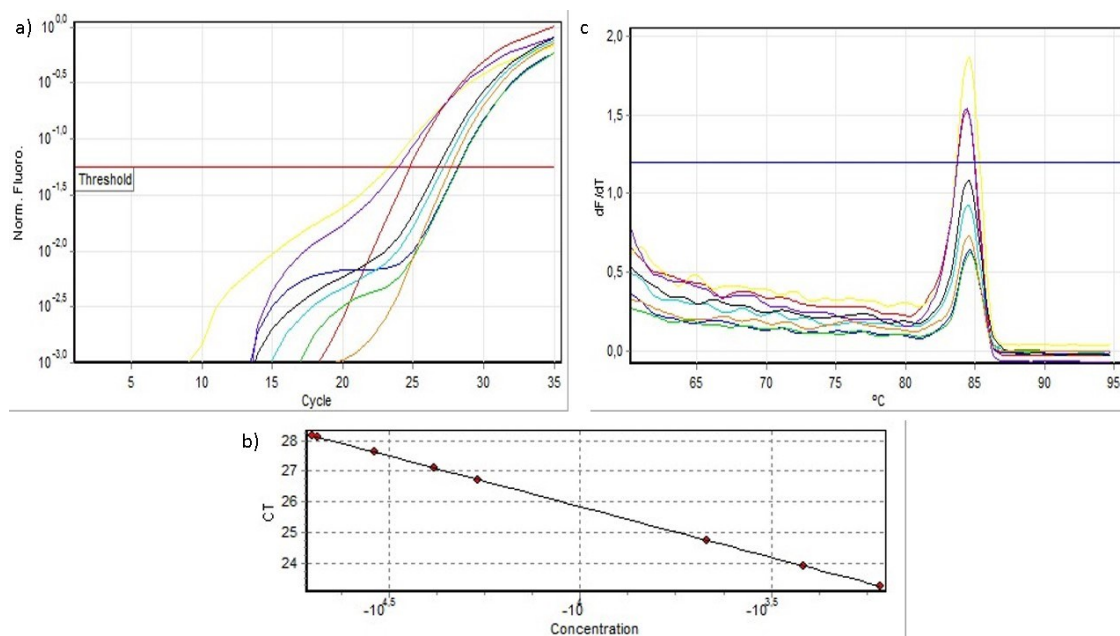









Figure 3.18 qPCR analysis of SCF samples (1-10). a) Normalized fluorescent signal vs. number of cycle and individuation of the threshold value. b) Standard curve showing determination of concentration of SCF samples. c) Melting curve analysis of positive and negative controls. Decrease in fluorescent signal (expressed as dF/dT) is plotted against temperature (°C).

In Table 3.16 and Table 3.17 the samples from 11 SCF TO 15SCF and from 16 SCF to 20 SCF respectively. The normalized fluorescent signal and the melting curve for the samples from 11 SCF to 15 SCF are reported in Figure 3.19 and for the samples from 16 SCF and 20 SCF in Figure 3.20 Only one sample resulted positive, the 17 SCF.

From the total data reported the SCF samples can be analyzed without the need for dilution and 2SCF, 3SCF, 8SCF, 10SCF, and 17SCF are positive to the presence of *Campylobacter*.

Table 3.16 SCF samples (11-15), Ct value, quantification and melting data.

#	Col	Name	C _T	Calc Conc (ng/μL)	T _m (C°)
1		11 SCF TQ	28.12	0.000021	-
2		12 SCF TQ	26.39	0.000068	-
3		13 SCF TQ	27.30	0.000036	-
4		14 SCF TQ	26.70	0.000055	-
5		15 SCF TQ	26.64	0.000057	-
6		<i>E. coli</i>	27.15	0.000040	-
7		NTC	26.79	-	-

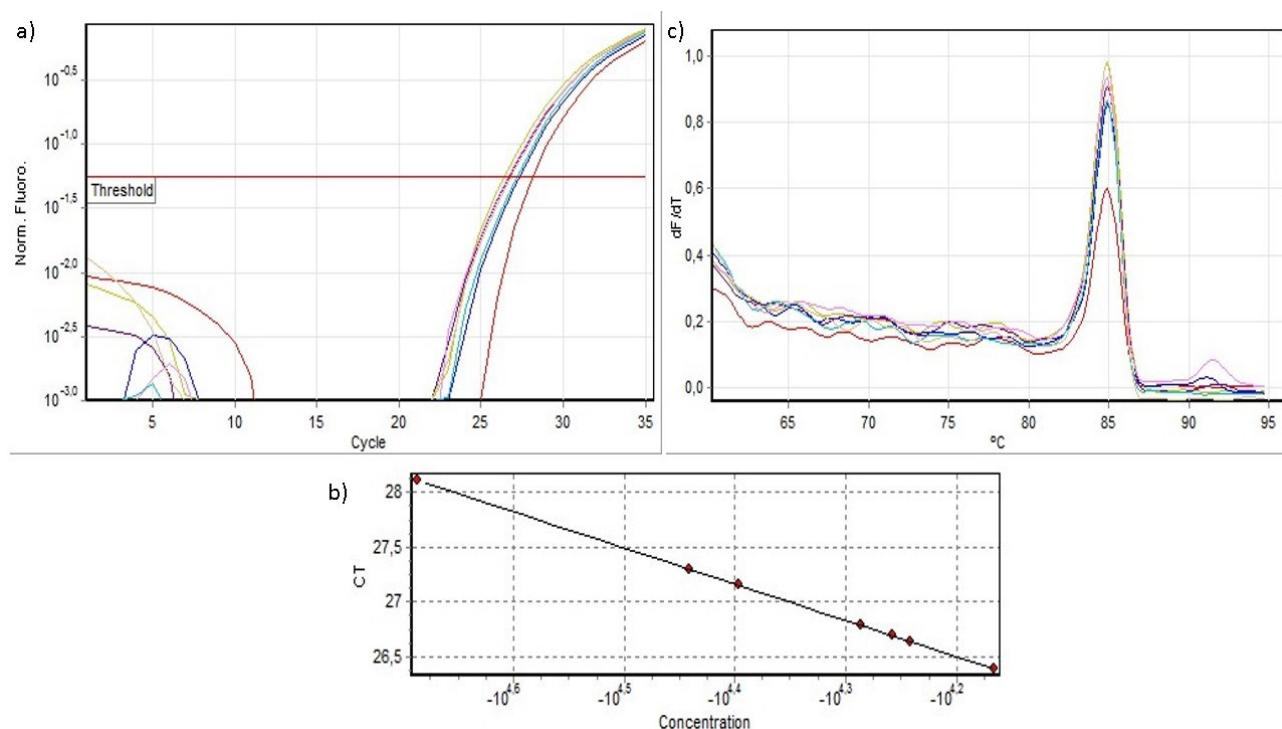









Figure 3.19 qPCR analysis of SCF samples (1-10). a) Normalized fluorescent signal vs. number of cycle and individuation of the threshold value. b) Standard curve showing determination of concentration of SCF samples. c) Melting curve analysis of positive and negative controls. Decrease in fluorescent signal (expressed as dF/dT) is plotted against temperature (°C).

Table 3.17 SCF samples (16-20), Ct value, quantification.

#	Col	Name	C _T	Calc Conc (ng/μL)	T _m (C°)
1		16 SCF TQ	27.27	0.000037	-
2		17 SCF TQ	25.62	0.000116	-
3		18 SCF TQ	30.44	0.000004	-
4		19 SCF TQ	28.39	0.000017	-
5		20 SCF TQ	28.77	0.000013	-
6		NTC	27.47	0.000032	-
7		<i>E. coli</i>	27.76	0.000026-	-

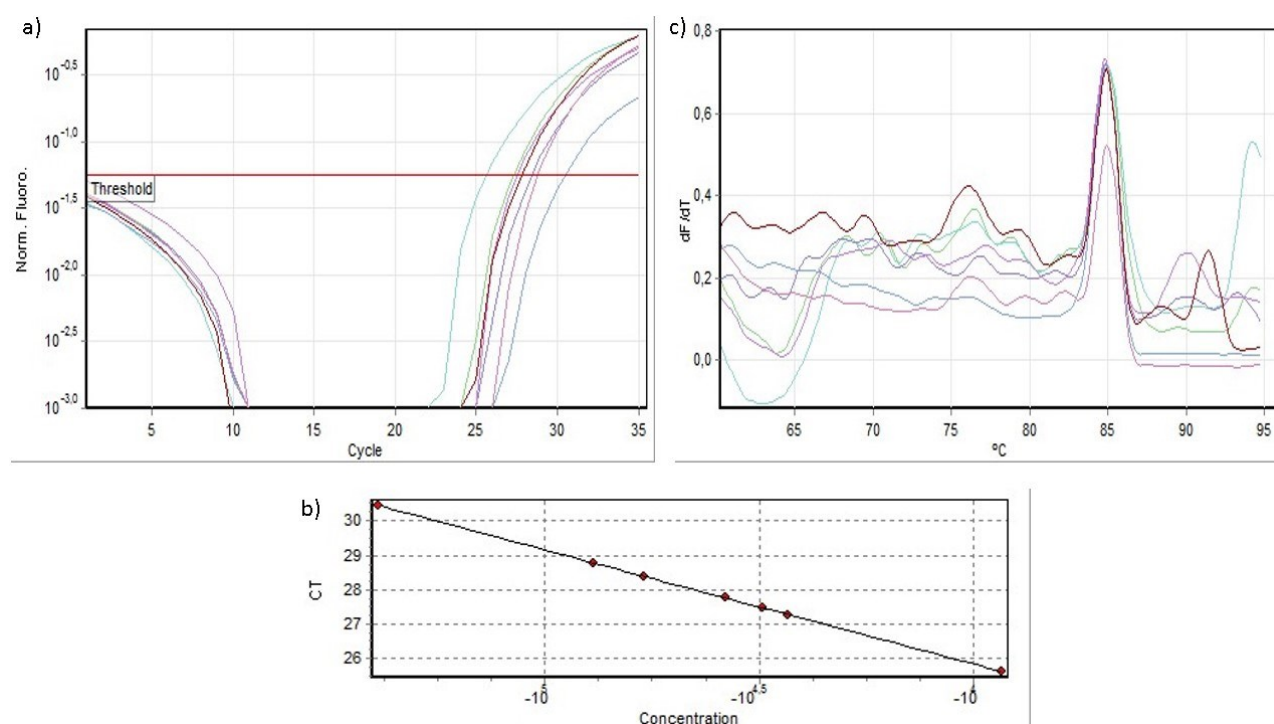


Figure 3.20 qPCR analysis of SCF samples (16-20). a) Normalized fluorescent signal vs. number of cycle and individuation of the threshold value. b) Standard curve showing determination of concentration of SCF samples. c) Melting curve analysis of positive and negative controls. Decrease in fluorescent signal (expressed as dF/dT) is plotted against temperature (°C).

Samples extracted from Bolton broth at TQ dilution

The qPCR analysis of SC samples was conducted also on DNA extracted after 48 h of enrichment in Bolton broth. In Table 3.18 and Figure 3.21 are reported the data obtained for samples from 1 to 10 SCB. The results obtained are in agreement with the results obtained for SCF samples. 2SCB, 3SCB, 8SCB, and 10 SCB were positive to the presence of *C. jejuni*. Taking into account the calibration curve, samples were diluted to increase the accuracy of the analysis

Table 3.18 SCB samples (1-10), Ct value, quantification and melting data.

#	Col	Name	Ct	Calc Conc (ng/ μ L)	T _m (C°)
1	■	2 SCB TQ	5.20	168.45	84.85
2	■	3 SCB TQ	6.84	53.79	84.85
3	■	6 SCB TQ	30.51	0.000004	-
4	■	7 SCB TQ	27.72	0.000027	-
5	■	8 SCB TQ	13.29	0.611224	84.85
6	■	9 SCB TQ	-	-	-
7	■	10 SCB TQ	16.34	0.07360	84.85
8	■	NTC	-	-	-

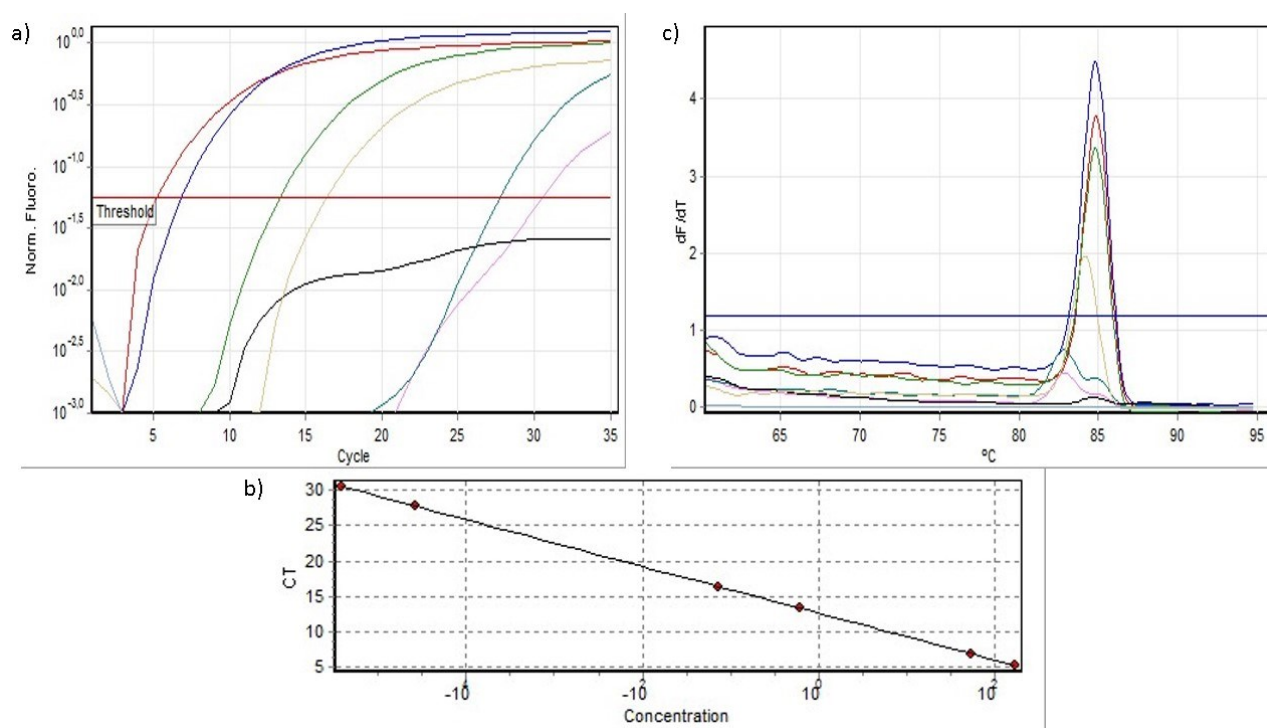


Figure 3.21 qPCR analysis of SCB samples (1-10). a) Normalized fluorescent signal vs. number of cycle and individuation of the threshold value. b) Standard curve showing determination of concentration of SCF samples. c) Melting curve analysis of positive and negative controls. Decrease in fluorescent signal (expressed as dF/dT) is plotted against temperature (°C).

Samples extracted from Bolton broth at 1:100 dilution

Samples from 1 to 10SCB were diluted 1:100 to increase the accuracy of the analysis. The presence of *Campylobacter* spp. was detected in samples 2SCB, 3SCB, 8SCB, and 10SCB, while 9SCB was considered negative (Table 3.19 and Figure 3.22).

Table 3.19 SCB samples (1-10), diluted 1:100, Ct value, quantification and melting data.

#	Col	Name	C _T	Calc Conc (ng/μL)	T _m (C°)
1	■	2 SCB 1:100	13.38	0.572837	84.65
2	■	3 SCB 1:100	12.94	0.779398	84.60
3	■	6 SCB 1:100	29.82	0.000006	-
4	■	7 SCB 1:100	28.23	0.000019	-
5	■	8 SCB 1:100	18.79	0.013392	84.50
6	■	9 SCB 1:100	22.63	0.000928	-
7	■	10 SCB 1:100	19.00	0.011548	84.50
8	■	NTC	26.88	0.000049	-

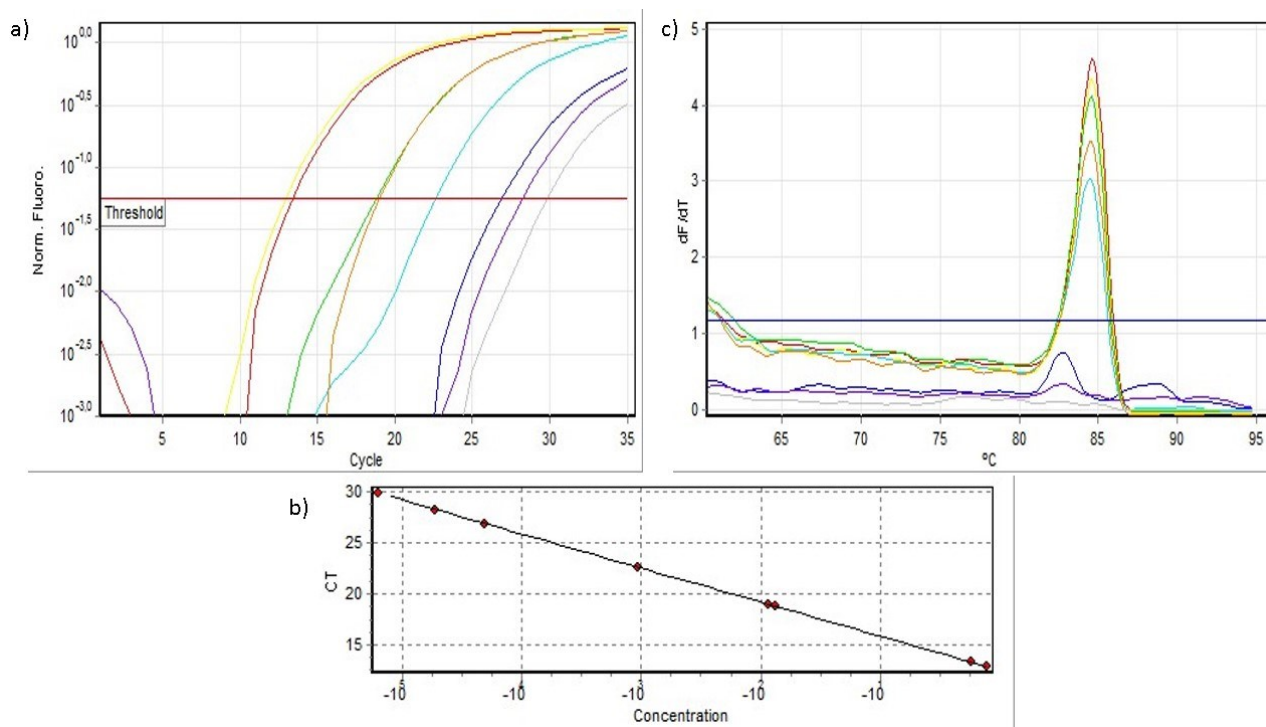









Figure 3.22 qPCR analysis of SCB samples diluted 1:100 (1-10). a) Normalized fluorescent signal vs. number of cycle and individuation of the threshold value. b) Standard curve showing determination of concentration of SCF samples. c) Melting curve analysis of positive and negative controls. Decrease in fluorescent signal (expressed as dF/dT) is plotted against temperature (°C).

Samples from 11 to 15 SCB are all negative considering the Ct value of the NCT and the melting temperature under the threshold reported in Table 3.20 and in Figure 3.23.

Table 3.20 SCB samples (11-15), diluted 1:100, Ct value, quantification and melting data.

#	Col	Name	Ct	Calc Conc (ng/ μ L)	T _m (C°)
1		11 SCB 1:100	27.44	0.000033	-
2		12 SCB 1:100	26.57	0.000060	-
3		13 SCB 1:100	26.36	0.000070	-
4		14 SCB 1:100	26.94	0.000047	-
5		15 SCB 1:100	26.85	0.000049	-
6		<i>E. coli</i>	27.15	0.000040	-
7		NTC	26.79	0.000052	-

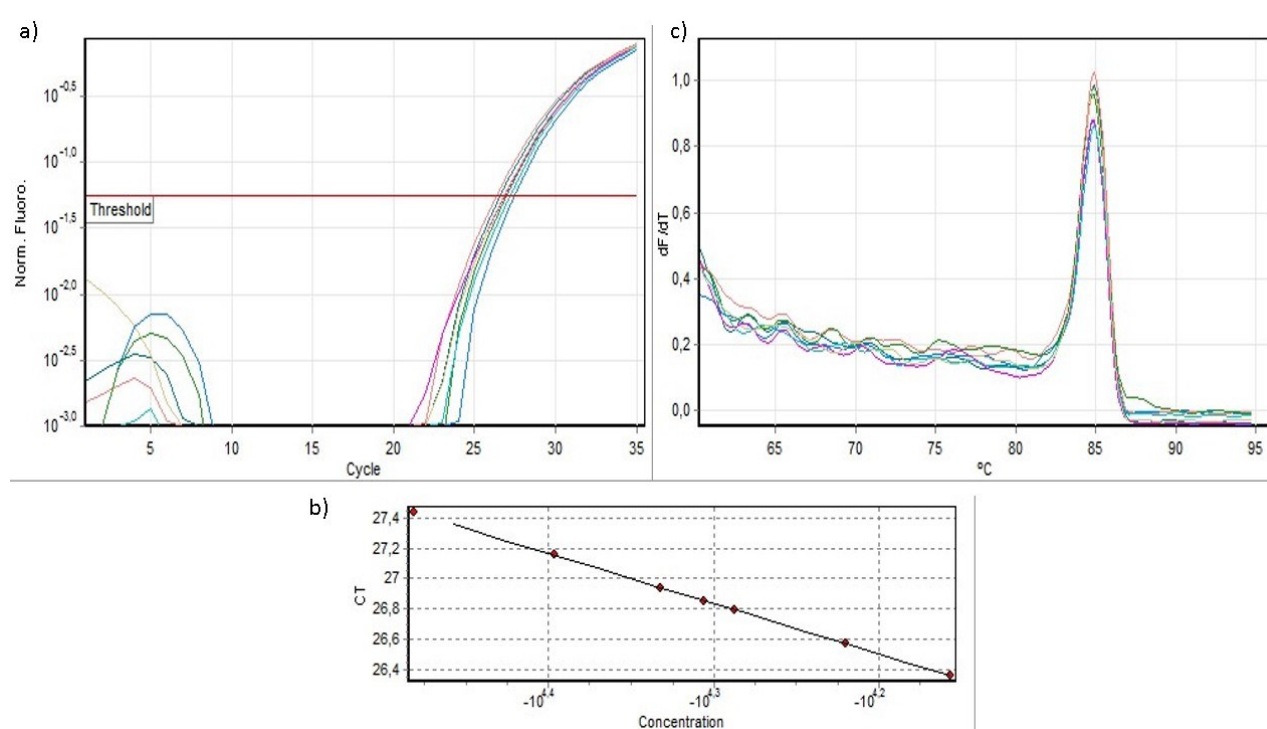






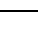


Figure 3.23 qPCR analysis of SCB samples diluted 1:100 (11-15). a) Normalized fluorescent signal vs. number of cycle and individuation of the threshold value. b) Standard curve showing determination of concentration of SCF samples. c) Melting curve analysis of positive and negative controls. Decrease in fluorescent signal (expressed as dF/dT) is plotted against temperature (°C).

In Table 3.21 and in Figure 3.24 are shown the data of the samples from 16 to 20 SCB. Based on the value of the Ct only sample 17 SCB was positive.

Table 3.21 SCB samples (16-20), diluted 1:100, Ct value, quantification and meltig data.

#	Col	Name	C _T	Calc Conc (ng/μL)	T _m (C°)
1		16 SCB 1:100	26.07	0.000085	84.65
2		17 SCB 1:100	22.30	0.001172	84.75
3		18 SCB 1:100	26.99	0.000045	84.75
4		19 SCB 1:100	26.63	0.000058	84.65
5		20 SCB 1:100	26.78	0.000052	84.75
6		<i>E. coli</i>	27.26	0.000037	84.60
7		NTC	26.50	0.000063	84.65

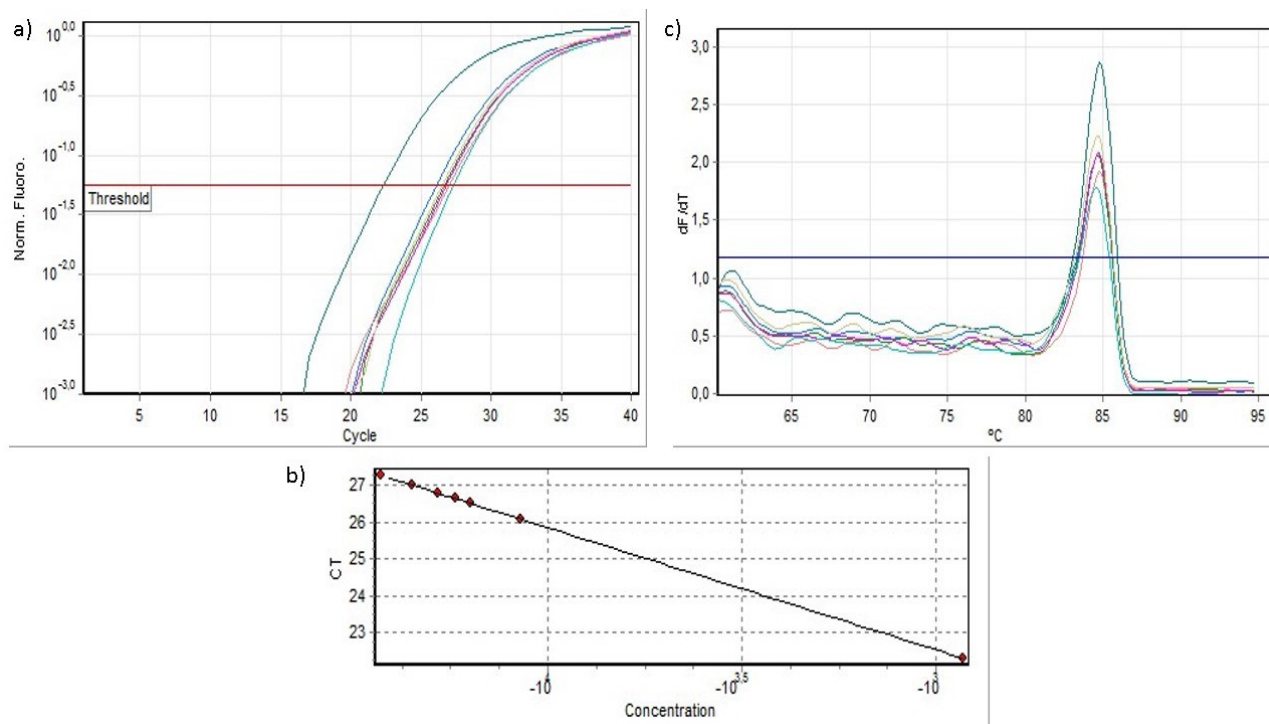


Figure 3.24 qPCR analysis of SCB samples (11-15). a) Normalized fluorescent signal vs. number of cycle and individuation of the threshold value. b) Standard curve showing determination of concentration of SCF samples. c) Melting curve analysis of positive and negative controls. Decrease in fluorescent signal (expressed as dF/dT) is plotted against temperature (°C).

The results reported previously confirm the capability of the primers CampyPFW and CampyPRW to detect *Campylobacter* spp. in saline peptone water without dilution, and in Bolton broth. In the case of enrichment, the best performance of the qPCR analysis was obtained by diluting the DNA at 1:100. The CampyP primer and qPCR protocol are able to discriminate positive samples from the negative samples. This method reliable is faster than the alternative for the ISO method and is precise

3.2.5 CAMPYP3 PROBE

The CampyP3 probe is under patent.

3.2.5.1 Features of the probe

The DNA probe, named CampyP3, was designed within the 16S gene of *Campylobacter* spp. to detect *C. jejuni*, *C. coli*, *C. lari*, and *C. upsaliensis*.

For the design of CampyP3, of 36 nucleotides (nt) length, DNA sequences with accession numbers NR_117760.1 for *C. jejuni*, N.: JX912505.1 for *C. coli*, N.: NR_115289.1 for *C. lari*, and N.: NR_115289.1 for *C. upsaliensis*.

The optimal features of the probe are as follow (Table 3.22):

Table 3.22 Features of the probe CampyP3.

FEATURES	CampyP3	Score
Length	36	/
Melting Temperature	64 °C	Good
Content ofGC %	47 %	Good
Stability at 3' end	2	Good
Repeated sequence in tandem (Poly x)	0	Good
Self dimer	16	Good
Self end dimer	0	Good

Based on the data reported, the CampyP3 probe shows the optimal features. The melting temperature is in the range 55-80°C, the % of guanine and cytosine (GC) is in the range 40-60%, there are not repeated sequence in tandem and dimers.

3.2.5.2 In silico specificity test for the probe

The specificity was tested in silico by the software Amplifx, Fast PCR 6.1 and Blast. The first two software are able to simulate the probe hybridization as shown in Figure 3.25.

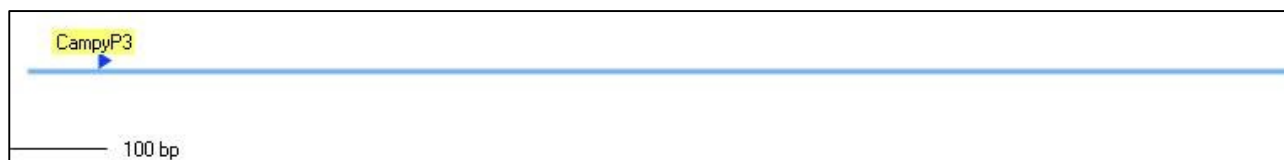


Figure 3.25 Example of *in silico* probe hybridization with the sequence of *C. jejuni*, NR_117760.1 by Ampliflix.

Tests on hybridization gave positive results with *Campylobacter jejuni* NR_117760.1, JX912519.1, *C. coli* JX912505.1, *C. lari* NR_117762.1, *C. upsaliensis* NR_115289.1.

The probe was also tested on bacteria that can be present in food samples like chicken and pig, including other species of *Campylobacter*. Accession numbers corresponding to 16S, 16S -23S and whole genomes of species tested are listed in Table 3.2. No *in silico* amplifications were possible for all the sequences tested. The results were also confirmed with the software FAST PCR 6.1. The sequence chosen for the CampyP3 probe analyzed with BLAST, according to the studies conducted by Zhang et al. (2000) and Morgulis et al. (2008), confirmed that the selected sequence belongs to the genus *Campylobacter* (Figure 3.26).

Lineage Report		Organism Report Taxonomy Report		
Organism	Blast Name	Score	Number of Hits	Description
Bacteria	bacteria		104	
• Campylobacter	e-proteobacteria		103	
• • Campylobacter coli	e-proteobacteria	67.6	15	Campylobacter coli hits
• • Campylobacter sp. CA656	e-proteobacteria	67.6	1	Campylobacter sp. CA656 hits
• • Campylobacter jejuni	e-proteobacteria	67.6	53	Campylobacter jejuni hits
• • Campylobacter sp. B571	e-proteobacteria	67.6	1	Campylobacter sp. B571 hits
• • Campylobacter sp. B716b	e-proteobacteria	67.6	1	Campylobacter sp. B716b hits
• • Campylobacter sp. B423b	e-proteobacteria	67.6	1	Campylobacter sp. B423b hits
• • Campylobacter sp. W677a	e-proteobacteria	67.6	1	Campylobacter sp. W677a hits
• • Campylobacter sp. W441b	e-proteobacteria	67.6	1	Campylobacter sp. W441b hits
• • Campylobacter volucris	e-proteobacteria	67.6	1	Campylobacter volucris hits
• • Campylobacter helveticus	e-proteobacteria	67.6	2	Campylobacter helveticus hits
• • Campylobacter jejuni subsp. jejuni	e-proteobacteria	67.6	9	Campylobacter jejuni subsp. jejuni hits
• • Campylobacter hepaticus	e-proteobacteria	67.6	1	Campylobacter hepaticus hits
• • Campylobacter sp. MIT17-670	e-proteobacteria	67.6	1	Campylobacter sp. MIT17-670 hits
• • Campylobacter sp. MIT17-664	e-proteobacteria	67.6	1	Campylobacter sp. MIT17-664 hits
• • Campylobacter sp. MIT10-5678	e-proteobacteria	67.6	1	Campylobacter sp. MIT10-5678 hits
• • Campylobacter insulaenigrae	e-proteobacteria	67.6	1	Campylobacter insulaenigrae hits
• • Campylobacter jejuni subsp. doylei	e-proteobacteria	67.6	4	Campylobacter jejuni subsp. doylei hits
• • Campylobacter lari	e-proteobacteria	67.6	1	Campylobacter lari hits
• • Campylobacter upsaliensis	e-proteobacteria	67.6	1	Campylobacter upsaliensis hits
• • Campylobacter sp.	e-proteobacteria	67.6	2	Campylobacter sp. hits
• • Campylobacter avium LMG 24591	e-proteobacteria	67.6	1	Campylobacter avium LMG 24591 hits
• • Campylobacter cuniculorum DSM 23162 = LMG 24588	e-proteobacteria	67.6	1	Campylobacter cuniculorum DSM 23162 = LMG 24588 hits
• • Campylobacter jejuni subsp. jejuni D42a	e-proteobacteria	67.6	1	Campylobacter jejuni subsp. jejuni D42a hits
• • Campylobacter jejuni subsp. jejuni M129	e-proteobacteria	67.6	1	Campylobacter jejuni subsp. jejuni M129 hits
• uncultured bacterium	bacteria	67.6	1	uncultured bacterium hits

Figure 3.26 Lineage analysis of sequence CampyP3 by BLAST.

3.2.6 DOT BLOT ALKALINE PHOSPHATASE (ALP) ASSAY

The validation of CampyP3 was conducted by an enzymatic immunoassay as shown in Figure 3.27a and 3.27b. Therefore, the sensitivity and specificity of CampyP3 were tested using a CampyP3 labeled with a digoxigenin at 5' end.

In Figure 3.27a the sensitivity of the probe was tested using the target CP3 (sequence complementary to campy P3) with concentration from 100 ng/ μ L to 100 fg/ μ L. A blue spot was the confirmation of the positive hybridization reaction. The limit of detection (LOD) for CampyP3 was 1 ng/ μ L. The results of the specificity test, shown in Figure 3.28b, were conducted on negative controls such as *E. coli*, *S. enterica*, *H. pylori*, and *Arc. butzleri*, bacteria that can be present in meat samples (Figure 3.27b Row A).

In Figure 3.27b Row B, several species of *Campylobacter* spotted at the concentration of 100 ng/ μ L. Only *C. jejuni* produced the blue spot indicating positivity.

In Figure 3.27b row C, high DNA concentrations of *Campylobacter* spp. were spotted. The probe had shown the ability to detect the targeted species.

3.2.7 DOT BLO CHEMILUMINESCENT ASSAY

The results obtained by traditional chemiluminescent techniques are presented in Figure 3.27c, d and e. Figure 3.27c and 3.28d show the sensitivity test, while Figure 3.27e shows the specificity test. The experiments were conducted applying the CampyP3 probe labeled with Biotin at 5' end. In Figure 3.27c the target was represented by the sequence complementary to CampyP3 probe (CCP3), used at concentrations from 1 ng/ μ L to 5 pg/ μ L. The LOD obtained was 0.1 ng/ μ L. Figure 3.27d shows the results of the sensitivity carried out on *C. jejuni* whole DNA from 100 ng/ μ L to 1 ng/ μ L, considered as the positive control. The LOD was 5 ng/ μ L for the whole DNA of *C. jejuni*. The specificity of the probe CampyP3-Bio was tested also on short sequences of DNA, PR and PE probe, used in comparison with CCP3 (Figure.3.27e). PR is a negative short sequence, instead, PR is a short probe with a random distribution of the nucleotides present in the sequence complementary to CampyP3.

The Concentrations from 0.8 ng/ μ L to 0.1 ng/ μ L were used. The CampyP3 probe showed specificity only for positive controls.

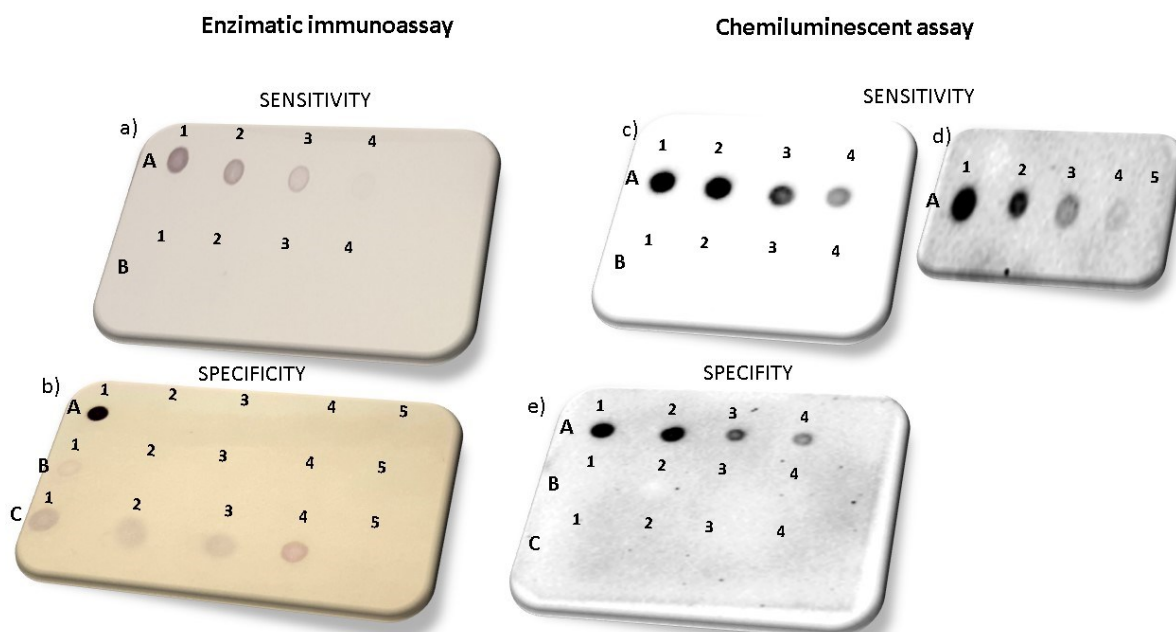


Figure 3.27 Enzymatic immunoassay and chemiluminescent results. Membrane a) Row A, A1: 100 ng/ μ L, A2: 50 ng/ μ L, A3: 10 ng/ μ L, A4: 1 ng/ μ L. Row B, B1: 0.1 ng/ μ L B2: 0.01 ng/ μ L B3: 0.001 ng/ μ L B4: 0.0001 ng/ μ L. Membrane b) Row A, A1: CCP3 100 ng/ μ L, A2: *E. coli* 100 ng/ μ L, A3: *H. pylori* 100 ng/ μ L, A4: 100 ng/ μ L A5: 100 ng/ μ L. Row B, B1: 100 ng/ μ L B2: 100 ng/ μ L B3: 100 ng/ μ L B4: 100 ng/ μ L B5: 100 ng/ μ L. Row C, C1: 256 ng/ μ L C2: 206 ng/ μ L C3: 612 ng/ μ L C4: 386 ng/ μ L C5: 218 ng/ μ L Membrane c) Row A, A1: 1 ng/ μ L A2: 0.5 ng/ μ L A3: 0.2 ng/ μ L A4: 0.1 ng/ μ L. Row B, B1: 0.05 ng/ μ L, B2: 0.02 ng/ μ L, B3: 0.01 ng/ μ L, B4: 0.005 ng/ μ L Membrane d) Row A, A1: 100 ng/ μ L A2: 50 ng/ μ L A3: 10 ng/ μ L A4: 5 ng/ μ L A5: 1 ng/ μ L. Membrane e) CCP3 in Row A A1: 0.8 ng/ μ L A2: 0.4 ng/ μ L A3: 0.2 ng/ μ L A4 0.1 ng/ μ L. PR in Row B: B1: 0.8 ng/ μ L B2: 0.4 ng/ μ L B3: 0.2 ng/ μ L B4 0.1 ng/ μ L. PE in Row C C1: 0.8 ng/ μ L, C2: 0.4 ng/ μ L, C3: 0.2 ng/ μ L, C4 0.1 ng/ μ L.

3.2.8 DOT BLOT Si-NPs CHEMILUMINESCENT ASSAY

3.2.8.1 Si-NPs chemiluminescent readout for CCP3

Figure 3.28 (a and b) shows the sensitivity obtained without and with Si-NPs respectively. Concentrations from 0.1 ng/ μ L to 0.78 pg/ μ L were tested, and the LOD was 0.1 ng/ μ L (Figure 3.28a) like previously obtained for Figure (3.28c). Figure 3.28b produced an improved value of LOD, 6 pg/ μ L, due to the application of 10^6 NPs. Figure 3.28c shows the data related to the increase of the signal with the utilization of NPs. The specificity was tested on the bacteria listed in Table 3.1. Based on the values obtained with the analyses of the spots produced on the membrane with the CampyP3-Bio using the Image LabTM Software, it is possible to consider as positive only samples with a normalized value above 1. As shown in Figure 3.29 only *Campylobacter jejuni*, *C. coli*, *C. lari*, and *C. upsaliensis* resulted in detected.

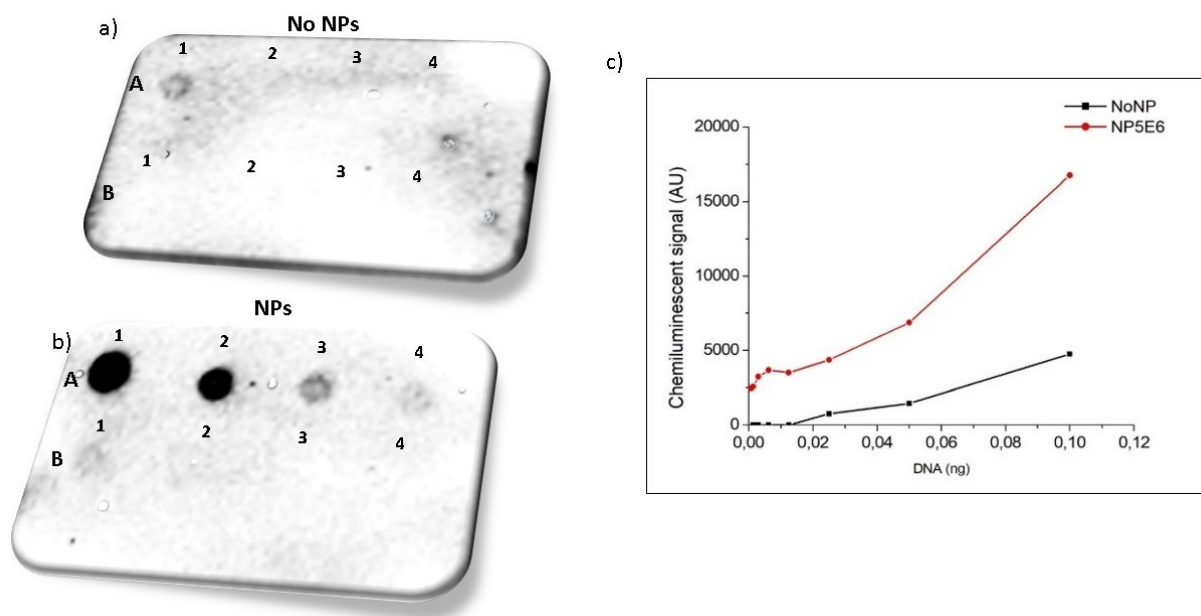


Figure 3.28 New Chemiluminescent results without and with NPs tested with complementary probe CP3. a) Row A, A1:0.1 ng/ μ L, A2: 0.05 ng/ μ L, A3: 0.025 ng/ μ L, A4: 0.0125 ng/ μ L; Row B B1:0.006 ng/ μ L, B2: 0.0031 ng/ μ L, B3:0.0015 ng/ μ L, B4 0.00078 ng/ μ L. b) Row A, A1 0.1 ng/ μ L, A2:0.05 ng/ μ L, A3: 0.025 ng/ μ L, A4: 0.0125 ng/ μ L; Row B, B1: 0.006 ng/ μ L, B2: 0.0031 ng/ μ L, B3: 0.0015 ng/ μ L, B4 0.00078 ng/ μ L. c) Comparison between the value obtained without NPs (black curve) and with NPs (red curve).

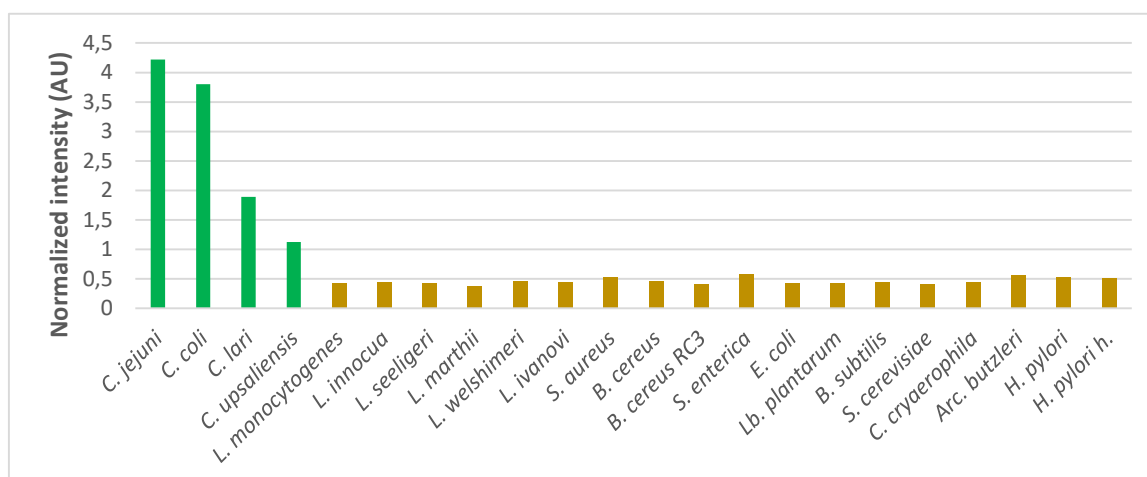


Figure 3.29 New chemiluminescent specificity test results. Several DNA Microorganism strains standardized at 100 ng/ μ L were tested with the probe CampyP3-Bio associated with Si NPs. In green the *Campylobacter* spp. and in yellow the negative controls.

3.2.8.2 Scanning electron microscopy

In Figure 3.30 (a, b, c, d, and e) are reported the images related to the nylon membrane used (3.30a), the spot of the analyses on *C. jejuni* using the chemiluminescent protocol (3.30b), and a detail of the analyses in Figure 3.30c. Figure 3.30d and 3.30e show the membrane surface of the spot with *C. jejuni* analyzed using the Si-Nps protocol. All the images were obtained with the utilization of the Scanning Electron Microscope (SEM).

The probe CampyP3-Bio was used in both the protocols, the first with chemiluminescence (3.30b) and with Si-NPs (3.30d). The target in both experiments was whole DNA from *Campylobacter jejuni*.

It is possible to suppose that the difference between Figure 5a and 5b is due to the deposition of the target DNA, while in Figure 5d is possible to see white particles that can be considered the Si-NPs used for the protocol.

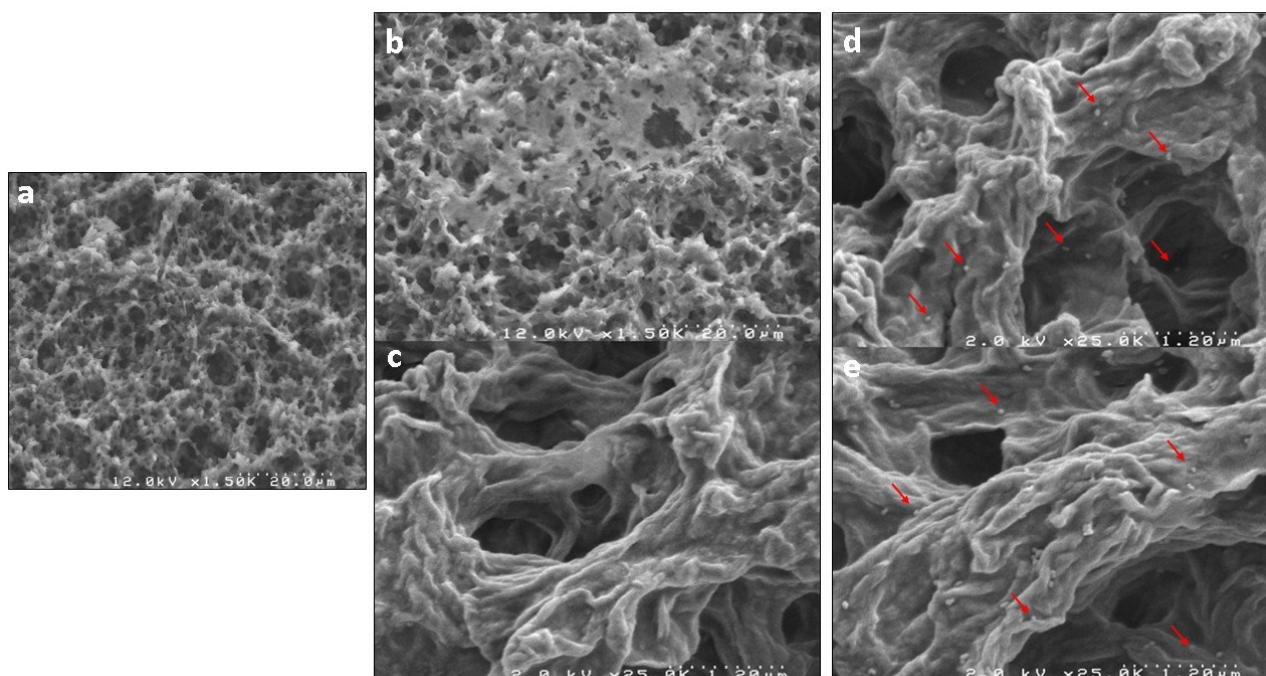


Figure. 3.30 Characterization of the functionalized membrane by Scanning Electron Microscopy (SEM). a) Surface of nylon membrane. b) Surface attached *C. jejuni* DNA-probe-biotin-streptavidin complex in the lower and c) a detail of the membrane. In 5c the surface attached *C. jejuni* DNA- probe-biotin-streptavidin-SiNPs complex.

3.2.8.3 *Campylobacter* spp. detection in chicken samples

The results obtained by the analysis of chicken samples are reported in Figure 3.31. Positive signals were obtained for samples 3SCB and 10SCB, while no signals were obtained for samples SCB4, SCB5 and SCB6 as shown. The data are confirmed by the data obtained with the method ISO 10272-1:2006.

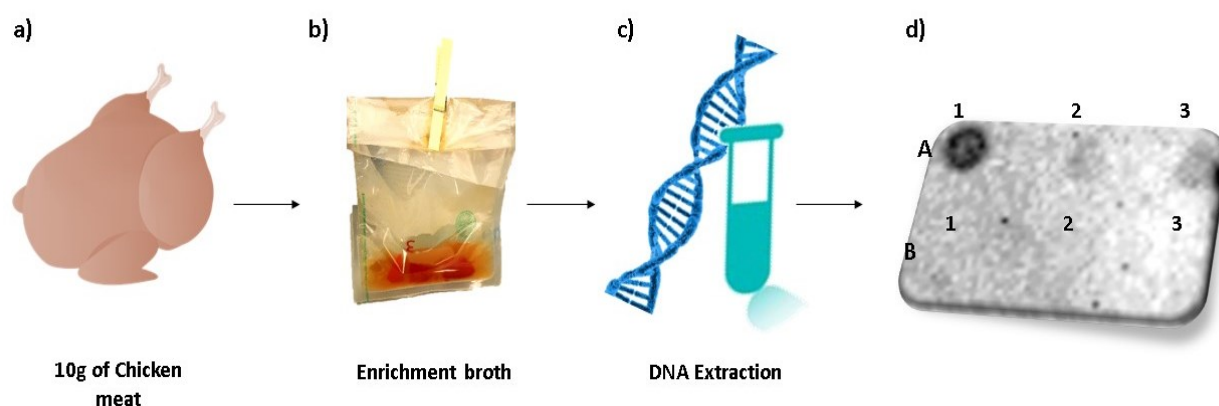


Figure 3.31 Scheme of the analysis of chicken meat samples. Chicken sample (a) was treated with enrichment step (b), the DNA was extracted (c) and was analysed by Si-NPs protocol (d). In d) the results obtained; Row A: A1: CCP3, A2: 3SCB, A3: 10SCB; in Row B, B1: SCB4, B2: SCB5 B3: SCB6.

3.2.9 ELECTROCHEMICAL BIOSENSOR

3.2.9.1 PBS BUFFER OPTIMIZATION 1X vs 4X

The buffer PBS 1X and 4X were tested to evaluate the influence of the concentration on voltammetric behavior.

The functionalized screen-printed gold electrodes (SPAuE), named 1.0, 1.1 and 1.2 were hybridized using PBS 1X, while the SPAuE named 2.0, 2.1 and 2.2 were functionalized and hybridized using PBS 4X.

The data of SPAuE 1.0 correspond to the electrode functionalized and blocked with MCH 10 mM, while the data of SPAuE 1.1 correspond to an electrode 1.0, after hybridization with CCP3 at 1 ng/ μ L. The SPAuE 1.2 corresponds to the electrode directly measured after the hybridization (it lacks the data related to functionalization). The same procedure was carried out for 2.0, 2.1 and 2.2 respectively. This experiment was aimed to decide if the utilization of one SPAuE for all the measurements could have affected the final value.

The analysis was conducted by immersion of the SPAuE in 8 mL of ferrocyanide.

The anodic current (I_{pa}) and the ΔI_{pa} (I_{pa} Blank- I_{pa} samples) measured by CV and by DPV are reported in Table 3.23, for each sample.

Table 3.23 Measurement of anodic peak current (Ipa) obtained by CV and DPV to compare PBS 1X and PBS 4X signal expressed in ampere (A) and microampere (μ A).

PBS buffer	Samples		CV			DPV		
			Ipa A	Ipa μ A	Δ Ipa μ A	Ipa A	Ipa μ A	Δ Ipa μ A
1X	1.0	Blank	0.000193	0.19312	0	0.000455	0.45536	0
	1.1	CCP3 1ng/ μ L	0.000187	0.18728	-0.00584	0.000433	0.43315	-0.02221
	1.2	CPP3 1ng/ μ L	0.00018	0.17999	-0.01313	0.000398	0.3983	-0.05706
	2.0	Blank	0.000169	0.16903	0	0.000484	0.48366	0
4X	2.1	CCP3 1ng/ μ L	0.000173	0.1725	0.00347	0.000491	0.49142	0.00776
	2.2	CCP3 1ng/ μ L	0.000199	0.19936	0.03033	0.000553	0.55327	0.06961

The data of the Δ Ipa are reported in Figure 3.32 for CV and in Figure 3.33 for DPV. For both measurements, CV and DPV, the anodic current (Δ Ipa) due to the oxidation of ferrocyanide showed a correct decrease after the hybridization of the target using the buffer at 1X for the samples 1.1 and 1.2. There was, on the contrary, an increase of the anodic current using the buffer at 4X for the samples 2.1 and 2.2. Therefore, the buffer at 1X was chosen to proceed with the experiments.

The signal obtained by DPV is more sensitive in comparison to CV as shown in Figures 3.32 and 3.33 as expected.

It is interesting to note that comparing the data obtained for SPAuE analyzed before functionalization and after hybridization (1.1 and 2.1) to the data obtained for SPAuE only analyzed after hybridization (1.2 and 2.2) the intensity of the signal (Δ Ipa) is higher for the SPAuE 1.2 and 2.2.

However, the measurements were conducted also after functionalization to study the assay protocol and to have major control of the signal.

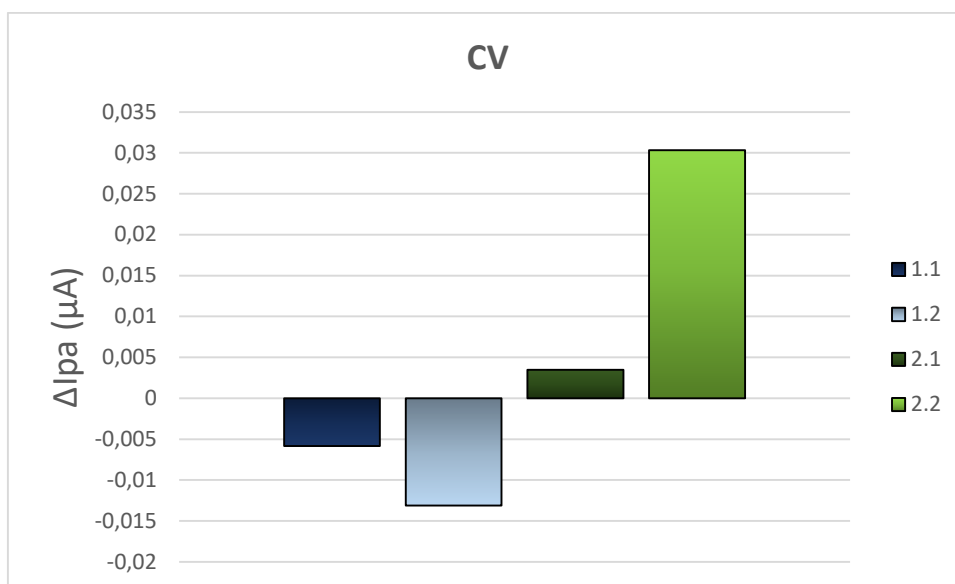


Figure 3.32 Cycle voltammetry ΔI_{pa} data of samples treated with PBS 1X (1.1- 1.2), blue and samples treated with PBS 4X (2.1- 2.2).

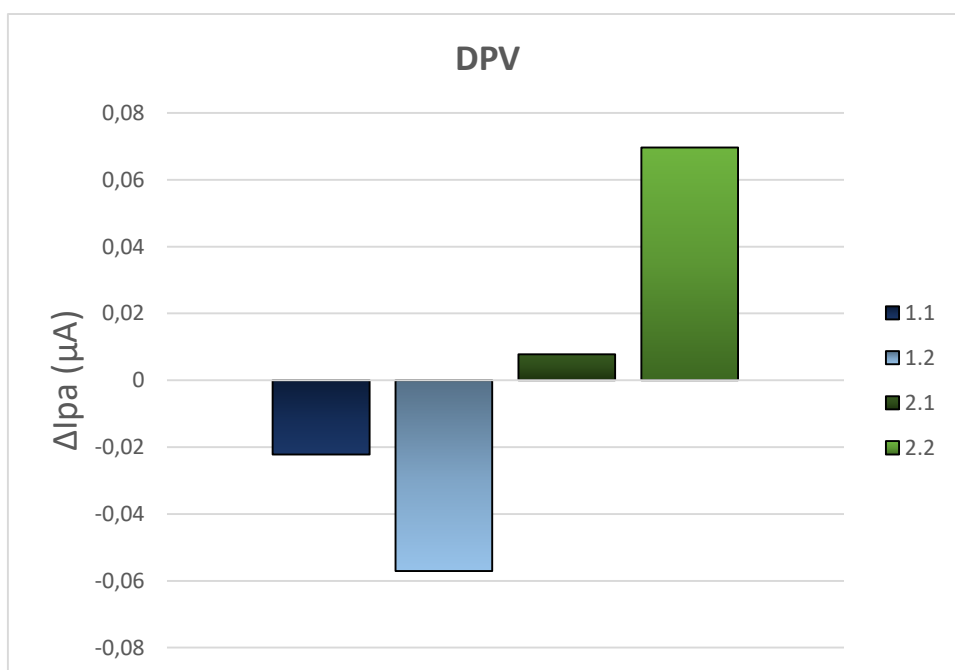


Figure 3.33 Differential pulse voltammetry ΔI_{pa} data in comparison of samples treated with PBS 1X (1.1- 1.2) and samples treated with PBS 4X (2.1- 2.2).

3.2.9.2 Optimization of MCH and time deposition.

The concentration of MCH was optimized testing 1 mM and 10 mM and also the blocking time was optimized testing 30 min and 60 min. The measurement of the I_{pa} , ΔI_{pa} obtained using the CV and DPV were reported in Table 3.24. The measurements were conducted: after

functionalization (1.0 and 2.0) and subsequently after hybridization of CCP3 at 1 ng/ μ L (1.1 and 2.1) and directly after functionalization and hybridization (1.2 and 2.2). The reading was conducted by immersing the SPAuE in 8 mL of ferrocyanide.

Table 3.24 Measurements of anodic peak current by CV and DPV for the several concentration and time deposition of MCH. The I_{pa} values are expressed in ampere (A) and microampere (μ A).

MCH	Time	Samples	CV			DPV		
			I_{pa} A	I_{pa} μ A	ΔI_{pa} μ A	I_{pa} A	I_{pa} μ A	ΔI_{pa} μ A
	30 min	1.0 Blank	0.00019659	0.19659	0	.,00047499	0.47499	0
	30 min	1.1 CCP3 1ng/ μ L	0.00000659	0.00659	-0.19	0.00002435	0.02435	-0.45064
1mM	60 min	1.2 CCP3 1ng/ μ L	6E-06	0.006	-0.19059	0.00001638	0.01638	-0.45861
	30 min	2.0 Blank	0.00019475	0.19475	0	4.55E-04	0.45536	0
	30 min	2.1 CPP3 1ng/ μ L	0.00000607	0.00607	-0.18868	0.00002221	0.02221	-4.3315E-01
10 mM	60 min	2.2 CPP3 1ng/ μ L	0.00000733	0.00733	-0.18742	0.00002161	0.02161	-4.3375E-01

The data of the ΔI_{pa} are reported in Figure 3.34 for CV and in Figure 3.35 for DPV.

For both measurements, CV and DPV, the anodic current (ΔI_{pa}) showed greater decrement using MCH at 1 mM for samples 1.1 and 1.2 in comparison to the MCH at 10 mM for samples 2.1 and 2.2.

The ΔI_{pa} was not influenced by the time of the blocking deposition (MCH), 30 min and 60 min, as shown for the samples 1.1 compared to 1.2 and 2.1 and 2.2.

Therefore, the MCH at 1 mM with 60 min of deposition were chosen to proceed with the following experiments.

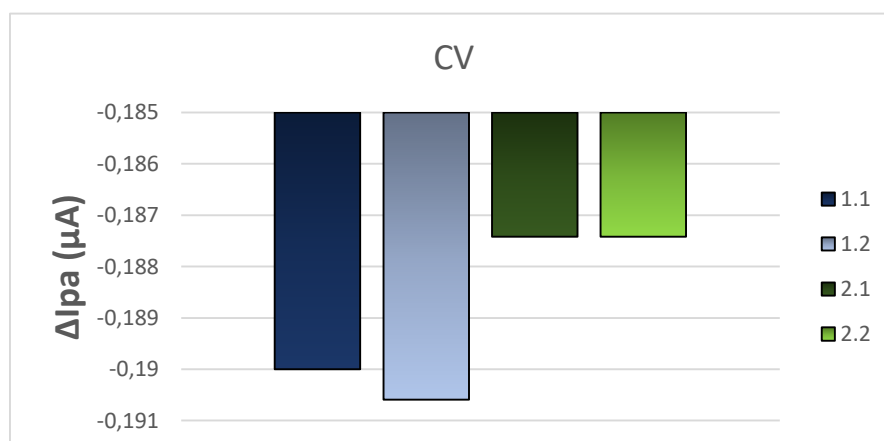


Figure 3.34 Cycle voltammetry ΔI_{pa} data of samples treated with 1mM MCH (1.1- 1.2) and with 10mM MCH (2.1- 2.2). Moreover sample treated with deposition of MCH for 30 min (1.1 -2.1) and for 60 min (1.2-2.2).

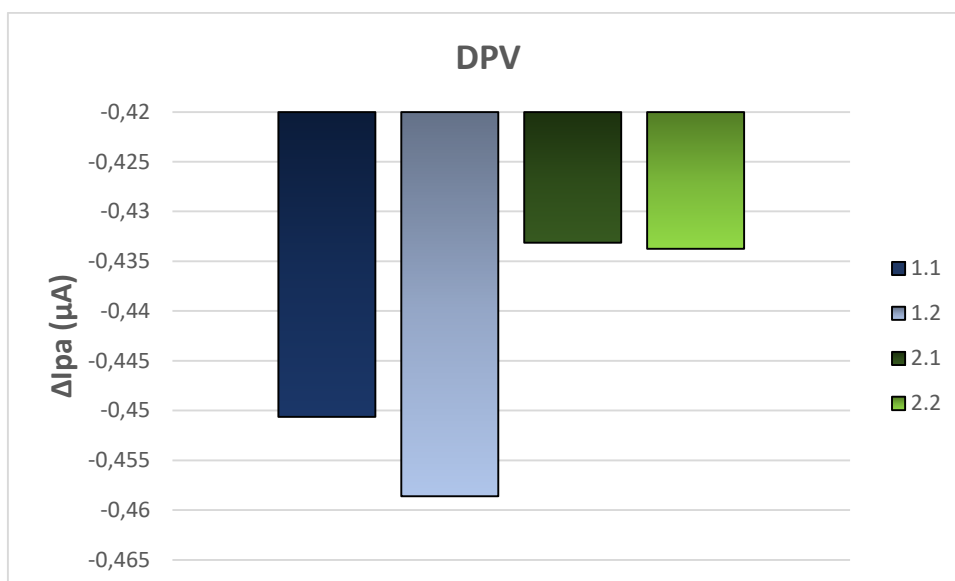


Figure 3.35 Differential pulse voltammetry ΔI_{pa} data of samples treated with 1mM MCH (1.1- 1.2) and with 10mM MCH (2.1- 2.2). Moreover sample treated with deposition of MCH for 30 min (1.1 -2.1) and for 60 min (1.2-2.2).

3.2.9.3 Optimization of reading by drop-casting

The reading measurements were tested by immersion in ferrocyanide and by drop-casting. In this last case, the measurements by CV and DPV were carried out depositing 80 μL of ferrocyanide. The data are reported in Table 3.25. The ΔI_{pa} current signals are -0.17796 for CV value and -0.40944 for DPV value. Thus, a little higher current signal was obtained with the reading by immersion (Table 3.24 sample 1.2) with -0.19059 for CV value and -0.45861 for DPV value.

However, the reading by drop-casting was chosen for the following experiments, considering the possibility that the SPAuE could be damaged by multiple immersions in ferrocyanide solution (exp. calibration curve) that could have lead to significant differences in current signal and reproducibility of the analysis.

Table 3.25 Measurements of anodic peak current by CV and DPV carried out reading by ferrocyanide drop. The I_{pa} values are expressed in ampere (A) and microampere (μA).

Reading	Samples	CV			DPV		
		I_{pa} A	I_{pa} μA	ΔI_{pa} μA	I_{pa} A	I_{pa} μA	ΔI_{pa} μA
1	Blank	0.00019659	0.19659	0	0.00047499	0.47499	0
Drop	1.1 CCP3 1ng/ μL	0.00001863	0.01863	-0.17796	0.00006555	0.06555	-0.40944

3.2.9. 4 Optimization of washing step

The optimization of the washing steps was carried out by testing three washing methods by simulating 5 measurements to produce a calibration curve using 5 concentrations.

Washing method n.1: five washing for each concentration, of which 4 washing with PBS 1X, and one, the last, with sterilized water. Washing method n.2: five washing for each concentration with sterilized water. Washing method n.3: two washing for each concentration with sterilized water. The Ipa measurements by CV and by DPV and the respective standard deviation of the ΔIpa are reported in Table 3.26.

To assess the washing method that gave less interference on the current signal it was considered the value of the standard deviation. Method 3, presented the lower value of standard deviation for CV and DPV, therefore it was chosen to proceed with the further experiments.

3.2.9.5 Calibration curves with complementary probe CCP3.

To test the capability of the sensor to detect the target, the following experiments were performed using the sequence complementary to the probe CampyP3, named CCP3, as the template. Before, the SPAuE functionalization with CampyP3 probe at 10 ng/ μ L, the CCP3 probe was serially diluted from 10 ng/ μ L, 1 ng/ μ L, 100 pg/ μ L, 10 pg/ μ L and 1 pg/ μ L; and hybridized to the probe. The mean of three measurements of the voltammetric response, cyclic voltammetry (CV) and differential pulse voltammetry (DPV) were reported. Moreover, the difference between anodic peak current recorded after hybridization (Ipa samples) and the anodic peak current recorded at the functionalized electrode (Ipa blank) were reported in Table 3.27 for CV (ΔIpa CV) and DPV (ΔIpa DPV).

Table 3.26 Measurement of the anodic peak current (Ipa) and the ΔIpa by CV and by DPV and the standard deviation (ST DV) of complementary probe CCP3. The Ipa values are expressed in ampere (A) and microampere (μ A).

Washing mode	Samples	CV			DPV			ST DV Δ CV	ST DV Δ DPV
		Ipa A	Ipa μ A	ΔIpa μ A	Ipa A	Ipa μ A	ΔIpa μ A		
1	Blank	0.000178	178.21	0	0.000399	399.06	0		
	1.1	0.000182	181.91	3.7	0.000409	409.42	10.36		
	1.2	0.000182	181.61	3.4	0.00041	409.75	10.69	2.266	8.066
	1.3	0.000183	182.51	4.3	0.000394	394.44	-4.62		
	1.4	0.000177	176.95	-1.26	0.000391	391.1	-7.96		
	1.5	0.000178	177.99	-0.22	0.000394	394.38	-4.68		

2	Blank	0.000174	174.19	0	0.000393	392.76	0		
	2.1	0.000177	177.11	2.92	0.0004	399.57	6.81		
	2.2	0.00018	180.14	5.95	0.000401	401.19	8.43	1.897	4.715
	2.3	0.00018	180.40	6.21	0.000391	390.68	-2.08		
	2.3	0.000176	176.33	2.14	0.00039	390.15	-2.61		
	2.4	0.000176	175.98	1.79	0.000392	391.79	-0.97		
3	Blank	0.000176	176.02	0	0.000406	405.73	0		
	3.1	0.000179	179.14	3.12	0.000411	411.36	5.63		
	3.2	0.000181	181.15	5.13	0.000414	414.29	8.56	1.020	4.369
	3.3	0.000018	179.99	3.97	0.000411	410.64	4.91		
	3.4	0.000179	178.99	2.97	0.000403	402.81	-2.92		
	3.5	0.000178	178.13	2.11	0.000404	404.38	-1.35		

Table 3.27 Measurement of the average anodic peak current ($\overline{I_{pa}}$) and the ΔI_{pa} . By CV and DPV of complementary probe CCP3. The I_{pa} values are expressed in ampere (A) and microampere (μA).

Samples (pg/ μL)	Log	CV			DPV			ST DV	
		$\overline{I_{pa}}$ A	μA	ΔI_{pa} μA	$\overline{I_{pa}}$ A	μA	ΔI_{pa} μA	ΔCV	ΔDPV
Blank	/	0.000184	184.210	0	0.000419	418.907	0	0	0
CCP3 1	0	0.000181	180.807	-3.403	0.000414	413.743	-5.1633	4.179	16.907
CCP3 10	1	0.0001790	179.047	-5.163	0.000397	397.100	-21.807	2.823	4.308
CCP3 100	2	0.0001778	177.753	-6.457	0.000389	389.213	-29.693	0.768	10.065
CCP3 1000	3	0.0001766	176.637	-7.573	0.000374	373.665	-45.242	0.270	18.290
CCP3 10000	4	0.0001738	173.833	-10.377	0.000351	351.250	-67.657	2.300	21.009

Calibration curves reported in Figure 3.36 were obtained plotting the ΔI_{pa} CV and ΔI_{pa} DPV against the logarithmic concentration of the target (expressed in pg/ μL).

The data show a decrement of anodic peak current with both the reading methods and the ΔI_{pa} value inversely proportional to the DNA concentration. The range of CV values is from -3.403 to -10.337 μA and of DPV from -05.1633 to -67.657 μA .

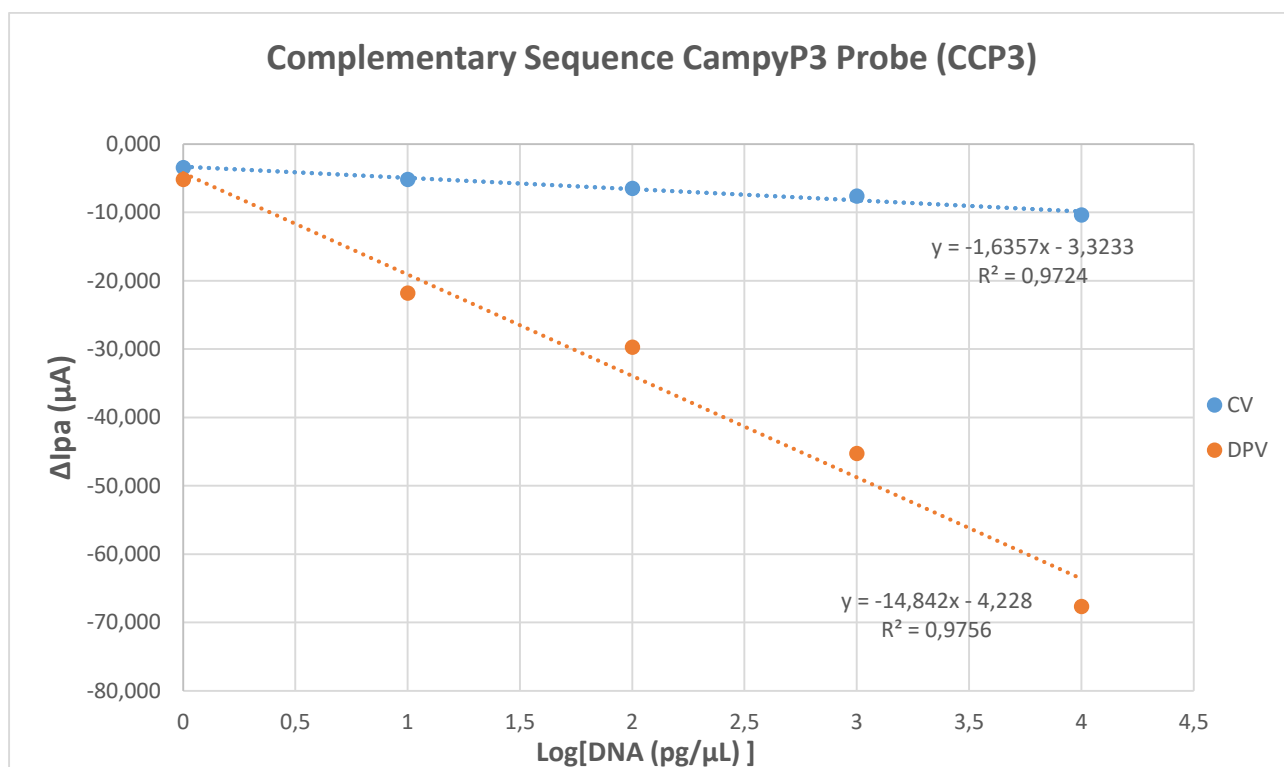


Figure 3.36 Calibration curves obtained by plotting ΔI_{pa} against CCP3 complementary probe concentration expressed in Log. The values were obtained by measurements in CV (blue) and DPV (orange).

3.2.9.6 Calibration curves with whole DNA

To verify the capability of the CampyP3 probe to detect also genomic DNA, the following test was performed using *Campylobacter jejuni* DSM 4688 genomic DNA. Several DNA dilutions from 10 ng/ μ L, 1 ng/ μ L, 100 pg/ μ L, 10 pg/ μ L and 1 pg/ μ L were hybridized to the probe CampyP3 at 10 ng/ μ L, previously immobilized on the gold working electrode. The electrodes were prepared with the same method reported previously. The mean of the I_{pa} by CV and DPV were measured and the respectively ΔI_{pa} values were calculated (Table 3.28)

Calibration curves reported in Figure 3.37 were obtained plotting the mean ΔI_{pa} CV and ΔI_{pa} DPV against the logarithmic concentration of the target (expressed in pg/ μ L).

The data show that there is a decrement of anodic peak current with both the reading methods and that the ΔI_{pa} is inversely proportional to the DNA concentration. The calibration curves (Figures 3.35 and 3.36) show that at the same concentration the higher decrement of the current is as expected correctly, corresponding to the whole DNA.

Table 3.28 Measurement of the average anodic peak current ($\overline{I_{Pa}}$) and the ΔI_{Pa} . By CV and DPV of *C. jejuni* whole DNA. The I_{Pa} values are expressed in ampere (A) and microampere (μA).

Samples (pg/ μL)	Log	CV			DPV			ST DV	
		$\overline{I_{Pa}}$ A	I_{Pa} μA	ΔI_{Pa} μA	$\overline{I_{Pa}}$ A	I_{Pa} μA	ΔI_{Pa} μA	ΔCV	ΔDPV
Blank	/	0.000189	189.403	0	0.000454	453.6867	0	0	0
<i>C. j.</i> 1	0	0.000193	193.140	3.737	0.000451	451.050	-2.637	8.676	39.065
<i>C. j.</i> 10	1	0.000183	182.566	-6.837	0.000412	411.7633	-41.923	4.959	7.852
<i>C. j.</i> 100	2	0.000175	175.173	-14.230	0.000388	388.050	-65.637	7.126	24.191
<i>C. j.</i> 1000	3	0.000171	171.146	-18.257	0.000362	362.2067	-91.480	8.172	10.510
<i>C. j.</i> 10000	4	0.000171	171.400	-18.003	0.000368	367.8733	-85.813	5.052	17.498

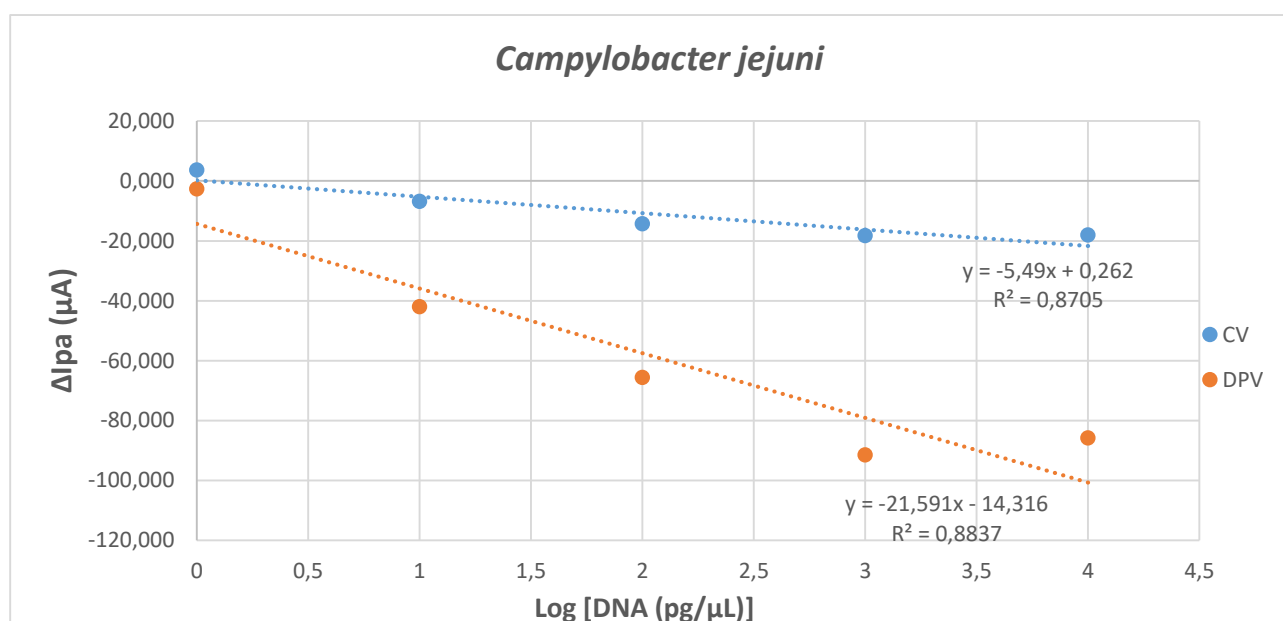


Figure 3.37 Calibration curves obtained by plotting ΔI_{Pa} against *C. jejuni* concentration expressed in Log. The values were obtained by measurements in CV (blue) and DPV (orange).

3.2.9.7 Calibration curves for the specificity

SPAUEs cleaned and functionalized were used to test the specificity of the assay using the negative controls *Campylobacter fetus*, *Escherichia coli*, and *Listeria innocua*. *C. fetus* was used for the high similarity of the whole genome with *C. jejuni* and *C. coli*, *E. coli* was tested because usually present in chicken food samples, instead, *L. innocua* was used to test a Gram-positive.

C. fetus – negative control

To verify the capability of the CampyP3 probe to be specific once applied to the biosensor, also the genomic DNA of *Campylobacter fetus* DSM 5361 was tested as very close to the four *Campylobacter* species target.

Several DNA concentrations from 1 to 10000 pg/μL were hybridized to the probe CampyP3 at 10 ng/ μL, previously immobilized on the working electrode. The electrodes were prepared with the same method as compared to the previous test. Tests were carried out three-time and in Table 3.29 the mean of I_{pa} by CV and DPV ($\overline{I_{pa}}$) measured and the mean of the ΔI_{pa} were reported.

Table 3.29 Measurement of the average anodic peak current ($\overline{I_{pa}}$) and the ΔI_{pa} . By CV and DPV of *C. fetus* whole DNA. The I_{pa} values are expressed in ampere (A) and microampere (μA).

Samples (pg/μL)	Log	CV			DPV			ST DV	
		$\overline{I_{pa}}$	μA	ΔI_{pa}	$\overline{I_{pa}}$	μA	ΔI_{pa}	ΔCV	ΔDPV
Blank	/	0.000187	187.4567	0	0.000407	406.940	0	0	0
<i>C. fetus</i> 1	0	0.000187	186.5833	-0.873	0.000407	407.390	0.450	2.842	10.824
<i>C. fetus</i> 10	1	0.000188	188.4367	0.980	0.000410	409.530	2.590	4.141	10.387
<i>C. fetus</i> 100	2	0.000186	186.0767	-1.380	0.000407	406.9467	0.007	2.615	14.344
<i>C. fetus</i> 1000	3	0.000189	189.2733	1.817	0.000410	409.7867	2.847	0.701	12.674
<i>C. fetus</i> 10000	4	0.000193	192.510	5.053	0.000395	394.6333	-12.307	4.839	15.706

Calibration curves reported in Figure 3.38 were obtained plotting the ΔI_{pa} CV and ΔI_{pa} DPV against the logarithmic concentration of the target (expressed in pg/μL).

The data show that there is no proportional decrement of the anodic peak current at the increase of the concentration of DNA, as expected.

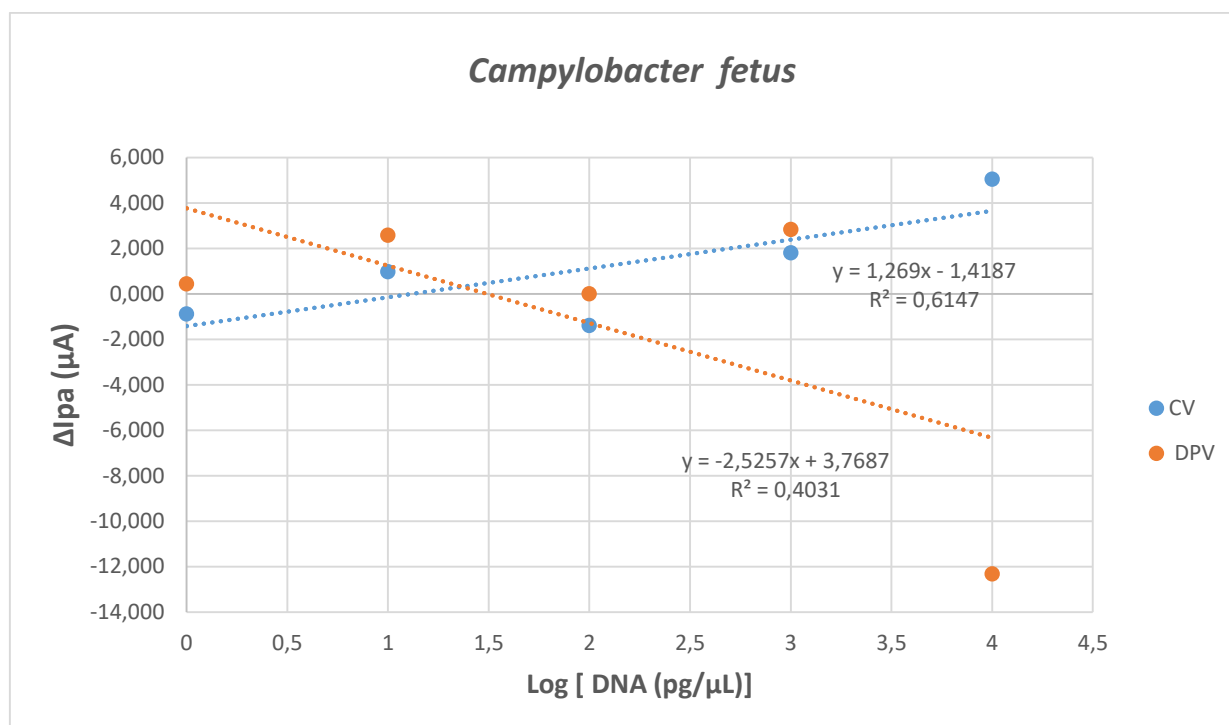


Figure 3.38 Calibration curves obtained by plotting ΔI_{pa} against *C fetus* concentration expressed in Log. The values were obtained by measurements in CV and DPV.

E. coli negative controls

The data are reported in Table 3.30 and the calibration curves in Figure 3.39. The data show that there is not a proportional decrement of the anodic peak current with the increase of the concentration DNA as expected, and already seen for *C. fetus*.

Table 3.30 Measurement of the average anodic peak current ($\overline{I_{pa}}$) and the ΔI_{pa} . By CV and DPV of *E. coli* whole DNA. The I_{pa} values are expressed in ampere (A) and microampere (μA).

Samples		CV			DPV			ST DV	
(pg/ μL)	Log	$\overline{I_{pa}}$ A	I_{pa} μA	ΔI_{pa} μA	$\overline{I_{pa}}$ A	I_{pa} μA	ΔI_{pa} μA	ΔCV	ΔDPV
Blank	/	0.000188	188.0633	0	0.000456	456.460	0	0	0
<i>E. coli</i> . 1	0	0.000192	192.170	4.107	0,000460	45.8967	3.437	2.686	8.208
<i>E. coli</i> 10	1	0.000193	193.3133	5.250	0.000461	461.310	4.850	2.748	7.989
<i>E. coli</i> 100	2	0.000198	197.730	9.667	0.000462	461.800	5.340	11.209	7.703
<i>E. coli</i> 1000	3	0.000192	191.530	3.467	0.000450	450.140	-6.320	2.984	8.775
<i>E. coli</i> 10000	4	0.000188	187.770	-0.293	0.000434	4339833	-22.477	2.935	11.640

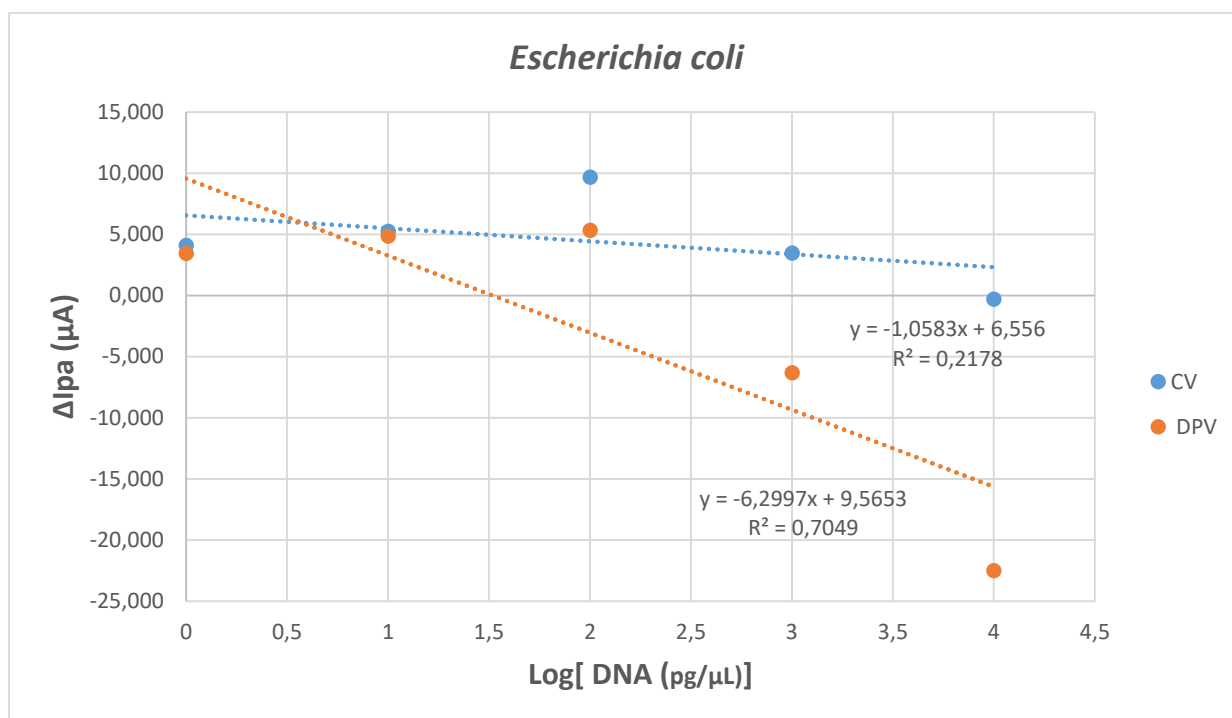


Figure 3.39 Calibration curves obtained by plotting ΔI_{pa} against *E. coli* concentration expressed in Log. The values were obtained by measurements in CV and DPV.

L. innocua

The data are reported in Table 3.31 and the calibration curves in Figure 3.40. The data show that there is not a proportional decrement of the anodic peak current with the increase of the concentration of DNA as expected.

Table 3.31 Measurement of the average anodic peak current ($\overline{I_{pa}}$) and the ΔI_{pa} . By CV and DPV of *L. innocua* whole DNA. The I_{pa} values are expressed in ampere (A) and microampere (μA).

Samples (pg/ μ L)	Log	CV			DPV			ST DV	
		$\overline{I_{pa}}$ A	I_{pa} μ A	ΔI_{pa}	$\overline{I_{pa}}$ A	I_{pa} μ A	ΔI_{pa}	ΔCV	ΔDPV
Blank	/	0.000176	175.850	0	0.000355	354.990	0	/	/
<i>L. innocua</i> 1	0	0.000174	173.7333	-2.117	0.000354	354.100	-0.890	6.863	25,261
<i>L. innocua</i> 10	1	0.000175	174.7833	-1.067	0.000350	350.480	-4.510	8.608	27.933
<i>L. innocua</i> 100	2	0.000175	174.5133	-1.337	0.000356	355.7167	0.727	9.326	37.541
<i>L. innocua</i> 1000	3	0.000176	175.890	0.040	0.000349	348.5867	-6.403	8.386	34.899
<i>L. innocua</i> 10000	4	0.000173	173.3933	-2.457	0.000334	334.140	-20.850	10.410	43.737

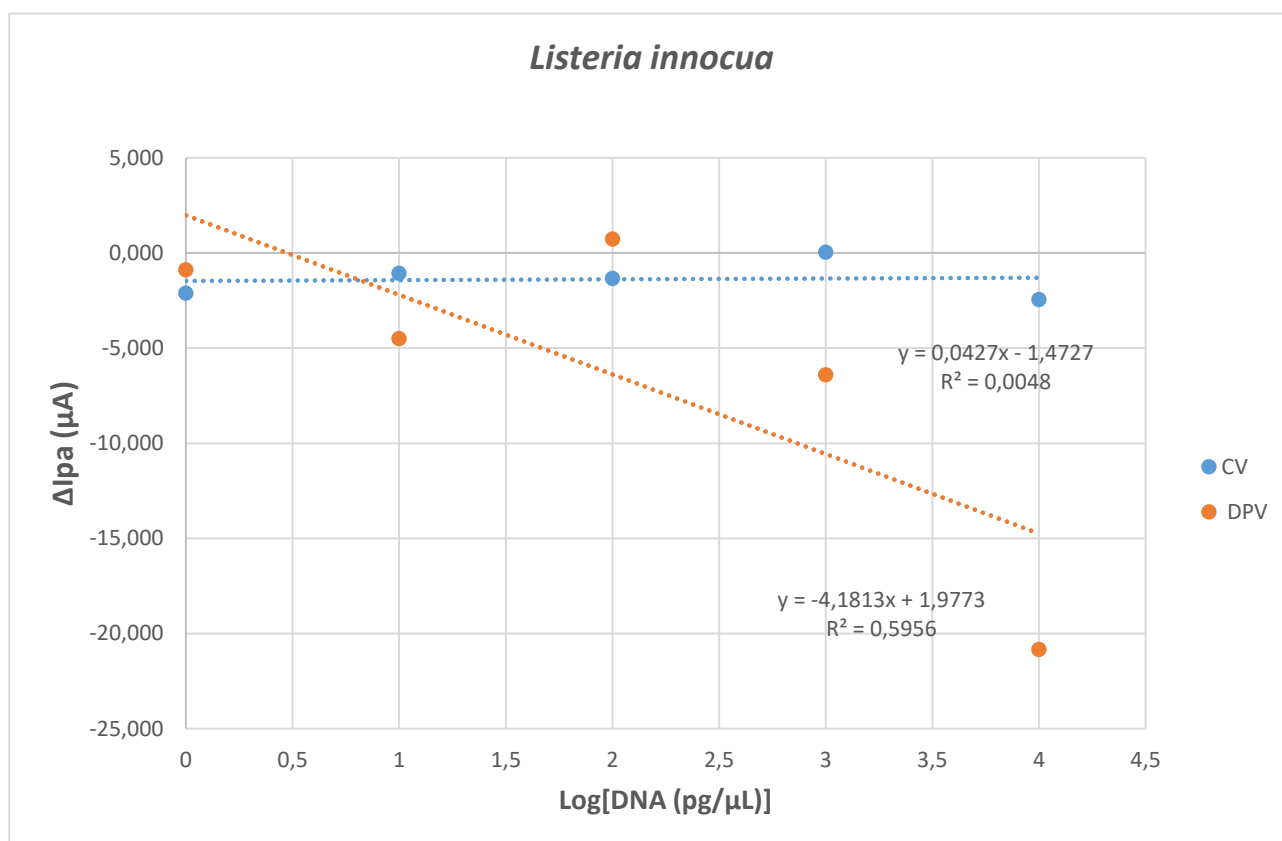


Figure 3.40 Calibration curves obtained by plotting ΔI_{pa} against *L. innocua* concentration expressed in Log. The values were obtained by measurements in CV and DPV.

In Table 3.32 the slope ratio is reported for all the negative controls in comparison with *C. jejuni*. Greater is the slope ratio value of the calibration curve, greater is the sensitivity of the assay to discriminate the positive controls from negative controls. From the slope ratio value seems to be that CV measurements are more sensitive than DPV measurements to discriminate *E. coli* and *L. innocua*.

In the regression line of *C. jejuni*, the intercept value is higher in DPV measurement with 14.316, in comparison to values of the negative controls in DPV. The intercept value represents the decrement of the current signal at the lower concentration tested. Thus, the assay seems to be more able to discriminate a negative from a positive control using the DPV measurements at a lower concentration.

Table 3.32 Slope ratio value obtained between the slope value of *C. jejuni* and the slope value of negative controls *C. fetus*, *E. coli* and *L. innocua*.

CV	<i>C. jejuni</i> $y = -5.49x + 0.262$				
	<i>C. fetus</i>	$y = 1.2683x - 1.418$	<i>E. coli</i>	$y = 1,269x - 1,4187$	<i>L. innocua</i> $y = 0.0427x - 1.4727$
	Slope ratio	4.32	Slope ratio	4.43	Slope ratio 128.6
DPV	<i>C. jejuni</i> $y = -21.591x - 14.316$				
	<i>C. fetus</i>	$y = -2.5257x + 3.7687$	<i>E. coli</i>	$y = -6,2997x + 9,5653$	<i>L. innocua</i> $y = -4.1813x + 1.9773$
	Slope ratio	8.54	Slope ratio	3.42	Slope ratio 5.16

Figure 3.41 and 3.42 show the behavior of the calibration curves of *C. jejuni*, *C. fetus*, *E. coli* and *L. innocua* obtained by CV and by DPV. The best specificity and sensitivity were obtained by DPV measurements. From Figure 3.41 the limit of detection of the system seems to be between 1 pg/μL and 10 pg/μL. It is necessary a measurement of the concentration between 1 pg/μL and 10 pg/μL, to verify if the limit of detection is really 10 pg/μL or lower. The analysis on food sampled was carried out only considering the DPV measurements as more sensitive than CV.

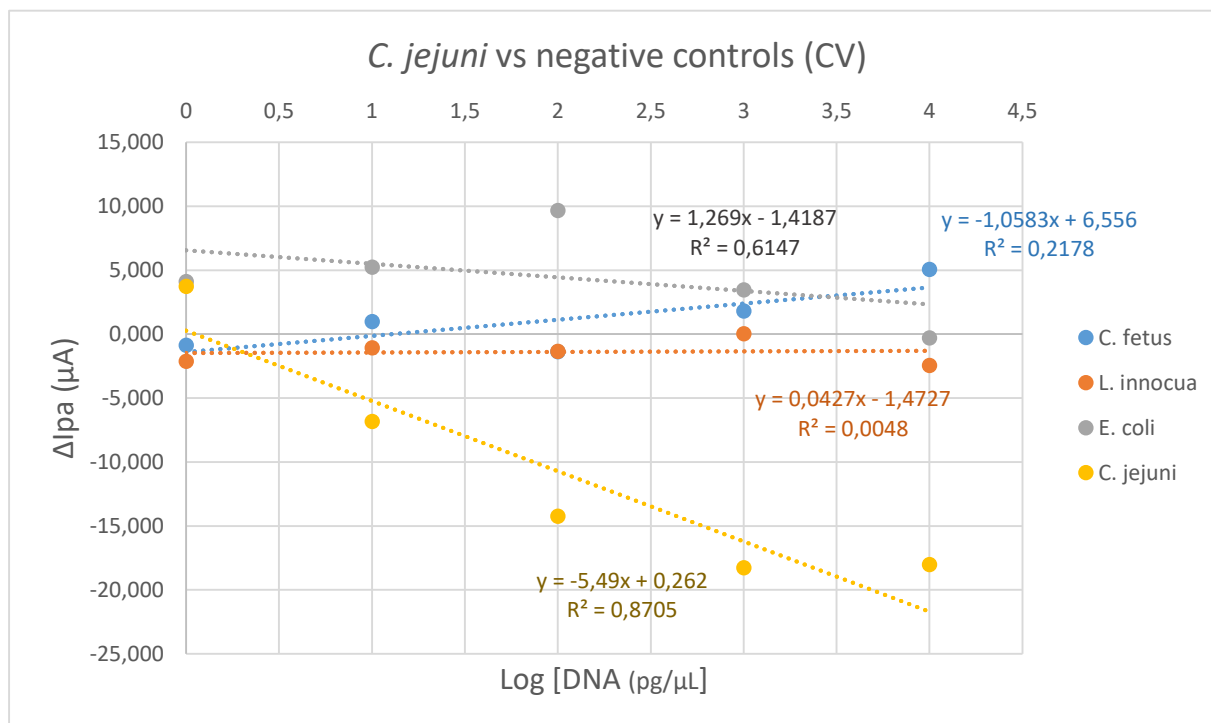


Figure 3.41 The calibration curves obtained by CV measurement of *C. fetus* (blue), *L. innocua* (orange), *E. coli* (grey) and *C. jejuni* (yellow).

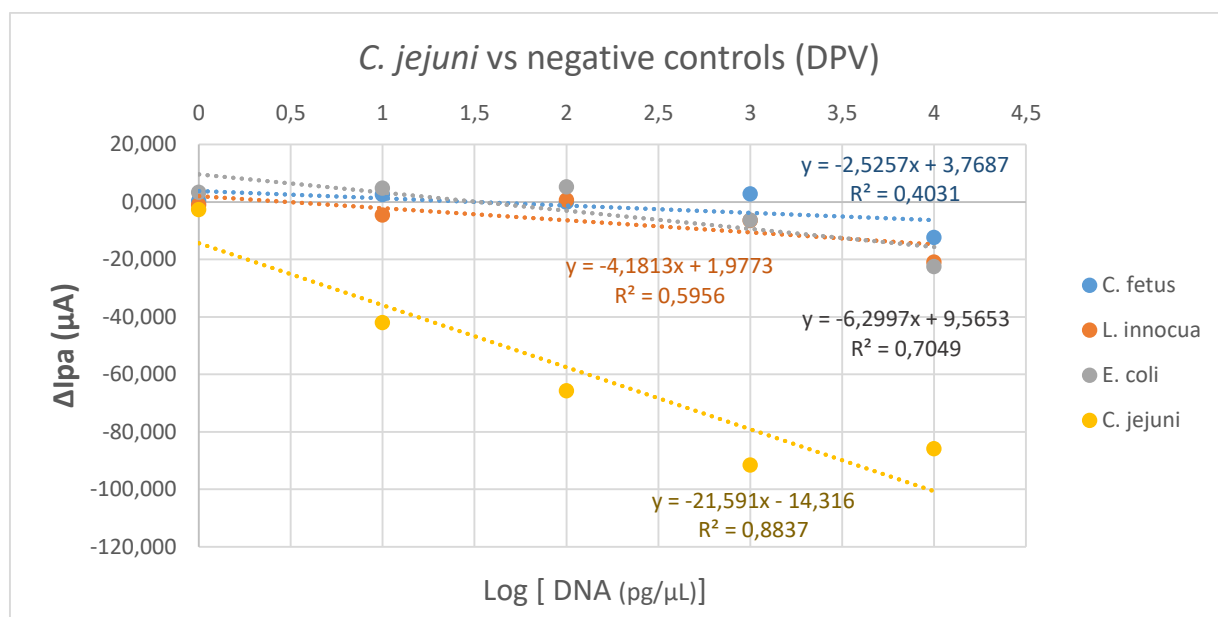


Figure 3.42 The calibration curves obtained by DPV measurement of *C. fetus* (blue), *L. innocua* (orange), *E. coli* (grey) and *C. jejuni* (yellow).

3.2.9.8 Detection of *Campylobacter* spp. in food

Three chicken samples were analyzed by the electrochemical biosensor. The DNAs were extracted by phenol: chloroform: isoamyl alcohol protocol after enrichment in broth (Bolton broth) (48h at 41.5°C). The extracted DNA was diluted 1:10 and 12 μL of DNA were hybridized on the gold functionalized surface of the working electrode. For the analysis, *E. coli* at 10 ng/μL was used as the negative control. The data of the measurements performed using the DPV protocol for each sample are reported in Table 3.34. The X value of each sample, *E. coli*, 2SCB, 3SCB, 7SCB, was calculated using the equation of the DPV regression line of *C. jejuni* and added in the plot of Figure 3.42.

Table 3.33 Measurement of the anodic peak current (Ipa) and the ΔIpa by DPV of whole DNA chicken samples.

Samples			DPV		
			Ipa A	Ipa μA	ΔIpa μA
1	Blank	0.000393	393.14	-	
	<i>E. coli</i>	0.000409	409.04	15.900	
2	Blank	0.000473	473.42	-	
	2SCB	0.000394	393.81	-79.610	
3	Blank	0.000479	479.2	-	

	3SCB	0.000421	420.94	-58.260
4	Blank	0.00046	460.09	-
	7SCB	0.000447	446.74	-13.350

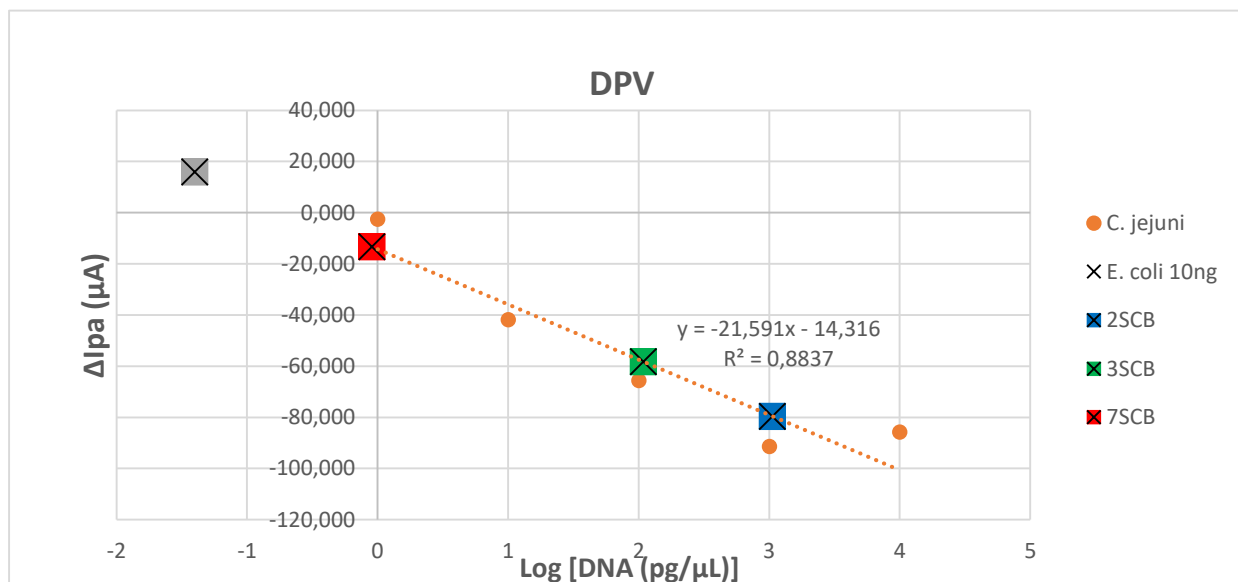


Figure 3.43 Food samples plotted in the regression line of *C. jejuni* obtained by DPV.

The X value and the Y value were replaced for each sample in the regression line. Thus, the value of the DNA detected was calculated and expressed in ng/μL and presented in Table 3.34. The values of *E. coli* samples gave negative results as expected, based on the range used (between 10 ng to 1 pg). Samples 2SCB and 3SCB resulted positive for *Campylobacter* spp. and the value calculated was 1.056 ng/μL. Sample 7SCB was considered negative for *Campylobacter*, even if the value 0.0009 ng/uL is borderline considering the limit of the detection to the assay.

Table 3.34 The X and Y values of samples used to calculate the DNA concentration by *C. jejuni* DPV regression line.

Samples	Y	X	pg/μL	ng/μL
<i>E. coli</i>	15.9	-1.399	0.039902	0.00004
2SCB	-79.61	3.024	1056.818	1.0568
3SCB	-58.26	2.035	108.3927	0.1084
7SCB	-13.35	-0.044	0.903649	0.0009

REFERENCES

- Bonnet R., Farre C., Valera L., Vossier L., Léon F., Dagland T., Pouzet A., Jaffrézic-Renault N., Fareh J., Fournier-Wirth C., Chaix C. (2018). Highly labeled methylene blue-ds DNA silica nanoparticles for signal enhancement of immunoassays: application to the sensitive detection of bacteria in human platelet concentrates. *Analyst.*, 143 (10):2293-2303.
- Cocolin L., Aggio D., Manzano M., Cantoni C., Comi G. (2002). An application of PCR-DGGE analysis to profile the yeast populations in raw milk. *International Dairy Journal* 12 (5): 407-411.
- Fontanot M., Iacumin L., Cecchini F., Comi G., Manzano M. (2014). Rapid detection and differentiation of important *Campylobacter* spp. in poultry samples by dot blot and PCR. *Food Microbiol.* 43:28-34.
- Klijn N., Weerkamp A.H., de Vos W.M. (1991). Identification of mesophilic lactic acid bacteria by using polymerase chain reaction-amplified variable regions of 16S rRNA and specific DNA probes. *Appl. Environ Microbiol.* 57(11):3390-3.
- Morgulis A., Coulouris G., Raytselis Y., Madden T.L., Agarwala R., Schäffer A.A. (2008). Database Indexing for Production MegaBLAST Searches. *Bioinformatics* 24:1757-1764
- Zhang Z., Schwartz S., Wagner L., Miller W. (2000). A greedy algorithm for aligning DNA sequences. *J. Comput. Biol.*, 7 (1-2):203-14.

SOFTWARE

- Altschul S.F., Gish W., Miller W., Myers E.W., Lipman D.J. (1990). Basic local alignment search tool. *J. Mol Biol.*, 215(3):403-410 (<http://blast.ncbi.nlm.gov/Blast.cgi>).
- Corpet F. (1988). Multiple sequence alignment with hierarchical clustering. *Nucleic Acid Res.*, 16(22):10881-10890 (<http://multalin.toulouse.inra.fr/multalin/>).
- IDT OligoAnalyzer 3.1 (<http://eu.idtdna.com/calc/analyzer>).
- Jullien N. (2013). AmplifX 1.7. CNRS, Aix-Marseille Université (<http://crn2m.univ-mrs.fr/pub/amplifx-dist>)

CONCLUSIONS AND FUTURE PERSPECTIVE

Taking into account the detection techniques developed, optimized and applied for the analysis of real food samples, several considerations can be done.

The plate count-based approach ISO 10272:2006 for *Campylobacter* and the Listeria Precip method need a long analysis time, from 5 to 8 days. It is considered too long for food companies releasing short shelf-life foods. Moreover, the detection of living cells can be difficult due to food industries treatments used for food stabilization, that can stress cells that enter a VBNC (viable but not culturable) state and are unable to grow on agar medium.

The procedures are also laborious.

The molecular approach based on PCR/qPCR is specific, but to get high sensitivity an enrichment step is still needed for the detection of *L. monocytogenes* as demonstrated by the negative results obtained from CSS samples (t_0). On the other hand the application of the qPCR for the detection of the *Campylobacter* spp. at t_0 has confirmed the result of ISO 10272-1:2006. This can depend on several factors: features of primer and the efficiency of the calibration curve used. These techniques although more expensive can reduce the time for analysis to 2-3 days if the enrichment step is necessary or if not the analysis time is 24h.

The novelty approach with the electrochemical biosensors described can match with the need for rapidity and sensitivity for the detection of food pathogens. The sensitivity obtained although not optimal to detect the pathogen without an enrichment step is promising. In both biosensors construction, some parameters will require more experiments to improve sensitivity.

For the OECT biosensor in order to improve the sensing performance, the modification of the gate electrode with nanoparticles or changing the nanostructure needs further study. Instead, for the biosensor based on voltammetry, the best result was obtained from the CampyP3 in comparison with the ListE shown that the design probe step is very important. For the electrochemical biosensor, the immobilization step will be studied testing new probes and buffers. This is the first step for the point of care analysis in food processing.